Università degli Studi di Cagliari

DOTTORATO DI RICERCA

Difesa e Conservazione del Suolo, Vulnerabilità Ambientale e Protezione Idrogeologica

Ciclo XXVIII

STUDY OF LAND DEGRADATION AND DESERTIFICATION DYNAMICS IN NORTH AFRICA AREAS USING REMOTE SENSING TECHNIQUES

Settore scientifico disciplinare di afferenza

GEO/04

Presentata da: Gabriela Mihaela Afrasinei

Coordinatore Dottorato Prof Giorgio Ghiglieri

Tutor Prof Giorgio Ghiglieri

PhD Dr Maria Teresa Melis

Esame finale anno accademico 2014 – 2015

Abstract

In fragile-ecosystem arid and semi-arid land, climatic variations, water scarcity and human pressure accelerate ongoing degradation of natural resources. In order to implement sustainable management, the ecological state of the land must be known and diachronic studies to monitor and assess desertification processes are indispensable in this respect. The present study is developed in the frame of WADIS-MAR (www.wadismar.eu). This is one of the five Demonstration Projects implemented within the Regional Programme "Sustainable Water Integrated Management (SWIM)" (www.swim-sm.eu), funded by the European Commission and which aims to contribute to the effective implementation and extensive dissemination of sustainable water management policies and practices in the Southern Mediterranean Region. The WADIS-MAR Project concerns the realization of an integrated water harvesting and artificial aquifer recharge techniques in two watersheds in Maghreb Region: Oued Biskra in Algeria and wadi Oum Zessar in Tunisia.

The WADIS MAR Project is coordinated by the Desertification Research Center of the University of Sassari in partnership with the University of Barcelona (Spain), *Institut des Régions Arides* (Tunisia) and *Agence Nationale des Ressources Hydrauliques* (Algeria) and the international organization *Observatorie du Sahara et du Sahel*. The project is coordinated by Prof. Giorgio Ghiglieri. The project aims at the promotion of an integrated, sustainable water harvesting and agriculture management in two watersheds in Tunisia and Algeria. As agriculture and animal husbandry are the two main economic activities in these areas, demand and pressure on natural resources increase in order to cope with increasing population's needs. In arid and semiarid study areas of Algeria and Tunisia, sustainable development of agriculture and resources management require the understanding of these dynamics as it withstands monitoring of desertification processes.

Vegetation is the first indicator of decay in the ecosystem functions as it is sensitive to any disturbance, as well as soil characteristics and dynamics as it is edaphically related to the former. Satellite remote sensing of land affected by sand encroachment and salinity is a useful tool for decision support through detection and evaluation of desertification indicating features.

Land cover, land use, soil salinization and sand encroachment are examples of such indicators that if integrated in a diachronic assessment, can provide quantitative and qualitative information on the ecological state of the land, particularly degradation tendencies. In recent literature, detecting and mapping features in saline and sandy environments with remotely sensed imagery has been reported

successful through the use of both multispectral and hyperspectral imagery, yet the limitations to both image types maintain “no agreed-on best approach to this technology for monitoring and mapping soil salinity and sand encroachment”. Problems regarding the image classification of features in these particular areas have been reported by several researchers, either with statistical or neural/connectionist algorithms for both fuzzy and hard classifications methods.

In this research, salt and sand features were assessed through both visual interpretation and automated classification approaches, employing historical and present Landsat imagery (from 1984 to 2015).

The decision tree analysis was chosen because of its high flexibility of input data range and type, the easiness of class extraction through non-parametric, multi-stage classification. It makes no *a priori* assumption on class distribution, unlike traditional statistical classifiers. The visual interpretation mapping of land cover and land use was undergone according to acknowledged standard nomenclature and methodology, such as CORINE land cover or AFRICOVER 2000, Global Land Cove 2000 etc. The automated one implies a decision tree (DT) classifier and an unsupervised classification applied to the principal components (PC) extracted from Knepper ratios composite in order to assess their validity for the change detection analysis. In the Tunisian study area, it was possible to conduct a thorough ground truth survey resulting in a record of 400 ground truth points containing several information layers (ground survey sheet information on various land components, photographs, reports in various file formats) stored within the a shareable standalone geodatabase. Spectral data were also acquired *in situ* using the handheld ASD FieldSpec 3 Jr. Full Range (350 – 2500 nm) spectroradiometer and samples were taken for X-ray diffraction analysis. The sampling sites were chosen on the basis of a geomorphological analysis, ancillary data and the previously interpreted land cover/land use map, specifically generated for this study employing Landsat 7 and 8 imagery. The spectral campaign has enabled the acquisition of spectral reflectance measurements of 34 points, of which 14 points for saline surfaces (9 samples); 10 points for sand encroachment areas (10 samples); 3 points for typical vegetation (halophyte and psammophyte) and 7 points for mixed surfaces.

Five of the eleven indices employed in the Decision Tree construction were constructed throughout the current study, among which we propose also a salinity index (SMI) for the extraction of highly saline areas. Their application have resulted in an accuracy of more than 80%. For the error estimation phase, the interpreted land cover/use map (both areas) and ground truth data (Oum Zessar area only) supported the results of the 1984 to 2014 salt – affected areas diachronic analysis

obtained through both automatic methods. Although IsoDATA classification maps applied to Knepper ratios Principal Component Analysis has proven its good potential as an approach of fast automated, user-independent classifier, accuracy assessment has shown that decision tree outstood it and was proven to have a substantial advantage over the former. The employment of the Decision Tree classifier has proven to be more flexible and adequate for the extraction of highly and moderately saline areas and major land cover types, as it allows multi-source information and higher user control, with an accuracy of more than 80%.

Integrating results with ancillary spatial data, we could argue driving forces, anthropic vs natural, as well as source areas, and understand and estimate the metrics of desertification processes. In the Biskra area (Algeria), results indicate that the expansion of irrigated farmland in the past three decades contributes to an ongoing secondary salinization of soils, with an increase of over 75%. In the Oum Zessar area (Tunisia), there was substantial change in several landscape components in the last decades, related to increased anthropic pressure and settlement, agricultural policies and national development strategies. One of the most concerning aspects is the expansion of sand encroached areas over the last three decades of around 27%.

Acknowledgements

I wish to express my utmost appreciation and gratitude to my supervisors Prof Giorgio Ghiglieri and Dr. Maria Teresa Melis for their invaluable guidance and confidence and especially for their patience throughout this period of three years of both instructive and exploratory thrilling experiences. Sincere thanks goes to Prof. Giorgio Ghiglieri for offering me the opportunity of starting and building my research in a constructive, multi-national cooperation and multi-disciplinary yet familial environment, as well as the privilege to be enriched intellectually and culturally throughout the various research-related expeditions. Moreover, I sincerely thank Dr. Maria Teresa Melis for setting the basis and giving me invaluable support, guidance and expertise in remote sensing and well as modern scientific views, providing an effective research environment with a commitment beyond professorship. Words cannot be enough to express the gratitude and feelings that gathered throughout these years, not even the ones you have heard so often: *Scusami, Titi, per il ritardo,...ti ringrazio per la comprensione!* ...thank you prof. Ghiglieri, thank you Titi for all that you have done for all of us, young researchers of the TeleGIS laboratory, but also students all across the faculty...the Red TeleGIS office is of reference to us all.
I am deeply thankful to the NRD Centre (*Nucleo Ricerca Desertificazione*) of the University of Sassari and the WADIS-MAR project for the possibility of conducting the current research. High appreciation and gratitude go to Prof. Giuseppe Enne, Prof. Pier Paolo Roggero and Prof. Luciano Gutierez for the support and the opportunities they have given me in participating in this project. Special thanks go to the NRD colleagues and fellows for all their support, collaboration and friendship, among which Alberto Carletti, Oumelkheir Belkheir, Ileana Ioccola, Nadia Maio, Alessandra Paulotto, Anna Paola Dessena...

I would like to express my appreciation to the TeleGIS Laboratory team of the University of Cagliari (Italy) for their invaluable support and to the researchers and professors of the Chemical and Geological Department of the University of Cagliari for their collaboration and support among which Prof. Antonio Funedda, Prof. Andrea Vacca and Prof. Alfredo Loi. Special thanks go to Prof. Franco Frau for his important support and expertise provided for the mineralogical analysis and X-ray diffraction.

To you, my dear friends and colleagues, Dr. Cristina Buttau and PhD student Claudio Arras, I owe much of my knowledge, research and I must say I could not have wished for better colleagues to share bad and wonderful moments, adventures in Tunisia...A chent'annus e attrus'annus di aici, picciochedusus!
To Sonia Cristina Aldana Martinez, with warmth and esteem...you were the missing link and the missing piece of the puzzle...
Sincere thanks to my TeleGIS Blu office colleagues, for your support, patience and frienship: Patrizia Fenza and Fabrizio Cocco.

I would also like to thank the Algerian and Tunisian WADIS-MAR partners, Institut Technique de Développement de l'Agronomie Saharienne, Biskra, Algeria (ITDAS) and Agence Nationale des Ressources Hydrauliques, Algeria (ANRH), Institut des Regions Arides (IRA, Ministry of Agriculture, Tunisia) and Observatoire du Sahara et du Sahel (OSS) for the provided data and collaboration.
Special thanks go to the Emorology Laboratory of IRA, for their hospitality, support and guidance throughout the undertaken research internship at IRA headquarters for the three fruitful and culturally enriching months. My utmost gratitude goes to Mr. Mohamed Ouessar, Mr. Kamel Nagaz, Mohamed Moussa, Mongi Ben Zaied, Dalel Ouerchefani, Hanen Dhaoui, Mohamen Labidah for their expertise and support during my research there and thereafter. Deep sincere gratitude are dedicated to the field survey group of technicians Ms. Amar Zerrim, Ms. Messaoud Guied, Amor Jlali for the both instructive and adventurous field campaign, for showing me the perfect combination of deep commitment for work and research with friendly, warm and joyful attitude.

Many thanks go to my IRA colleagues and friends: Hanen Jarray,Lazhar Atoui...
Baba Sy...
To Mr. Mohamed Talbi...
To Nabil Gasmi and his wife...
I wish to express my gratitude also to the Spatial Analysis Laboratory team of the University of Wollongong, Australia for their support provided during the undertaken research programme. Special thanks go to Dr. John Bradd, my Australian supervisor, more than a professor, more than a supervisor...a Friend...you have taught me how to teach myself and not only to learn... thank you for your trust, guidance and encouragements...I will not forget to keep my timetable updated... Thank you and your family for your warm, hearty hospitality and friendship...
Special thanks go to Prof. Alberto Marini for his guidance and support since my arrival in Sardinia, as an Erasmus student...thank you for the many opportunities and many doors you opened for me...thank you for making it possible for me to continue my studies here, thank you and your family for your support and friendship, for your hospitality...
Thanks go to the University of Iasi (Romania) professors and fellow colleagues which have set the scientific and academic background throughout the years of Bachelor and Master Studies which have consented me to cope with various challenges thereafter and to my goals go far.
My sincere esteem and gratitude to PhD. Lecturer Aurelian-Nicolae Roman from the University of Iasi for acquainting me to Remote Sensing in such a dedicated and lively manner that it became my passion, beyond work...for all the support and shove to go beyond my horizons, without which I would not be here now...Iti multumesc, Nae!
My father, for all his support and love throughout these years, which words cannot describe...my dear most beloved mother: Sărut-mâinile vouă, mamă și tată!...Mioara and Juan Mari, who gave me parent-like support throughout these years, supporting me in my ambitions...to my cousin Ramon, for his brotherly affection and support...to my whole family...To my beautiful country who gave birth to my passion for geography and the love for culture and tradition...Romania...
To Sardinia, my second home, for giving me a second family...My sincere and hearty gratitude to the Pistis family for all their support and affection...
Last but not least, to Marco, for the intellectual and moral support, for the life you have given me, for being You...please receive my greatest esteem and gratefulness...the rest is beyond words...

Dedicated to my mother

to my father

to Marco

...to you

...a vous

...para vos

...dumneavoastră

...a Lei

...a fustei

Table of Contents

1. CHAPTER ONE: Introduction

1.1. Research Background

In fragile ecosystems of arid and semiarid lands, climatic variations, water scarcity and human pressure accelerate ongoing degradation of natural resources. The main impact that results from the interaction between climatic and ecologically unbalanced human interventions is often summarised as desertification. The increasing water demand induced by the increasing social and economic development, needs sustainable and efficient water and soil management. Land degradation, a form of desertification, (e.g. soil degradation, productivity loss and accelerated erosion, the reduction of the quantity and diversity of natural vegetation) is widely spread in these environments. North Africa arid land of Maghreb suffers under scarce water conditions. Erratic behaviour of rainfall events over brief intervals often produces short and intense flood events along ephemeral *wadi* beds. Most part of the available surface waters is thus lost, providing limited benefits for households living in villages of such semi-desert areas. In this research we focus on two study areas in Algeria and Tunisia, characterised by an arid and semiarid climate, where sustainable development requires the understanding of the aforementioned dynamics as it withstands monitoring of desertification processes. As agriculture and animal husbandry are the two main economic activities in these areas, demand and pressure on natural resources increase in order to cope with increasing population's needs.

The PhD research is inserted in and partly supported by WADIS-MAR, one of the five Demonstration Projects implemented in the framework of the Regional Programme "Sustainable Water Integrated Management (SWIM)", funded by the European Commission. The project aims to contribute to the effective implementation and extensive dissemination of sustainable water management policies and practices in the Southern Mediterranean Region. It has been designed in the context of increasing water scarcity, combined pressures on water resources from a wide range of users, desertification processes and climate change impacts. The overall objective of the WADIS-MAR project is the realization of an integrated water harvesting and aquifer recharge techniques in two watersheds in the Maghreb Region, Oued Biskra in Algeria and Oum Zessar in Tunisia, characterized by water scarcity, overexploitation of groundwater resources and high vulnerability to climate change risk. It addresses the overall objective of Sustainable Water Integrated Management (SWIM) Programme - Component B which is "to actively promote the

extensive dissemination of sustainable water management policies and practices in the region in the context of increasing water scarcity, combined pressure on water resources from a wide range of users and ongoing desertification processes in connection with climate change", and specifically Lot 2 – point 1, "Water and Climate Change" which priority is "adapting to climate change and enhancing drought and flood management" giving particular attention to the water-agriculture-food-environment link.

Taking into account also past local traditional experiences, the project focuses on the implementation of a sustainable water and agriculture management system based on a participative and bottom-up approach as to enable local communities to manage groundwater resources, starting from a more efficient use of water harvesting techniques (WHT) and from a sustainable agricultural practices application. The project also involves regional, national, local institutions and associations to:

- safeguard and promote "soft" modern intervention on traditional systems
- enhance inter-sectorial coordination and regional cooperation
- increase capacity building
- create an enabling technical, policy and institutional environment for the promotion of a sustainable water and agriculture management model.

WADIS-MAR is coordinated by Prof. Giorgio Ghiglieri whereas the leading institution is NRD-UNISS Desertification Research Group of the University of Sassari (Italy). The partnership is composed of the UB University of Barcellona (Spain, as European partner 1) and two national organizations of North Africa countries: IRA, *Institut des Régions Arides* (Partner 3) of Tunisia and ANRH, *Agence Nationale des Ressources Hydrauliques* (Partner 4) of Algeria. The international organization OSS, *Observatorie du Sahara et du Sahel* (Partner 2) complete the consortia. The project is also supported by other local associations and organizations such as local NGOs and institutions (CRSTRA- Centre for Scientific and Technical Research on Arid Regions of Biskra, DGRE - General Direction of Water Resources in Tunisia).

Some phases of the project and of the current PhD research have been undergone in collaboration with several groups of researchers and professors of the Chemical and Geological Department of the University of Cagliari:

- Geological analysis and geological conceptual model: Dr. Cristina Buttau, Prof. Antonio Funedda, PhD student Claudio Arras and Dr. Maria Teresa Melis
- X-ray diffraction analysis: Prof. Franco Frau

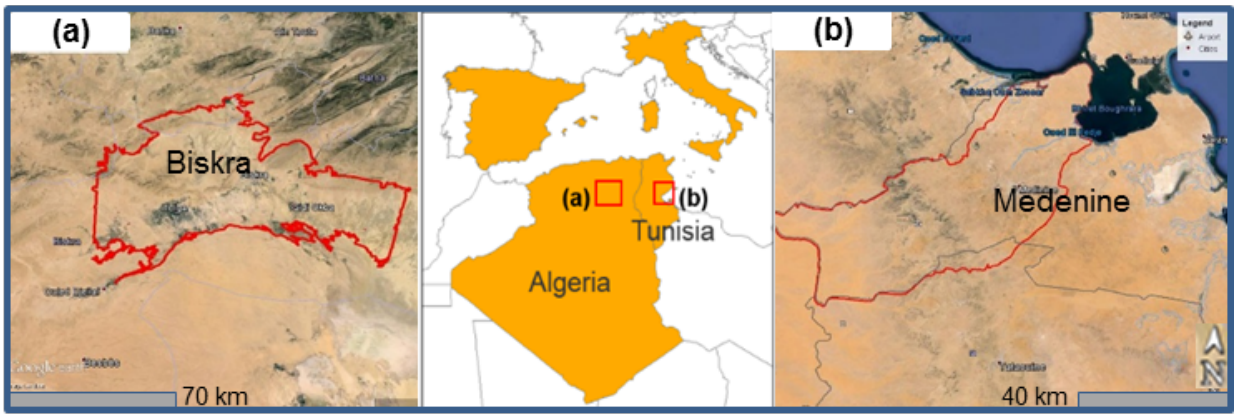

Figure 1. Study areas: Biskra, Algeria (a) and Oum Zessar, Tunisia (b). The WADIS-MAR partners are highlighted in orange

In the two study areas of the WADIS-MAR project, two of the strong local interests are the phenomena of soil salinization and sand encroachment, which are typical of arid and semiarid climatic regions and particularly felt by local communities as a limitations for agriculture. The understanding of the dynamics related to these phenomena is strongly connected to the knowledge of the physical-economical context, particularly the geologic setting in the broadest sense. Therefore the assessment of these dynamics rely also on the availability of spatial data and thematic maps on one hand and the anthropic related features, namely land use and management or modifications of the territory that can have a certain impact (water harvesting techniques, *Jessour*, *tabias* etc), on the other hand.

In the area of Oued Biskra in Algeria and Oum Zessar in Tunisia land cover and geological data are not available with the thematic and spatial detail necessary for the planning of interventions and therefore remotely sensed data were acquired intended for the preparation of maps of the evolution over time of main land cover classes and specific features of interest chosen as indicators of desertification. Therefore, as a first phase, salt and sand features were assessed through both visual interpretation and automated classification approaches, employing historical and present Landsat imagery (from 1984 to 2015). The visual interpretation mapping of land cover and land use was undergone according to acknowledged standard nomenclature and methodology, such as CORINE

land cover or AFRICOVER 2000, Global Land Cove 2000 etc, as presented in section 4.3 of Chapter 4 *Methodology and Data*.

In the last decade, satellite remote sensing has been proven a useful tool for multi-temporal analysis through detection and evaluation of desertification indicating features for decision support (Abbas, Khan et al. , Allbed and Kumar). Problems regarding the image classification of features such as sand and salt features in these particular areas have been reported by several researchers, either with statistical or neural/connectionist algorithms for both fuzzy and hard classifications methods. (Pal and Mather 2003, Khan, Rastoskuev et al. 2005, Fares and Philip 2008, Farifteh, van der Meer et al. 2008, Elnaggar and Noller 2010, Ouerchefani, Dhaou et al. 2013, Afrasinei, Melis et al. 2015). Therefore, two different automated classification schemes are proposed in this study: 1) a decision tree analysis (DTA) (Matthew 2012, Srimani and Prasad 2012), (Elnaggar and Noller 2010) and 2) unsupervised IsoData classification applied to Principal Component Analysis (PCA) of Knepper ratios.

In the Oum Zessar study area, the classification methods, either visual or automatic, are supported by a thorough, systematic ground truth (GT) campaign, but in the Biskra area, this was difficult to achieve and available ancillary data were used throughout the study phases. In both areas' cases, the decision tree was built based on a previous spectral analysis and existing indices assessment and nonetheless, the construction of new ones according to current purpose. Five of the eleven indices employed in the Decision Tree construction were constructed throughout the current study, among which we propose a salinity index (SMI) for the extraction of highly saline areas. The decision tree was constructed in such a manner that it fits both areas' of study needs, hence trying to solve the replicability issue mentioned earlier. Thirdly, the PCA was applied to Knepper ratios composite, as a support for the decision tree verification. The error assessment of the DTA resulting maps of the 2011 scene was calculated using the previously interpreted land cover map and the IsoDATA classified Knepper ratios' PC images.

Proximal sensing techniques were applied in this study: spectral field data and X-ray diffraction analysis were undergone for the estimation of quantitative and qualitative change of degradation – indicating features, namely soil salinization and sand encroachment.

The final objective of this study is the engagement of remote sensing tools in defining valid mapping methods for change detection of salt and sandy areas, respectively. Consequently, a

consistent number of scientific works (section 2.2. of Chapter 2 *Literature review*) have been reviewed for the current study (Kang, Yu et al. 2005, Bouaziz, Gloaguen et al. 2011, Avelar and Tokarczyk 2014, Fu, Gu et al. 2014) which reported issues regarding discrepancy of results and the degree of the replicability of algorithms or methods applied (Nutini, Boschetti et al. 2013) in similar context of study employing similar toos and satellite data type. We try to minimise these issues through the proposed aforementioned methodology and methods described in the following chapters and sections.

In the current chapter, in the following sections, the driving reasons and necessity of this study are argued, as well as the main and specific objectives and purpose of this research.

1.2. Rationale

Drought and desertification affect the arid watershed of Oued Biskra and Oum Zessar that are characterized by unfavourable climatological and hydrological conditions. Low and erratic rainfall results in frequent periods of serious drought alternating with episodes of floods that cause major damages and soil erosion. During the occasional floods, infiltration through beds of wadis is the major source of aquifer recharge. The wadis often carry large volumes of water during a flood but most of this water is lost. In addition to these climate constraints, in the last decades, other socio-economic changes are impacting on both environment and rural livelihood systems of these areas: the first is that many farmer and herdsman from mountains migrated to urban centres or Europe to seek employment and more income; the second is the enormous boom in the tourist sector which generated demand not only for labour but also for fresh vegetables and fruit; the third is the descent of sedentary farmers from the mountains into the plains that lead to a progressive abandonment of upstream areas and Jessour systems. These changes are causing:

- In the upstream area, a reduction of available water and an increasing of erosion because the traditional harvesting systems required an up-to-date maintenance;
- In the downstream area, an overexploitation of groundwater that needs to cope with increasing needs of rapidly expanding urbanization, as well as agricultural demands.

Ideally, if intermittent surface water floods are optimally managed they can help respond to the increasing demands for water in arid area. Moreover the use of aquifers to store water in arid regions eliminates the disadvantages associated with surface storage, such as evaporation, pollution, siltation, and health hazards (NRD 2011).

As a first requisite towards an efficient soil and water management and agricultural sustainability, regular monitoring of land features and environmental state is essential in order to have, for which a valid and replicable mapping method is indispensable.

The second requisite is mapping and multi – class environmental risks maps are required for a sustainable agriculture and modern management of arid lands in many parts of the world. However, in order to inventory and monitor a major land – degradation problem, such as soil salinization or sand encroachment over large areas, time – effective, less expensive and more efficient mapping techniques are needed, as opposed to conventional techniques.

In order to cope with these needs, in this research we propose the employment of remote sensing as mapping tool and two classification approaches, namely visual and automatic ones. We also considered necessary to support this analysis with ancillary data, indispensable in any similar study, field collected data as well as proximal sensing and X-ray diffraction analysis. The logical flow that conducted us into establishing our objectives and setting-up work phases also according to WADIS-MAR framework is summarised in figure 1.

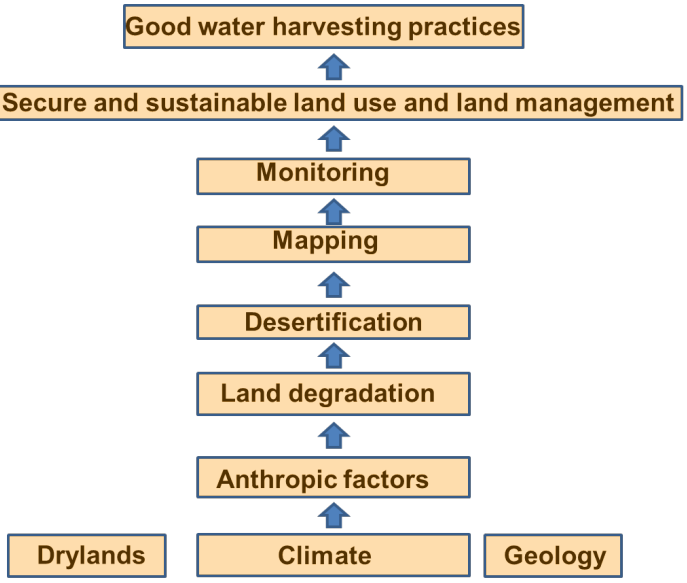

Figure 2. Rationale flow

Out of the various forms of land degradation, the Biskra area of Algeria and Oum Zessar area of Tunisia are interested primarily by soil salinization and sand encroachment, respectively (Fares and Philip 2008). In the first study area of Biskra in Algeria, soil salinization is the main menace for sustainable agriculture. In the second area, of Oum Zessar in Tunisia, sand encroachment represents

the main threat, followed by soil salinity is also taken into consideration for analysis in order to understand to which extent the secondary salinization occurs.

1.2.1. Biskra area and soil salinization

The Biskra region is a key agricultural region at national level with a high value on the international market of date production. Biskra area needs sustainable and efficient water and soil management, given the high risk of land degradation. This environmental issue is primarily related to natural climatic and bio – physical background and already scarce and fragile land and water resources. These processes are further accelerated by the increasing water and land resources demand induced by the growing social and economic development.

The identification and constant monitoring of the salt – affected areas in the semi – arid to arid environment of the *Wadi* Biskra area of Algeria is of major importance for stakeholders and end-users, being necessary for drafting and implementing rational and sustainable development policies of land resource management.

The geological information is essential to the understanding and analysis of salinity and salinization mechanism, enhancing the prediction accuracy (Elnaggar and Noller 2010). In the Biskra study area, the geological setting consists of mainly limestone, alluvial deposits and other sedimentary deposits with a strong component of evaporite minerals (mainly gypsum and halite). These geological characteristics give an *a priori* favourable background for the leaching and mobility of soluble salts, mainly Na chlorides and Ca sulphates (no sodic or alkaline soils issue) and their deposition in lower topographies. Secondary salinization mostly occurs in low – land areas, where groundwater frequently rises up through the soil profile through seepage. At a bigger scale, it must be mentioned also that soil salinity is not only influenced by the morphology of the soil profile but also by the soil physical, chemical and biological properties (Metternicht and Zinck 2008).

Added to this primary setting, the climatic conditions of high temperature, sporadic torrential rainfalls and an extremely high evapo-transpiration rate led to a secondary salinization, especially because it is corroborated with the continuous and intense irrigation with relatively saline water over extended areas. In the Biskra area of Algeria, documentation of vegetation and soil conditions are not available or do not have the necessary detail to sustain local or regional studies. Conventional mapping approaches either are excluded, because of insufficient or lack of

standardisation and repeatability of surveys, prohibitive costs, time consuming and deficient mapping quality in difficult or inaccessible terrain, or out of political context.

Through this research, we sought not only to identify and assess the spatial distribution and temporal variation of salt – affected areas but also to construct a valid workflow of an analysis targeted towards the qualitative and quantitative estimation of changes and deepening the understanding of the driving forces of this phenomena: natural *vs* anthropogenic or both and to what extent each has its contribution. This is done employing remote sensing data and techniques in a temporal analysis of the spatial distribution of salt – affected areas either inter-seasonal or inter-annual. Although ecosystem processes that have led to various forms of desertification have been widely studied, it is not clear how findings at patch scale in arid and semi – arid areas can be expanded to similar areas and at larger scales or vice – versa.

1.2.2. Oum Zessar area and sand encroachment

Sand encroachment is one of the most serious environmental problems in South Tunisia and previous research show that several irrational human activities have contributed to the intensification of this process, namely overgrazing, change in land use, from pasture to agriculture and other disturbances coming from inappropriate agricultural practices (Ouerchefani, Dhaou et al.). In the Oum Zessar study area, in Tunisia, the main desertification issues are related to sand accumulation due to rapid and extensive changes in land use and management, as pressure increased in recent years due to changes in socioeconomic policies. The effect of this issue has been an increasingly irrational use of natural resources, and as a consequence a state of severe degradation: accelerated expansion of rain fed and irrigated agriculture (specially olive trees and annual crops, cereals, respectively), significant change of agrarian system and land use and the development of multi sectors activities for income support (urbanization, services, migration etc.). Soil salinity comes second as land degradation process, since it is a primary salinity, yet to become secondary salinization and its spatial distribution is restricted to the coastal areas.

The studies conducted in the Southern Tunisia that approach the sand encroachment and salinization issue are limited to either local test sites or regional scale and results on driving forces and trends need more insight. This is also because of the difficult access to data or the lack of necessary detail in order to conduct a consistent study. Other studies related to aeolian transport argue that the aeolian sand transport and the dynamics of sand dunes (barkhans) in Southern Tunisia

are influenced by the predominant active winds (> 3 m/s), coming from the East, South East and North, thus inducing a movement towards Sahara and not the opposite (Khatelli and Gabriels 1998). However, there is an insignificant number of studies that approach in a comprehensive and valid manner the problem of the origin and dynamics of sand encroachment in this region of Jeffara Plain, which, among all, is a key agricultural area for the entire Southern Tunisia.

1.3. Research Objectives

The main purpose of this research is to illustrate and quantify the environmental degradation and risks associated with the salinization and sand encroachment processes in the two study areas of Algeria and Tunisia, respectively. The main objectives are to:

- Assess and design one single classification approaches that would accomplish the requirements for mapping both salinity and sand encroachment areas
- Detect changes of main land degradation indicators: land cover, land use, soil salinization and sand encroachment
- Obtain quantitative and qualitative information
- Driving forces and trends

The scope of this study was not only to map the land cover and soil conditions for a certain point in time but to construct a valid method in order to repeat this investigation in different stages or moments in time and different environmentally sensitive areas. We aim to achieve this throughout the design of a methodological approach employing remotely sensed data for automatic multi-temporal replicable mapping of salt-affected soils and sand encroachment in agricultural areas, hence change detection analysis.

For the representation and analysis integration, there was the need to have an overall knowledge of land cover/land use, geomorphology and spatial distribution of the saline soils and sand encroached areas. This was achieved through GIS data integration and analysis of pedology, geology, land cover, climate, hydrogeology information, either as continuous or discrete variables, prior to the processing of remotely sensed data such as satellite imagery or derivate products.

Remote sensing from space platforms offers alternative information sources which scientific community has already proven its potential in providing information on features used as indicators for land degradation assessment. Vegetation and soil are primary indicators: they give direct and

relatively fast feedback on any changes in physical and chemical regime of the subsequent ecological components and their interrelationships. These features are, to a certain extent, spectrally detectable.

A classification scheme based on decision tree is proposed in this study, as it is a nonparametric classifier (Matthew 2012, Srimani and Prasad 2012), allowing the user to define decision ruled based on ancillary, empirical data, spatial and spectral statistics. It has been reported as appropriate as it allows the use of different types of data, diminishing aforementioned spectral – related problems and promising high accuracy (Elnaggar and Noller 2010). After reviewing several remote sensing techniques reported as successful in delineating salt-affected areas and sand encroachment areas, respectively (Essifi, Ouessar et al. 2009, Wang, Yan et al. 2011, Allbed and Kumar 2013, Ouerchefani, Dhaou et al. 2013, Afrasinei, Melis et al. 2015), the results that emerged were not completely satisfactory and subsequent spectral analysis was undergone in order to choose optimal band operations for decision tree integration. The decision tree analysis was chosen because of its high flexibility of input data range and easiness of class extraction through multi-stage classification but at the same time because of its simplicity, being composed of "yes/no" decision nodes, which, according to a specified threshold, separates two classes from each node (Pal and Mather 2003, Rao, Chen et al. 2006, Elnaggar and Noller 2010, Hamid Reza and Majid Shadman 2012). Consequently, band ratios and indices (Khan, Rastoskuev et al. 2001, Allbed and Kumar 2013, Ouerchefani, Dhaou et al. 2013) have been derived in order to discriminate as accurate as possible the features of interest, in order to support decision rules used for a decision tree classifier scheme.

We thus concentrated our attention on the use of decision tree analysis and on spectral information extraction of salt mineralogy from Knepper ratios (Langford 2015). Both classification methods were supported by a thorough, systematic ground truth campaign in the Tunisian study area. In the Biskra area ground truth was restricted and therefore some processing and method evaluation phases were skipped for this area. Integrating the remote sensed data outputs in a GIS environment, valid scenarios were interpreted for the identification of driving forces and the estimation of metrics and trends of desertification processes. We also discuss the decrease of several key land cover classes areas in the favour of others. The key ones act as ecological indicators and delineate anthropic dynamics.

To summarise, the matrix of this research consists of several specific objectives:

- Review and design a customised methodological workflow according to the specific characteristics of the study areas, purpose and object
- To review and define the integration of remote and proximal sensing in diachronic studies of salt-affected and sand encroachment areas
- Generate valid land cover and land use base maps and define specific nomenclature
- Evaluate and design optimal automated mapping techniques according to purpose of study, environmental context and availability of data
- Assess and define appropriate spectral indices for the construction of a replicable decision tree classifier
- Detect, qualitatively and quantitatively estimate changes of the spatial and temporal distribution of main land degradation indicators: land cover, land use, soil salinization and sand encroachment
- Argue driving forces and trends
- Assess the accuracy of the results, highlight limitations and make recommendations

Since one of the most prevalent uses of remote sensing imagery is in change detection, in the following chapter a consistent number of works have been reviewed that discuss or use VNIR imagery in this scope and highlight that the results show a discrepancy in the accuracy assessment and the degree of the replicability of algorithms or methods applied (Nutini, Boschetti et al. 2013).

In the next chapters, the study sites are described briefly in terms of physical and socio – economic characteristics (Chapter three), then materials and data are presented which were used for the further preparation and processing (Chapter four), thus evaluating the classification method that best fitted the final purpose of this study: change detection (Chapter five). In the last chapter, the sixth, conclusions are conferred, as well as limitations and novelty of outcomes.

2. CHAPTER TWO: Literature Review

2.1. Land Degradation and Desertification

Land degradation and desertification are among the most serious environmental issues at global, regional, and local scales. Both are global processes that are especially active in arid, semi-arid, and dry sub-humid areas, and that have been enhanced in recent decades by factors including climatic variations and human activities. Indicators generally simplify reality to make complex processes quantifiable so that the information obtained can be communicated (Feranec and Otahel 2000).

Desertification is the persistent degradation of dryland ecosystems due to anthropogenic activities and variability in climate. The United Nations Conference on Environment and Development (UNCED) defines desertification as "land degradation in arid, semi-arid and dry sub-humid areas resulting from various factors, including climatic variations and human activities". Land degradation can occur everywhere, but it is defined as desertification when it occurs in the drylands. In these areas, scarcity of water limits the production of crops, forage, wood and other services that ecosystems provide to humans. Drylands are therefore highly vulnerable to increases in climatic variability and anthropogenic pressures.

Land degradation is known to reduce the physical, chemical, or biological quality of land and lowers its productive capacity. Climatic variations and increasing anthropic activity could increase the potential for land degradation, including loss of organic matter and nutrients, weakening of soil structure, decline in soil stability, thus causing an increase in soil erosion and salinization (Li, Ustin et al. 2009).

Common indicators of desertification include loss of biodiversity or declining habitat, loss of water-retention capacity, reduced soil fertility and increasing wind and water erosion (Bullock and Houerou 1995). The chief drivers of desertification include deforestation, overgrazing, over-cultivation, pressure of population, industrialization and poor land use practices. According to the MEA report, nearly 10–20% of drylands are already degraded, and ongoing desertification threatens many of the world's ecosystems, including those inhabited by some of the poorest human populations (D'Odorico, Bhattachan et al. 2013) (Dregne 2002). Droughts may trigger or accelerate desertification by reducing the growth of important plant species. The amount of precipitation

needed to sustain growth varies with the temperature, soil moisture capacity, and species. Therefore, desertification is one of the greatest environmental challenges today and a major barrier to meeting ecological and human needs especially in drylands. Adaptation to drought and desertification may rely on the development of diversified production systems, such as agroforestry techniques and ranching of animals better adapted to local conditions. However, adaptation also needs political, social, extension service, and educational inputs (Bullock and Houerou 1995).

In the current PhD study we address the processes related to land degradation and not soil degradation. It is important that a clear net distinction should be made between the two concepts. (Escadafal, Barbero-Sierra et al. 2015) highlights that in literature the concept of Land is defined as a multidimensional concept, including rocks, soils, and everything they carry (vegetation, animals, water bodies, infrastructures, landscape, and time), including environmental change driven by human interferences. Soils on the other hand are considered part of land, mainly comprehended in biophysical terms through their vertical dimension (depth).

(Escadafal, Barbero-Sierra et al. 2015) argues that a focus on land is approaching the issue of degradation and sustainability at the landscape level, whereas studying soil degradation will usually imply a more local and focused analysis. He continues by emphasizing that land and soil are intrinsically bound to each other, thus they cannot be regarded independently from the scientific perspective. He gives the example of land degradation caused by the removal of vegetation that can have far reaching consequences on soils and soil degradation, which usually impact the landscape level. He emphasizes that the keyword ‘land’ shows additional connections with sociology, anthropology, economics, public administration, business, and even mathematics. The keyword ‘soil’ has unique links with applied microbiology, biotechnology, optics, and even astronomy. Through his analysis, he concludes that a clear trend is observed: ‘land’ is associated more with disciplines of the domain of social sciences, whereas ‘soil’ has more connections with natural or physical science usually known as ‘hard sciences’ (Escadafal, Barbero-Sierra et al. 2015).

2.1.1. Salinity and Salinization

Soil salinity is in the first instance a natural feature, while soil salinization is mainly a human – induced process. Soil salinity is an environmental hazard, but soil salinization is a form of land degradation that potentially leads to desertification. It is a worldwide environmental issue that adversely affects plant growth, crop production, soil and water quality (Gorji, Tanik et al. 2015,

Scudiero, Skaggs et al. 2015). It is estimated that more than half of the irrigated land in arid and semiarid regions of the world is affected to some degree by salinization and that millions of hectares of agricultural land have been abandoned because of salinity build-up (Masoud and Koike , Fares and Philip , Elnaggar and Noller). The global extent of primary salt-affected soils is about 955 M ha, while secondary salinization affects some 77 M ha, with 58% of these in irrigated areas. Nearly 20% of all irrigated land is salt-affected, and this proportion tends to increase in spite of considerable efforts dedicated to land reclamation. (Metternicht and Zinck 2003).

However, FAO reports that salt-affected soils occur in all continents and under almost all climatic conditions and that their distribution, however, is relatively more extensive in the arid and semiarid regions compared to the humid regions. The nature and properties of these soils are also diverse such that they require specific approaches for their reclamation and management to maintain their long term productivity. For any long-term solutions, it is, therefore, necessary to understand the mode of origin of salt-affected soils and to classify them, keeping in view the physical-chemical characteristics, processes leading to their formation and the likely approaches for their reclamation and successful management (FAO 1999).

Salt is often derived from geological formations featuring shale, marl, limestone, sylvite, gypsum, and halite. Variability of soil salinity is affected by parent material, soil type, and landscape position (van der Meer, van der Werff et al. 2012). Salinization is characterised by its development in both time and space due to accumulation of soluble salts of sodium, magnesium and calcium in soils and it usually happens in poorly drained land under semiarid and arid climates where large quantities of salt have been leached from higher areas in the drainage basins (Metternicht and Zinck 2008, Abbas, Khan et al. 2013). Leached salts from higher areas concentrate in slow – flowing drainage basins groundwater, can be transported to the soil surface by capillary action (seepage) from brackish water tables and accumulated due to evaporation (Fares and Philip). They can also accumulate as a result of anthropogenic activities such as fertilization or oil production.

FAO asserts that the presence of excess salts on the soil surface and in the root zone characterizes all saline soils. During the process of chemical weathering, which involves hydrolysis, hydration, solution, oxidation, carbonation, and other processes, the salt constituents are gradually released and made soluble. The released salts are transported away from their source of origin through surface or groundwater streams. The salts in the groundwater stream are gradually concentrated as the water with dissolved salts moves from the more humid to the less humid and relatively arid areas. The

predominant ions near the site of weathering in the presence of carbon dioxide will be carbonates and hydrogen-carbonates of calcium, magnesium, potassium and sodium; their concentrations, however, are low. As the water with dissolved solutes moves from the more humid to the arid regions, the salts are concentrated and the concentration may become high enough to result in precipitation of salts of low solubility. Apart from the precipitation, the chemical constituents of water may undergo further changes through processes of exchange, adsorption, differential mobility, etc., and the net result of these processes invariably is to increase the concentration in respect of chloride and sodium ions in the underground water and in the soils (FAO 1999).

2.1.2. Sand Encroachment

As a form of land degradation through wind erosion, mainly reflecting excessive human activities and climate change in arid, semi-arid, and part of sub-humid region (UNCCD 2004), sand desertification has become worrying in the last decades especially in prone arid and semi-arid areas (Afrasinei, Melis et al. 2015, Ge, Dong et al. 2016). The main form of sandy desertification in the desert is the evolution of anchored dunes into semi-anchored and mobile dunes, and the main form of reversal is the evolution of mobile dunes into semi-anchored and anchored dunes. Given the fragile natural environment and hydrothermal sensitivity of the desert, the historical and modern sandy desertification processes have received considerable attention over the past several decades. Sandy desertification in arid and semi-arid regions are mainly presented as the degradation and recovery of vegetation, and is closely associated with regional aeolian activities. Previous studies have also suggested that aeolian activities are important in the development of the aeolian morphology and regional ecological environment (Wang, Wang et al. 2013, Duan, Wang et al. 2014, Li, Zhao et al. 2016)

Understanding landscape changes is regarded as one of the key steps in revealing the processes and mechanisms of sandy desertification (Hirche, Salamani et al. 2011). Some researchers claim that landscape fragmentation resulting from human reclamation and grazing activities could destroy the integrity of vegetation cover and land cover changes could create higher opportunities for soil exposure to wind which contributed to land degradation and sandy desertification (Ge, Dong et al. 2016)

(Ge, Dong et al. 2016) reached the conclusion that landscape fragmentation may be related to the sandy desertification processes. Results indicated that grass land and arable land contributed the

most to landscape fragmentation processes in the regions adjacent to bare sand land during the period 1980 to 2010 (Ge, Dong et al. 2016).

2.2. Remote and proximal sensing approach

2.2.1. Proximal Sensing and Spectral Analysis

2.2.1.1. Spectral analysis

Spectral analysis may be undertaken using radiometric, spatial and spectral enhancement, analysis of horizontal and vertical spectral profiles, 2D scatter plots but also through comparison of in situ collected spectral signatures with existing spectral libraries, either software incorporated either web-based (e.g. SPECCHIO) (Melis, Afrasinei et al. 2013, Afrasinei, Melis et al. 2015, Afrasinei, Melis et al. 2015)

The band ratio is a simple technique that has been used for many years in remote sensing to display spectral variations effectively. It is based on highlighting the spectral differences that are unique to the materials being mapped. Identical surface materials can give different brightness values because of their physical and chemical characteristics, topographic slope and aspect, shadows, or seasonal changes in sunlight illumination angle and intensity. These variances affect the viewer's interpretations and may lead to misguided results. The band ratio images are known for enhancement of spectral contrasts among the bands considered in the ratio operation and have successfully been used in mapping of alteration zones (Mia and Fujimitsu 2012) (Langford 2015).

A review of the most known combinations of ratios for mapping hydrothermal altered mineral deposits is presented below. Ratios of 3/1, 5/7, 5/4 are known to be useful for iron oxides, hydroxyl bearing minerals, ferrous oxides identification, respectively. The Abrams ratio (5/7:3/2:4/5) Kaufmann ratio (7/4:4/3:5/7), Chica-Olma ratio (5/7:5/4:3/1) are successful in the identification of minerals containing iron ions, hydrothermal altered iron-oxide, clay minerals (and altered), hydroxyl minerals or vegetated zones, ferrous oxide (Mia and Fujimitsu 2012).

Knepper (1989) proposed specific band ratios for the delineation of hydroxyl – bearing minerals, hydrated sulphates and carbonates, vegetation and iron oxides and hydroxides, namely the 5/7:3/1:3/4 red-green-blue (RGB) combination, used mainly for geological remote sensing mapping (Langford 2015).

Starting from band operations, indices of various types have been successfully used due to their simplicity and applicability. A number of researchers have developed different salinity indices such as Normalized Difference Salinity Index (NDSI) or the Salinity Index (SI), several vegetation indices (VIs) such as Normalized Differential Vegetation Index (NDVI) and Soil Adjusted Vegetation Index (SAVI), water/wetness indices etc. which have been used as indirect indicators assess and map soil salinity (Mulder, de Bruin et al. 2011, Allbed and Kumar 2013, Allbed, Kumar et al. 2014).

Another method of spectral analysis is the Principal Components Analysis (PCA), which uses the principal components transformation technique for reducing dimensionality of correlated multispectral data. The analysis is based on multivariate statistical technique that selects uncorrelated linear combinations (eigenvector loadings) of variables in such a way that each successively extracted linear combination, or principal component (PC), has a smaller variance (2013). The statistical variance in multispectral images is related to the spectral response of various surficial materials such as rocks, soils, and vegetation, and it is also influenced by the statistical dimensionality of the image data. Eigenvector loadings (eigenvalues) give information using magnitude and sign of about which spectral properties of vegetation, rocks and soils are responsible for the statistical variance mapped into each PC (Metternicht and Zinck 2003, Mia and Fujimitsu 2012, van der Meer, van der Werff et al. 2012).

Spectral transformation can reduce multi-spectral data volume with minimal information loss and generate a new image, which loads main information of original data. It is an effective technique in improving classification accuracy and change. (Haijiang, Chenghu et al. 2008).

The Tasseled Cap transformation, also called as K-T transformation and originally applied to the Landsat Multispectral Scanner (MSS) data, is a principal component analysis technique, which linearly transforms multi-spectral data and creates 3 uncorrelated bands: Brightness (B), Greenness (G) and Wetness (W). The Tasseled Cap transformation is scene independent and has fixed coefficients, and therefore the multi-date TM, ETM+ and OLI data can be transformed through this technique and the results are comparable over time. The BGW bands are directly related to specific physical attributes and can be easily interpreted. Brightness was interpreted as change in total reflectance or albedo at the surface, and is mainly driven by soil reflectance variations; Greenness

measures the contrast between visible bands and near infrared band, and has a close correlation with vegetation coverage, just like the vegetation index; Wetness is sensitive to soil and plant moisture.

2.2.1.2. Proximal sensing

A spectral library is a collection of reflectance from the target object recorded using radiometers. With the advent of new generation sensors, like hyperspectral sensors, the importance and use of reflectance spectra of objects in Remote Sensing has increased manifold (Guo, Shi et al. 2013). As compared to multispectral sensors these sensors collect reflectance from objects simultaneously in hundreds of narrow adjacent spectral bands and thus due to their high spectral resolution, they are more efficient in discriminating soils, minerals, vegetations and manmade materials. In order to harness the full potential of Hyperspectral data, spectral library is a pre-requisite.

Consequently, many organizations across the globe are working on development of such libraries. The U. S. Geological Survey has developed a digital reflectance spectral library for 423 minerals, 17 plants and some miscellaneous materials (http://speclab.cr.usgs.gov/ spectral.lib04/spectral_lib.html). The Jet Propulsion Laboratory (JPL) spectral library includes spectra of 160 minerals in digital form (http://speclib.jpl.nasa.gov/ documents/jpl_desc). The ASTER spectral library is a compilation of over 2,400 spectra of natural and man made materials, which includes data from three other spectral libraries such as Johns Hopkins University (JHU) Spectral Library, JPL Spectral Library, and United States Geological Survey (USGS - Reston) Spectral Library (http://speclib.jpl.nasa.gov/). The spectrum database SPECCHIO (Spectral Input/Output) has been developed, that offers ready access to spectral data, modelled data, and existing spectral libraries. An extensive library of spectra (n=1,336) for coastal wetland communities, across a range of biocli- matic, edaphic, and disturbance conditions were developed and used to classify and delineate vegetation at different location (Zomer et al. 2008) (Afrasinei, Melis et al. 2015). Thermal infrared spectra minerals, rocks, soils, etc. have been developed by Mars Space Flight Facility at Arizona StateUniversity (http://speclib.asu.edu/). Besides, spectral databases have been developed for specific case studies related to soil and vegetations. A spectral library for 83 species that includes tropical crops and trees used for agroforestry, and manure samples (39) for the purpose of soil and livestock management in tropical agro-ecosystems using near-infrared spectroscopy has been constructed (Shepherd et al. 2003). Similarly, a mid-IR reflectance spectral library of soil samples for cotton-growing re- gions of eastern Australia is also

available. A diverse library of over 1,000 archived topsoils from eastern and southern Africa was prepared for the assessment and management of risk in soil evaluations in agricultural, environmental, and engineering applications (Shepherd and Walsh 2002). The development of plant spectral libraries has not previously succeeded be- cause of the large number of potential plant species that are required to characterize a terrestrial vegetation library. In addition, there has been no resolution on how to characterize the spectral variability expressed in changing phenological states and environmental conditions. Crop-specific spectral library for three important varieties of each of rice, chilly, sugar cane, and cotton crops in Andhra Pradesh state of India is also available (Rao 2008) (Rao, Chen et al. 2006). However, such information on forest species is not yet available. Traditionally, the information for forest resource management was produced using field surveys, which are very tedious and time consuming. With the advent of digital remote sensing using multispectral images the situation improved, whereby a large area could be monitored in less time and with less effort. However, these images could only broadly classify the forest cover (Martin et al. 1998) and provide little information on the biochemical characteristics of species. The presence of more number of bands covering wide range of spectrum in the hyperspectral sensors make them efficient in studying biochemical and structural properties of plants (Underwood et al. 2003), wherein a spectral library of forest species would be of great help. Developing spectral library is key to improve our capacity to utilize the full mapping potential from new sources of data provided by airborne and advanced space borne hyperspectral imagers (Zomer et al. 2008).

2.2.2. Landsat archive and Landsat 8

Since the project's inception in 1965, the Landsat mission has stood at the forefront of space-based Earth observation and has been the trailblazer for remote sensing. Landsat 8 was launched on February 11, 2013 and orbits the entire Earth every 16 days in an 8-day offset from Landsat 7 satellites, providing this temporal coverage. Currently (2016), both Landsat 8 and Landsat 7 collect data, each following a near-polar, sun-synchronous orbit on the Worldwide Reference System (WRS-2). Most acquired scenes are downlinked to the Landsat Ground Network and made available for download within 24 hours of acquisition. Landsat Level 1 standard data products are processed to standard parameters, and distributed as scaled and calibrated digital numbers (DN). The DN’s can be scaled to calibrated absolute radiance or reflectance values using metadata distributed with the product (conversion algorithms for Landsat 1-7 and Landsat 8).

The collected data are orthorectified and available to download at no charge. Landsat 8 carries two different instruments: 1) the Operational Land Imager (OLI) sensor involves refined heritage bands and 2) the Thermal Infrared Sensor (TIRS) provides two thermal bands. Both sensors supply improved signal-to-noise (SNR) radiometric performance quantized over a 12-bit dynamic range. They provide 4096 potential gray levels in an image compared with only 256 gray level in the previous 8-bit instrument. Therefore, the improved signal to noise performance enables better characterization of land cover state and condition. The final products are delivered as 16-bit images scaled to 55,000 gray levels. Its additional reliability has already been proven in various studies (Roy, Wulder et al. 2014, Aldabaa, Weindorf et al. 2015).

Concerning metadata and data descriptions, Landsat metadata files contain information that can be useful in locating specific data files in the archive inventory, and is valuable to users in terms of certain product characteristics. Changes are occasionally made to the metadata files, in order to improve data quality and usability.

Calibration and validation are important aspects of any remote sensing system. The calibration of the Landsat sensors is supported by pre-flight, post launch-onboard, and ground reference data. Calibration parameter files are provided for all sensors below, along with notices that describe any changes that may have been made to the files and affect data products. Bias parameter files are also available for Landsat 8 satellite data products. Definitive Ephemeris is useful in the geometric correction of Landsat 4-5 Thematic Mapper and Landsat 7 data. Calibration validation is an ongoing quality check for the Landsat sensors, along with software research and development to enhance or improve the algorithms used to produce Level 1 products. Data quality measures are in place to inform users whether the integrity of Landsat data has been affected by anything from instrument artefacts to production software updates.

The Quality Assessment (QA) band is an important addition to Landsat 8 data files. Each pixel in the QA band contains integers that represent bit-packed combinations of surface, atmosphere, and sensor conditions that can affect the overall usefulness of a given pixel. Used effectively, QA bits improve the integrity of science investigations by indicating which pixels might be affected by instrument artefacts or subject to cloud contamination.

The Landsat data is also supplied with “Known Issues” information, which describe known artefacts that exist in the Landsat product. These artefacts vary widely between the MSS, TM,

ETM+ and OLI/TIRS sensors caused by specific sensor characteristics and anomalies identified after launch. Landsat data are systematic, geometric, radiometric, and terrain corrected to provide the highest quality data to the user communities. Occasionally, anomalies occur and artefacts are discovered that require research and monitoring. The Landsat Calibration and Validation (Cal/Val) team investigates and tracks anomalous data. Details about a number of anomalies that have been discovered and investigated can be found in the Landsat Known Issues information.

Most of the above information were extracted from the official USGS site: landsat.usgs.gov.

2.2.3. Classification methods

2.2.3.1. An Overview of Classification Methods

Remote sensing includes the interpretation of measured electromagnetic energy reflected from or emitted from a target. Sensors mounted on aircraft or satellite platforms record this electromagnetic radiation in digital form, which is then processed by a computer. Computer-processing applications range from the calibration of the data for the effects of such factors as the changing response of sensors over time to the identification of patterns in multi- and hyperspectral data that relate to ground features. Classification of satellite images is one of the most commonly applied techniques used to process remotely sensed data. Image classification is the process of creating a meaningful digital thematic map from an image data set. The classes shown on a map are derived either from known cover types or by algorithms that search the data for similar pixels. Once data values are known for the distinct cover types in the image, a computer algorithm can be used to divide or segment the image into regions that correspond to each cover type or class.

In remote sensing, choosing a classification approach, method or algorithm (image classifiers) must be made upon specific criteria that takes into account the aim, type and object of the study, feature to classify (associate each pixel to a class) and identify (relate classes to a known land cover/use), data dimension, computation requirements, time and costs etc. In our case, of a change detection thus multi-temporal study of land features (not clouds or aerosols etc), at a local-regional scale using Landsat series images, decision tree classification seems to be the optimal one.

Conscerning change detection, the semi-automatic change detection methodology described in (Aleksandrowicz, Turlej et al. 2014) was developed to deal with different very high spatial resolution images acquired over different European landscapes. The methodology is a fusion of

various change detection methods ranging from layer arithmetic, vegetation indices differentiating, texture calculation and methods based on canonical correlation analysis (multivariate alteration detection (MAD)). They used statistical thresholds in most of the processing steps, obtaining an overall change recognition accuracy of 89%. Moreover, several researchers have emphasized the importance of a polyvalent or hybrid methodological approach for mapping and detecting changes spatially and temporally with an increased accuracy (Nutini, Boschetti et al. 2013, Aleksandrowicz, Turlej et al. 2014, Olofsson, Foody et al. 2014, Zhu and Woodcock 2014).

Remote sensing data is a successful tool in mapping land features over large areas and it has proven its efficiency in certain circumstances, but the problem of spectrally similar features remain as it has been approached and discussed by several authors in different studies (Metternicht and Zinck 2003, Metternicht and Zinck 2008).

Traditionally, classification tasks are based on statistical methodologies such as Minimum Distance-to-Mean, Maximum Likelihood and Mahalanobis Distance Classification (Mather and Paul, 1987). The most used ones, like maximum likelihood classifier (MLC) are generally based on statistical parameters such as mean and standard deviation. These classifiers are generally characterized by an explicit underlying probability model and are ideally suited for data in which the distribution of the data within each of the classes can be assumed to follow a normal distribution in multispectral space. The performance of this type of classifier depends on how well the data match the pre-defined model (Srimani and Nanditha, 2010). If the data are complex in structure, then to model the data in an appropriate way can become a real problem. In order to overcome this problem, sophisticated statistical and neural/connectionist algorithms, Rule-based classifiers, image segmentation, expert classification, support vector machines for both fuzzy and hard classifications of data have been developed during the 30 years-lifetime of the remote sensing scientific community and are increasingly being used. (Pal 2012, Srimani and Prasad 2012, Richa Sharma 2013). Nonparametric classifiers have frequently been found to yield higher classification accuracies than parametric classifiers because of their ability to cope with non-normal distributions and intra-class variation found in a variety of spectral data sets (Rogan, Franklin et al. 2002, Pal and Mather 2003, Otukei and Blaschke 2010, Pal 2012).

Most of these techniques do not make any a priori assumption about the data distribution, hence are essentially non-parametric in nature. Decision Tree classification (DTC) is one such technique

which is very effective and useful for the remote sensing community for LULC classification. This is intuitive, simple, flexible, and efficient in computing non-normal, non-homogenous and noisy data as well as non-linear relation between features and classes, missing value, and both numeric and categorical inputs(Pal and Mather 2003). Decision tree classification techniques have been used successfully for a wide range of classification problems, but only recently been tested in detail by the remote sensing community(Pal and Mather 2003). Several studies have compared DTC methods with other classifiers. Otukei and Blaschke (2010) compared decision tree, maximum likelihood and support vector machine based techniques for land cover change assessment using Landsat TM and ETM+ data and found decision tree based methods performed better than others. Punia et al. (2011) used C5.0 based decision tree classifiers to classify IRS-P6 AWiFS data and reported very high accuracy (Richa Sharma 2013).

DTA may incorporate several environmental variables that significantly influence the development of soil salinity and not only the spectral properties of soil surface, for example, the use of surficial geology, terrain, and landform map layers (Farifteh 2007). Using this technique, Elnaggar and Noller (2010) reported that it could significantly enhance the productivity and accuracy of multi – class soil salinity mapping compared to conventional mapping methods especially in such remote inhospitable areas. Furthermore, they have concluded that vegetation indices did not have significant correlation with electro - conductivity values, but instead, the wetness ones did, as saline soils tend to retain high moisture content.

Even if decision tree algorithms have been shown to perform less well in higher dimensional feature spaces when compared to maximum likelihood classifier they still outperform it (Rogan, Franklin et al. 2008, Otukei and Blaschke 2010).

Decision tree classifiers can perform automatic feature selection and complexity reduction, while the tree structure gives easily understandable and interpretable information regarding the predictive or generalization ability of the data. DTC computational time is minimal. (Srimani and Prasad 2012) applied some of the popular machine learning Decision tree classifiers and results have shown that it could provide accurate and efficient methodology for classification of Land use and Land cover mapping by using remote sensing data.

The advantages that decision trees offer include an ability to handle data measured on different scales, lack of any assumptions concerning the frequency distributions of the data in each of the

classes, flexibility, and ability to handle non-linear relationships between features and classes (Pal and Mather 2003). In contrast to neural networks, decision trees can be trained quickly, and are rapid in execution. They can be used for feature selection/reduction as well as for classification purposes. Finally, the analyst can interpret a decision tree, it has significant intuitive appeal because the classification structure is explicit and easily interpretable. It is not a 'black box', like the neural network, the hidden workings of which are concealed from view (Pal and Mather 2003) (Rao, Chen et al. 2006).

2.2.3.2. Salinity mapping

Soil salinity is generally measured via electrical conductivity (EC) in soil saturated paste (ECp), its liquid extract (Becerril-Piña, Mastachi-Loza et al.), or using different soil to water suspensions. Soil with an ECe N 4dSm−1 is referred to as saline (Metternicht and Zinck 2008). Plant tolerance of salinity is species specific, but values N4dSm−1 constrain the growth of many agronomic crops. However, cost and time efficient tools are necessary for a regular monitoring of soil salinity as it is essential for efficient soil and water management and sustainability of agricultural lands (Metternicht and Zinck 2003), especially in arid and semiarid environments.

Detecting and mapping features in saline environments with remotely sensed imagery has been successful through the use of both multispectral and hyperspectral imagery (Kang, Yu et al. 2005) (Allbed, Kumar et al. 2014). Approaches include artificial neural network, classification and regression tree, fuzzy logic generalized Bayesian analysis, geostatistics, etc (Metternicht and Zinck 2003). Yet the limitations to both image types maintain "no agreed-on best approach to this technology for monitoring and mapping soil salinity" (Allbed and Kumar, 2013). Researchers are hesitant to use multispectral imagery for salinity mapping since low spatial resolution can cause pixel misclassification (R.L. Dehaan 2002) (Allbed and Kumar, 2013). Due to significantly higher resolution and more bands acquired by hyperspectral imagery, better quantitative analysis can be performed for saline soil identification (R.L. Dehaan 2002). Undeterred by its shortcomings, multispectral imagery has been stated in the literature to be a "preferred method for mapping and monitoring soil salinity" (R.L. Dehaan 2002, Allbed and Kumar 2013). Furthermore, multispectral data such as that captured by Landsat satellites are much more accessible and affordable (free downloads are available from the USGS EE) than hyperspectral images. Imagery acquired from Landsat TM has been successfully interpreted for soil salinity and soil type identification studies,

and is the most common type of imagery cited throughout numerous publications (Elnaggar and Noller 2010). To account for data limitations and accuracy, literature suggests additional ancillary data inputs such as field data, geographic information systems (GIS), and digital elevation models (DEM) with multispectral images (Sah et al., 1995; Eklund et al., 1998; Metternick and Zinck, 2003; Allbed and Kumar, 2013). In addition to this, researchers also emphasize the effectiveness of a conceptual framework of a method where the data obtained from optical remote sensing sensors are integrated with the results of simulation models or geophysical survey, or both, in order not only to predict different levels (low, moderate, severe) of salinization/alkalinisation in a cost-attractive and efficient way, but also to track down the salinization as a pedogenic process (Farifteh, Farshad et al. 2006, Farifteh 2007, Farifteh, Van der Meer et al. 2007, Farifteh, van der Meer et al. 2008). Other researchers propose field and laboratory methods (soil sampling and various measurements) in order to extract useful information on salt – affected soils (such as saturation percentage, pH and EC values etc.) (Farifteh, van der Meer et al. 2008). This information, corroborated with vegetation indices, transformation operations (e.g. Tassel Cap) and band ratios, have the potential of a preliminary distinction between the main classes.

Salinity can be also identified indirectly throughout other land components, such as vegetation, which is the first one to give the first input on the health state of a land. Changes in the reflectance, composition and morphology of a single leaf can be used to detect salinity effects at an early stage. Authors noted that visible reflectance of leaves from plants growing on salt-affected soils is lower than reflectance of non-salt-affected leaves before plant maturation and higher after; near-infrared reflectance increases without water stress due to a succulent (cell thickening) effect and increases in other cases (Escadafal and Pouget 1985, Anna, Megan et al. 2008, Eyal, Graciela et al. 2008).

Bands in the near- and middle-infrared spectral bands give information on soil moisture and salinity (Melis, Afrasinei et al. 2013, Afrasinei, Melis et al. 2015). Near- to middle-infrared indices are indicators for chlorosis in stressed crops (normalized difference for Thematic Mapper bands 4 and 5). This ratio is immune to colour variations and provides an indication of leaf water potential. Biophysical response to a salty environment is manifested in low fractional vegetation cover, low leaf-area index (LAI), high albedo, low surface roughness and high surface resistance compared with healthy crops (Metternicht and Zinck 2003).

Salinized and cropped areas can also be identified with a salinity index based on greenness and brightness that indicates leaf moisture influenced by salinity, with classical false-colour composites of separated bands or with a computer-assisted land-surface classification (Metternicht and Zinck 2008, Allbed, Kumar et al. 2014, Gorji, Tanik et al. 2015). A brightness index detects brightness appearing at high levels of salinity. The contribution of false-colour composites and visual interpretations is demonstrated in various studies. Geomorphological patterns are helpful in distinguishing salinization.

2.2.3.3. Sand encroachment mapping

Aeolian desertification is one of the most devastating environmental and socio-economic problems in arid, semi-arid and dry semi-humid climate zones (Wang, Wang et al. 2013. Aeolian desertification destroys land resources, reduces ecosystem productivity, depresses ecosystem services and exacerbates poverty (Duan, 2014 #2043). Multi-temporal remote sensing data provide an opportunity to extract spatio-temporal information on aeolian desertification (Afrasinei, Melis et al. 2015). In particular, multi-spectral satellite sensors, such as Landsat MSS, TM and ETM+, are important tools for land desertification monitoring, at the regional scale. At the same time, since the strip noises of the Landsat 7 satellite and the retirement of Landsat 5 satellite in recent years, for the purpose of extending the Landsat record into the future and maintaining continuity of observations, the satellite Landsat 8 alternatives have successfully been launched in 2013 which is very important for global change research (Roy, Wulder et al. 2014).

In south –eastern Tunisia, the main desertification issues are of anthropic origin, as pressure increased in recent years due to changes in socio-economic policies (Schiettecatte, Ouessar et al. 2005, Ouessar 2007, Ouessar 2010, Sghaier, Ouessar et al. 2010, Afrasinei, Melis et al. 2015). Sand encroachment is one of the most serious environmental problems in central and south Tunisia and previous research show that several unwary human activities have contributed to the intensification of this process, namely overgrazing, change in land use, from pasture to agriculture and other disturbances coming from inappropriate agricultural practices (Ouerchefani, Dhaou et al. 2013). The studies conducted in the south-eastern Tunisia that approach the sand encroachment and salinization issues (Dalel Ouerchefani 2008, Essifi, Ouessar et al. 2009, Ouerchefani 2012, Lorenz, Gasmi et al. 2013) are limited to either local test sites or regional scale and results on driving forces

and trends need more insight. The contributing factors are reported as being mainly of anthropogenic nature and not mostly of natural, windborne one, with the Grand Oriental Erg is the source area. In this sense, studies argue that the aeolian sand transport in Southern Tunisia is influenced by the predominant active winds (u > 3 m^{-1}), coming from the East, South-East and North, thus inducing a movement towards Sahara and not the opposite (Khatelli and Gabriels 1998, Khatelli and Gabriels 2000), but the results need further validation. The studies conducted in the Southern Tunisia that approach the sand encroachment and salinization issue are limited to either local test sites or regional scale and results on driving forces and trends need more insight. This is also because of the difficult access to data or the lack of necessary detail in order to conduct a consistent study. However, Ouerchefani et al. have combined Geographic Information System (GIS) and remote sensing for a 31 years analysis of sand encroachment phenomenon in the area of Oglet Merteba of about 20 000 ha, north of Matmata, in Southern Tunisia (Ouerchefani, Dhaou et al.). They concluded that over the last decade this phenomenon has intensified, with a more aggressive period in 2006 and with newly affected areas located in the central plain zone. The contributing factors were reported as being mainly of anthropogenic nature. Other studies related to aeolian transport argue that the aeolian sand transport and the dynamics of sand dunes (barkhans) in Southern Tunisia are influenced by the predominant active winds (u > 3 m1), coming from the East, South East and North, thus inducing a movement towards Sahara and not the opposite (Khatelli and Gabriels 1998).

(Ouerchefani 2012) emphasizes in her PhD dissertation that in the classic literature, several studies have focused on the study of wind erosion (The Houérou 1969; Mainguet 1978; Khatteli, 1981 and Floret Pontanier 1982; Chahbani Kardous 1992 and 2005), in which several authors associate a type of wind deposition (defined as aeolian formations: barkhane, Nebka etc .) to a sedimentary processes (deflation, transport or deposition) without relying on precise experimental measures to demonstrate the reliability of these aeolian indicators of deflation, transit or deposit. From a methodological point of view, conventional methods using data point of land and old aerial photographs do not allow to have a real synoptic view of the problem and its consequences. She highlights also the importance of remote sensing, due to its applicability in constant monitoring due to accessibility, repetitiveness and spatial coverage. In addition, the Geographical Information Systems represent an essential tool for coping with large volumes of spatial different entities and

multisource types of data. GIS has become indispensable as it offers users the possibility of processing manipulation and storage capacity of large volumes of data (Ouerchefani 2012).

3. CHAPTER THREE: Study Areas

3.1. Biskra area

3.1.1. Physio-Geographical Description

The study site is located in north-eastern Algeria, in the north of the great Chotts of Melrhir and Felrhir, and covers an area of about 5000 km^2 (figure 1). It mainly overlaps the piedmont area that passes from the Aures mountainous and hilly domain in the North to the Sahara plain in the South, with fine-clayey deposits and vast alluvial fans and small mountain ranges in the middle - slope area.

Morphologically, it presents a piedmont area, passing from a hilly relief in the Northern part to gross deposits at the foot slope to fine-clayey deposits to the South, with vast alluvial fans and small mountain ranges in the middle - slope area. To the East, the landscape is characterised by a vast plain modelled by *wadi* courses, with their source area in the Atlas and eventually fading into the great depression of the greater watershed of Chott Melrhir, reaching an average of – 80 m below sea level. Wadi Djeddi and Wadi Biskra are equally important water resources for the adjacent area, as they collect a large amount of tributaries and their surface runoff of the southern hillside of the Saharian Atlas and of the south-western Aurès and North of Biskra, respectively. The vegetation cover is mainly characterised by the presence of steppe vegetation, in the northern part and associations of desert species, including halophytic and psamophyte ones unevenly distributed in the rest of the area, apart from well vegetated wadi courses.

The area can be divided into two zones: the *Occidental Zab* and the *Oriental* one (as shown in figure 1), where Oued Biskra constitutes the limit between the two zones. Locally known as the *Zibans palmeraie* (palm grove) or the *Occidental Zab*, the irrigated area exceeds 65 000 ha and draws more than 600 million of m^3 per year, whereas the Tolga area is an international exporter of high – quality dates (*Deglet Nour*). The importance of these palm groves is due mostly to the presence of very productive and shallow aquifers highly exploited for more than one century

(Ghiglieri, Sy et al. 2014), with an average salinity from 2 to 4 g/l, hence the increase of surface salinity and gypsum encrustment. The land use mainly regards date palm plantations and extended greenhouse cultivations (vegetable cultivations), followed by open field cultivations.

To the East, the *Oriental Zab* domain of the *Zibans* area, the landscape is characterised by vast alluvial fans and a plain modelled by *wadi* courses, with their source area in the Atlas and eventually fading into the great depression of the greater watershed of Chott Melrhir, reaching an average of – 80 m below sea level. Open field and industrial cultures have become an intense practice in the last decades, as these ones, unlike phoeniciculture, do not require a shallow aquifer (Bougherara and Lacaze 2009), but usage of deep groundwater has increased in the last decades.

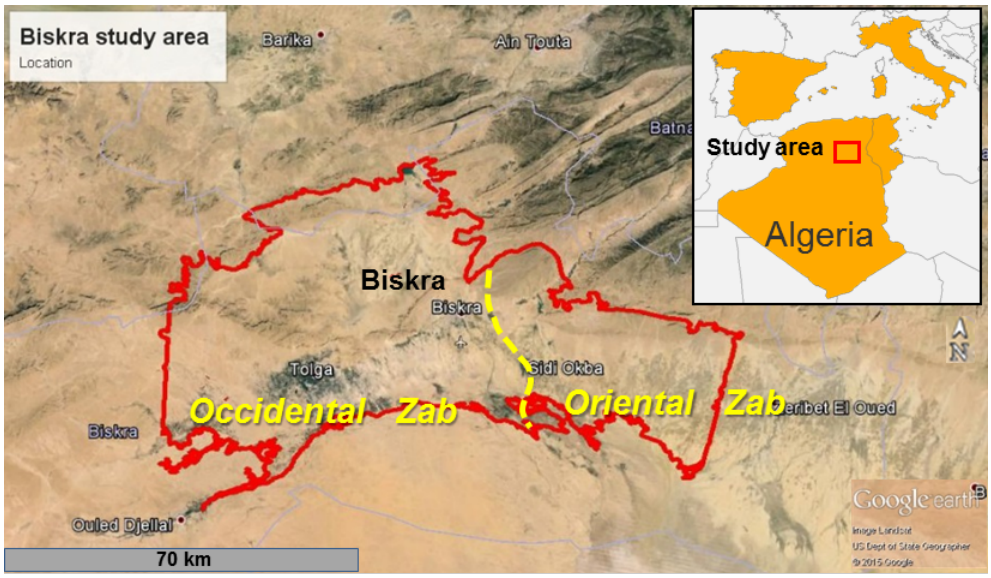

Figure 3. Biskra study area (Algeria)

3.1.2. Geological and Hydrogeological Setting

From the geological point of view, the Biskra area is located in the eastern part of the Saharan Atlas (Aures), between the folded Atlas domain in the northern part of the area and the desert and flat domain of Sahara, in the South. This zone is a part of the intra-continental mountain chain that was formed between Tertiary and Quaternary during the geodynamic events in the peri-Mediterranean area (opening of the Ocean Tethys and the opening of the Atlantic basin and subsequent closure of the western Maghrebide Tethys) (Bracene and Lamotte 2002).

The area is characterized by the superposition of several folding events occurring from Middle Eocene to Pleistocene that strongly influence the geometry of the main aquifers (Algerienne 1980, Buttau, Funedda et al. 2013). Terrigenous and carbonate successions that range from Early Jurassic to Holocene crop-out in the study area.

The deformation history that has affected these formations, in agreement with most of the authors, provides the following series of events:

- "Atlas Event" (Lower Eocene, Lutetian) (Guiraud, Bosworth et al. 2005). It involved the formations ranging from the Triassic to Lower Eocene. This created several structures orientated NE-SW which were developed from a shortening trending NW-SE and are contemporary to an uplift.
- Relative quiescence and rapid uplift in the Miocene, characterized by sedimentation of molasse-type deposits that cover the oldest formations (Bracene and Lamotte 2002).
- "Villafranchian phase", characterized by a N-S shortening and uplift responsible for the tilting of the Miocene formations and development of the folds with E-W axial trend. The uplift has occurred in several stages, the last being in the Pleistocene and involved the entire Atlas zone(Frizon de Lamotte, Saint Bezar et al. 2000).

The study area mainly consists of sedimentary successions aging from Mesozoic to Pliocene (Guiraud, Bosworth et al. 2005). The lowest Mesozoic unit consists of evaporitic and terrigenous clastic rock deposits, Triassic in age, outcropping in the study area for diapirism phenomena. The permeability of the Triassic gypsum is high and the deposit plays an important role in conditioning the groundwater salinity. The Jurassic formations consist of alternations of marl and dolomitic and carbonate deposit, which shows highly variable thickness and medium permeability.

The Lower Cretaceous (Albian-Aptian) successions consist of terrigenous clastic and carbonate rocks, up to 400 m thick. The Upper Cretaceous sequence also consist of limestone with an important intercalation of arenaceous or sandstone or sandy marls, the total thickness is about 2000 m. On the Mesozoic sequence rest a terrigenous clastic and carbonate successions of Eocene and Miocene age. Quaternary aeolian sand and loose sediments consisting of alluvial sand and gravels cover the most of the plans in the depression zone, occurring as piedmont slope deposits and valley fill materials that range in thickness from 10 to 20 m. All these deposits have generally a good permeability, allowing infiltration into the lower aquifers.

From the hydrogeological point of view, in the study area it is possible to distinguish two first-order aquifer systems: The Complex Terminal aquifer (CTa) and the Continental Intercalary aquifer (CIa) that are divide by Cenomanian impermeable level (Ci) (Buttau, Funedda et al. 2013).

The Continental Intercalary (CI) aquifer of North Africa is one of the largest confined aquifers in the world, it covers about 600,000 km² with a potential reservoir thickness of between 120 and 1,000 m. The CI aquifer, present both in Tunisia and Algeria, may be considered as large artesian basin type of area, especially since the results may be extrapolated to the west (Grand Erg Septentrionale) and to the east (to the Fezzan of Libya) as well as to the south to the basins of the southern Sahara. This aquifer includes the Lower Cretaceous deposit and in several zone Triassic and Jurassic deposits (Castany, 1985). Terminal Complex (CTa) is the name used for a group of several aquifers located in different geological formations of Early Cretaceous and detrital Mio-Pliocene (Ould Baba Sy & Besbes, 2007). The CTa extends over the major part of the sedimentary basin in Algeria and Tunisia, it is unconfined or semi-confined, with its main recharge area in the central Sahara. The CT aquifer system is generally unconfined, and direct recharge has taken place in the past and is possibly occurring at present the Saharan Atlas. Groundwater development has mainly taken place in the sandy Mio–Pliocene formation, except to the north of the Chotts where the carbonates have been exploited (Guendouz et al., 2003).

The thickness of the Complex Terminal aquifer (CTa), in this area, is known only approximately because of the uncertainties associated with the deep erosion that occurred during Cenozoic. However, in the CTa is possible to recognize Turronian aquifer (Ta), Maestrichtin-Campanian aquifer (MCa), Tolga acquifer (AT), Aquifer of sand (As), Mio-Pliocene aquifer (MPa) and Quaternary aquifer (Qa) which are divided into Coniancian Santonian-impermeable (CSi) and Middle Eocene-impermeable level, respectively.

In this area, the CIa, , has a depth between 1600 and 2500 m, the average yield is 80 L/s and the temperature is higher than 60° (Sedrati N., 2011). The Albian and Aptian aquifers are included in the Continental Intercalary (CI).

The CTa is made up of Benhamida S, 2008, MdH 1980:

- Quaternary aquifer (Qa), located in alluvial deposits and it is fed by vertical infiltration. The water of the aquifer is of good quality and it is used for drinking and domestic use. The thickness ranges from100 to 300 m and with a flux between 05 and 20 l/s.
- Mio-Pliocene aquifer (MPa), Aquifer of sand (As) (MdH 1980), a wide aquifer in this wilaya, representing a succession of clay, sand and gravel levels. The permeability parameters change because it is a heterogeneous aquifer system. The thickness varies from 20 to 150m and has the average yield is 15 l/s.
- Tolga acquifer (AT) in the south area, Maestrichtin-Campanian aquifer (MCa) in the north. This aquifer is located in the fissured limestone of lower Eocene age. The depth of this aquifer ranges from 100 m to 500 m in the Tolga and Louis, respectively. The yield of this aquifer ranges from 10 l / s (when pumping) to 30 l / s (when under pressure).
- Turronian aquifer (Ta)

The hydraulic potentiality is estimated to 2113,86 hm3/an, of which 96,62 % is groundwater (namely 2042,43 hm^3) but only 43% is used and the 3,38% is represented by superficial water (namely 71.43 hm^3) used for livestock watering points and Foum El Gherza water supply. The daily requirement is 262 L/ab in urban zone and 226 L/ab in the rural zone, which is higher than the national average.

The water of the aquifers of the Biskra wilaya is exploited for various economic sectors (domestic-rural-industrial, table 1). The Water has an important role in all human activities in this region, hence the rapidly changing socio-economic context has generated an increase in demand for water. In fact, from 1950 to 2008 the volume of water collected has increased from 3.2m^3/s to 18m^3/s because of the growth in the number of wells (from 1,141 to 9,908 wells). This situation has resulted in the depletion of the underground resource and increased salinity. In order to meet the high water demand, the fossil aquifers of the CTA were exploited, a valuable and non-renewable resource.

The aquifers suffered a process of quantitative degradation. The pumping tests carried out in the region of Tolga, W of the city of Biskra, indicate rather good values of transmissivity, with values ranging between $20x10^{-2}$ m^2 / s and $5x10^{-2}$ m^2 / s in the Eocene deposits. However, the overexploitation of groundwater for irrigation purposes in palm groves induced a progressive

lowering of the water table and therefore the depletion of springs. The Cenomanian, characterized by a clayey-evaporite series, constitutes a second waterproof limit separating the CTa aquifer from the deep CI one. The CI aquifer is quite known and exploited mostly by sinks of Sidi-Khaled and Ouled-Djellal for irrigation of the palms. The exploitation is particularly costly because of the high depth at which it is located.

Aquifer	N.Tot.Well	N.Well AEP	N.Well IRR	N.Well IND	Q (hm^3/y)
Quaternary	1486	76	1409	1	60.269
Mio-Pliocene	5891	101	5780	10	265.21
Upper Miocene (Pontiano)	55	38	17		6.506
Lower Eocene	1408	64	1341	3	166.889
Mastrictian -Campanian	39	2	37		15.949
Turonian	24	10	14		0.529
Albo-Barremian	19	12	7		39.408

Table 1. Exploration of aquifers in the study area (legend: AEP – drinking water; IRR - irrigation water, IND - water for industrial use (Benhamida S, 2008).

3.1.3. Climatic Context

The climate regime of this area is characterized by hot and dry climate, stretching over the semiarid, arid and pre-desert zones, with an average annual temperature of about 22°C. The lower temperatures are registered usually in December and January while the higher occur in July and August. Regarding precipitation, the rainfall frequency peaks usually occur in November and March, mainly with the prevalence of overnight rain. The maximum frequency of rainfalls is in November and March and the total annual rainfall average is about 150 mm but the annual mean rainfall is less than 30 mm, as shown in figure 2. The only the areas in the North East region have a relatively higher rainfall raging between 200 and 500mm. However the average rainfall within a year is less than 20 mm. The minimum rainfall is almost null in the months of July and August. Biskra area is characterised by a hot and dry climate, with an annual mean of 21^{o}C. The maximum frequency of rainfalls is in November and March and the average annual total received rainfall is about 200 mm but the annual mean rainfall is less than 30 mm, as shown in figure 2. The minimum

rainfall is almost null in the months of July and August. The annual values do not vary much but the inter-annuals contrast considerably. Therefore, from the climatic point of view, the years can be classified as: dry years (approx. 40 mm), intermediate years (approx. 145 mm) and humid years (approx. 300 mm). The annual mean of evaporation ranges about 2600 mm, showing a high unbalance between rainfall and loss, hence the necessity of much irrigation for the development of agriculture.

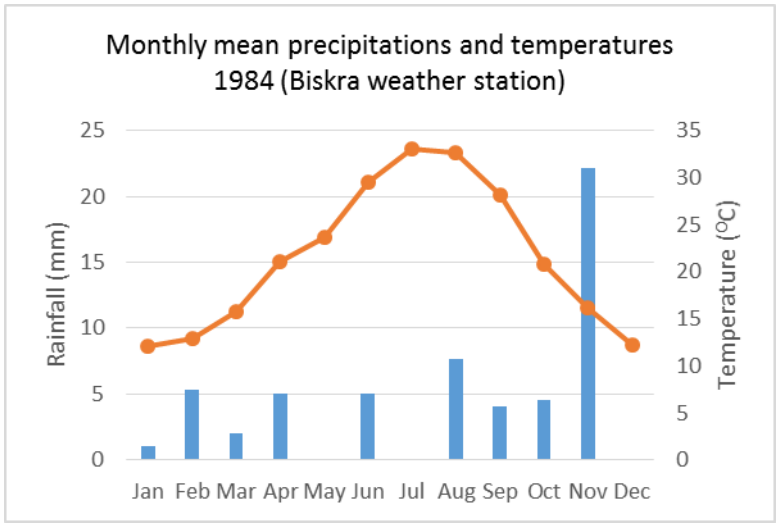

Figure 4. Monthly mean precipitations and temperatures 1984 (Biskra weather station)

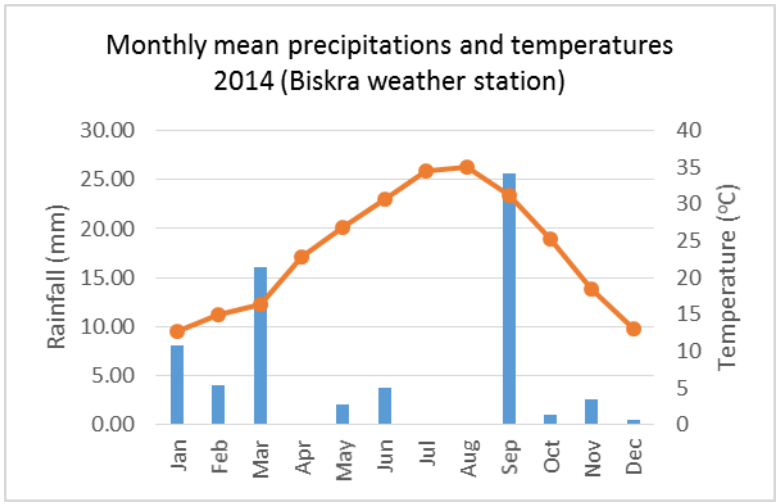

Figure 5. Monthly mean precipitations and temperatures 2014 (Biskra weather station)

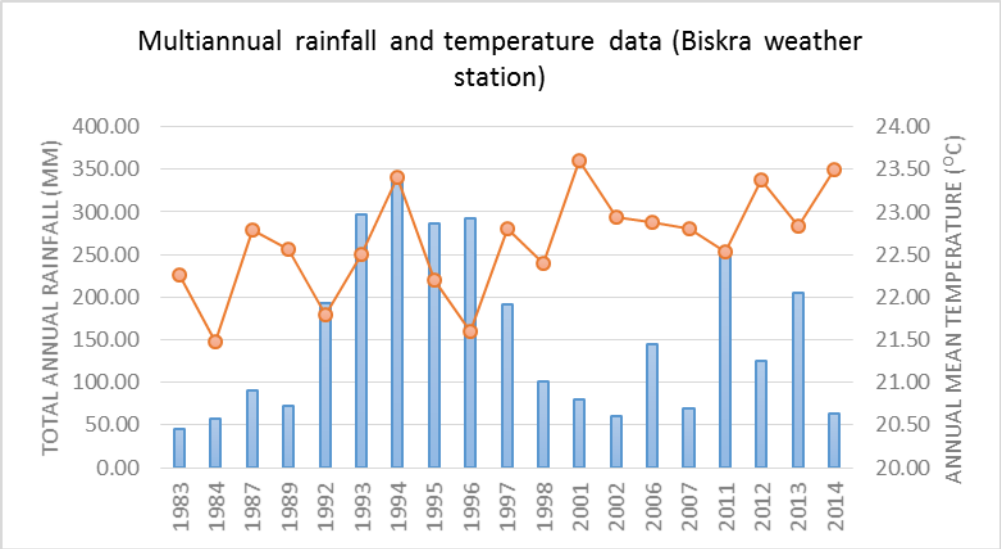

Figure 6. Multiannual rainfall and temperature data (Biskra weather station)

3.1.4. Socio-Economic Context

Including the city of Biskra the population overcome 210,000 inhabitants. Given its geographical position, the entire wilaya of Biskra is characterized by a type of forestry-oriented agro- pastoral agriculture which is characterized by a large area of date palm cultivation. The irrigated area in the whole wilaya exceed 65.000 ha and draws more than 600 million m3 of water per year, mainly trough groundwater pumping from thousands of boreholes and private local wells. According to the inventory campaign of water points, made by ANRH in 2000 and 2008, 34 water wells are currently exploited inside the Oued Biskra: 90% of which are used for drinking water supply for the city of Biskra and 10% for farm's irrigation. The volume of annual water withdraw is estimated to be about 5,000,000 m3 with chemical quality properties variable depending on zones and with an average salinity from 2 to 4 g/l. In recent years, following the development of the city of Biskra and to address the need of water from farming activities the demand has increased leading to a considerable exploitation of the aquifer and automatically a significant decrease of water table levels. View the importance of this aquifer for both the city of Biskra and its surrounding areas, it become necessary as well as strategic, to think for new or more efficient use of aquifer artificial

recharge methods in order to solve the problem of water table drawdown and the decrease of salinity up to 50% (NRD 2011).

3.2. Oum Zessar Area

3.2.1. Physio-Geographical Description

The 4000 km^2 watershed of Oum Zessar can be considered, from the ecological, hydrological as well as socio-economical point of view, as representative of the arid south-eastern area of Tunisia. The study site belongs to the province of Médenine (guvernorat) and it covers administratively several counties, stretches from the limit of the Great Oriental Erg in the West and crosses the Dahar Plateau and Jeffara plain before ending into the Mediterranean Sea (Gulf of Gabès).

The agricultural systems in the watershed are marked by their diversity, from upstream to downstream, and are essentially characterized by a non-regular agricultural production that varies from year to year, depending on the rainfall regime; the development of arboriculture and the extension of newly cultivated fields at the expense of rangelands; the predominance of olive trees and the development of episodic cereals; the gradual intensification of the livestock husbandry systems; the development of irrigated agriculture exploiting surface- and groundwater resources. Massive water harvesting projects were initiated in the province of Médenine, and particularly in the watershed of Wadi Oum Zessar, in the 1980s. The focus was on micro-watershed treatment and maintenance of existing structures. Moreover, a large number of recharge and spreading units were installed. In total, investments of several millions of USD were made for both province. During the 1990s, international's work mainly comprised the construction of traditional systems (i.e. in Tunisia Jessour, Tabias). By the end of 2000, recharge and spreading units were built and recharge wells installed. However, during the last years, an overexploitation of groundwater occurred due to drillings, development of irrigated crops and extension of fruit trees orchards. Those systems are marked by a competition for the access to the natural resources, especially for land ownership and water use (Genin et al., 2006).

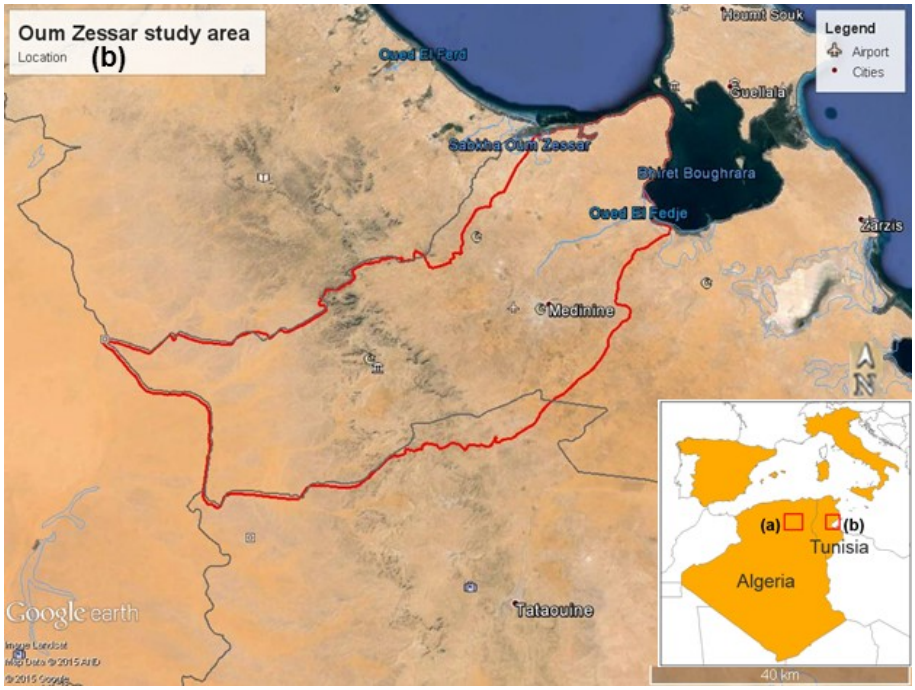

Figure 7. Oum Zessar study area (Tunisia)

3.2.2. Geological Setting

The hydrogeology of this area is conditioned by of morphostructural and geological features, these characteristics allow to distinguish two domains (Buttau, Funedda et al. 2013):

(1) the sedimentary-Mesozoic basin of Jeffara, formed since the Lower Palaeozoic and (2) the Jeffara escarpment including the Tunisian Dahar domain.

The Jeffara escarpment and Tunisian Dahar domain represents the southern side of a wide gentle anticline, first thrusting unit above the southern Tellian Tunisian deformation front. The NNW-SSE trending anticline axis weakly dipping toward SE . The southern flank is slightly dipping of 1° to 2° westward (Busson, 1967; Gabtni et al., 2009) and south-west (Bouaziz et al., 2002; Bodin et al., 2010). The northern flank of the Jeffara escarpment is absent because it is collapsed and after filled by the Jeffara soft Cenozoic/Quaternary deposits. The Dahar was built up trough the reactivation of the Panafrican faults systems (Ben Ayed and Kessibi, 1981; Gabtni et al., 2012) and affected by E-W and NW-SE Tethysian faults (Bahrouni et al., 2014).

In this domain outcroping Triassic, Jurassic, Cretaceou formations covered by Tertiary, Quaternary deposits.

The Tunisian Jeffara basin represents a low-flat-sub-tabulary topography that is bordered by the Gabes gulf and the Mediterranean Sea to the north, the southern morphologic edge of the Dahar domain whose layers are covered by Tertiary, Quaternary deposits. The geology of the Jeffara basin is poorly known even if it is characterized by the continental Jeffara which constitutes a transition area to the Mesozoic/Cenozoic outcrops of the Dahar, and the coastal plain of the maritime Jeffara (Gabtni et al., 2009). In the Jeffara basin mainly outcrop Cenozoic continental deposits with increasing thickness towards the coast. In the continental Jeffara Lower to Middle Triassic formations outcrop along the *wadi* because of the erosional processes affecting the Cenozoic deposits and there are small Jurassic and Cretaceous outcrops in north of the study area. The jeffara basin is affected by E-W right lateral strike-slip faults NW-SE normal faults (es: Medenine fault).

In the jeffara basin in according to Ouessar and Yahyaoui (2006), the groundwater system of the region can be subdivided into shallow and deep aquifers.

The shallow aquifers include the quaternary formation while the deep aquifer include the lower Triassic, Jurassic, Cretaceou and Mio-pliocene aquifers.

In this study area, there are four main aquifers, divided into two groups according to their lithological characteristics: the shallow and phreatic group correspondent to recent alluvial deposits and the deep aquifers set up in the lithological units of Triassic, Jurassic and Cretaceous. The shallow aquifers of the Mio – Plio – Quaternary deposits that cover up the Jeffara Plain and the dolomitic limestone of Turonian are recharged naturally via infiltration and are exploited for the domestic use of the nearby localities. The salinity varies between 0, 6 and 1g/l in correspondence to carbonate lithology and between 1, 5 and 5 g/l when the lithological setting is related to alluvial deposits. The water table ranges from 30 to 2 – 3 meters near the coastal plain.

Among the deep aquifers, the Lower Triassic aquifer of sandstone (in the upstream part) and the Zeuss Koutine aquifer (in the middle and downstream parts) are the main ones. The first one provides the freshest groundwater of the region (salinity less than 1 g/l), which is mainly used for irrigation and drinking water, while the second one is the main source of water supply for the province of Medenine.

3.2.3. Climatic Context

The study watershed receives between 150 and 240 mm of total annual rainfall and is defined by a climate regime with a contrasting temperature pattern with mild to cold winters (up to 3 °C, occasional freezing) and warm to very hot summers (up to 48°C). The wettest months are from December to March while the dryer from May to August. Rainfalls are mainly concentrated in winter (40%), in autumn (32%) and spring (26%) whereas summer is almost rainless. Most of the rainfall does not exceed 10 mm but relatively high intense rainfall showers (more than 80 mm and 100 mm) could be expected once per decade and within 35 years, respectively.

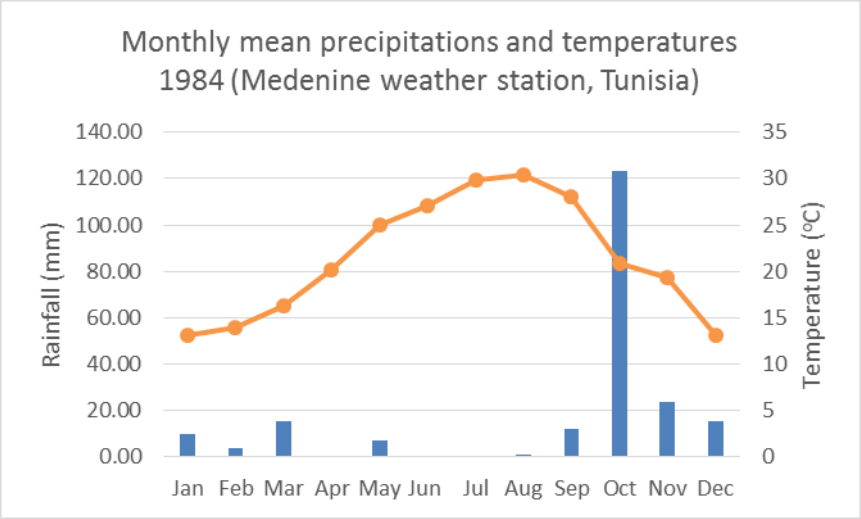

Figure 8. Monthly mean precipitations and temperatures 1984 (Medenine weather station, Tunisia)

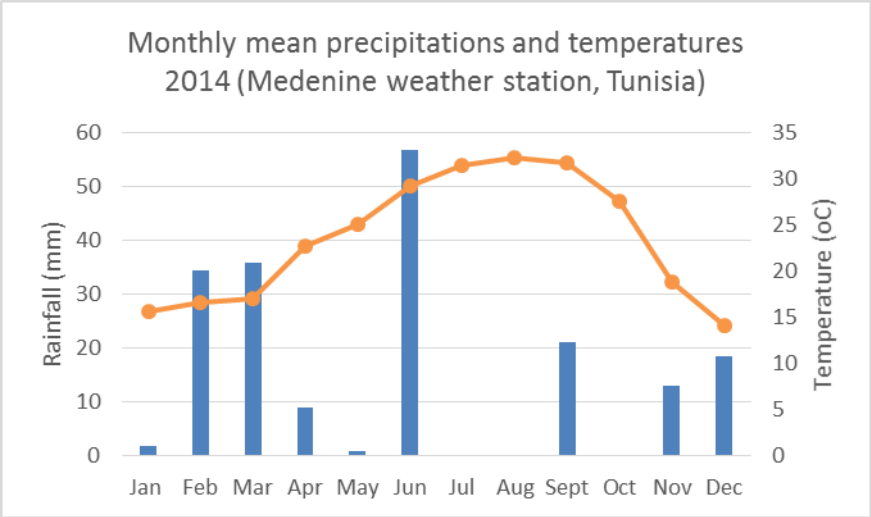

Figure 9. Monthly mean precipitations and temperatures 2014 (Medenine weather station, Tunisia)

3.2.4. Socio-Economic Context

The agricultural systems in the watershed are marked by their diversity, from upstream to downstream, and are essentially characterized by a non-regular agricultural production that varies from year to year, depending on the rainfall regime. The development of arboriculture and the extension of newly cultivated fields at the expense of rangelands; the predominance of olive trees and the development of episodic cereals; the gradual intensification of the livestock husbandry systems; the development of irrigated agriculture exploiting surface and groundwater resources. Cropped sites, mainly arboriculture, are found on terraces behind water harvesting structures practiced by the local farmers: *jessour* and *tabias* (Ouessar 2011). *Jessour* are mainly found in the mountainous areas of the watershed and are constructed in the intermountain and hill watercourses to intercept runoff and sediments. *Tabias* are essentially situated in the piedmont areas in the middle of the watershed on gentle slopes and gains its water directly from its impluvium or by the diversion of wadi runoff.

4. CHAPTER FOUR: Methodology and Data

4.1. Methodological approach

The methodology used in this study arises from the need to tackle with two types of problems:

1) the two main environmental issues present in the areas of study, hence soil salinity and sand encroachment, defining their current state, driving forces and trends

2) from the methodical point of view, hence the spectral confusion among very reflective desert features; in some cases, limited or no access to field data or to undergo field survey oneself. A schematic workflow is presented in figure 9. Firstly, the visual interpretation of Landsat imagery was undergone, sustained by a large set of ancillary data. Two different automated classification schemes were considered in this study (Afrasinei, Melis et al. 2015), according to reported limitations of various experimented classification methods in similar case study contexts by the scientific community (Pal and Mather 2003, Elnaggar and Noller 2010): 1) a decision tree analysis (DTA) employing also indices constructed through thorough spectral analysis, band transformation techniques, image statistics and expert-knowledge (Rao, Chen et al. 2006) (Matthew 2012, Srimani and Prasad 2012), (Elnaggar and Noller 2010) and 2) IsoDATA classification applied to the Principal Components Analysis (PCA) of Knepper ratios, adequate in the fast, user-independent, spectral-based delineation of mineral components. In the Biskra area, ground truth data was difficult to achieve in the correct amount needed for such studies, thus available ancillary data were used as basis throughout the study phases. Thirdly, the IsoDATA of Knepper rations PCA resulting maps were compared with the DTA results and with the visually interpreted land cover/use map, through and error assessment confusion matrix. Change detection is applied in both cases and the results are discussed through correlation to social and economic ancillary data.

This study approaches an inter- and intra-annual change analysis, thus 2 images per each one of the four years were chosen: one at the beginning and one at the end of the dry season. Further details are given in section 4.2.1.

The ArcGIS 10.2 software was employed for geospatial data analysis and geoprocessing and ENVI 5.2 software (Exelis VIS, Boulder, CO) was used for the satellite data pre-processing and processing and partially for the spectral signatures processing. Regarding the powder X-ray diffraction analysis, all the measurements and data interpretation were undertaken in the XRD Laboratory of the University of Cagliari, using the PalyticalX'Pert Pro instrument and the corresponding X'Pert HighScore software for the identification of the mineral phases of each sample.

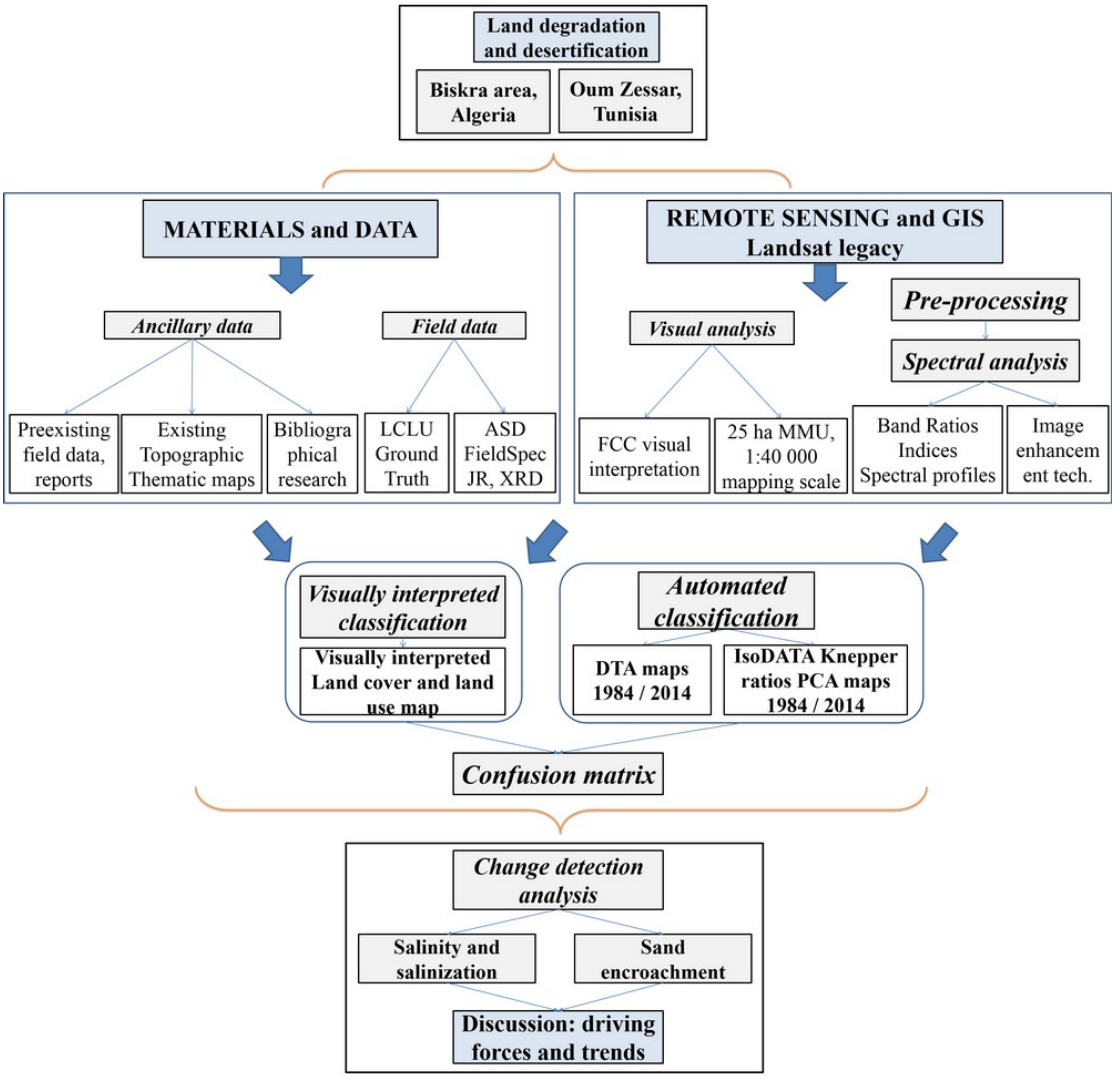

Figure 10. Methodological workflow

4.2. Data and Materials

A large set of ancillary data, organised in a database was used for the visual interpretation phase of the land cover and land use (LCLU), consisting of ground truth data acquired in June, 2014, available spatial data aerial photography, geological and topographical maps, agricultural calendars, statistics and pedologic reports, mainly provided by local entities and institutions such as *L'Agence Nationale des Ressources Hydrauliques,* Algeria, (ANRH), Institut Technique de Développement de l'Agronomie Saharienne (ITDAS), Institut des Regions Arides (IRA), Observatoire du Sahara et du Sahel (OSS) and others (figure 11).

For the easiness of comprehension, the main data, materials, tools and software engaged in this research are as follows:

- Bibliographic data
- Ancillary data (hardcopy)
- Spatial data
- Remote sensing data: satellite imagery of Landsat series TM5, ETM+, 8 OLI (1984-2015) and 1 arc-second DEM (newly released SRTM in October 2016)
- Field instruments
- Field observation data: land cover survey and spectroradiometric survey sheets
- Saline crusts/sand samples
- Proximal sensing data: ASD FieldSpec 3 Jr. Full Range (350 – 2500 nm) spectroradiometer data
- X-ray diffraction data
- ArcGIS 10.2; ENVI 5.2 (Exelis); ASD ViewSpec Pro; SAMS (University of California); PANalytical X'Pert Pro diffractometer and X'Pert HighScore software

The spectral campaign has enabled the acquisition of spectral reflectance measurements of 34 points, of which 14 points for saline surfaces (9 samples); 10 points for sand encroachment areas (10 samples); 3 points for typical vegetation (halophyte and psammophyte) and 7 points for mixed surfaces.

	A	B	C	D	E	F	G	H	I	J	K	L
1	File name	Typology	Type	Content	Georeferenced	Datum	Projection	Scale	comment	delivery date	delivered by	Layer Type
2	wilaya_region	vector							corrupted	2012-01-19	ANRH	unknown
3	S.BASSINS.TAB	vector	polygon	watersheds	yes	WGS84	Geographic		topological errors	2012-01-19	ANRH	administrative
4	S.BASSINS2.TAB	vector	polygon	watersheds	yes	WGS84	Geographic			2012-01-19	ANRH	administrative
5	RN.bmp	raster		Carte des reseau hydroclimatique et de la surveillance de la qualite des eaux	no	WGS84	Geographic	1:500,000		2012-01-19	ANRH	hydrogeological
6	Bikra-Daira.TAB	vector							corrupted	2012-01-19	ANRH	unknown
7	BISKRA.TAB	vector	polygon	communes of the wilaya of biskra	yes	WGS84	Geographic			2012-01-19	ANRH	administrative
8	BISKRA1.TAB	vector	polygon	polygon of the wilays of biskra	yes	WGS84	Geographic			2012-01-19	ANRH	administrative
9	BISKRA2.TAB	vector	polygon	communes of the wilaya of biskra	yes	WGS84	Geographic			2012-01-19	ANRH	administrative
10	BISKRA_Daira.TAB	vector	polygon	district of the wilaya of biskra	yes	WGS84	Geographic			2012-01-19	ANRH	administrative
11	Blskra.jpg	raster		Carte des Sols de Algerie (Biskra)	no	no	Geographic	1:500,000		2012-01-19	ANRH	soil
12	busson.jpg	raster		Carte geologique du Bassin Mesozoique du Sahara Algero-Tunisien	no	no	Geographic	1:2,000,000	higly deformed	2012-01-19	ANRH	geology
13	comgeo	vector	polygon	communes of the whole Algeria	yes	WGS84	Geographic			2012-01-19	ANRH	administrative
14	Sol Agri Sah.doc	doc		LES SOLS AGRICOLES AU SAHARA - Caractéristiques, contraintes et propositions d'aménagement					generic document	2012-01-19	ANRH	soil
15	ANRH-ALGER_biskra.pdf	pdf		ETUDE SUR MODELE MATHEMATIQUE DE SYSTEME AQUIFERE DE LA REGION DE BISKRA					generic document	2012-01-19	ANRH	hydrogeological
16	MODELE MATHEMATIQUE_BISKRA.doc	doc		ETUDE SUR MODELE MATHEMATIQUE DE LA NAPPE DE BISKRA – NORD des CHOTTS CONSTRUCTION et CALAGE du MODELE					detailed document	2012-01-19	ANRH	hydrogeological
	rapport-biskra-simulation.doc	doc		EXPLOITATION du MODELE MATHEMATIQUE Définition et Réalisation des					detailed document	2012-01-19	ANRH	hydrogeological

Figure 11. Ancillary data organised in an accessible database for both areas provided by WADIS-MAR project

4.2.1. !Image Acquisition

All Landsat images were obtained by the courtesy of the US Geological Survey (USGS, earthexplorer.usgs.gov) and they were chosen avoiding exceptional humid years, which were irrelevant for this study. The imagery was chosen based on climate data, avoiding exceptionally rainy years, days or rainy periods prior to the selected date, the choice of the scenes being very restricted by cloud coverage. ArcGIS 10.2 was employed for geospatial data consultation and geoprocessing and ENVI 5.2 software (Exelis VIS, Boulder, CO) was used for the satellite data pre-processing and processing.

In the Biskra area, the study approached an inter- and intra-annual change detection analysis and 2 images per each one of the four years (1984, 1995, 2007 and 2015, as presented in table 1) were chosen: one at the beginning and one at the end of the dry season. This is because there is a maximum vegetation peak at the end of May, after the winter – spring rainfalls and a minimum vegetation peak at the end of the dry season, in August-September. We have taken into account the

fact that, in these particular areas, substantial changes in various types of land cover types and especially salt features are influenced by seasonality, as reported by literature, and that the most appropriate period for satellite data choice is the end of the dry season (Khan, Rastoskuev et al. 2005, Masoud and Koike 2006, Fares and Philip 2008, Elnaggar and Noller 2010, Allbed and Kumar 2013). Therefore, in this study, we also consider this seasonal variation in order to assess to what extent and degree this theory applies in this case study, nevertheless being an arid, pre-desert environment.

The years were chosen at an interval of about 10 years, according to possibility, starting with 1984, from the oldest one available and valid for analysis. These were chosen after a careful consultation of climate data (Biskra weather station, tutiempo.org) in order to avoid anterior heavy rainfall days, especially for the post dry season dates. The 2011 scene used for visual interpretation was not inserted in the multi-temporal analysis, being used only for comparison purposes, through an error assessment.

For both areas, images from 1984 and 2014 were chosen, as presented in table 2 and 3.

In the Oum Zessar area, multiple image acquisition was restricted by cloud coverage, especially because the criteria was much more difficult to meet. Two scenes were needed for the full coverage of the study area, so the closest dates as possible (not more than 15 days between the scenes, due to change in plant growth, compromising accuracy of results) had to be chosen for the mosaic construction of each year. Thus, both images had to be cloud-free and very close in time. We also encountered difficulty in finding appropriate pairs even within an year. For this reason, in the case of Oum Zessar, the analysed scenes are only the ones of June for both 1984 and 2014. However, given the amount og ground truth available for this area in the same month of June in 2014, it was more important to focus on the delineation of a valid decision tree and its integration with the collected field spectra.

Table 2. Landsat scenes used for Biskra area

Satellite	WRS Path	WRS Row	Acquisition Year	Day of acquisition- Julian Day Number (JDN)	Date
LT5	194	36	1984	182	30 June
LT5	194	36	1984	246	2 Sept
LT5	194	36	1995	148	28 May
LT5	194	36	1995	228	16 Aug

LT5	194	36	2007	149	29 May
LT5	194	36	2007	229	17 Aug
LT5	194	36	2011	160	9 June
LC8	194	36	2015	123	3 May
LC8	194	36	2015	219	7 Aug

Table 3. Landsat scenes used for Oum Zessar area

Landsat	WRS Path	WRS Row	Acquisition Year	Day of acquisition- Julian Day Number (JDN)	Date
LT5	190	37	1984	170	18 Jun
LT5	191	37	1984	177	25 Jun
LC8	190	37	2014	163	21 Jun
LC8	191	37	2014	172	28 Jun

4.3. Land Cover and Land Use Mapping Through Visual Interpretation

The observed biophysical cover of the earth's surface, termed land-cover is composed of patterns that occur due to a variety of natural and human-derived processes.

On the other hand land-use is human activity on the land, influenced by economic, cultural, political, historical, and land-tenure factors. Remotely-sensed data (i.e., satellite or aerial imagery) can often be used to define land-use through observations of the land-cover (Abubaker Haroun Mohamed Adam 2013). Up-to-date land-use information is of critical importance to planners, scientists, resource managers, and decision makers. Optical remote sensing plays a vital role about defining land cover/use and monitoring interactions between nature and human activities. Additionally, remote sensing provides time, energy and cost saving. Today, data such as satellite sensor images and aerial photos are used widely to detect land cover and land use dynamics.

Land use refers to man's activities on earth, which are directly related to land, whereas land cover denotes the natural features and artificial constructions covering the land surface [35]. The geospatial phenomena are changing over time and the land cover information has to be up-date periodically. Up-to-date knowledge of land cover is an important tool for the various planning authorities with responsibilities for the management of territory [19]. However, it should be noted that planners and land managers require accurate data to address land cover problems. Although the

priority is for land use (economic) information, land cover information is more easily mapped and can serve as an approximation of land use (Hamid Reza and Majid Shadman 2012).

Visual interpretation is still one of the most widely used methods for detecting, identifying and characterizing the spatial features on an image. The visual interpretation of LCLU maps assisted as reference data due to its detail, quality and expert knowledge validity (Elnaggar and Noller 2010): acknowledged methodology (ETC/LC and Agency 1999, Büttner, Maucha et al. 2000, Feranec and Otahel 2000, Jaffrain and EEA 2011), large set of ancillary data, 1:40 000 mapping scale, 25 hectares minimum mapping unit (MMU) and 37 LCLU classes of 4th level of detail (according to CORINE land cover (ETC/LC and Agency 1999)). It was also supported by ground truth data, according to possibility (Elnaggar and Noller 2010). The methodological and classification approach was adapted from various land cover programs implemented either in Europe, such as CORINE land cover or the African ones (ETC/LC and Agency 1999, Büttner, Maucha et al. 2000, Feranec and Otahel 2000, Jaffrain and EEA 2011) which allowed us to define visual interpretation keys and variables and a land cover nomenclature and class description adapted to the local context.

Photointerpretation keys are a tool with which to describe the appearance of the various categories of land cover on satellite images. These variables enable the photointerpreter to make comparable descriptions of units from the total number of items of the nomenclature and thus facilitate the interpretation work. Each unit appearing on a satellite image can be described using the variables shown in figure (ETC/LC and Agency 1999). Subsequently, a few examples of interpretation phases are given, as well as examples of variables, ancillary data, snapshots of the digitalization phases etc.

Variables	Options
Precision of contours: nature of the boundary between two units	Sharp Blurred Angular Regular
Colour/hue: depending on vegetation density, slope, orientation	All colours Variations: - Light - Dark - Pale - Variable
Size: indication of the most frequent surface area of units in the category	Small: less than 1 km2 Medium: between 1 and km2 Large: more than 5 km2
Texture: arrangement of different tones on the image. Texture is defined by them configuration of the which are too small to be seen individually. Texture must not be confused with detail. Texture expresses the average size of the constituent elements of the image	Fine: < 50 m Medium: 50 to 250 m Coarse: > 250 m . Smooth Visible texture
Structure: spatial organization of the constituent element of the image,described solely in terms of their spatial properties. Structure expresses 'breaks' in average pixel values.	Homogeneous Linear Cellular Irregular Speckled Spaghetti
Spatial distribution: indication of the geographical distribution of units in the satellite image as a whole.	Longitudinal Dispersed Regular Irregular Sporadic Erratic Concentrated Grouped Variable
Location: description of the normal physiographic positions of the category within an overall landscape.	Example: port area near an urban area

Figure 12. Various options available for each variable used in visual image interpretation (ETC/LC and Agency 1999)

4.3.1. Biskra Area

The visual interpretation process was undergone through several phases:

- Preliminary research on the area of interest, gathering and consultation of available ancillary data: topographical, geological, hydro - geological maps, statistical information on soil profiles; information of contour, administrative boundaries, sand dunes, canals, main towns, roads, villages – as base map. In addition: published soil survey reports, soil maps, geological maps, land cover/land use (or update the existing), water quality reports, hydro - geological reports.
- Preparation of satellite images and pre-processing of the Landsat imagery:
  - False colour composites generation: RGB 432 and 543, image enhancing
  - Generation of other image processing derivates supportive to image interpretation (various colour composites targeting best visibility of single land cover features and salt – affected soils, NDVI[1], ENVI SPEAR tools – vegetation delineation)
- Land cover/land use computer aided photo - interpretation of the areas of research: Biskra, Algeria and Oum Zessar, Tunisia.
  - Enhanced false colour composite: 1: 30.000 mapping scale visually interpreted for land cover features as well as visible salt – affected areas, with the help of image interpretation variables: precision of contours, colour/hue, size, texture, structure, spatial distribution and location.(Corine land cover technical guideline was used as reference methodology)
  - Provisional interpretation key; provisional nomenclature and class addition or adaption to local context

Examples of ancillary data employed in the visual interpretation phases are given in figures 13-16, using also ancillary data provided by the Google Earth community. Figure 17 illustrates the digitalisation phase, with a minimum mapping unit of 25 hectares, at a mapping scale of 1:40 000.

[1] Normalized Difference Vegetation Index

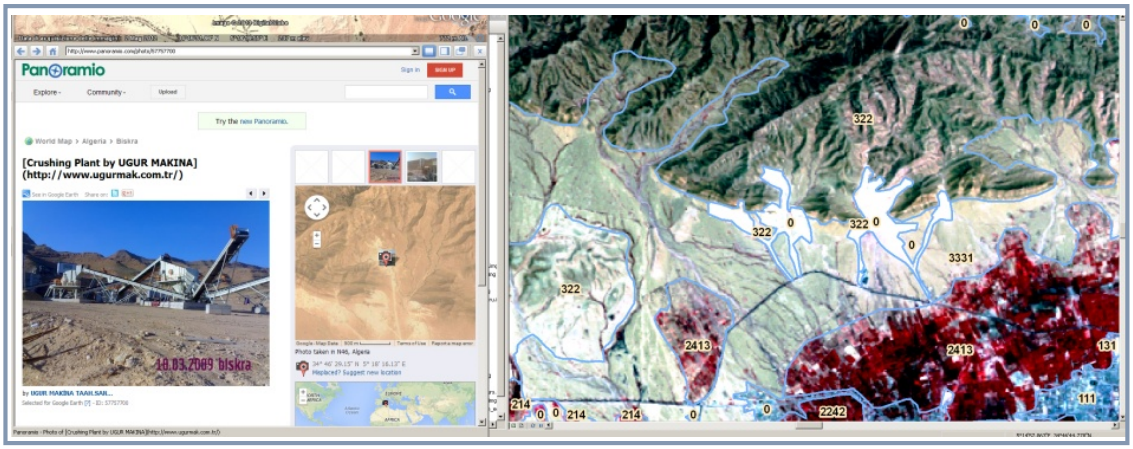

Figure 15. Example of ancillary data provided by the Google Earth community: construction site north of Tolga, Biskra area, Algeria.

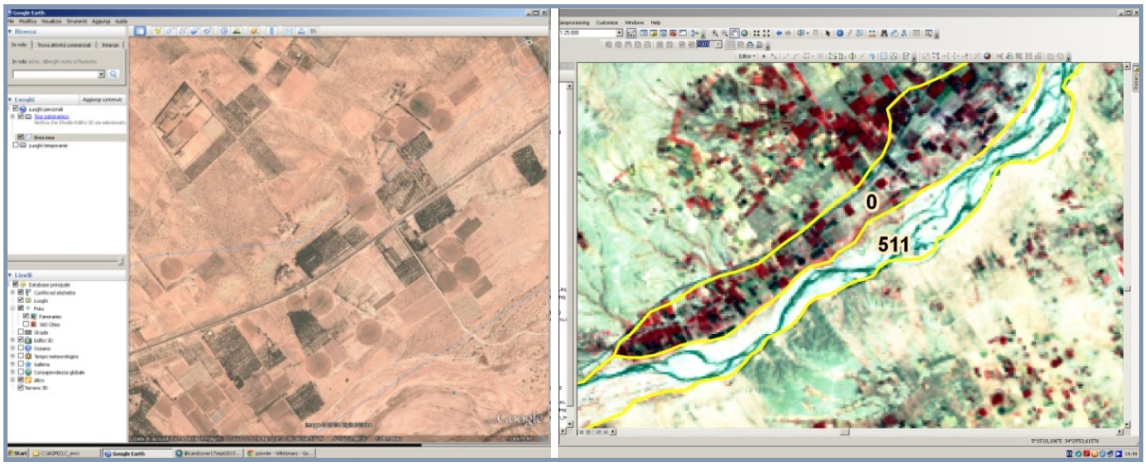

Figure 14. Example of ancillary data provided by the Google Earth community: recognisable centre pivot irrigation patterns in the south-western part of the Biskra study area, Algeria

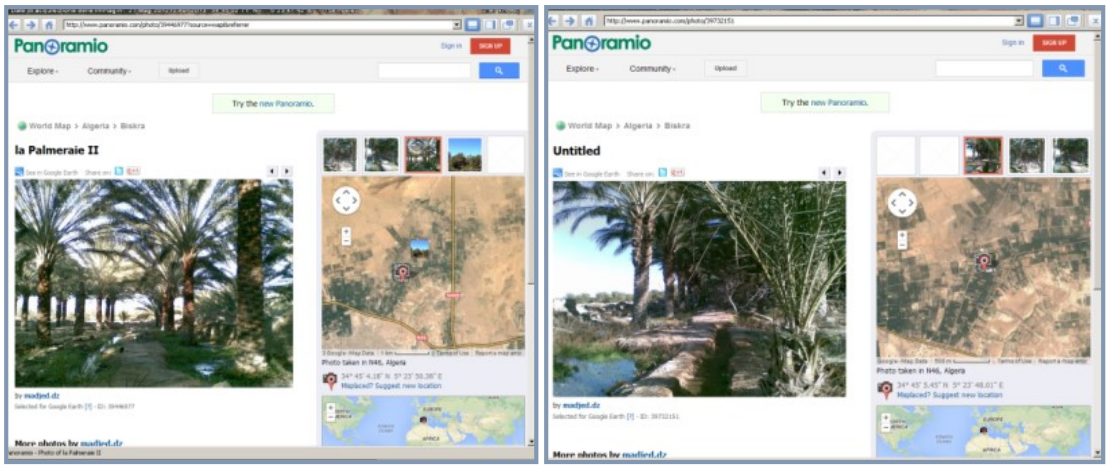

Figure 13. Example of ancillary data provided by the Google Earth community: multi-level plantation system with annual crops in the lower part, fruit trees in the 2nd level and date palm in the third. Surrounding areas of Tolga, Biskra wilaya, Algeria

Figure 17. Example of ancillary data provided by the Google Earth community: distinguishable greenhouse pattern north of El Amri, near Tolga, Biskra area, Algeria

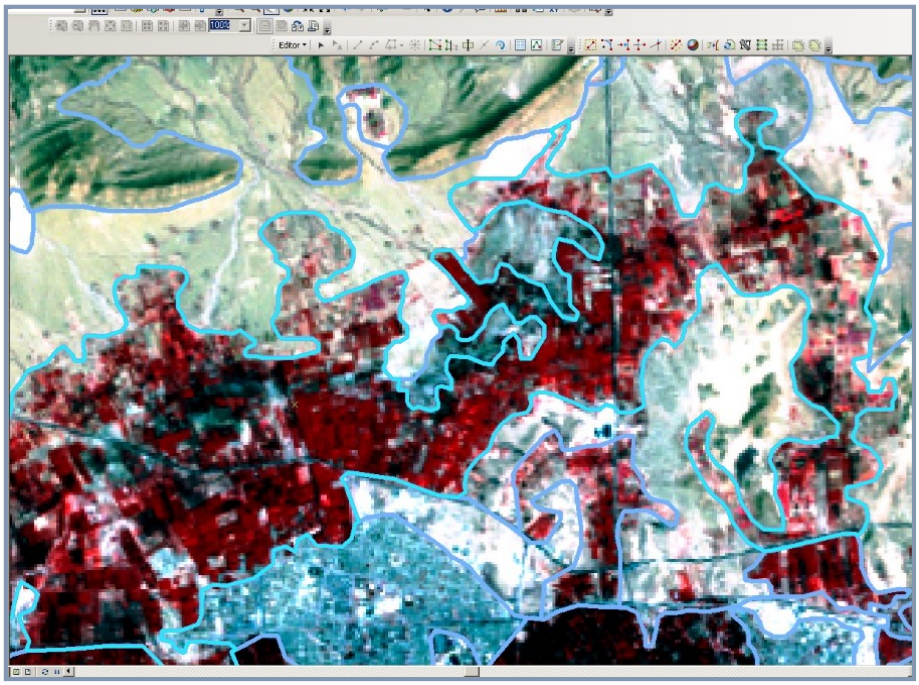

Figure 16. Digitalization phase at 1:40.000 mapping scale and 25 ha minimum mapping unit. Tolga area, Biskra wilaya, Algeria

Figures 18 and 19 represent examples of visual interpretation keys used for standardisation. The resulting land cover map is presented in figure 20, prior to land use conversion using ground truth information. It was also used as a basis for establishing doubt points for ground verification.

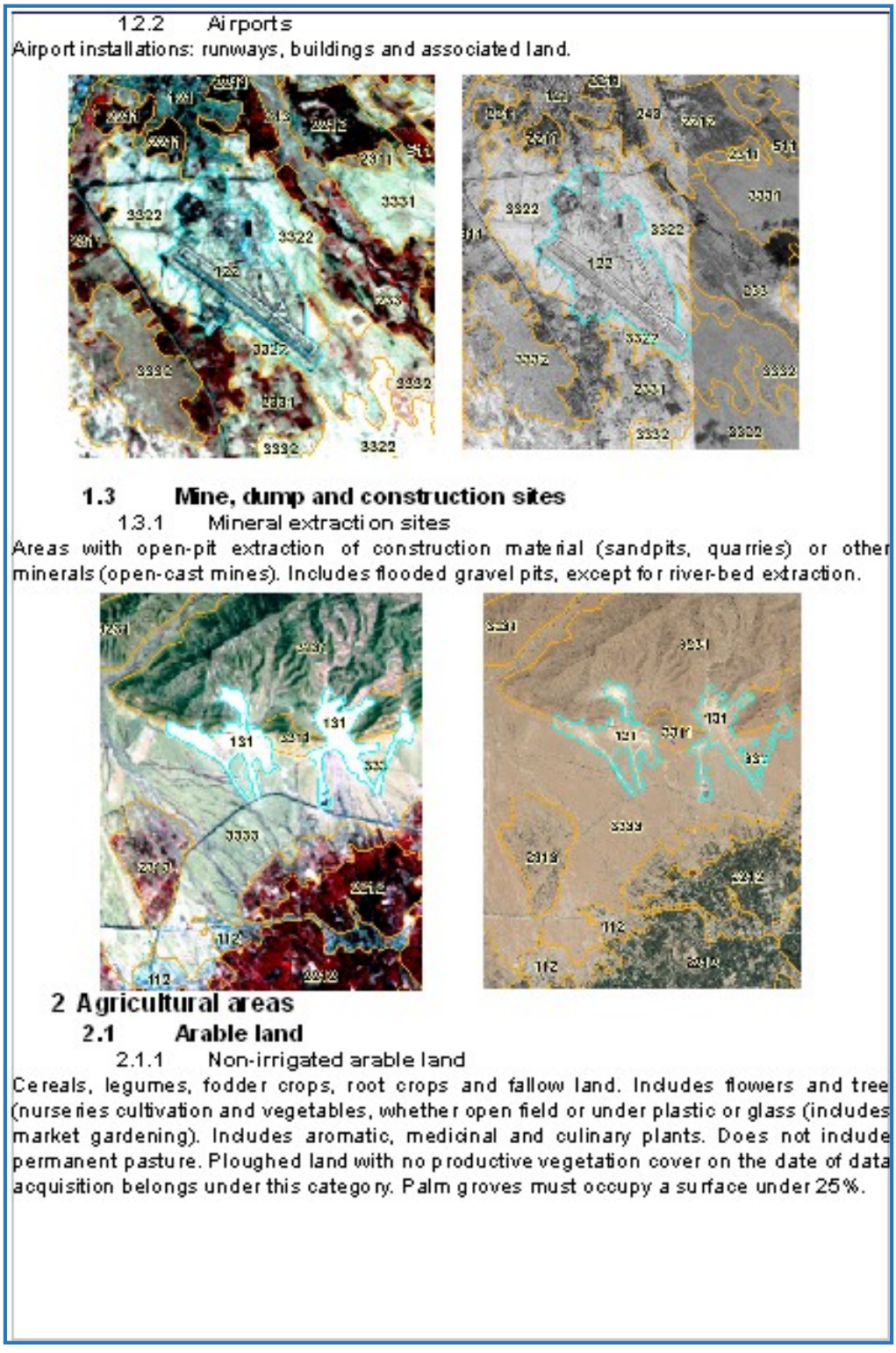

Figure 18. Example of interpretation keys for land cover and land use classes. Left images: FCC 432 used for interpretation. Right images: Online ArcGIS Bing maps used only for visualization.

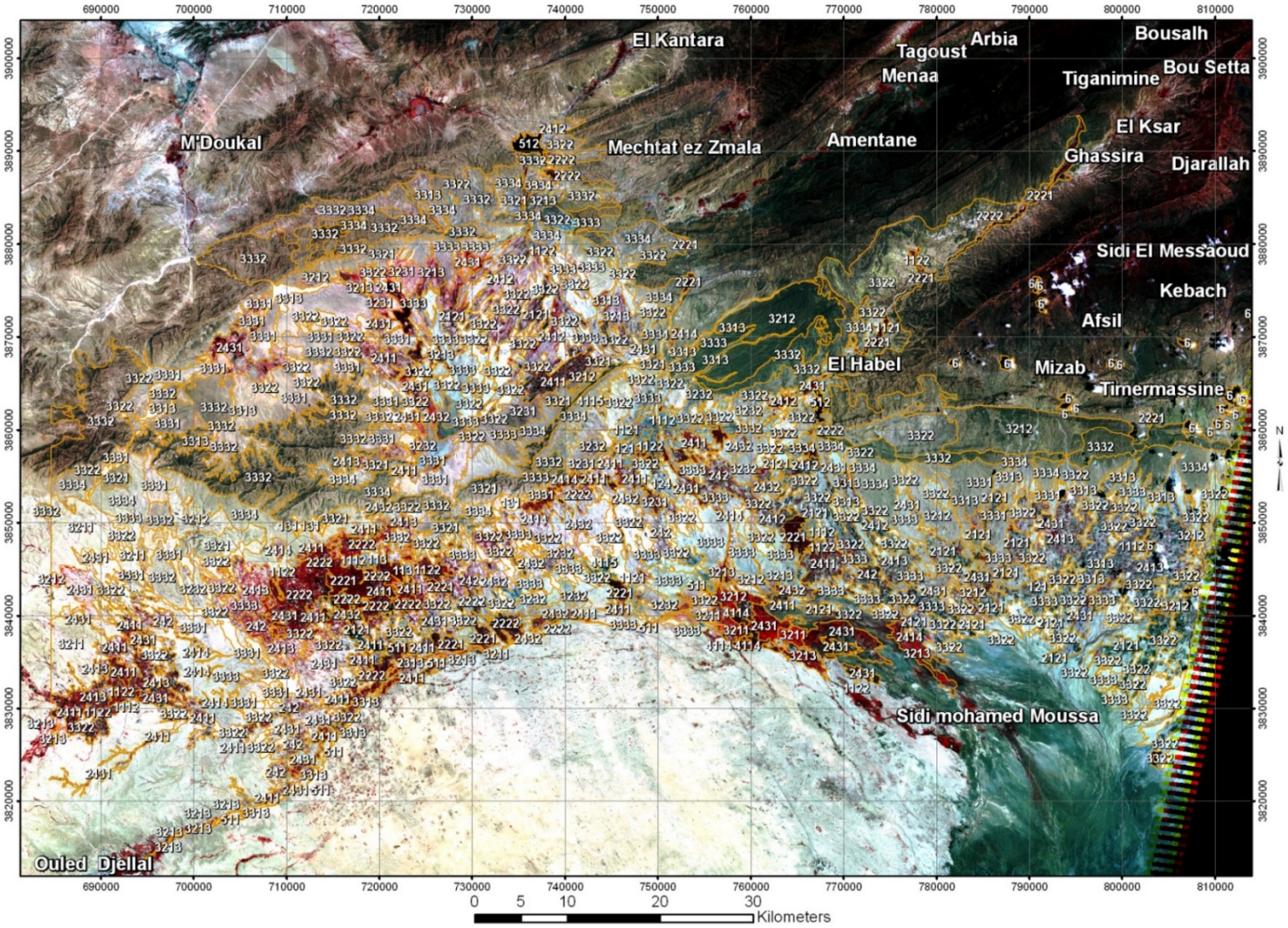

Figure 19. Complete digitalization of the Biskra study area, Algeria before ground truth validation

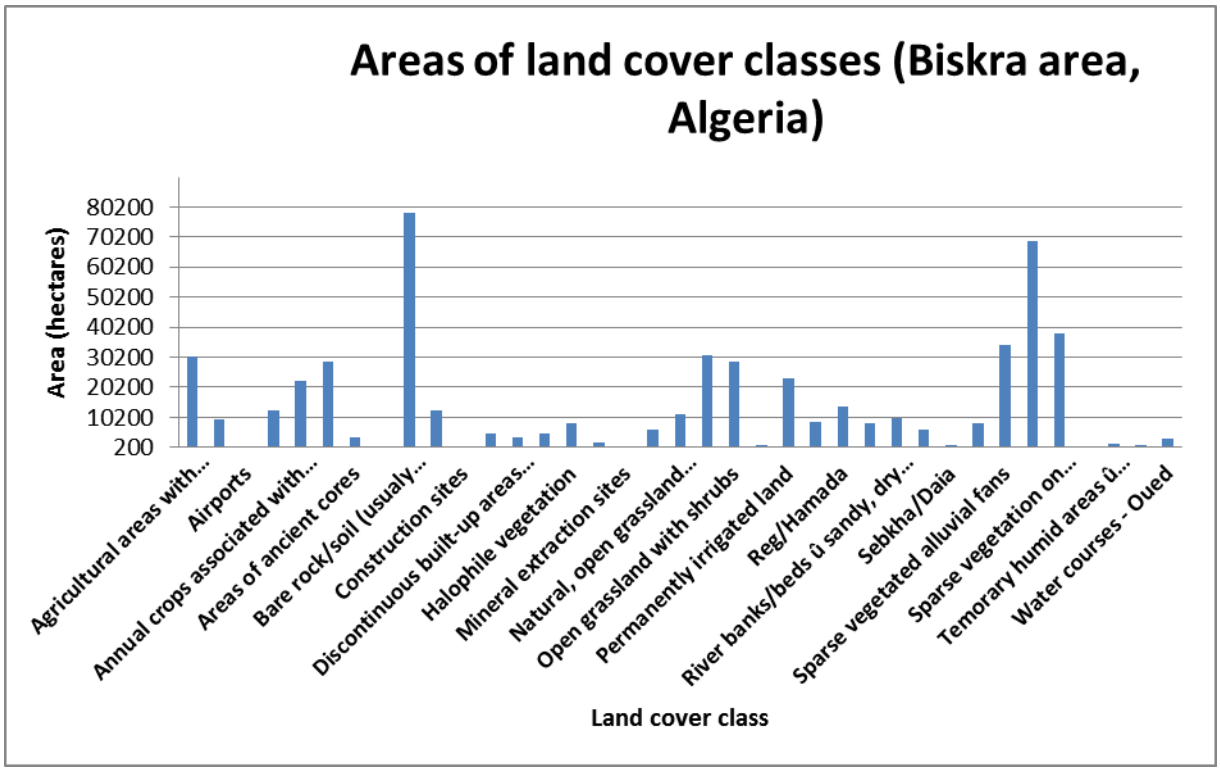

Figure 20. Areas of land cover classes (Biskra area, Algeria). Biskra total area: 526947 ha

4.3.1.1. Ground truth and conversion to land use

Ground truth information was acquired in this area in order to adjust previously interpreted land cover classes.

After establishing doubt points, ground truth sheets and high detail topographic maps containing access points were prepared and sent to the Algerian partners for ground verification, since it was not possible to have access to the study area, from socio-political reasons.

In the figures below, examples of the land cover sheet (figure 21), topographical access maps (figures 22 and 23) to doubt points, location and attributes and ground truth photographs of verified points (figures 24-26) are given. The access maps are reproduced in 1: 40 000 scale and doubt points are highlighted in colours varying from green to red denoting priority and importance of their description: red - high priority, yellow-medium priority, green-low priority. The location of the points were chosen based also on accessibility of infrastructure.

A	B	C	D	E	F
Id	LULCcode	Descriptio	REAL CODE	Verità a terra	Immagine
0	3322	3322 Bare soils/3332 Sparse vegetation on rocks	24312	Terreno preparato per orticoltura /colture annuali	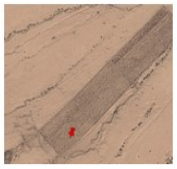
1	2414	4114Saline inland marshes/2432Visible cultivation pattern, not srouted vegetation	242	Zona salata (El Maleh); Secondary palmeraie; Vegetazione sparsa	
2	2413	2413Palms with greenhouse, maraichers/2222secondary oasis	2413Palms with greenhouse, maraichers	Secondary palmerie con colture sotto serra	
3	2414	2414Discont arable with palm nurseries/2432Visible cultivation pattern, not srouted vegetation	2414	Suolo in preparazione per arboricoltura	
4	1122	1122Discont urban fabric with Palms/1111areas of urban centers	1111areas of urban centers	Giardino pubblico	

Figure 21. Extract example of the "Land cover validation sheet" employed for the Biskra area ground truth

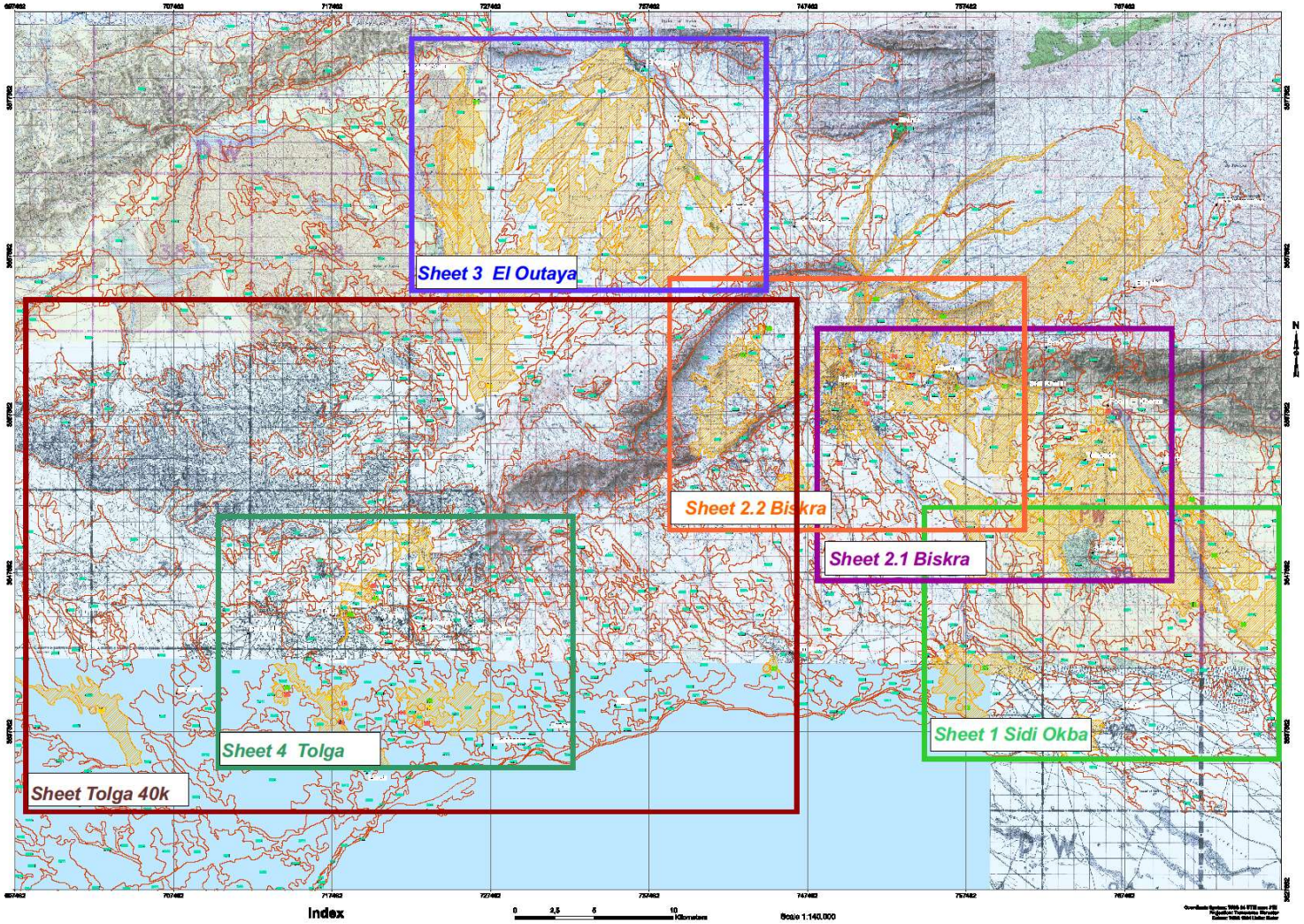

Figure 22. Index of <u>all</u> ground truth maps containing ground truth points for the interpreted land cover map.

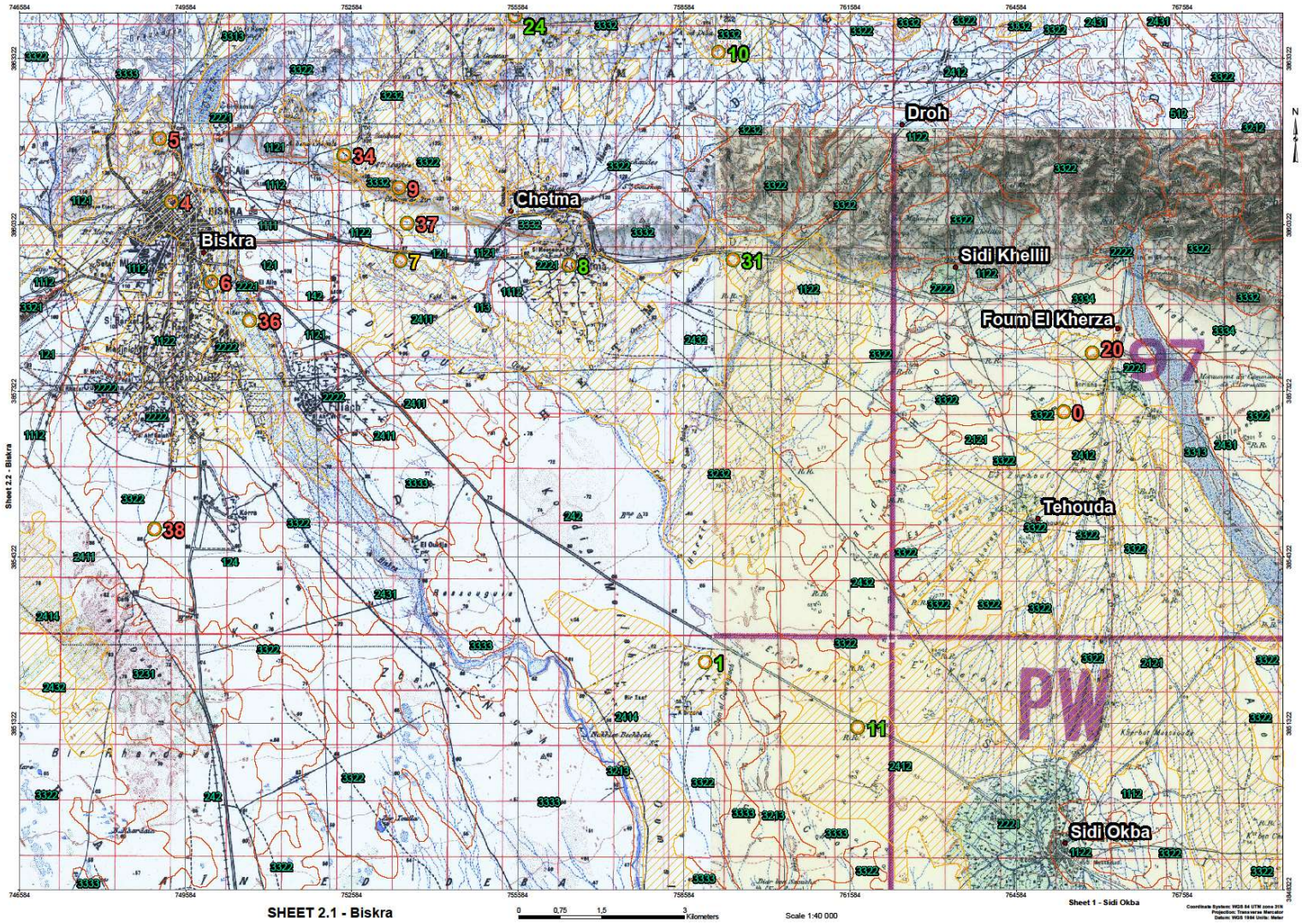

Figure 23. Example of a ground truth map sheet prepared for ground verification. Doubt points are highlighted in colours varying from green to red denoting priority and importance of their description: red - high priority, yellow-medium priority, green-low priority

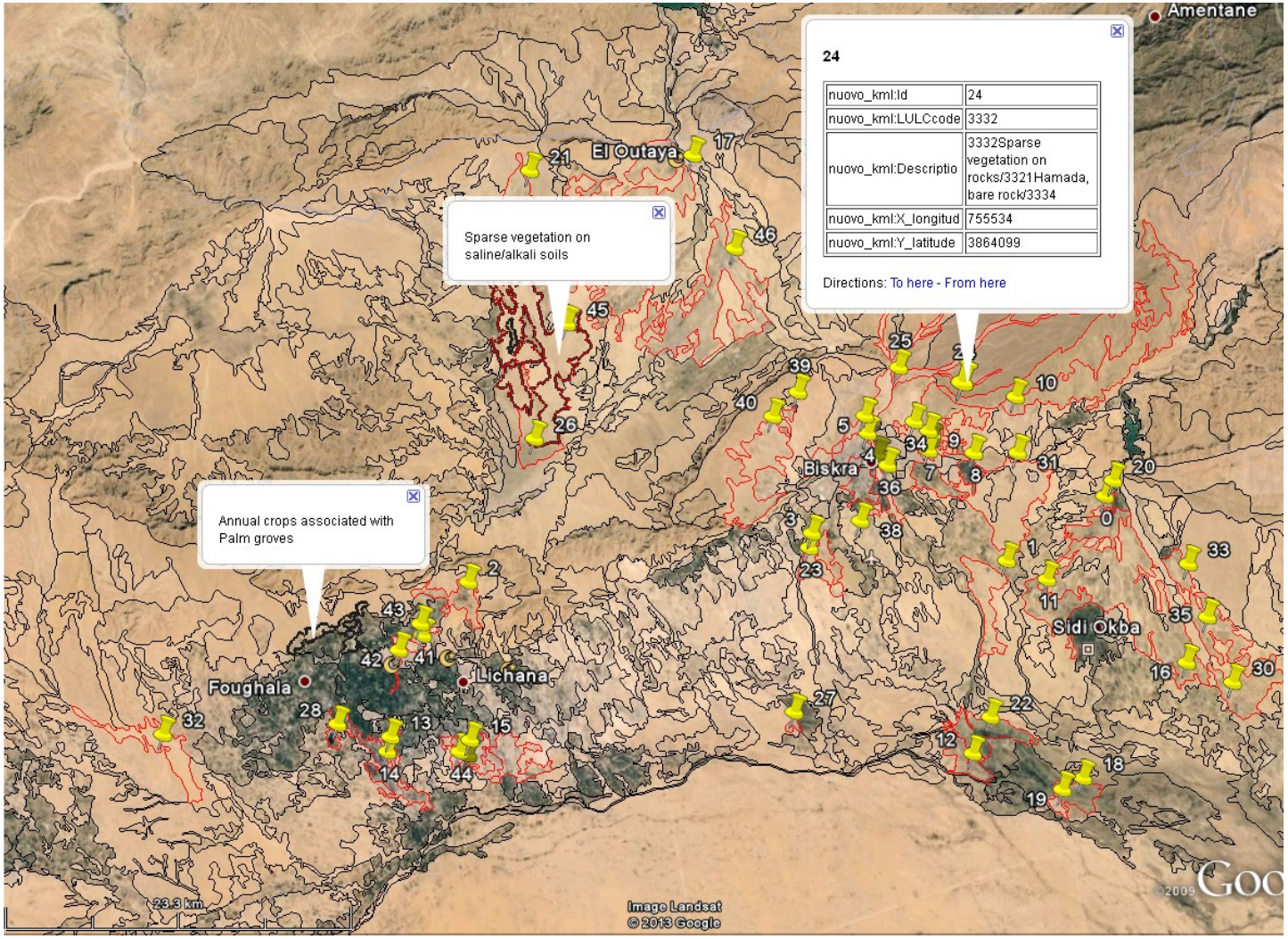

Figure 24. Ground validation points. Google image used only for visualization easiness purposes.

Figure 25. Example of ground truth photographs related to point 34 in figure 48

Figure 26. Ground truth photographs: examples of crops and land use correspondent to point 43 in figure 48

4.3.2. Oum Zessar

For the Oum Zessar area, the interpretation phases respected the same workflow as described for Biskra area. Below, examples of various phases are given, such as digitalisation phase (figures 27 and 28), example of one type of ancillary data employed for the better understanding of possible land cover types (figure 29, where olive trees are visible, not distinguishable from Landsat images), and finally the example of complete digitalization of the Oum Zessar study area, with established land cover classes, before ground truth validation and conversion to land use.

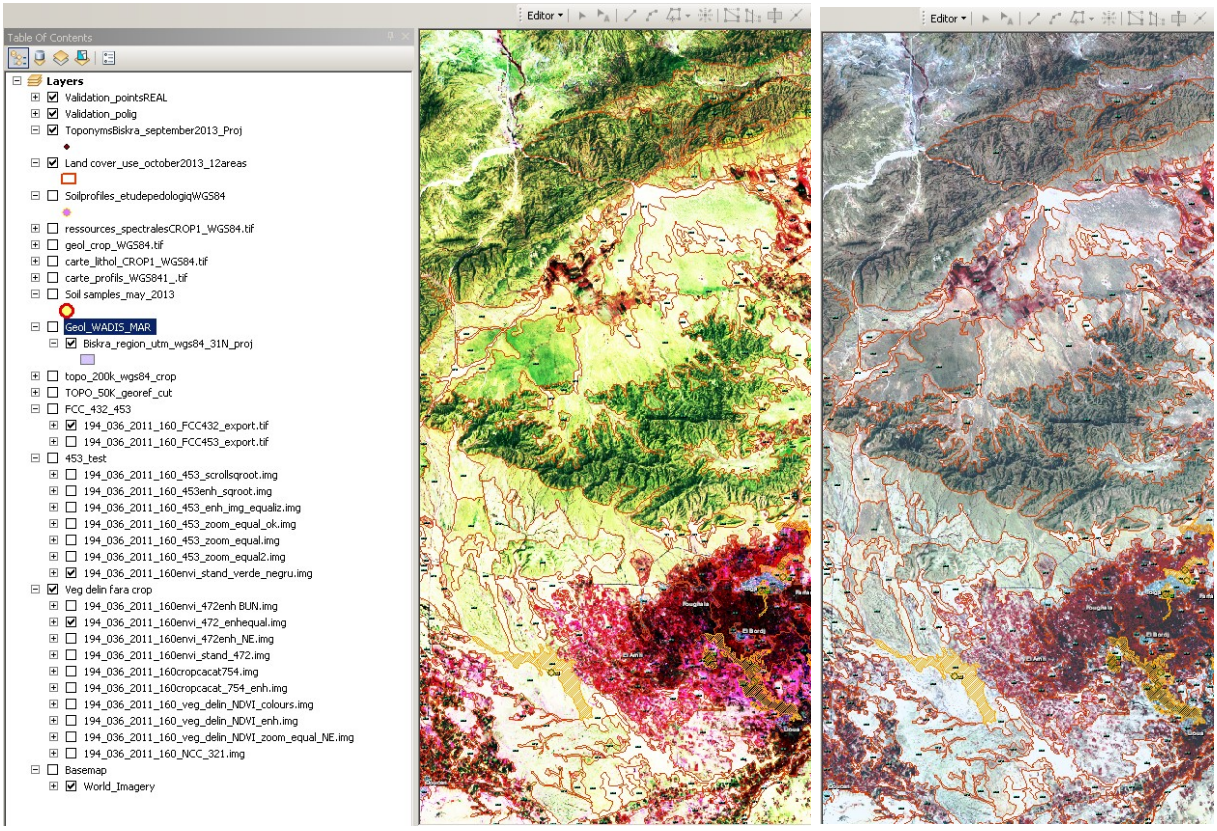

Figure 27. Example of interpretation phase, using FCC 432 Landsat TM bands with histogram stretch

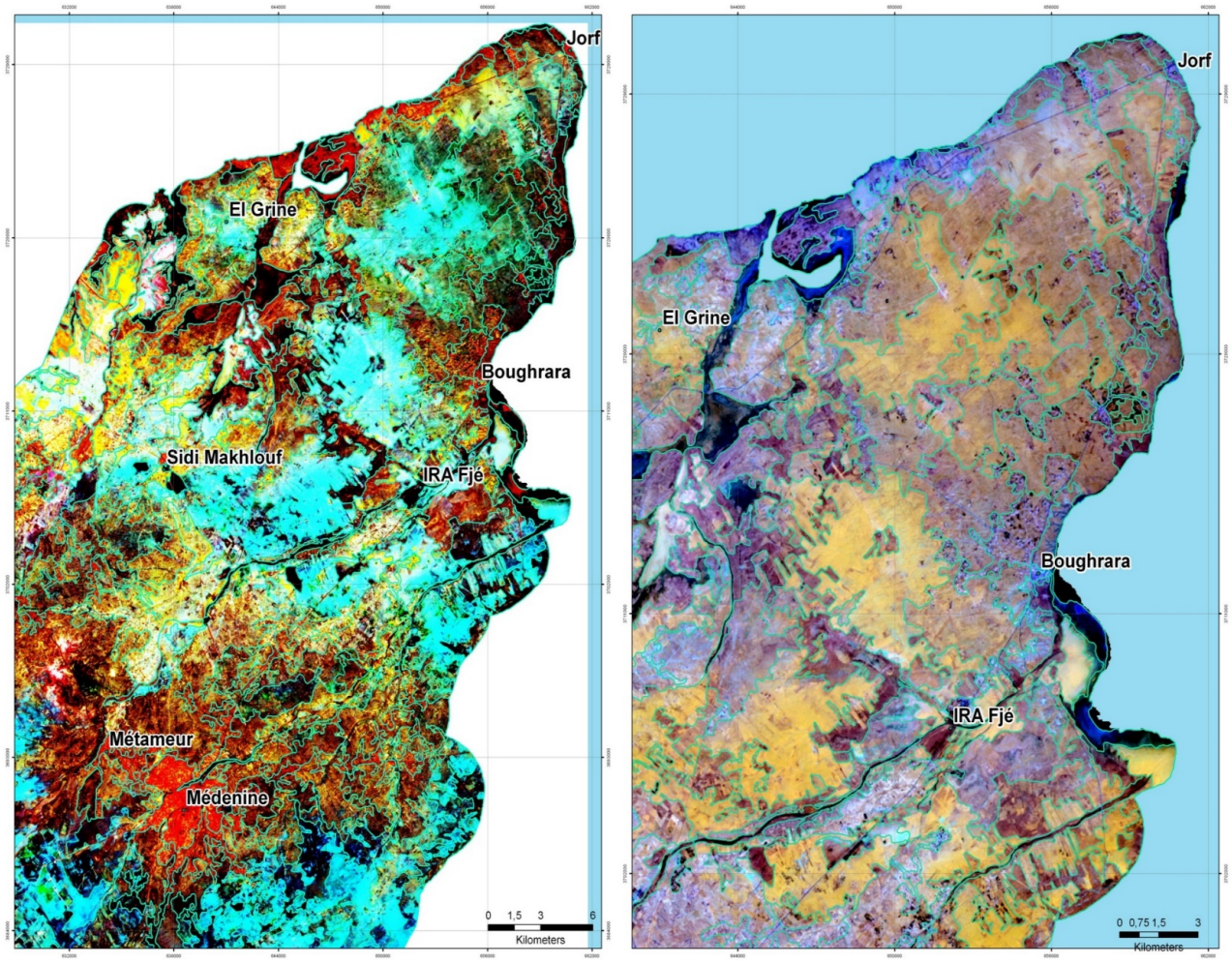

Figure 28. Example of interpretation and digitalisation phase, using FCC 256 (stretched) and 752 Landsat 8 bands with histogram stretch

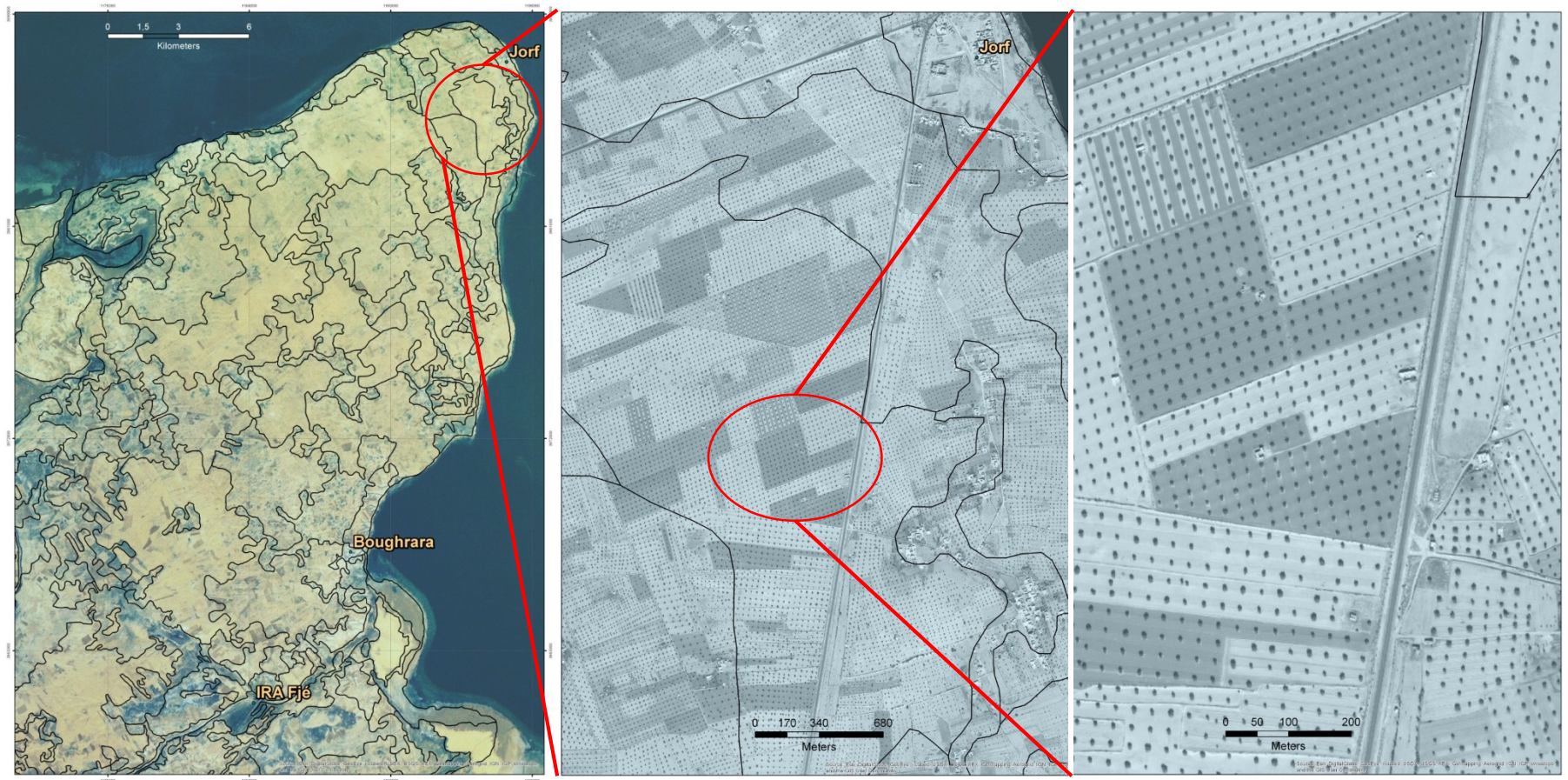

Figure 29. Example of use of ancillary data: visual inspection of previously digitalized polygons overlaid to Quickbird (Google Earth) images in order to understand the type of crops or land use. GE images were used only for visual inspection, since only Landsat data was used for digitalization or polygon boundaries adjustment.

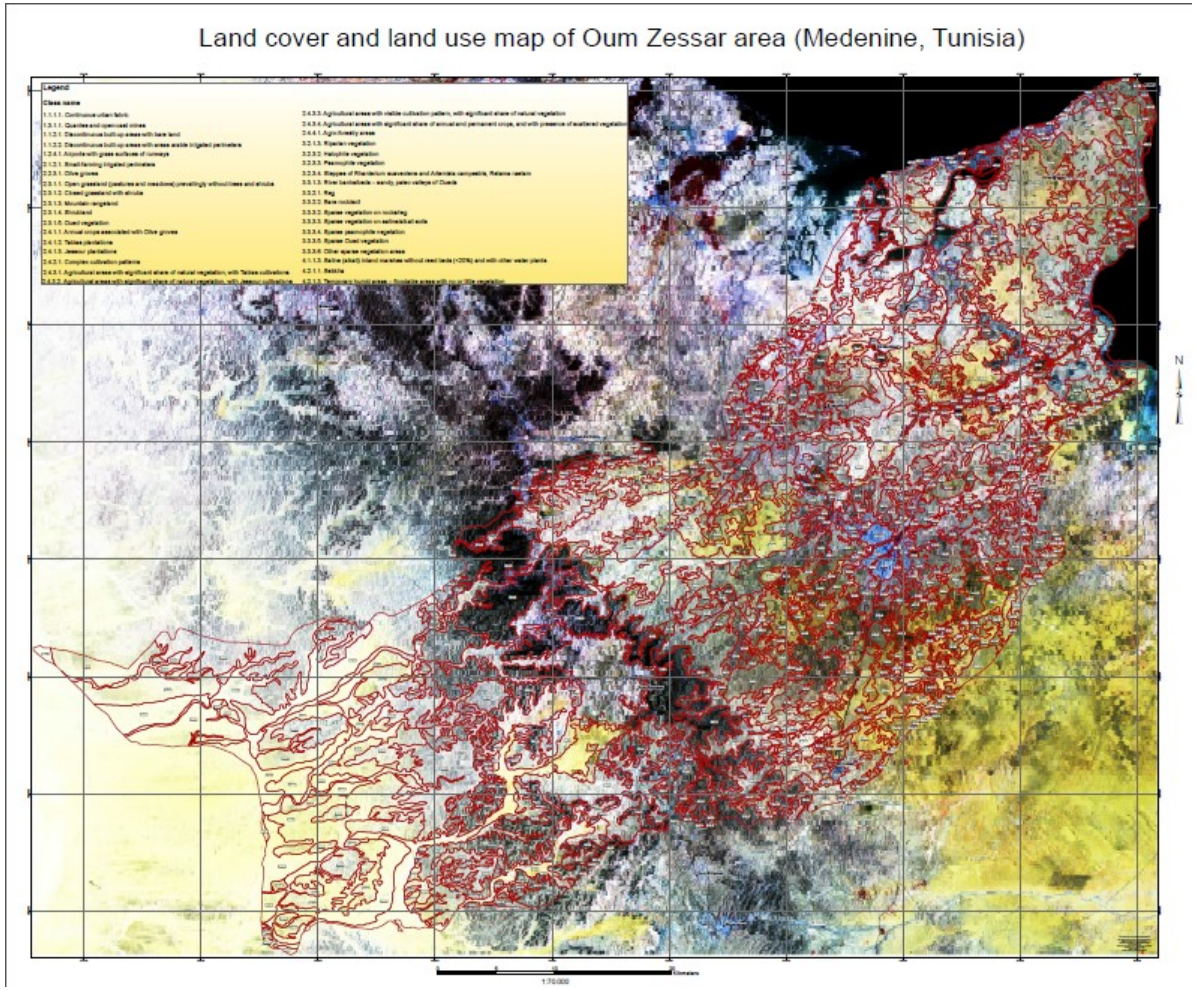

Figure 30. Complete digitalization of the Oum Zessar study area, Tunisia before ground truth validation

4.3.2.1. Ground truth and conversion to land use

The undertaken field research is an important step in the current study. The land cover features and their specific multi – temporal analysis represent a valuable information level, thus tributary to the management of resources according to a plan of economic and political development.

The conversion to land use was possible only through ground truth information, especially because our aim was to obtain a high precision of class nomenclature and description, up to the fourth level-equivalent of CORINE land cover.

Ground truth information was acquired in this areas in order to adjust previously interpreted land cover classes and, respectively, to compare with spectral signatures from satellite images in order to identify them and assess changes of their spatial distribution in time.

4.3.2.1.1. Internship at the Institut des Regions Arides

In the first two weeks at IRA headquarters there have been scheduled several meetings with local experts in order to address each geographical component individually, consult the bibliographical material provided by the local library and understand the studies that each laboratory was undertaking for eventual similarities and searching contribution or collaboration opportunities.
The following meetings were held with the main experts of the main laboratories, with material collecting and guidance on the land cover and geomorphological field data collection:

- The Eremology and Combating Desertification Laboratory: Prof. Mohamed Moussa – expert in pedology and biodiversity.
- The GIS Laboratory: Amar Zerrim – expert in spatial analysis and thematic mapping; Messaoud Guied – field technician, Pedological laboratory assistant; Mongi Ben Zaied – expert in hydrology, erosional processes and spatial data analysis; PhD Student Bouajila Essifi
- The Pedological Laboratory: Dalel Ouerchefani – expert in land degradation risk assessment, GIS and Remote sensing; Phd Student Ibtissem Enneb
- The Agronomical Laboratory: Prof. Naggaz Kemel – for agronomical data and consultation.
- The Aeolian Erosion Laboratory: Prof Mohamed Labiadh – for aerosol data and consultation.

- For climate data: Mondher Fetoui

There are two main types of activities carried out during the mission:

Field work: scheduling activities for land cover ground truth and associating land use.

- Identifying and scheduling the proposed research activities in terms of priority: first and second week
- Overall acquaintance with the study area, planning, gathering local information and bibliography
- Preliminary verification of proposed land cover nomenclature
- Establishing the terms of field survey and (methods, location, means of transport, daily program)
- Ground truthing
- Verification of new data by consulting local experts

Office activity:

- Image processing methods study for supervised image classification (ENVI and IDRISI)
- Study of the sand encroachment phenomenon
- Bibliographical information collection
- Spatial data collection

The ground truth campaign was undertaken mostly during the last week of April and the month of May 2014, according to a stepwise methodology, in order to collect field information for the adjustment of polygon boundaries, interpretation keys and land cover nomenclature as well as class assignment of previously photo-interpreted land cover features using Landsat imagery.

The ground truth campaign was previously organized under the coordination of PhD Maria Teresa Melis and PhD Giorgio Ghiglieri. The field campaign activities were conducted on site by PhD Student Gabriela-Mihaela Afrasinei and supported by IRA technicians and experts: PhD Mohamed Ouessar, Amar Zerrim, Messaoud Guied and Omar Jlali.

The used material consisted of: compass, GPS-incorporated camera, (as shown in the figures 32 and 33), Mobile Mapper GPS with ArcPAd software installed (figure 34) for the collection of doubt points (figure 31) and on-site attribute compilation, land cover sheets (figure 37).

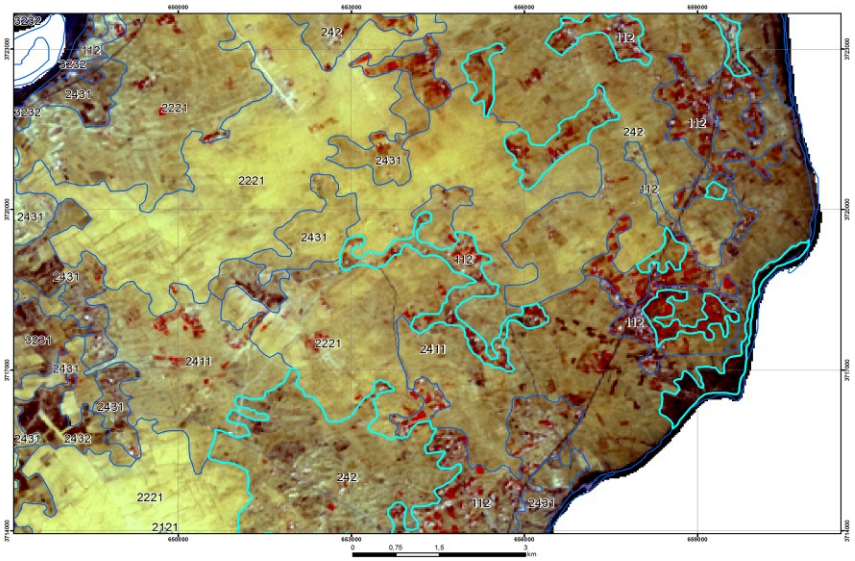

Figure 31. Example of interpretation doubt polygons (highlighted in blue turquois) in a small region of the study area, used for establishing doubt points to be verified in the field

Figure 32. Instruments used for ground truth data collection: GPS incorporated Photo Camera, compass, GPS

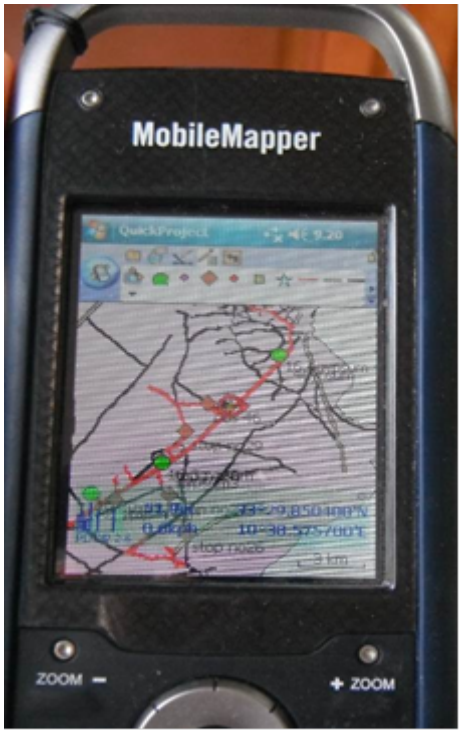

Figure 33. GIS software ArcPad installed on Mobile Mapper GPS; the visible loaded layers are: study area limit, GPS tracklog, doubt points, routes and toponyms, on site collected ground truth points (with attributes)

The collected points are classified as interest points and auxiliary observation points. The interest points represent points of doubt, with description containing:

- lithology
- geomorphological aspects: landform/processes/agents
- vegetation: physyignomy/main species
- land use: agriculture/main crops/rotation/afforestation
- soil: texture/salinization
- land cover facets
- other information/data/sketch

The photographs for each point are panoramic (3 panoramic photos for the 360 degrees view), as seen in figure 35 with the specification of compass Northing angle of the left starting part of the first photograph and photographs of particular details (soil texture, presence of salt efflorescence, vegetation) with dimension mark (usually a pen, figure 36).

Figure 34. Example of overall landscape, panoramic photos taken for doubt point description, with the specification of the North angle direction of the starting point of first photo: N120.

Figure 35. Examples of photos of details of various landscape components, relevant for the current study

Institution

Name AGM

Email

LAND COVER

Ground Truth Sheet

Stop no 1.

Date 7.04.2014	Surveyors G Mărăsineț	Location Midway Kautine - Hamet
GPS Lat 33,4219	GPS Long 10,3671	GPS file Quick project 04042014
Altitude ~~164~~ 152,6 m	Projection Geographic lat/long WGS-84	

Photo no.	Orientation (compass)	Photo no.	Orientation
8927 - 8928	start N150	8941 - 8943	N 240
8931 - 8932	start N195	8946 - 8950	observations
8933 - 8939	N 110	8988	right - N???

Geophysical aspects (relevant information)

Bedrock : triasic, ~~evoluat~~ arenaria, (strato argilla sottile) overlaid by silt -> limon de epandage recent

Oued terrace - upper (interfluviu) + confluență

graminaceae, veg steppic

land use: main = pasture; sec -> agr;

Describe in terms of geology:lithology/structure; geomorphology:landform/processes/agents/flooding -> Oued; vegetation: physiognomy/main species; land use: agriculture/main crops/ rotation/ afforestation; soil: texture/salinisation etc

Possible Land cover class/es:photo-interpreted	Field observation: land cover description	
Land Facet #1 - Name Description	Steppic veg.; grassland with shrubs, graminaceae	~~60~~ %
Land Facet #2 - Name Description	Arable area - grain (along oued), surrounding area	20 %
Land Facet #3 - Name Description	Olives - jessour	20 %
Land Facet #4 - Name Description		%

Other information/data/sketch

Land use - within the oued bed - pasture

- on the river banks and terraces -> jessour -> olives and agriculture on ~~sa~~ surrounding area.

- dopo il gabbione, -> scarpata di erog fluviale.
- tabias are much smaller than jessour; usually used by small farmers
- jessour have also gabions?

Figure 36.Example of land cover sheet (Oum Zessar area, Tunisia)

At the end of each day, the data from the GPS was downloaded and organised into individual folders, containing corresponding photos and point shapefile, mostly in order to prevent loss of data or overwrite.

Once the field campaign has concluded, all the shapefiles collected individually per day have been merged together and it has been proceeded to the verification of data, comparing GPS collected data attributes with the descriptions of the land cover sheets and filling in missing information observed in the field, creating columns such as "Field_LU" (field land cover), "Field_lith" (field lithology), "Field_morp" (field morphology), "Field_pedo" (field pedology), "Location", per each interest point. For each point, either interest or auxiliary information, there have been also verified the photographs, whether description in "Comments" field matches with observable features in the photo.

For each point, with few exceptions, there is the field "Photos" in which there are specified the names of the corresponding photos with the North angle direction. In the "Comments" column, there are also comments on detail photos, such as close-ups of salt efflorescence or particularities of specific species of interest such as psamophytes, halophyte or pelophyle.

This step was necessary in order to separate the photos with no/incorrect coordinates or shifts greater than 100m, considering that the final land cover map is in 1:100 000 scale. The verified photos were consequently imported to ArcGIS 10.2. through the tool *GeoTagged Photos to Points* from *Data Management* Tools which allows the creation of points with primary attributes of the camera GPS and with hyperlinked and attached photos to each point.

The results consist in a ready-to-use database of 450 observation points (figures 38-40) divided in primary points (with Land cover Sheet full description containing notes on lithology, geomorphology, vegetation, land use, soil, land cover facets and other information) and auxiliary observation points. The auxiliary observation points are generally points of particularities, such as surface wells, factories, vegetation species, salt efflorescence, outcropping of geological formations or geological structures, very helpful for the verification of interpreted data as they are well distributed within the territory, covering 80% of it, as shown in figure 38.

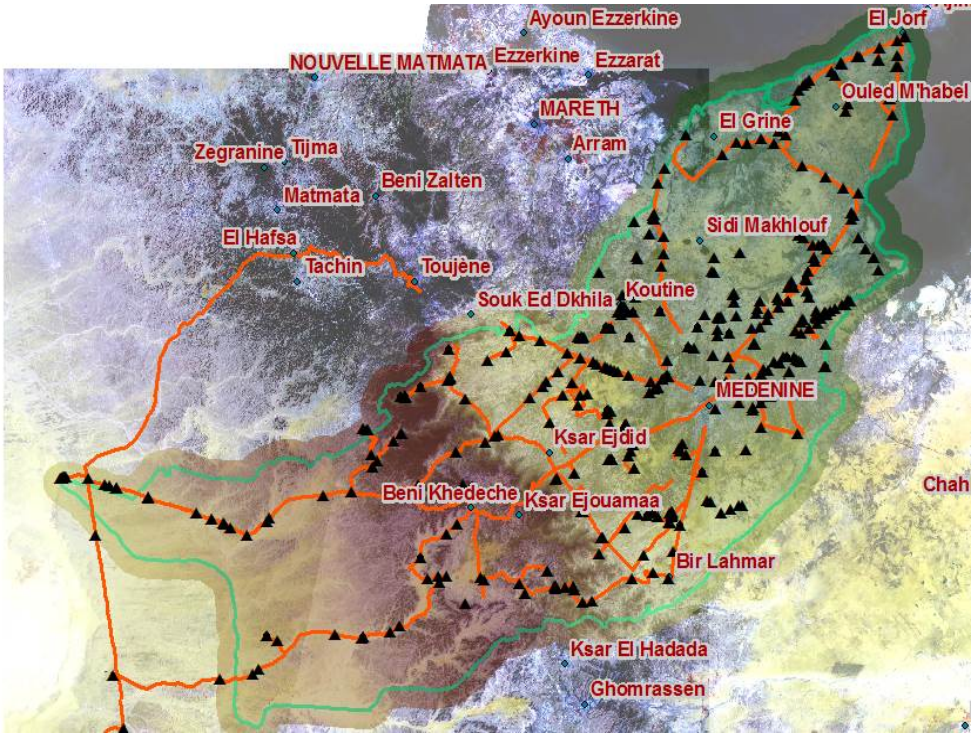

Figure 37. Collected field data, consisting of two entities: linear (tracklog, in red) and point data with description (black triangles)

Shp_7apr_22may_2014_32N

OBJ	Shap	NAME	CA	DATE	Attach	COMMENTS	PHOTO	ELEVA	X	Y	Field_LC	Field_LU
11	Point	stop no26		05/05/2014	yes	GT sheet26, Oued Medenine, sebkha	N100, panoram f0602-0604;	74,85	10,622279	33,428136	natural vegetation with areas of	pasture and agriculture
12	Point	stop no27		05/05/2014	yes	GT sheet27	N30, panoram f(110)0615-17	66,97	10,613534	33,448696	closed grassland with sparse ar	pasture and arboriculture, ce
13	Point	stop no28		05/05/2014	yes	gypsum crystalization	f0619-0620;f0621-0624-halo	60,84	10,609374	33,46723	arable land, olive groves	discontinuous urban with ara
14	Point	stop no29		05/05/2014	yes	GT sheet 29; gypsum	f0640-0641-soil observation,	43,87	10,620537	33,483823	steppe,open shrubland, olive par	pasture and arboriculture
15	Point	stop no30		05/05/2014	yes	GT sheet 30	f0649-0656-panoramic;N290	83,21	10,587063	33,445635	irrigated perimeter	maraichere and arboriculture
27	Point	stop	5	05/06/2014	yes	Oasis Metameur, main supplier for ve	N252 f0760, panoramic	134,64	10,428523	33,364532	annual crops, greenhouses, veg	agricultural
41	Point	stop5	1	04/07/2014	yes	sparse shrub	f9010-9015, f9020-9023	170,62	10,337627	33,413006	open grassland with bushy veget	pasture
42	Point	observatio	2	04/07/2014	yes		PHOTO_20140407_161844.j	177,44	10,338899	33,413347	olives, figues	arboriculture, ploughed land
43	Point	stop4	1	04/07/2014	yes	Oued Ennaued	N164-PHOTO_20140407_13	173	10,336794	33,413764	natural vegetation, retma reteam	pasture
44	Point	stop no2	1	04/07/2014	yes	GT sheet2	f8957-8973	166,64	10,370108	33,421418	closed grassland, jessour and ta	pasture, arboriculture
45	Point	stop no1	1	04/07/2014	yes	GT sheet1. steppic oued vegetation	N50-f8972-8928; N95-f8931/	152,6	10,367132	33,421907	graminaceae and shrub vegetatio	pasture
46	Point	stop no3	1	04/07/2014	yes	GT sheet 3; tabias on the other opposi	f8974-gypsum, f8975-8985	147,32	10,366353	33,422753	wheat, natural grassland and shr	cerealiculture, pasture
51	Point	obs		05/07/2014	<Null>	surface well ,Khlifa Benammaer, culti		124,85	10,494986	33,394051	irrigated area	agriculture
61	Point	agricult	5	05/07/2014	yes	irrigated perimeter, cucurbitaceae, oliv	f1299 N96	87,95	10,521951	33,445288	irrigated perimeter	agriculture
64	Point	stop	5	05/07/2014	yes	grenadier, fig, arboriculture with olive	1342-48	106,12	10,51531	33,415495	irrivated private perimeter	arboriculture
65	Point	obs		05/07/2014	yes	private irrigated perimeter	f1431-37 start N240	71,43	10,622173	33,423544	irrigated perimeter	
68	Point	stop	5	05/07/2014	<Null>	natural closed grassland	f1610-6 N104	198,99	10,32462	33,369798	closed grassland	pasture
72	Point	stop no6	3	04/08/2014	<Null>	oued arnien riverbed	PHOTO_20080101_140233.j	153,29	10,388901	33,327245	open grassland with shrubs	pasture
79	Point	stop no7	1	04/08/2014	<Null>	GT sheet7; agricult olive nursery	N140-f9080;N90-f9081;N210	165,46	10,390958	33,326536	arable land, irrigated maraichere,	cultivation
81	Point	observatio	1	04/08/2014	<Null>	gypsum pseudo	start panoramic N56 f9120-f	162,13	10,367632	33,342794	shrub dense vegetation, open gr	pasture
82	Point	stop no9	1	04/08/2014	<Null>	GT sheet9; gypsum pseudo	N68 f9130;f9134-f9140-detai	172,82	10,366968	33,34273	ploughed land, olive plantation	arboriculture
94	Point	stop no11	1	04/09/2014	<Null>	GT sheet11	f9283 strt N90 end N190	204,37	10,371578	33,294972	olive,fig, almond nursery, private	agriculture,pasture and arbor
96	Point	stop no10	2	04/09/2014	<Null>	GT sheet10; left oued terrace, closed	N276-f9147;panoramic N234	186,21	10,442683	33,241728	arboriculture(almond, pistache, oli	pasture and arboriculture wit
196	Point	obs		05/13/2014	<Null>			177,26	10,349816	33,389432	closed grassland with small dens	
199	Point	stop	5	05/13/2014	<Null>	olives	f2995 N10	196,72	10,286255	33,411181	olive groves	agriculture
220	Point	stop	5	05/13/2014	<Null>	potatoes	strt N120, 3403	204,61	10,288267	33,367021	irrigated perimeter	agriculture
229	Point	stop	5	05/13/2014	<Null>		f3422	149,47	10,420041	33,370599	closed grassland	pasture
257	Point	stop	3	05/15/2014	<Null>	f3669-N280; veg artemisia erba alba p	f3669-N280	529,35	10,077258	33,326558	steppic vegetation, artemisia herb	pasture
428	Point	stop19	5	04/29/2014	<Null>	peach, orange, almond, olive cultivatio	puit f 0192 start N001, f0192	138,17	10,399059	33,436914	private irrigated perimeter, discon	agriculture
460	Point	stop	5	04/30/2014	<Null>	sheet	f 0488-495 N 250	119,59	10,565072	33,354463	steppic vegetation, olive plantatio	pasture, agriculture
461	Point	stop puit	5	04/30/2014	<Null>	small irrigated arboricult privat,		142,51	10,537978	33,365167	irrigated perimeter	
468	Point	stop no8	1	04/08/2014	<Null>	GT sheet8, oued Gatar	N356 f9117;N28 f9118;N70 f	192,03	10,36885	33,341553	open grassland with sparse shru	pasture, tabias

Figure 38. Example of field collected data transfer from Land Cover Sheets into attribute table in GIS environment

Field_LU	Field_lith	Field_morp	Field_pedo	X_UTM	Y_UTM	Location
pasture and agriculture	Quaternary conglomerate	left river terrace, rill erosion on river bank	alluvional sandy loam, calcareou	650818,386532	3699928,23326	
pasture and arboriculture, ce	loam and gypsum conglomerates	medium terrace	sandy loam, calcareous encrust	649969,871949	3702195,30923	
discontinuous urban with ara	recent alluvional and aeolian deposits	inferior terrace	alluvional deposits, gypsum comp	649551,391659	3704244,50361	
pasture and arboriculture	loam and gypsum conglomerates	medium terrace	loam, gypsum component	650560,050927	3706100,52828	
maraichere and arboriculture	aeolian and alluvuinal deposits	inferior terrace	aeolian and alluvinal deposits	647514,472049	3701818,05537	
agricultural	red clay and conglomerates	Oued riverbed	sandy soil with red clay beneath	632900,704023	3692611,42031	
pasture	red clay and conglomerats	upper terrace	clayey sandy loam	624374,557907	3697873,89376	Oued Ennaoued
arboriculture, ploughed land	recent aeolian and alluvial deposits	inferior terrace	loam	624492,39857	3697913,24436	Oued Ennaoued
pasture	alluvial clasts,Sidi Stout Triassic sandston	detrital riverbed deposits	scheletic, mineral soil	624296,095934	3697956,96417	Oued Ennaoued
pasture, arboriculture	red clay and conglomerates, alluvial depo	Oued upper terrace	gypsum loam	627382,707686	3698845,96361	Oued Hallouf
pasture	Triassic sandstone outcropping	Oued medium terrace, confluence, fault a	loam, recent deposits	627105,225782	3698896,50495	Oued Hallouf
cerealiculture, pasture	gypsum conglomerats	medium terrace deposits	thin gypsum loam	627031,561889	3698989,41314	Oued Hallouf
agriculture				639037,515883	3695971,32588	Khlifa Benammaer
agriculture	conglomerates, red clay	interfluvium, medium terrace	loam, clayey soil	641462,409038	3701688,99431	
arboriculture	carbonatic	inferior terrace	schelethic, carbonatic soil	640893,229066	3698376,41453	
				650816,491333	3699418,80202	
pasture	conglomerates, red clay	interfluvium, medium terrace	loam, clayey soil	623226,029609	3693067,54537	
pasture	gypsum clay, recent aeolian and alluvial d	detrital riverbed deposits	gypsum clay	629269,318938	3688427,24443	Oued Arnien
cultivation	red gypsum clay and conglomerates	upper river terrace	aeolian and alluvial loamy deposit	629461,849334	3688351,20235	Oued Arnien
pasture	red gypsum clay and conglomerates	upper river terrace	aeolian and alluvial loamy deposit	627266,945776	3690125,12656	Oued Gatar
arboriculture	red gypsum clay and conglomerates	upper river terrace	aeolian and alluvial loamy deposit	627205,260685	3690117,18287	Oued Gatar
agriculture,pasture and arbor	alluvial depoits, red caly and conglomerate	oued medium terrace	sandy loam, alluvial deposits	627703,974269	3684827,48564	
pasture and arboriculture wit	alluvial depoits, red caly and conglomerate	oued medium terrace	loam	634406,476986	3679013,19851	Oued Hajer
				625541,99111	3695274,68126	
agriculture	alluvial and aeolian deposits	Oued Inferior terrace	loam, sandy soil	619600,118515	3697611,33396	
agriculture	Medium terrace deposits, conglomerates,	medium terrace	clayey loam	619847,794919	3692717,23153	
pasture	red clay and conglomerates	mediun terrace, interfluvium	loam, clayey soil	632102,371412	3693273,35798	
pasture	dolomites	slope deposits and residual reliefs	calcareous concretions	600262,933045	3688007,97644	
agriculture	alluvial deposits of inferior terrace, aeolian	Oued inferior terrace	loam, sandy soil	630051,422538	3700599,9537	
pasture, agriculture	oued and aeolian deposits	Oued inferior terrace	sandy, alluvial soil	645622,285304	3691677,51508	
				643083,63022	3692826,92908	
pasture, tabias	Matmata aeolian deposits and loam, calcar	riverbed	thin loam	0	0	Oued Gatar

Figure 39. Example of field collected data transfer from Land Cover Sheets into attribute table in GIS environment, prolongation of figure 16.

4.4. Proximal Sensing Analysis

4.4.1. Collection of Field Spectra

Spectral data was acquired *in situ* using the handheld ASD FieldSpec 3 Jr. Full Range (350 – 2500 nm) spectroradiometer and samples were taken for X-ray diffractometric analysis. The spectral campaign has enabled the acquisition of spectral reflectance measurements of 34 points, of which 14 points for saline surfaces (9 samples); 10 points for sand encroachment areas (10 samples); 3 points for typical vegetation (halophyte and psammophyte) and 7 points for mixed surfaces. During the land cover field campaign, special attention has been given also to these areas of salt and sand encroachment, respectively, as they are a limitation for the agriculture in the study area. Reflectance measurements were made about 1m above the object with the sensor facing the object within 25° FOV. The spectroradiometer was calibrated with white spectrum (Spectralon) before and during each observation in order to minimize the effect of change in sun illumination. The readings were made during stable wind conditions to avoid the effect of wind on spectral reflectance. The choice of spectral measurement points of the two types of surfaces, saline and sandy and of specific vegetation were chosen on the basis of a geomorphological analysis, ancillary data and a land cover/land use map specifically generated for this study employing Landsat 8 imagery.

A geomorphological schematic map has been created through the interpretation of satellite data, high accuracy DEM (real 1 arc second SRTM, newly released in 2014) and available geological data.

The obtained geomorphic classes are:

- *Slope deposits and residual reliefs*
- *Scree and alluvial fans*
- *Regressive erosional valleys, slope deposits*
- *Oued chaotic detrital riverbed deposits and river terraces*
- *Mountain watersheds*
- *Medium terrace deposits, clay, conglomerates or loam with a gypsum component*
- *Inherited aeolian deposits, calcareous crusts*
- *Coastline sand deposits*

- *Coastal plain*
- *Coastal dunes*
- *Active aeolian landforms and deposits*

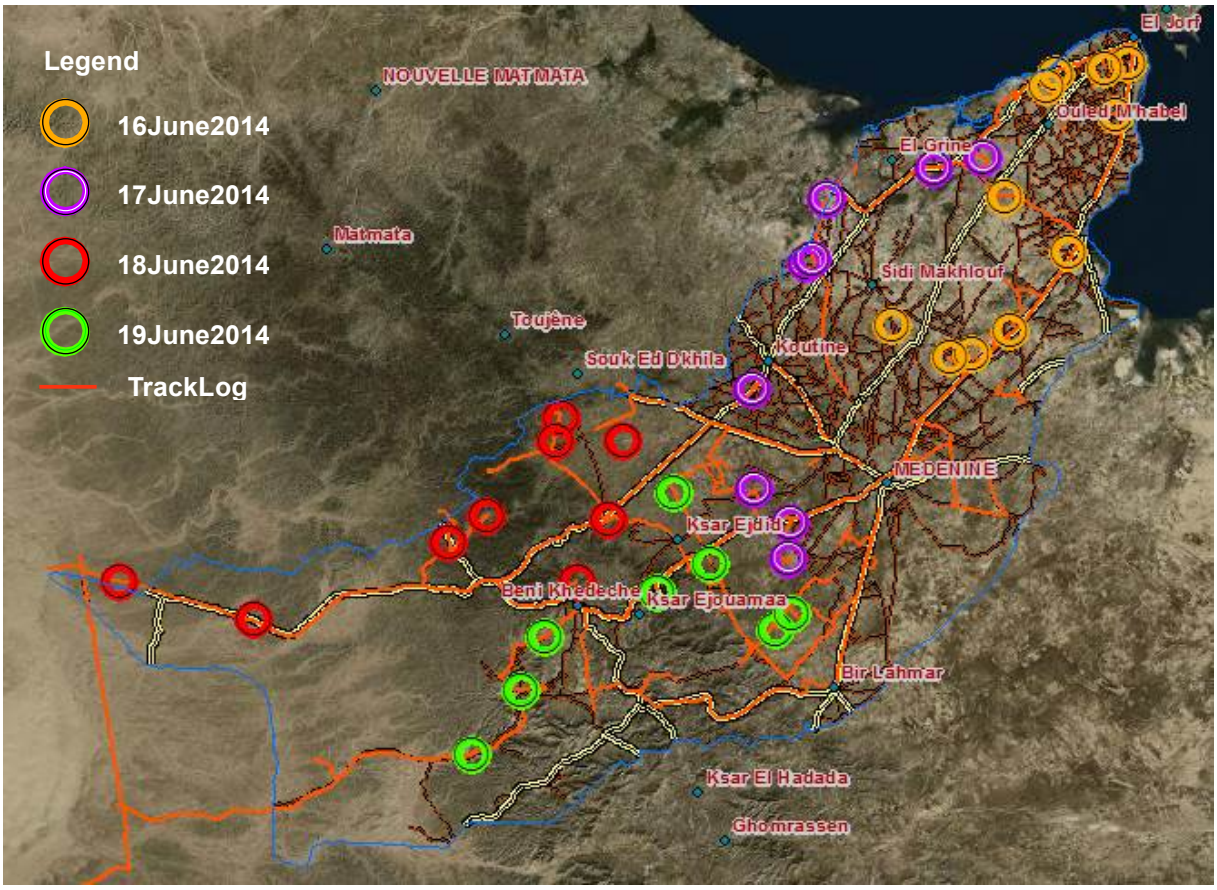

Figure 40. Spectroradiometric measurements: distribution of chosen target points. Colours indicate the points to be surveyed per each day.

the following equipment has been used for the spectroradiometric mesasurements:

- ASD FieldSpec 3 Jr. Full Range portable spectroradiometer and correspondent accessories (Spectralon reference panel, optic fiber, foreoptic, remote trigger)
- Ergonomic Pro-Pack with fiberoptic cable spool, instrument controller and battery pouch
- The belly board with laptop instrument controller and neck strap
- Instrument-linked Windows® 7 64-bit laptop as instrument controller
- Additional equipment: rolling tapes, compass, GPS receiver, plastic sampling bottles and paraffin liquid for the conservation of salt crystals.

Operational step on the field can be summarized as follows:

- Instrument equipment attachment to surveyor and testing
- On – site setting of the survey point (11cm diameter field of view according to 5^{o} foreoptic)
- The dark offset and white reference measurement
- Direct acquisition of reflectance spectra of the target sample to instrument controller (10 spectra recorded for each measurement)
- Compilation of Field Spectral measurements Sheet
- Photographs of targets and overall landscape.

The points of spectral measurement interest were divided in four days, with an average of 8 points per day, according to infrastructure, thus creating transects for time efficient and cost effective reasons. The point-entity shapefile was uploaded into Mobile Mapper GPS and was used as a navigator in order to reach each point directly.

Thus, upon a general inspection of the site, only the relevant points were then selected regarding the following features:

- gypsum crusts (inland), saline surfaces (near Sebkhas),
- ploughed mixed land of loamy-sandy soil with gypsum component,
- ploughed land of loamy-sandy soil with carbonate component
- sand accumulations/dunes in plain areas,
- sand accumulations/dunes in pre-desert areas
- sand dunes at the border of the Oriental Grand Erg
- Halophyte vegetation
- Psammophyte vegetation

These sets of spectral measurements were taken in order to create a spectral characterization of saline surfaces and sand encroachment areas, and the specific vegetation (halophyte, psammophyte) as it is very difficult to separate them spectrally from other land features. Detailed reports and spectral sheets have been employed in order to keep track of the collected data (figures 41 and 42).

Spectroradiometric measurements - detailed field report

Day 1:16-06-14

Departure at 7:00 am from Hotel El Ksour, Medenine

1 stop

Map: geological map of Medenine (1\100.000);
Age: Upper Pleistocene;
Lithology: silt, conglomerate, gypsum;
Measurements:
Dark offset and white reference measurement
1 point: 3 Measurements, 3 photos;
2 point: 3 Measurements, 3 photos;
3 point: 5 Measurements, 5 photos;
Landscape observation photos;
Samples: T1
Vegetation: sparse desert steppe;

2 stop

Map: Medenine (1\100.000);
Age: Upper Pleistocen;
Lithology: red silt, gypsum;
Measurements:
Dark offset and white reference measurement
1 point: 3 Measurements, 3 photos;
2 point: 3 Measurements, 3 photos;
Landscape observation photos;
Samples: T2,T3,T4;
Vegetation: sparse desert steppe, olive trees, palm trees;

3 stop

Map: Medenine (1\100.000);
Age: Upper Pleistocene;
Lithology: red silt, gypsum, conglomerate;

Figure 41. Detailed post-field report on the data acquired during field spectra collection

FIELD SPECTRORADIOMETER DATA

	Sample 3 Stop 2.1.
Campaign name	
Campaign description	
Investigator	Afrăsinei Gabriela
File path	
Capturing date	16.06.14
Capturing time	9:41
Latitude	1) 33° 26,9773 2) 33 26,9730 3) 33 26,9716
Longitude	10° 34,4896 10 34,4912 10 34,4741
Altitude	40m-45
Target homogeneity	
Landcover type	natural veg, big bushy veg, but sparse Ph.1641 - Fuji
Spectrum name	
Target type	gypsum crust (oxydized)
Pictures HIKON	1) 1056 2) 1057 3) 1058
Hand sample	T2
Sensor zenith angle	0°
Sensor azimuth angle	90°
Sensor distance	1 m.
Illumination zenith angle	
Illumination azimuth angle	~~90°~~
Illumination distance	~~1m~~
Number of averaged spectra	10
White reference	OK
White inter-calibration	
Sensor	
Instrument	
Instrument calibration number	
Foreoptic	
Illumination source	
Sampling environment	
Measurement type	
Measurement unit	
Goniometer model	
Cloud cover	50%.
Ambient temperature	
Air pressure	
Relative humidity	
Wind speed	
Wind direction	
Auto number	
User comment	- reddish loam, fine texture (very) - gypsum crust of 10-20cm thickness - sparse desert veg.
Spectral file name	1) 00281-290 2) 291-300 3) 301-310
File format	
Data structuring info	

Ph 1059 Hikon - vegetation

TeleGIS Laboratory
University of Cagliari
telegis@unica.it

- on some gypsum crusts -> black coloured alteration characteristic
- also olives and Palms in surrounding areas

Figure 42. Example of field spectroradiometric measurement sheet for measurement sample/target 3, stop 2.1. For each target, 3 measurements are taken in three different points and their each single set of coordinates is stored as it can be observed in the sheet.

Measrm_No	Stop	Sample	Photos	Y_DDDD	X_DDDD	Z	Target	Date	Time
1.1	1.1			33.4460	10.554	45		16-06-14	8:36:00 AM
1.2	1.1			33.4462	10.554	45		16-06-14	
1.3	1.1			33.4460	10.554	45		16-06-14	
2.1	1.2	T1	Nikon 1051, 1054, 1055	33.4458	10.553	45	fine loam, conglomerates, gypsum crust	16-06-14	8:55:00 AM
2.2	1.2			33.4458	10.553	45		16-06-14	
2.3	1.2			33.4460	10.553	45		16-06-14	
3.1	2.1	T2	Nikon 1056	33.4496	10.575	43	gypsum crust, oxydised	16-06-14	
3.2	2.1			33.4496	10.575	43	gypsum crust, oxydised	16-06-14	
3.3	2.1			33.4495	10.575	43	gypsum crust, oxydised	16-06-14	
4.1	2.2	T3	Nikon 1060, 1061	33.4512	10.574	45	gypsum crust	16-06-14	
4.2	2.2			33.4512	10.574	45	gypsum crust	16-06-14	
4.3	2.2			33.4512	10.574	45	gypsum crust	16-06-14	
5.1	2.3	T4	Nikon 1066	33.4517	10.574	45	sand dune	16-06-14	
5.2	2.3			33.4517	10.574	45	sand dune	16-06-14	
5.3	2.3			33.4517	10.574	45	sand dune	16-06-14	
6.1	3			33.5294	10.666	10	gypsum crust	16-06-14	11:20:00 AM
6.2	3			33.5293	10.666	10	gypsum crust	16-06-14	
6.3	3			33.5292	10.666	10	gypsum crust	16-06-14	
7.1	4		0	33.6387	10.713	8	carbonate	16-06-14	12:18:00 PM
7.2	4			33.6386	10.713	8	carbonate	16-06-14	
7.3	4			33.6387	10.713	8	carbonate	16-06-14	
8.1	5			33.6759	10.702		salt	16-06-14	1:02:00 PM
8.2	5			33.6757	10.702		salt	16-06-14	
8.3	5			33.6756	10.702		sand	16-06-14	
9.1	6	T5	Nikon 1088, 1089	33.6726	10.656	10	50m loam	16-06-14	3:02:00 PM

Measrm_No	Stop	Sample	Photos	Y_DDDD	X_DDDD	Z	Target	Date	Time
9.2	6			33.6726	10.656	10		16-06-14	
9.3	6			33.6726	10.656	10		16-06-14	
10.1	7			33.6114	10.612	11	sal crystals on top	16-06-14	3:40:00 PM
10.2	7			33.6624	10.649	11		16-06-14	
10.3	7			33.6623	10.649	11		16-06-14	
11.1	8	T6	Nikon 1108, 1109	33.6674	10.646	10	salt efflorescence	16-06-14	4:00:00 PM
11.2	8			33.6675	10.646	10	salt efflorescence	16-06-14	
11.3	8			33.6675	10.646	10	salt efflorescence	16-06-14	
12.1	9	T7	Nikon 1114, 1115	33.6447	10.599	9	sebkha	16-06-14	4:36:00 PM
12.2	9			33.6447	10.599	9	sebkha	16-06-14	
12.3	9			33.6446	10.599	9	sebkha	16-06-14	
13.1	A.1	T8	Fuji 116-6281/82	33.4987	10.623	14	sandy soil with efflorescence	18-06-14	8:37:00 AM
13.2	A.1			33.4987	10.623	14		18-06-14	
13.3	A.1			33.4987	10.623	14		18-06-14	
14.1	A.2			33.4986	10.623	14	dry vegetation	18-06-14	8:55:00 AM
14.2	A.2			33.4987	10.623	14		18-06-14	
14.3	A.2			33.4987	10.623	14		18-06-14	
15.1	A.3			33.4982	10.623	14	haloclinum, healthy halophyte	18-06-14	9:06:00 AM
15.2	A.3			33.4982	10.623	14		18-06-14	
15.3	A.3			33.4982	10.623	14		18-06-14	
16.1	A.4	T9	Fuji 6313/14	33.4983	10.623	14	reddish clay with salt efflorescence/gypsum	18-06-14	9:18:00 AM
16.2	A.4			33.4884	10.623	14		18-06-14	
16.3	A.4	T10	Fuji 6317/18	33.4982	10.623	14		18-06-14	

Measrm_No	Stop	Sample	Photos	Y_DDDD	X_DDDD	Z	Target	Date	Time
17.1	B.1			33.5807	10.591		reddish clay with salt efflorescence/gypsum	18-06-14	10:15:00 AM
17.2	B.1			33.5746	10.607			18-06-14	
17.3	B.1			33.5746	10.607			18-06-14	
18.1	B.2			33.5747	10.607		gypsum crust	18-06-14	10:36:00 AM
18.2	B.2			33.5747	10.607			18-06-14	
18.3	B.2			33.5747	10.607			18-06-14	
19.1	B.3			33.5747	10.608		Salt efflorescence	18-06-14	10:44:00 AM
19.2	B.3			33.5746	10.608			18-06-14	
19.3	B.3			33.5746	10.608			18-06-14	
20.1	C.1	T10b	Fuji 6351/52/53	33.5948	10.458	20	gypsum crust doubt	18-06-14	11:29:00 AM
20.2	C.1			33.5948	10.457	20		18-06-14	
20.3	C.1			33.5949	10.457	20		18-06-14	
21.1	C.2	T11	Fuji 6358/59	33.5948	10.458		gypsum crystalls, sebkha	18-06-14	11:40:00 AM
21.2	C.2			33.5948	10.458			18-06-14	
21.3	C.2			33.5948	10.458			18-06-14	
22.1	D.1			33.4763	10.497	60	gypsum crust, sebkha	18-06-14	12:29:00 PM
22.2	D.1			33.4763	10.497	60		18-06-14	
22.3	D.1			33.4763	10.496	60		18-06-14	
23.1	D.2	T12	Fuji 6377/78	33.4811	10.511	49	sand encroachment	18-06-14	12:50:00 PM
23.2	D.2			33.4811	10.511	49		18-06-14	
23.3	D.2			33.4811	10.511	49		18-06-14	
24.1	E.1			33.2426	10.402	181	regolith, carbonate	18-06-14	5:37:00 PM
24.2	E.1			33.2426	10.402	181		18-06-14	
24.3	E.1			33.2426	10.402	181		18-06-14	

Measrm_No	Stop	Sample	Photos	Y_DDDD	X_DDDD	Z	Target	Date	Time
25.1	A.1			33.3226	10.079	461	reg, clacareous concretions, structural surface of Cretacic	19-06-14	8:47:00 AM
25.2	A.1			33.3226	10.078	461		19-06-14	
25.3	A.1			33.3226	10.078	461		19-06-14	
25.4	A.1			33.3226	10.078	461		19-06-14	
26.1	B	T13	Nikon 1203/04	33.2640	10.019	338	sand dune, aeolian deposit	19-06-14	10:07:00 AM
26.2	B			33.2474	10.019	338		19-06-14	
26.3	B			33.2641	10.02	338		19-06-14	
27.1	C.1			33.2726	9.7749	223	bedrock outcrop, carbonate or gypsum crust	19-06-14	11:17:00 AM
27.2	C.1			33.2727	9.7749	223		19-06-14	
27.3	C.1			33.2727	9.7748	223		19-06-14	
28.1	C.2			33.2723	9.7596	223	Cretacic bedrock	19-06-14	11:23:00 AM
28.2	C.2			33.2723	9.7745	223		19-06-14	
28.3	C.2			33.2723	9.7745	223		19-06-14	
29.1	D.1	T14	Nikon 1238-44?	33.2849	9.7055	186	sand, oued valley, fine granulometry	19-06-14	12:05:00 PM
29.2	D.1			33.2849	9.7055	186		19-06-14	
29.3	D.1			33.2849	9.7055	186		19-06-14	
29.4	D.1	T15	Nikon 1250-56?	33.2849	9.7055	186	sand, coarse granulometry	19-06-14	12:05:00 PM
29.5	D.1			33.2849	9.7055	186		19-06-14	
29.6	D.1			33.2849	9.7055	186		19-06-14	
30.1	D.2	T16	Nikon 12????????	33.2852	9.7054	190	clay deposit in riverbed	19-06-14	12:50:00 PM
30.2	D.2			33.2852	9.7054			19-06-14	
30.3	D.2			33.2852	9.7054			19-06-14	

Measrm_No	Stop	Sample	Photos	Y_DDDD	X_DDDD	Z	Target	Date	Time
31.1	D.3		Nikon 1280	33.2840	9.7096	193	psamophyte vegetation-retama reatem. Third detector crashed - short medium infrared	19-06-14	2:13:00 PM
31.2	D.3			33.2841	9.7096	193		19-06-14	
31.3	D.3			33.2839	9.7096	193		19-06-14	
32.1	E	T17	Nikon 1317/18	33.0889	9.8957	310	sand dune, aeolian deposit on carbonate surface	19-06-14	3:20:00 PM
32.2	E			33.0889	9.8957	310		19-06-14	
32.3	E			33.0889	9.8957	310		19-06-14	
33.1	F	T18	Nikon 1347/48	33.0000	9	353	sand	19-06-14	4:20:00 PM
33.2	F			33.0000	9	353		19-06-14	
33.3	F			33.0000	9	353		19-06-14	
34.1	G	T19	Nikon 1370-72	33.2013	10.211	427	sand	19-06-14	5:04:00 PM
34.2	G			33.2013	10.211	427		19-06-14	
34.3	G			33.2013	10.211	427		19-06-14	

4.4.2. Spectral Signatures Processing

The generic metadata related instrument, reference standards, calibration, hyperspectral signal properties, illumination information, viewing geometry, environment information, atmospheric conditions, general project information, location information, general target and sampling information and vegetation specific metadata were considered keeping spectral library measurements protocol in view . The spectral signatures acquired in the field have been preprocessed and processed using ViewSpec Pro 5.6.8. software (ASD Inc. of Boulder, Colorado) and SAMS version 3.2 (Spectral analysis and management system, the University of California, Davis, figure 43) and resampled and visualised with ENVI 5.2 (Exelis Visual Information Solutions 2014) for comparison with the USGS mineral spectral libraries.

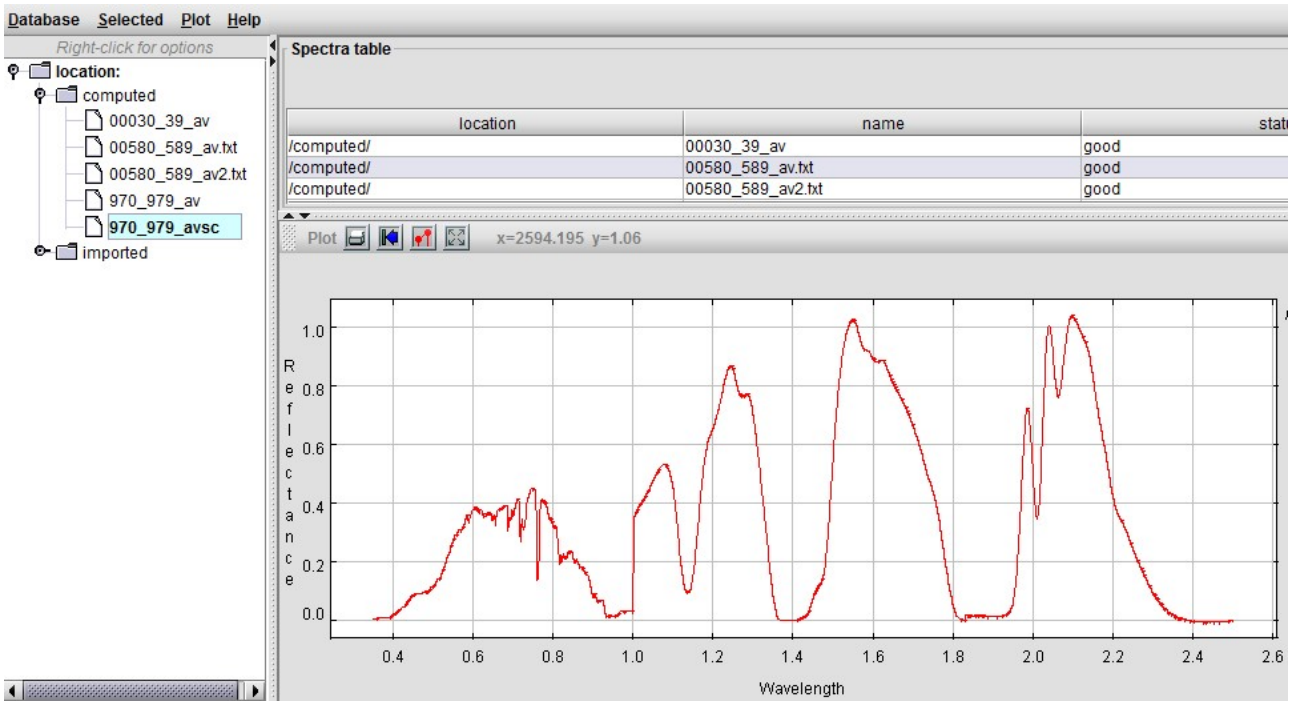

Figure 43. Processing field spectral data in SAMS 3.2. software

4.5. X-ray Diffraction Analysis

Powder X-ray Diffraction (XRD) is one of the primary techniques used by mineralogists and solid state chemists to examine the physico-chemical make-up of unknown solids. This data is represented in a collection of single-phase X-ray powder diffraction patterns for the three most intense D values in the form of tables of interplanar spacings (D), relative intensities (I/Io), and mineral name.

The XRD technique takes a sample of the material and places a powdered sample in a holder, then the sample is illuminated with x-rays of a fixed wave-length and the intensity of the reflected radiation is recorded using a goniometer. This data is then analysed for the reflection angle to calculate the inter-atomic spacing (D value in Angstrom units - 10-8 cm). The intensity (I) is measured to discriminate (using I ratios) the various D-spacings and the results are to identify possible matches.

4.6. Remote Sensing Approach

4.6.1. Image Preprocessing

The pre-processing and spectral analysis phases were partially addressed at the Spatial Laboratory of School of Earth and Environmental Sciences, University of Wollongong, New South Wales, Australia throughout a 4-months research training programme on general techniques and analysis of these two aspects.

The types of activities undertaken at the Internship at the Spatial Laboratory of School of Earth and Environmental Sciences, University of Wollongong, Australia, from the 15th of August to the 20th of November, 2014, can be divided as follows:

- Spatial Laboratory work - training on *Remote Sensing of the Environment* practice data on pre-processing methods provided by the school and applying these on own data with the support of the Laboratory technicians.
- Assessing features' spectral separability, their discrimination through known methods and assessment of accuracy

- Individual work - bibliographical consultation of local library, constructing EndNote library, preparation of future scientific article and continuing the rectification of previously collected data.
- Participation to School's activities such as work-in-progress scientific articles discussions of fellow PhD candidates, attending and participating as speaker at GeoQuest Research Centre seminars.

The downloaded data, level- L1T products were radiometrically calibrated and atmospherically corrected. Radiance and Reflectance were calculated following the procedure given in the literature as proper for the ecological context of the study area. Since the product employed ground control and relief models, geometric correction was not performed.

The surface reflectance image was eventually obtained (note in the image below, *Top of Atmosphere* image statistics before and after *Dark Object Substraction* and how the first bands are more sensitive to atmospheric scattering).

In this research, Dark Object Subtraction (DOS) is used as an approach for atmospheric correction, which is perhaps the simplest yet most widely used image-based absolute atmospheric correction approach for classification and change detection applications (Hamid Reza and Majid Shadman 2012) (Pons, Pesquer et al. 2014). No topographic correction was applied as it has been reported by several authors as prone to over-correct values in plain areas and lose valuable information, especially in regions where spectral separability has such sensitive thresholds. (Vanonckelen, Lhermitte et al. 2013). In order to perform the next steps, the two images have been mosaicked with the matching of colour balance, which does not alter the data values and performs a simple histogram matching between the two images and a mask have been applied for easiness of processing.

For both areas, the downloaded data, level L1T products were radiometrically calibrated and atmospherically corrected to obtain surface reflectance. Dark Object Subtraction (DOS) was applied for atmospheric correction and since the product employed ground control and relief models, (as delivered by the provider, namely USGS) geometric correction was not performed (Hamid Reza and Majid Shadman 2012, Pons, Pesquer et al. 2014). No topographic correction was applied as it has been reported by several authors as prone to over-correct values in plain areas and lose valuable

information, especially in regions where spectral separability has such sensitive thresholds (Vanonckelen, Lhermitte et al. 2014). Only in the Oum Zessar area, the two scenes have been mosaicked with the matching of colour balance, without altering the data values and a mask have been applied for easiness of processing and because of the presence of high coverage of water in the path 190 row 37 scene. All images were verified for co-registration.

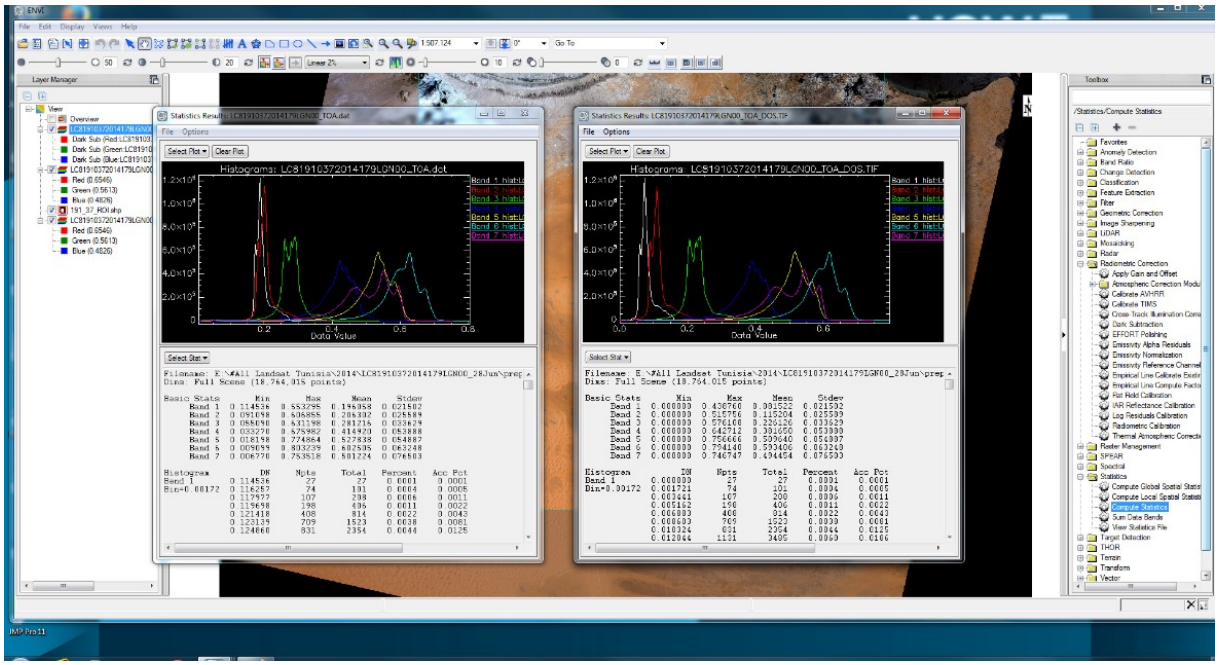

Figure 44. Example of bands histograms before and after atmospheric correction

4.6.2. Spectral analysis

4.6.2.1. Biskra area

A key preliminary phase that supported the spectral analysis took into account the key components of the Biskra area landscape: geomorphological units, land cover types, the distribution of the settlements and infrastructure, based either on previously interpreted land cover/use map or on other thematic maps and ancillary data. This step led to the recognition of a series of spectral classes that represent the main different land cover types and finally the saline areas. The multispectral data allows, by means of image processing, to extract and compare the different spectral components.

The spectral behaviour of salt-affected areas was undergone through the analysis of horizontal and vertical spectral profiles of point data using various band combinations. This gave a first input on which the key bands that can help discriminate them from other land features. The ones that can present similar spectral characteristics and confusion are carbonate-rich, clay-rich areas, bare land, urban fabric and outcropping rocks. This spectral characteristic of each pixel is called spectral signature, consultable via *Z profiles*. These were also assessed, but it is possible to visualise the reflectance values per one pixel at a time for all bands (multiple signatures through *collect spectra* function, figure 47 and 48), whereas horizontal and vertical profiles allow the visualization of reflectance values of multiple pixels but only in the displayed RGB bands. Analysis contained also 2D scatter plots visualization, which allows the assessment of the statistical relationships between groups of pixels (classes), constructing also ROIs and having the possibility to export and use them subsequently as training ROIs in supervised classifications (figure 49). In figures 50 and 51, the use of the ROI tool is given as example, as well as a way to obtain statistics of the average spectral information of the pixels contained in each ROI class which are useful in deriving optimal band operations for their spectral separation.

We have taken into consideration two factors: one is the maximum information content of the composite bands, as the larger the standard deviation is, the more the information content is derived from the composite bands; the other is the minimum affinity of the composite bands leading to significant independence and less redundant data.

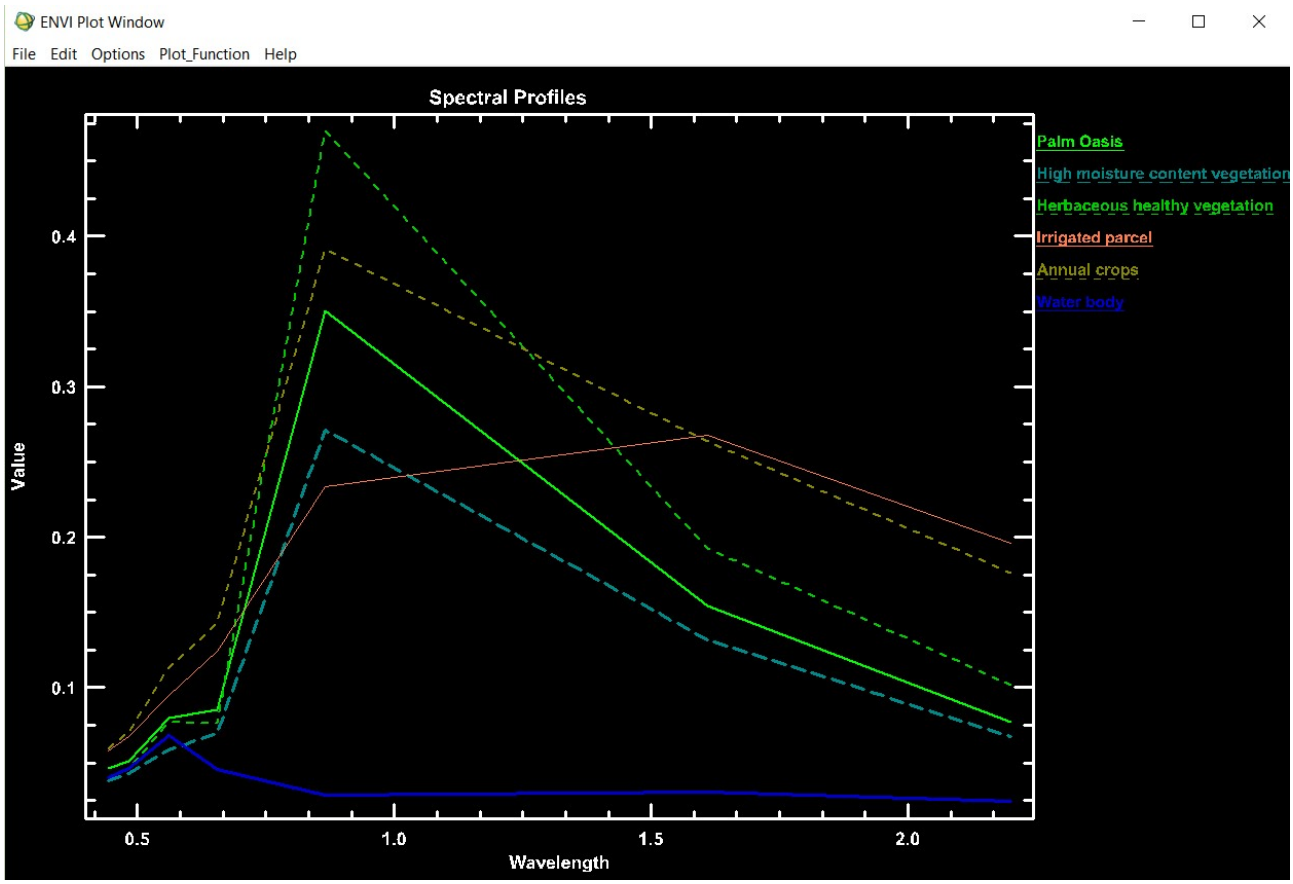

Figure 46. Spectral profiles of single pixels of different land cover types: examples of vegetation types and water bodies

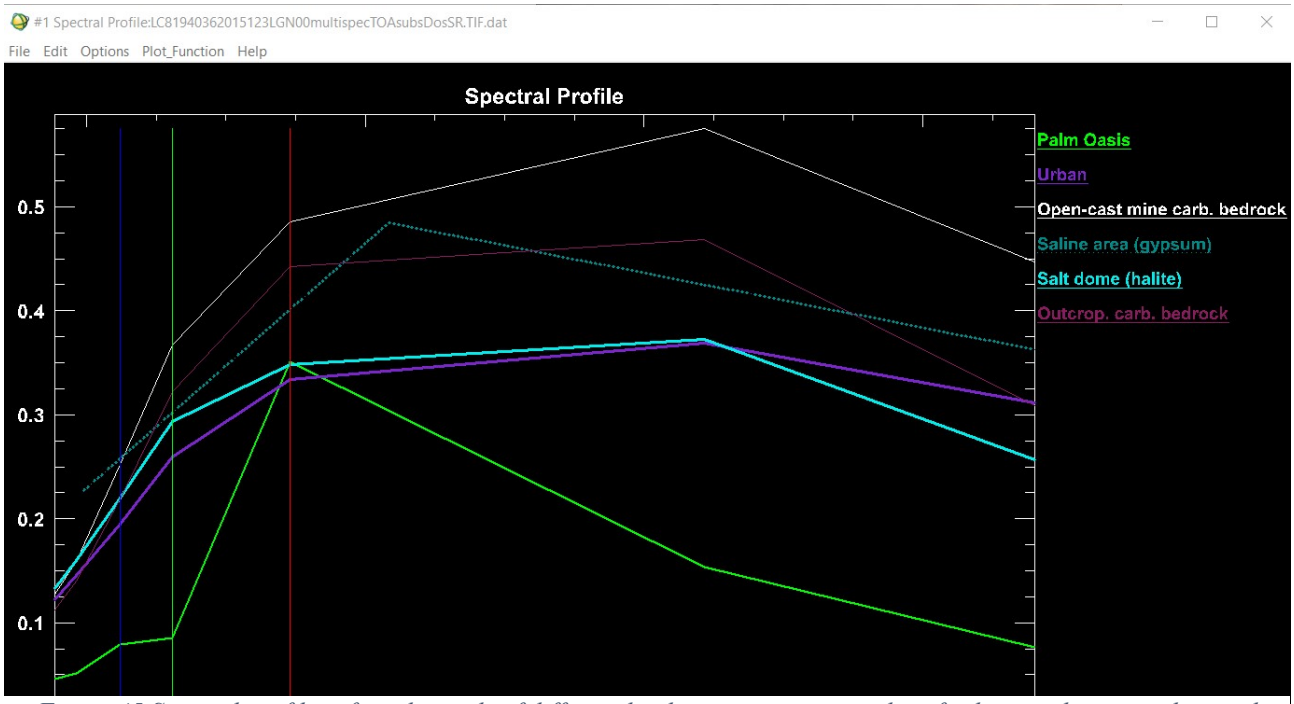

Figure 45 Spectral profiles of single pixels of different land cover types: examples of saline, carbonate, urban and vegetation features

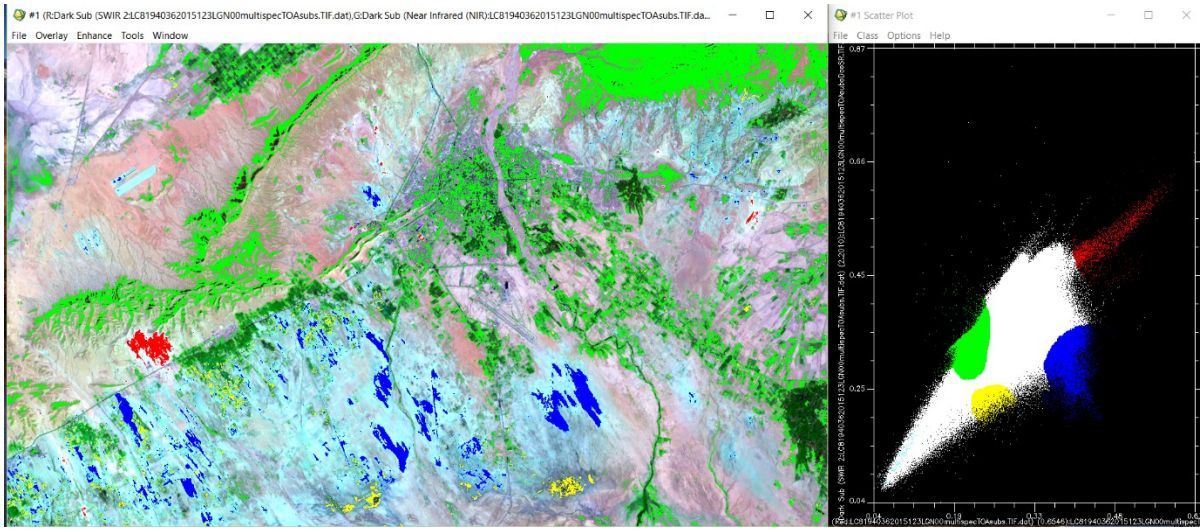

Figure 47. Identifying separable classes through 2D scatter plots. Shuffling pixels with the mouse on the image, correspondent values are highlighted within the scatter plot point cloud.

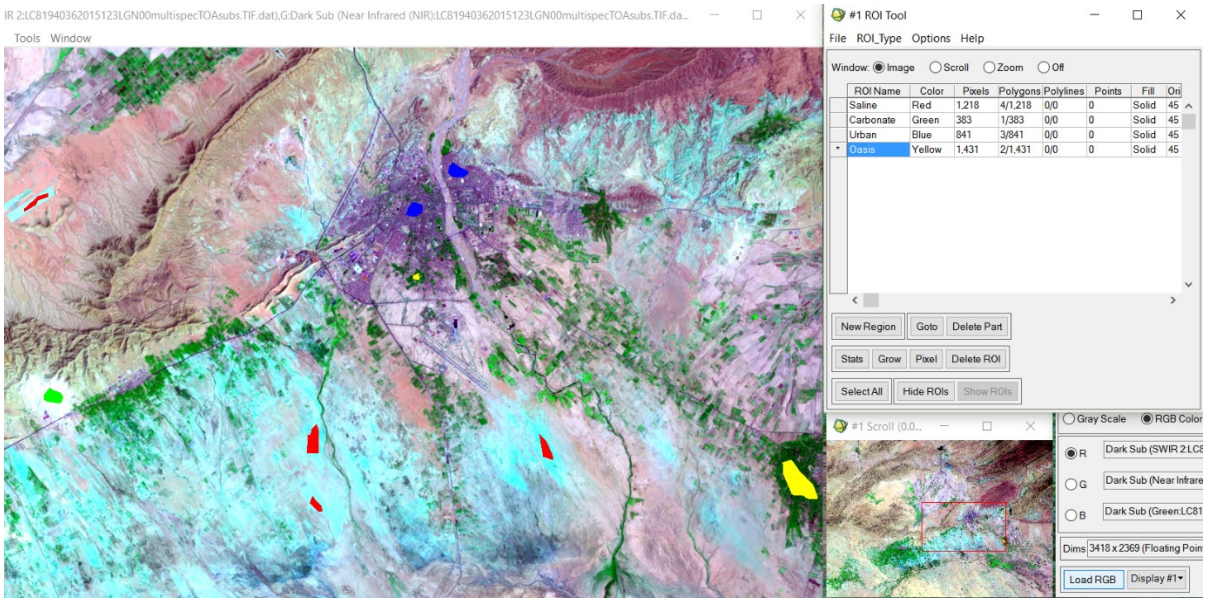

Figure 48. Using the ROI tool, it is possible to identify and assign pixels to classes (based on ancillary data, in the absence of ground truth), thus defining training data for classifiers

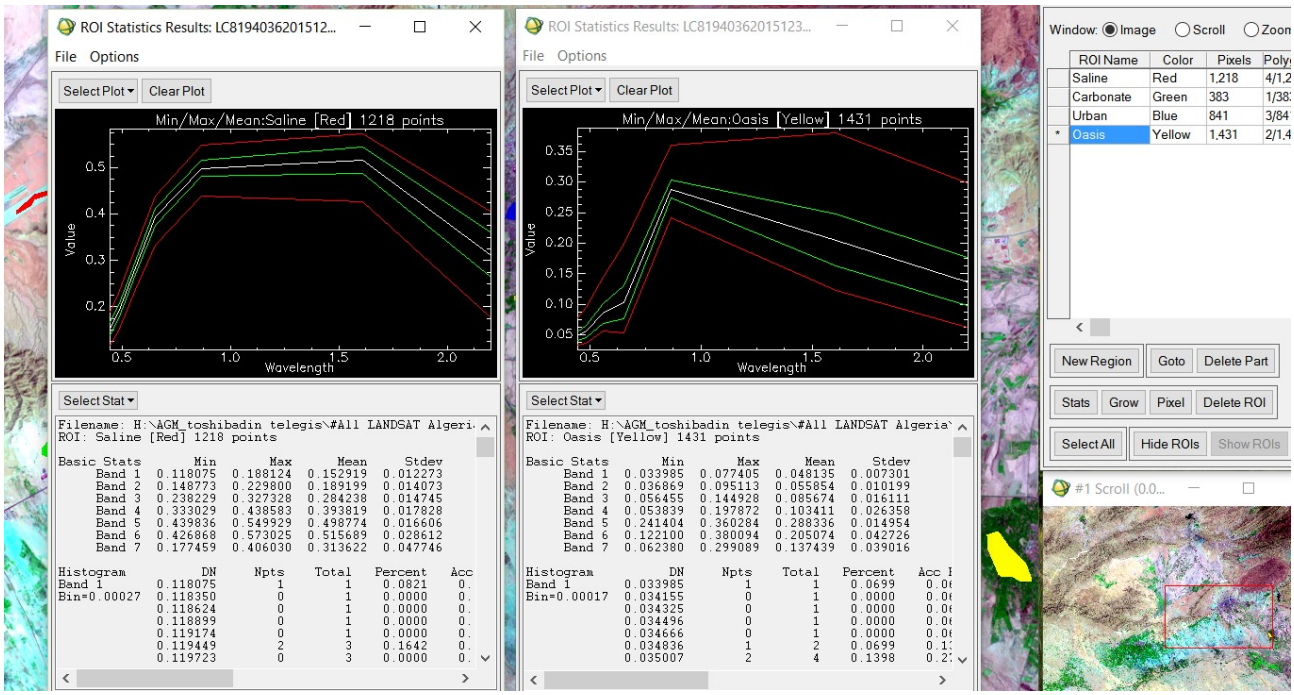

Figure 49. Statistical analysis of individual ROIs with respect to all Landsat bands which allow the definition of optimal band operations for their spectral separation

Radiometric, spatial and spectral enhancement are common operations for image analysis. Band ratios are a form of spectral enhancement, as they increase contrast, namely enhance certain features depending on bands choice and the spectral characteristics that those features present in the chosen bands. Band ratios and indices were derived in order to discriminate accurately the features of interest, in order to support decision rules used for a decision tree classifier scheme. Given the restricted access to ground truth survey (only 46 points verified by the WADIS-MAR Algerian partners), ancillary data, more specifically pedological and lithological remote sensing reports dating from 2006 provided by ITDAS Algeria, have been employed as "ground truth data", deriving correspondent ROIs for the statistical analysis of spectral separability of saline surfaces from other land features.

The spectral analysis of the entire set of Landsat bands (except the thermal ones) has shown the possibility to distinguish saline surfaces and has provided the background for ratios and indices construction to be integrated in a multi-stage classification process, based on a Decision tree classifier (Melis, Afrasinei et al. 2013(Afrasinei, 2015 #1929)).

4.6.2.2. Oum Zessar area

Given the availability of a more comprehensive ground truth data, in the case of Oum Zessar area, this phase consisted of spectral information analysis employing both remote and proximal sensing, namely Landsat imagery and spectral signatures derived from on-site spectroradiometric measurements, respectively. The proximal sensing spectral analysis, as described in section 3.4., was integrated for analysis throughout its assessment with the existing USGS spectral libraries (Afrasinei, Melis et al. 2015). Concerning satellite data, the spectral analysis was undergone through remote sensing techniques such as radiometric and spectral enhancement, analysis of horizontal and vertical spectral profiles passing through each single point of interest and 2D scatter plots investigation of salt features in order to understand their spectral behaviour in relation to other land features, especially those that can present similar spectral characteristics and confusion: carbonate-rich, clay-rich areas, bare land, urban fabric and outcropping rocks. For this phase, we have taken into consideration two factors: one is the maximum information content of the composite bands, as the larger the standard deviation is, the more the information content is derived from the composite bands; the other is the minimum affinity of the composite bands leading to significant independence and less redundant data.

Using the statistical summary of the 36 classes, the information of each of their Regions of Interest (ROI) was assessed in Excel in order to visualize their separability, as shown in figure 45, but also to calculate it. This have shown that the spectral profiles cannot be easily distinguished statistically and the error bars shown overlap of information. This has suggested the need of consequent band

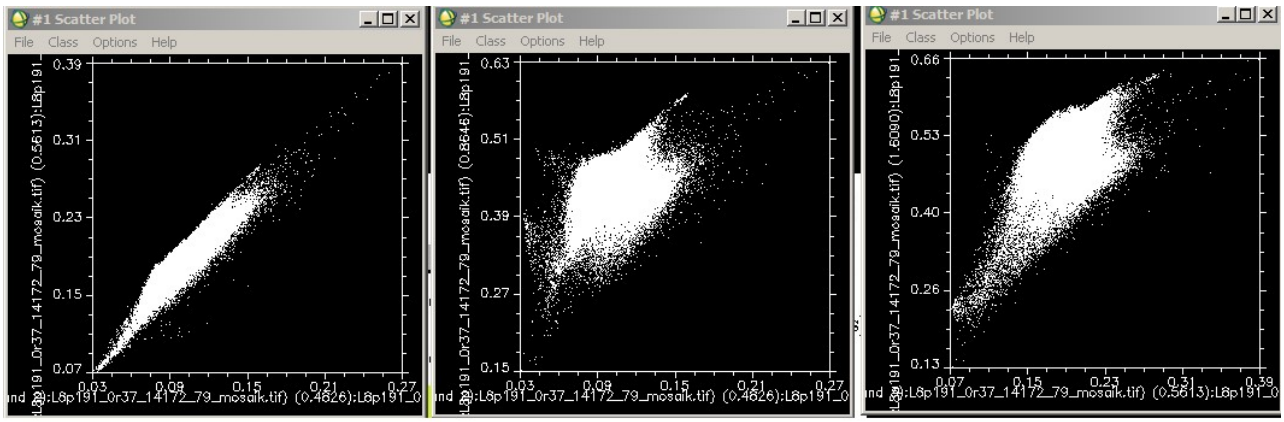

Figure 50. Scatter plots showing correlations or covariance: 1) band 1 against band 2; 2) band 2 against 7; 3) band 3 and band 6 (Landsat 8 bands)

transformation techniques in order to better discriminate the features of interest.

1	1.1.1.1. Continuous urban fabric [Green3] 18820 points				
	Basic Stats	Min	Max	Mean	Stdev
	Band 1	0,033982	0,210517	0,091377	0,012661
	Band 2	0,044625	0,260313	0,121491	0,015154
	Band 3	0,089054	0,380538	0,207437	0,019567
	Band 4	0,105225	0,503349	0,310840	0,026726
	Band 5	0,167078	0,615622	0,420670	0,029956
	Band 6	0,176109	0,628560	0,471311	0,039004
	Band 7	0,136067	0,490128	0,386315	0,031682
2	1.1.2.1. Discontinuous built-up areas with bare land [Blue] 56266 points				
	Basic Stats	Min	Max	Mean	Stdev
	Band 1	0,000000	0,158460	0,080584	0,011711
	Band 2	0,000000	0,201147	0,110455	0,014354
	Band 3	0,000000	0,301666	0,203680	0,020467
	Band 4	0,000000	0,450308	0,326303	0,028628
	Band 5	0,000000	0,584098	0,451993	0,031658
	Band 6	0,000000	0,634640	0,522959	0,033298
	Band 7	0,000000	0,499786	0,419802	0,029875
3	1.1.2.2. Discontinuous built-up areas with areas arable irrigated perimeters [Yellow] 47832 points				
	Basic Stats	Min	Max	Mean	Stdev
	Band 1	0,000000	0,257038	0,075217	0,011231
	Band 2	0,000000	0,317449	0,103154	0,013806
	Band 3	0,000000	0,413596	0,191518	0,019172
	Band 4	0,000000	0,513139	0,306598	0,030052
	Band 5	0,000000	0,627211	0,437690	0,025976
	Band 6	0,000000	0,658648	0,501093	0,037706

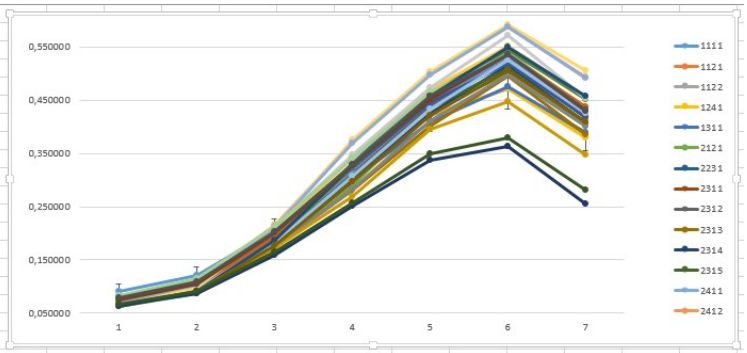

Figure 52. Each land cover and land use feature ROIs statistics

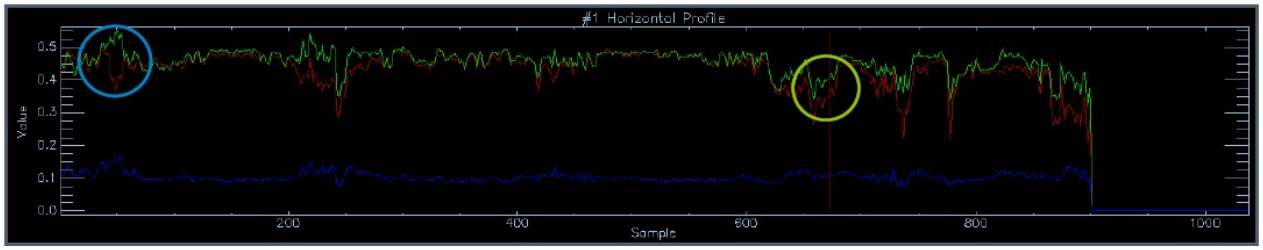

Figure 51. Example of spectral horizontal profile extracted from Landsat 8 image relative to the T8 sample, Tunisia. The spectral response of the halite is highlighted in yellow, whereas in blue the gypsum one is emphasized.

Band transformations

Apart from the original Landsat bands, a number of derivative bands were generated from the original data for analysis. These included decorrelation stretches, NDVI computation and all tasselled cap (TC) transformed bands.

The NDVI and NDWI

These two indices are usually used for vegetation studies especially assessing the health of vegetation, with higher NDVI values indicating good healthy vegetation while lower NDVI values show deprived vegetation. (Otukei and Blaschke 2010). However, there must be emphasised that there is a high covariance between the NDVI and NDWI (NIR-SWIR/NIR+SWIR) for certain features that denotes that these two indices in combination can be useful to discriminate certain species of vegetation, as for example xerophile species that may present reflectance in NDVI but none in NDWI as they do not contain moisture. On the other hand, the halophile vegetation would

have the opposite behavior, as it retains much water in the leaves, but do not present high values in NDVI.

The 2D scatter plot shows this positive covariance between the two indices, with the NDVI values on the Y axis, with values ranging from -0.244889 to 0.721790, with a standard deviation of 0.080546 and the NDWI on the X axis ranging from -0.233935 to 0.356424 with a SD of 0.043117, much more smaller than the one of NDVI, being restrictive in terms of features with moisture content (figure 53, 54).

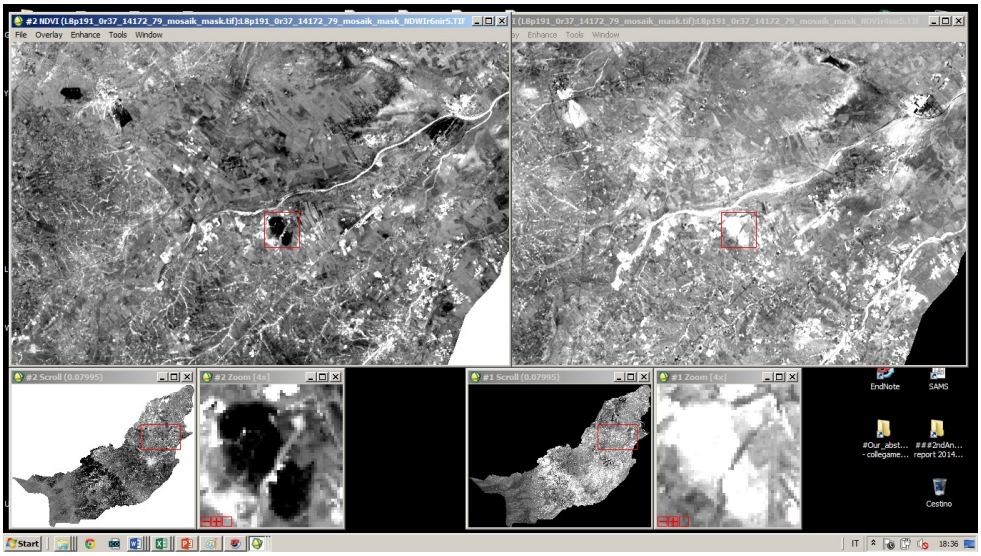

Figure 53

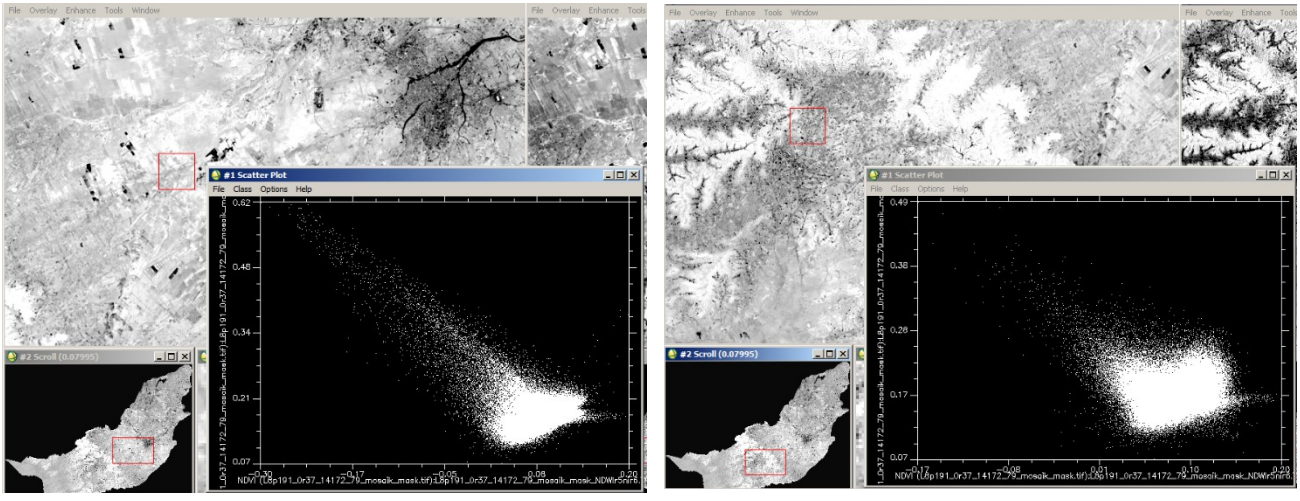

Figure 54

Tasseled Cap

Spectral transformation can reduce multi-spectral data volume with minimal information loss and generate a new image which loads main information of original data. It is an effective technique in improving classification accuracy and change. (Haijiang, Chenghu et al. 2008).

The Tasseled Cap transformation, also called as K-T transformation and originally applied to the Landsat Mul- tispectral Scanner (MSS) data, is a principal component analysis technique, which linearly transforms multi-spectral data and creates 3 uncorrelated bands: Brightness (B), Green-ness (G) and Wetness (W). The Tasseled Cap transformation is scene independent and has fixed coefficients, and therefore the multi-date TM, ETM+ and OLI data can be transformed through this technique and the results are comparable over time. The BGW bands are directly related to specific physical attributes and can be easily interpreted. Brightness was interpreted as change in total reflectance or albedo at the surface, and is mainly driven by soil reflectance variations; Greenness measures the contrast between visible bands and near infrared band, and has a close correlation with vegetation coverage, just like the vegetation index; Wetness is sensitive to soil and plant moisture. In order to overcome the ENVI 5.0. default settings of tasseled cap transformation to Landsat 7, a spectral subset of the mosaicked image was performed, removing the band 1, coastal aerosol of OLI sensor, leaving only the bands in the corresponding wavelengths as L7, in the same order. For thisdata, the tasseled cap transformation produced 6 output bands: Brightness, Greenness, Wetness, Fourth, Fifth, Sixth. The first 4 TC bands have shown particular usefulness for saline sulphate surfaces identification and separation from carbonate ones. In particular the tasselled cap of NIR band, brightness and wetness in a RGB combination allowed the visual inspection of the separability of these two types of saline surfaces, in yellow being represented the sulphate saline areas and the carbonate surfaces are further given an example of separation, through the application of a salinity index.

Other indices

The following indices were chosen for testing, due to the similarity of the characteristics of the study area in which they have shown high accuracy:

- Soil salinity index: SI = (Blue² * Rouge²)0,5, (Khan et al., 2001).

- Normalized Differential Salinity Index (NDSI); NDSI = (Red- NIR)/(Red+NIR), NIR : Near Infra Red, (Al-Khaier 2003)
- Salinity index (IS): IS = (Red + NIR²)0,5, (Douaoui and al. 2006);
- The vegetation indices such as the NDVI and brightness index (IB=(Rouge²+NIR²)0.5) are also used in the estimate of salinity (Fernandez-Buces et al., 2006). Brightness index (IB=(Rouge²+NIR²)0.5)

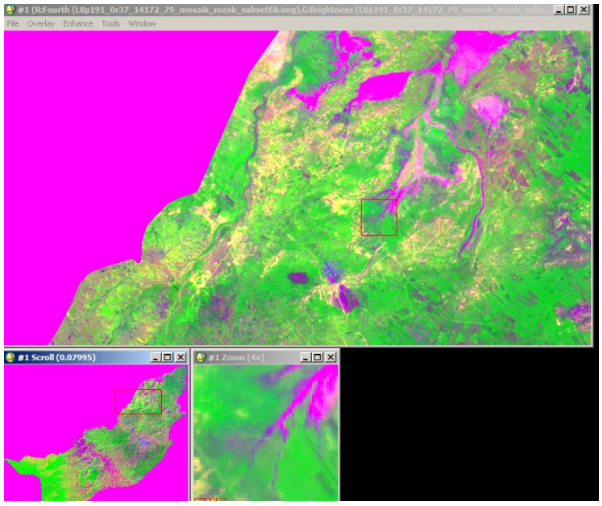

Figure 56

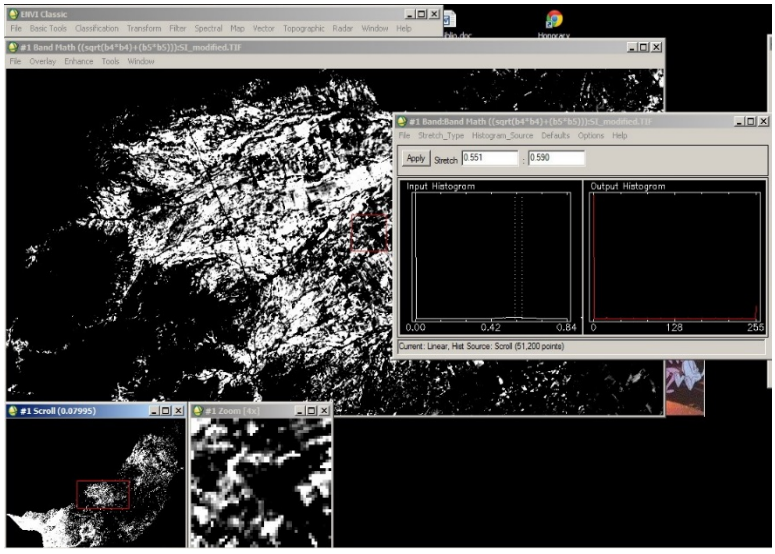

Figure 55 Establishing thresholds for mineralised or carbonate-mixed surfaces

These indices have shown that the strongest correlations are obtained with the lower wavelength spectral bands. It is surely in the band of blue that we find the most significant coefficients of correlation followed by a regular decrease towards the bands green and red, to become finally none significant with NIR band. Below there is an example of one of several methods to build decision rules and the correspondent threshold: by visual inspection combined with statistics analysis.

4.6.3. Image Classification

4.6.3.1. Oum Zessar Area: Traditional Classification Methods Assessment and testing

Conventional classification methods were assessed either through thorough literature review or by running a few test. In the case of Oum Zessar area, the traditional pixel-based image classification method was applied to the Landsat OLI image using training samples acquired in the field. The Maximum Likelihood classification was used because it is acknowledged as the most efficient among supervised pixel-based algorithms for image classification in similar studies. The ML classifier takes into account the variance and the covariance of the class signatures to assign a given pixel to a class depending on its feature characteristics (Antonio Di and Douglas 2012). The classified classes were 21 in total and there has also been performed the separation of the masked area from 1311 class as they were classified together. However, after the confusion matrix has been performed with the land cover and land use visually-interpreted map, an overall accuracy of 37.8904% has been obtained and a Kappa Coefficient = 0.3356. That may be interpreted as a very close spectral similarity between classes, the high number of classes set in the training areas and the heterogeneity within the classes, considering also that this is a general shortcoming of the single stage classifiers. The visual interpretation has taken into consideration 7 variables apart from ancillary data consultation and ground truth information: contours, colour or hue, size, texture, structure, spatial distribution and location, thus obtaining 36 classes, out of the 44 land cover and land use classes that include the standard CLC nomenclature (CLC2006TechnicalGuidelines 2007).

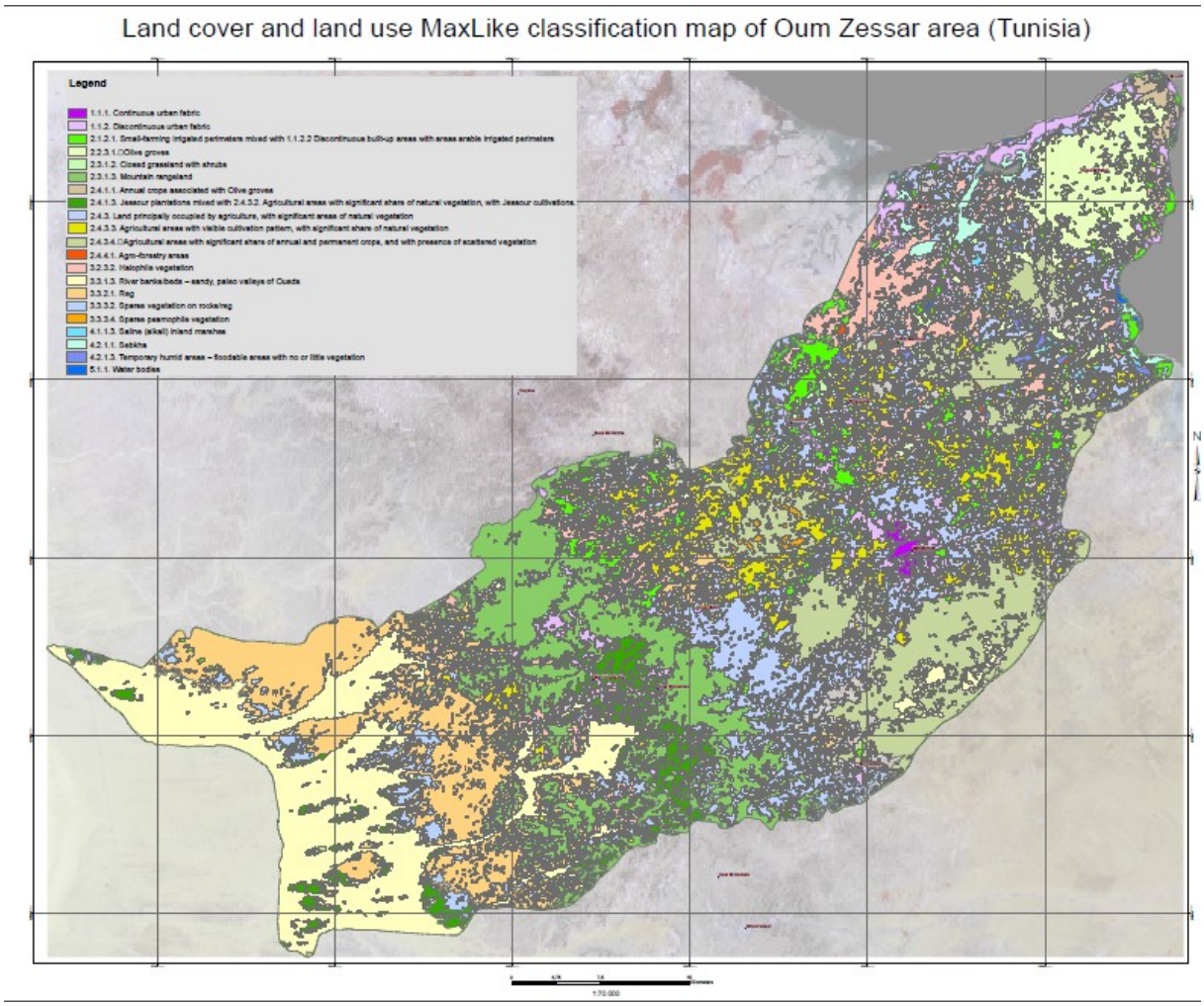

Figure 57. MaxLike classification applied to Oum Zessar area. Training ROIs derived from ground truth points

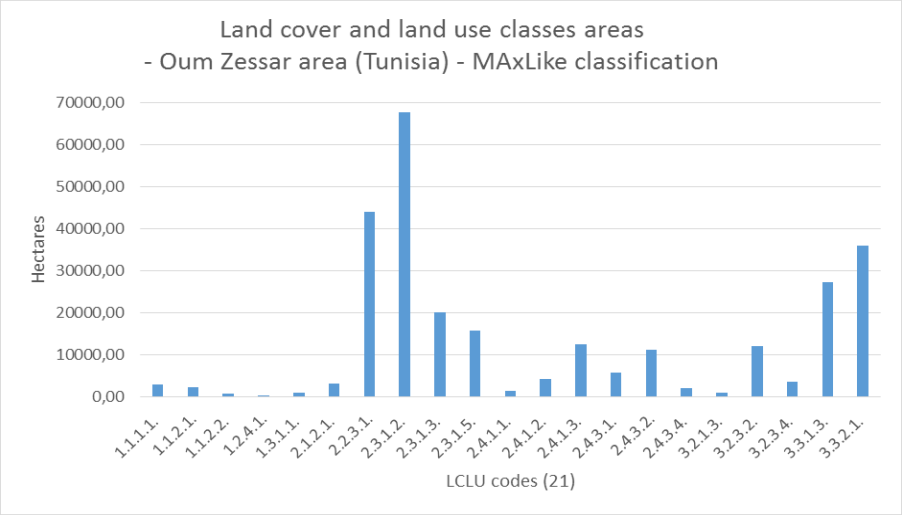

Figure 58. Land cover classes areas distribution resulting from MaxLike classification

.

	Classes	Comission	Omission	Producer Acc,	User Acc,
		(Percent)	(Percent)	(Percent)	(Percent)
1	1.1.1.1. C	53,35	20,35	79,65	46,65
2	1.1.2.1. D	72,14	89,59	10,41	27,86
3	1.1.2.2. D	85,27	98,82	1,18	14,73
4	1.2.4.1. A	94,47	33,6	66,4	5,53
5	2.1.2.1. S	73,15	60,74	39,26	26,85
6	2.2.3.1.OL	56,06	14,61	85,39	43,94
7	2.3.1.1. O	91,54	33,02	66,98	8,46
8	2.3.1.2. C	85,5	26,4	73,6	14,5
9	2.3.1.3. M	17,84	44,75	55,25	82,16
10	2.3.1.4. S	83,74	74,38	25,62	16,26
11	2.3.1.5. O	95,45	92,38	7,62	4,55
12	2.4.1.1. A	57,49	94,95	5,05	42,51
13	2.4.1.2. T	74,37	79,09	20,91	25,63
14	2.4.1.3. J	94,73	95,45	4,55	5,27
15	2.4.3.1. A	49,81	90,96	9,04	50,19
16	2.4.3.2. A	29,01	66,65	33,35	70,99
17	2.4.3.4. A	68,75	97,33	2,67	31,25
18	3.2.1.3. R	63,52	67,39	32,61	36,48
19	3.2.3.2. H	61,02	59,96	40,04	38,98
20	3.3.1.3. R	27,88	59,33	40,67	72,12
21	3.3.2.1. R	51,91	14,57	85,43	48,09
	Average	66,04761905	62,58666667	37,41333333	33,95238095

4.6.3.2. Decision Tree Analysis

The decision tree classifier is an efficient tool for land cover and land use classification. It is a hierarchal top-down approach, in which the decision rules are defined by a combination of several features, and a set of linear discriminate functions are applied at each test node, where a binary decision is made for splitting a complex decision into several simpler decisions so as to separate either one class or some of the classes from the remaining classes (Matthew 2012, Srimani and Prasad 2012).

As opposed to single stage classifiers in that only one decision is made about a pixel, as a result of which it is labelled as belonging to one of the available classes or is left unclassified. Multistage classification techniques are also possible in which a series of decisions is taken in order to determine the correct label for a pixel. A decision tree classifier is a non-parametric classifier that does not require any a priori statistical assumptions to be made regarding the distribution of data. The more common multistage classifiers are called decision trees. They consist of a number of connected classifiers (or decision nodes) none of which is expected to perform the complete segmentation of the image data set. Instead, each component classifier only performs part of the task. The advantages of using a multistage or tree approach to classification include that different data sources i.e. spectral data or GIS data e.g. elevation data, etc. different sets of features, and even different algorithms can be used at each decision stage (Hamid Reza and Majid Shadman 2012)

After reviewing and applying several vegetation and indices reported as successful in delineating salt-affected areas (Allbed and Kumar 2013) and sandy ones (Essifi, Ouessar et al. 2009, Ouerchefani, Dhaou et al. 2013), respectively, the results that emerged were not completely satisfactory and observations were made for both areas in order to choose optimal band operations for decision tree integration, as described in section 4.6.2.

The indices and band math operations employed in the DTA is summarized in table 4. Finally, the decision tree map was obtained by applying vegetation, wetness, mineral and salinity indices as well as simple band ratios, mostly derived from the analysis of bands statistics, scatter plots and vertical and horizontal profiles of interest features but also from literature, as presented in figure 2 and table 2 (Khan, Rastoskuev et al. 2001, Metternicht and Zinck 2008, Elnaggar and Noller 2010, Hamid Reza and Majid Shadman 2012, Allbed and Kumar 2013, Melis, Afrasinei et al. 2013, Mulder, de Bruin et al. 2013). The indices proposed for this study are constructed based on

choosing optimal band pairs/groups which have high spectral information covariance of each land feature of interest. For example, in the case of highly saline areas class extraction, Landsat visible bands of blue, green and red information are usually put together, as they present high correlation, in order to enhance the "brightness" features. They are subsequently divided by band SWIR2, which presented the lowest reflectance values of salt features, hence high covariance with the three aforementioned. The resulting indices are thus expressed as: sqrt(((b1^2)+(b2^2)+(b3^2))/b7) or (b1+b2+b3)/b7, Salt Minerals Index and Hue Salinity Index, respectively.

Exponential or square root functions were used to force the emphasis of extreme values, helping in delineating high or moderate saline areas. The statistics of each index/math image were used in order to establish the thresholds for each decision node. The decision nodes and the resulting map are thus obtained, for each of the eight dates. According to the lithological and vegetation cover of the area, the DT analysis and legend was adapted in order to classify the main land cover classes as well as classes of lithology distinguishable according to their spectral lithological response, which are described in table 3. JARS

The indices and band math operations employed in the DTA for Biskra area, are summarised in table 3, and for Oum Zessar area, in table 4. They were constructed differently for each area, depending on the spectral and physical-geographic particularities respectively, but also on the basis of the features of interest to be extracted: in Biskra area, salt-affected areas have priority, whereas in Oum Zessar area, the sandy ones.

Table 4. Indices analysed for decision tree construction, Biskra study area, Algeria (parent nodes only). Thresholds correspond to the indices applied for the 7 August 2015 image (Afrasinei, Melis et al. 2015).

Parent nodes-decision	Expression	Band math (TM bands)	Indices	Reference
NDVI	b1 GE 0.24	(b4-b3)/(b4+b3)	Normalised Difference Vegetation Index	(Gitelson, Kaufman et al. 1996, Gitelson, Peng et al. 2014)
NDWI	b2 GE 0.01	(b4-b5)/(b4+b5)	Normalised Difference Water Index	(Gao 1996, Kross, McNairn et al. 2015)
NDWI USGS	b3 GE -0.39	(b3-b4)/(b3+b4)	Normalised Difference Water Index - USGS	(McFeeters 1996), also known as Normalised Difference Salinity Index (NDSI) (Khan, Rastoskuev et al. 2005)
WR	b4 GE 1.0	b3/b4	Water Index	derived from (Kross, McNairn et al. 2015) (van der Meer, van der Werff et al. 2012)
SMI	b5 GE 0.74	sqrt(((b1^2)+(b2^2)+(b3^2))/b7)	Salt Minerals Index	proposed for this study
MI	b6 GE 0.028	(b1*b2*b3)/b4	Mineral Index	proposed for this study

IRI_SWIR1	b7 GE 0.88	sqrt(((b4^2)+(b7^2))/b5)	InfraRed Index – Short Wave InfraRed 1 (TM band 5)	proposed for this study
IRI_NIR	b8 GE 1.7	sqrt(((b5^2)+(b7^2))/(b4^2))	InfraRed Index – Near InfraRed (TM band 4)	proposed for this study
S2	b9 LE -0.32	(b1-b3)/(b1+b3)	Salinity Index 2	(Allbed and Kumar 2013)
HSI	b10 GE 1.74	(b1+b2+b3)/b7	Hue Salinity Index	proposed for this study
1/5	b11 GE 0.22	b1/b5	Ratio 1/5	(Melis, Afrasinei et al. 2013)

Table 5. Indices analysed for decision tree construction, Oum Zessar area, Tunisia (parent nodes only)

Parent nodes - decision	**Expression**	**Band math (L8 bands)**
NDVI	b1 GT 0.145	(b5-b4)/(b5+b4)
Ratio 5/2	b3 GT 4.2	(b5/b2)
Diff 5-2	b5 GT 0.37	(b5-b2)
Ratio 6/3	b7 GT 3.1	(b6-b3)
Diff NDVI-NDWI	b8 GT 0.26	((b5-b4)/(b5+b4))-((b5-b6)/(b5+b6))
MMI	b4 GT 0.6	(sqrt(b4*b4)+(b6*b6))
Modif SI	b6 GT 0.45	(sqrt(b2*b2)+(b5*b5))
NDWI	b2 GT -0.05	(b5-b6)/(b5+b6)

From the analysis presented in the previous phases we came to the conclusion that the spectral confusion resides in the particularity of the area, as desert features present a typical high reflectance even if the vegetation is present. In fact, the species that are commonly found are xerophyte in association with halophyte, psammophyte and pelophyte, but it is very important to identify and delineate their distribution because of the high economic value of the palatable ones, as the local economy relies on animal husbandry, mainly and secondly, agricultural production from small-scale farming. The study undertaken on the spectral separatability of the desertification – indicating features is an important step in the workflow of change detection analysis since there is a sensitive threshold in discriminating them and the mapping accuracy depends on it. Each single uncertainty will have a major impact on the final result.

In order to argue the need of a decision tree in order to optimise classification accuracy we needed to perform all the fore-mentioned tests of pre-existing methods and the spectral and spatial assessment of data that supports decision rules.

4.6.3.3. IsoDATA of Knepper Ratios' Principal Components

Soil salinity mapping through remote sensing is translated through spectral characterization of the contained abundant salt minerals. Knepper (1989) proposed specific band ratios for the delineation of hydroxyl – bearing minerals, hydrated sulphates and carbonates, vegetation and iron oxides and hydroxides, namely the 5/7:3/1:3/4 red-green-blue (RGB) combination, used mainly for geological remote sensing mapping (Langford 2015), but the novelty of the current study is that it is employed for salt features identification.

The principal components analysis was applied to Knepper composites of each year (Langford 2015) in order to obtain a fast spectral separation of main land cover types and especially to rapidly identify areas with different lithology and mineralogy. It was employed in order to evaluate its potential as an approach of fast automated, user-independent classifier, as opposed to decision tree analysis that needs thorough computation for rules choice and threshold calculation. It is based only on the spectral information contained within the employed bands, but it does not allow other manipulation, which was considered by us rigid, as it presents a consistent problem of mixed pixels. In fact, the obtained images presented difficulty in applying a classifier and in order to avoid further errors, IsoDATA unsupervised classification was chosen, as it proved to be the most suitable, with maximum 50 iterations, a threshold of 2 % and 12 classes requested. The PCA analysis was applied for each one of the 9 assessed years.

5. CHAPTER FIVE: Results and Discussion

5.1. Land Cover and Land Use Maps

For both areas, the land cover map was obtained through visual interpretation of land cover features from the standard false colour composites (RGB 432, 543, 742 bands), also applying image enhancement when needed, usually the radiometric one. Supported by ancillary data, it allowed the distinction of several vegetation types, impervious surfaces, different types of lithology etc.

5.1.1. Biskra area

In the Biskra area, the interpretation of the Landsat TM5 of 9th of June 2011, path 194, row 36 resulted in 37 LCLU classes that were defined based on ancillary data, given that ground truth data was difficult to obtain. This step served for the overall acquaintance with the study area in terms of land cover and land use and for the specific purpose of this study. However, for the quantitative comparison to DTA and Knepper PCA results, only the saline areas classes were merged and taken into consideration. On the other hand, all classes were considered for visual inspection and comparison with other classifiers' results. The correspondent LCLU classes to the legend codes in figure 4 are as defined within the nomenclature below, which follows the hierarchy of CORINE land cover programme (ETC/LC and Agency 1999):

1. Artificial surfaces

1.1. Urban fabric

1.1.1. Continuous urban fabric

1.1.1.1. Areas of urban centres

Areas of urban centres with public, administrative and commercial buildings, roads, parking lots and artificial surfaces (e.g. cemeteries without vegetation) cover more than 80% of the total surface. Urban greenery is exceptional.

1.1.1.2. Areas of ancient cores

Dense ancient cores (mainly residential buildings) with roads, parking lots, etc. Urban greenery is exceptional.

1.1.2. Discontinuous urban fabric

1.1.2.1. Discontinuous built-up areas with areas of bare soil

Most of the land is covered by structures. Buildings, roads and artificially surfaced areas are associated with bare soil, which occupy discontinuous but significant surfaces.

1.1.2.2. Discontinuous built-up areas with areas of Palm groves or Oasis vegetation

Most of the land is covered by structures. Buildings, roads and artificially surfaced areas are associated with Palms or other permanent crops, which occupy discontinuous but significant surfaces.

1.1.3. Peripheral urban wasteland

Area not included inside a systematic rotation of crops. Probably cultivated for several years but presently not used for agriculture purpose. There can be visible traces of human activity, even constructions, but not enough to include it in an urban fabric class or in one of the 1.2 classes; there are usually bare areas, presenting salinity.

1.2. Industrial, commercial and transport units

1.2.1. Industrial or commercial units

Artificially surfaced areas (cement, asphalt, tarmacadam, or stabilised, e.g. beaten earth) without vegetation occupy most of the area, which also contains buildings and/or vegetation.

1.2.4. Airports

Airport installations: runways, buildings and associated land.

1.3. Mine, dump and construction sites

1.3.1. Mineral extraction sites

1.3.1.1. Quarries and open-cast mines

Areas with open-pit extraction of construction material (sandpits, quarries) or other minerals (open-cast mines that include oil-shale mines, gravel, sand, and clay pits). Includes flooded gravel pits, except for river-bed extraction.

1.3.3. Construction sites

Areas under construction development for which earthworks and different stages of building constructions are typical.

1.4. Artificial, non-agricultural vegetated areas

1.4.2. Sport and leisure facilities

1.4.2.1. Sport facilities

Areas of playgrounds within or outside the urban fabric, running tracks, race-courses, ski resorts, golf grounds, etc.

2. Agricultural areas

2.1. Arable land

2.1.2. Permanently irrigated land

Crops irrigated permanently or periodically, using a permanent infrastructure (irrigation channels, drainage network). Most of these crops could not be cultivated without an artificial water supply. Does not include sporadically irrigated land. Because of the difficulty of separating non – irrigated arable land and the irrigated one, ancillary is necessary, such as topographic maps in which the irrigation network is marked or aerial photographs in which these networks may be visible. Furthermore, agricultural calendars, statistics and multi-date data should be used for a major precision of class assignment. (e.g. “Etude pedologique par teledetection de la region de Biskra”, 2006 and annexe from which it was possible to import into GIS the available information on the analysed soil profiles).

2.2. Permanent crops

2.2.2. Oasis

2.2.2.1. Primary Oasis

Palm groves that do not present an organised cultivation pattern, with a vissible random distribution denoting a natural growth. Usually these areas are characterized by multi – layer inter-cropping, with cereals, legumes or fodder crops on the first layer, fruit trees on the second layer and Palm trees as third, with a permanent infrastructure of irrigation.

2.2.2.2. Secondary Oasis

Parcels planted with Palm tree which can be mixed with fruit species but that cannot be clearly distinguished. Orchards of less than 25 ha surrounded by agricultural land (pasture or arable land) but which are nonetheless are included under item 2.4.2 (complex cultivation patterns). Orchards in which several types of tree are grown are included under 2.3.1.3. Nurseries and pasture planted with trees are not included under this heading.

2.4. Heterogeneous agricultural areas

2.4.1. Annual crops associated with permanent crops

2.4.1.1. Annual crops associated with Palm groves

Non-permanent crops (arable land or pasture) associated with Palm groves on the same parcel. This category covers associations within a single parcel, identifiable by specific spectral responses, rather than areas of polyculture with parcels given over either to annual crops or to permanent crops. Land units in a typical mosaic of small parcels of annual crops, pasture and permanent crops should be classified under category 2.4.2 (complex cultivation patterns).

2.4.1.2. Annual crops associated with other permanent crops

2.4.1.3. Arable land associated with greenhouses (*maraîchage*) with significant areas of Palm groves

2.4.1.4. Discontinuous arable land associated with Palm plantations

Non-permanent crops (arable land or pasture) associated with Palm groves on the same parcel, but unlike 2311 it is discontinuous spatially and it doesn't have the same homogeneity as it usually follows temporary torrents and small river beds and the Palm groves are usually in nursery phase or degraded state, thus having a weaker spectral response from the grown Palms.

2.4.2. Complex cultivation patterns

Juxtaposition of small parcels of diverse annual crops, pasture and/or permanent crops.

On satellite images this category always presents a very fine texture and an easily recognisable agricultural pattern. Topographic maps sometimes use symbols to indicate the biophysical content of this category.

This reading covers land units identifiable by characteristic spectral responses and composed of small parcels of diverse annual crops, pasture and/or permanent crops, provided that none of these three categories covers an identifiable surface unit of more than 25 ha within a single land unit. Arable land, pasture and orchards each occupy less than 75% of the total surface area of the unit. City gardens are included under this heading.

2.4.3. Land principally occupied by agriculture, with significant areas of natural vegetation

2.4.3.1. Agricultural areas with significant share of natural vegetation, and with prevalence of annual crops in late stage of phenophase

Areas principally occupied by agriculture, interspersed with significant natural areas. In these units, no homogeneous subset of 25 ha or more should be isolated in agricultural land or in natural areas (natural vegetation, forests, moors, grassland, water bodies or bare rock). Agricultural land occupies between 25 and 75% of the total surface of the unit.

2.4.3.2. Agricultural areas with visible cultivation pattern, with significant share of natural vegetation, with the prevalence of annual crops in early phenological stage or not yet sprouted (ploughed land prevailingly)

3. Forests and semi-natural areas

3.2. Shrub and/or herbaceous vegetation associations

3.2.1. Natural grassland and pastures

3.2.1.1. Natural, open grassland prevailingly without shrubs (<20%)

Low productivity grassland. Herbaceous cover between 20% and 40%, with <15% shrub or none.

3.2.1.2. Open grassland with shrubs

Herbaceous cover between 5% and 15%, with 20 - 40% shrub canopy.

3.2.1.3. Riparian vegetation

Rich riparian herbaceous and shrub vegetation (generally non xerophillous).

3.2.3. Xerophillous vegetation

3.2.3.1. Mixed xerophillous vegetation

3.2.3.2. Halophile vegetation

3.2.4. Matoraal

3.2.4.1. Matoraal

Xeric open degraded forest and shrubland often dominated by scattered tall shrubs and small trees: typical African and arid zones transitional woodland from forests to steppes.

3.3. Open spaces with little or no vegetation

3.3.1. Beaches, dunes, sands

3.3.1.3. River banks/beds – sandy, dry Oued

3.3.2. Bare rocks

3.3.2.1. Hamada

Vast rocky desert plateau

3.3.2.2. Bare rock/soil – usually saline/alkali

Scree, cliffs, including active erosion flats situated above the high-water mark. Processing at an interactive station (mineralization index, principal component analysis) may be used in order to better distinguish class 3321 from 3322, given that in semiarid areas the location and spatial distribution of salt-affected soils is primary for agricultural activities and not only.

3.3.3. Sparsely vegetated areas

3.3.3.1. Nebkhas

Coppice dunes, areas of sand plains (dunes) covered by sparse vegetation.

Typical semiarid aeolian dune landscapes consisting of areas covered by a rather thin layer of blowout sand and sometimes pebbles, forming coppice dunes, stabilised by vegetation, but too small to be considered a sand dune. They can be visually identified as they present a blurred homogenous colour indicating the blown - out sand. Isolated mounds are formed around individual plants, usually sparse within the defined area.

3.3.3.2. Sparse vegetation on rocks/hamada

Areas of xerothermic grasses and shrubs of karstic terrain, or areas of discontinuous grasslands.

3.3.3.3. Sparse vegetation on saline/alkali soils

3.3.3.4. Sparse vegetated alluvial fans

Linear pattern either herbaceous, but usually shrub vegetation, along the torrential water features.

4. Wetlands

4.1. Inland wetlands

4.1.1. Inland marshes

4.1.1.4. Saline (alkali) inland marshes without reed beds (<20%) and with other water plants

4.1.1.5. Sebkha/daia

Sebkha: Salt – flats characterized by evaporites – carbonate deposits with some siliciclastic.

Daia: depression, intermittent wetlands

4.1.1.6. Temporary humid areas – floodable areas with no or little vegetation

It differentiates from other wetlands through a shallow water level, it cannot be considered a marsh nor a Sebkha.

5. Water bodies

5.1. Inland waters

5.1.1. Water courses

5.1.1.1. Oued

By definition, they are temporary

5.1.2. Water bodies

5.1.2.1. Natural water bodies

Water areas of natural origin.

*) Etang – shallow stagnant water

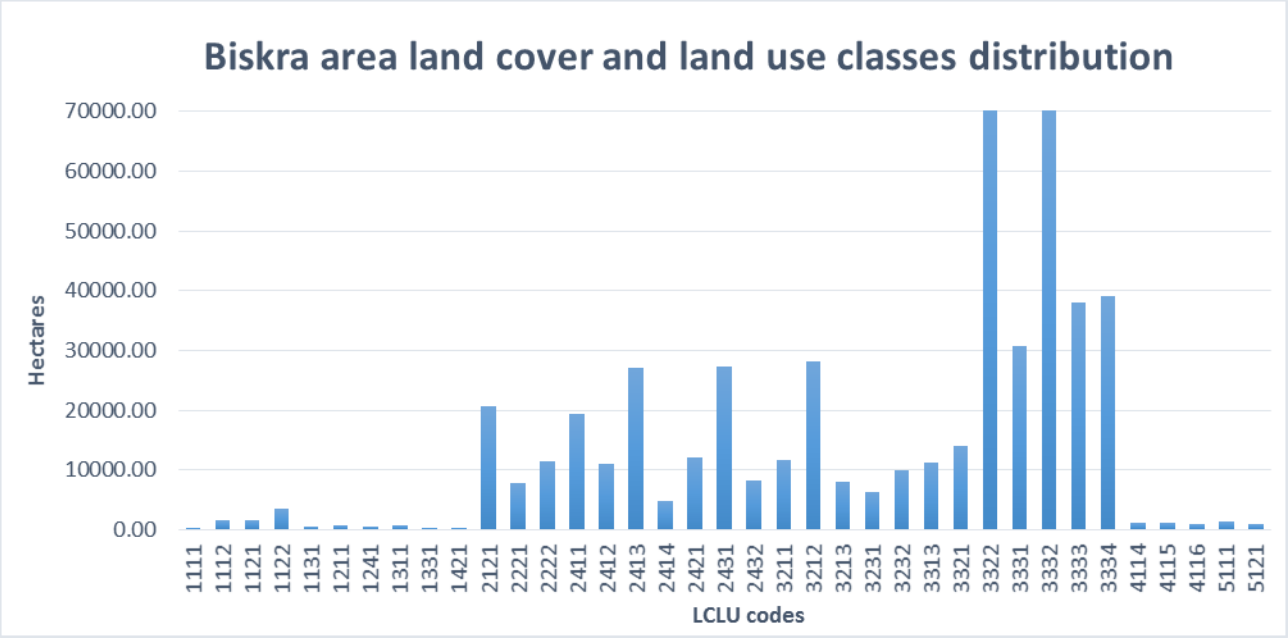

Figure 59

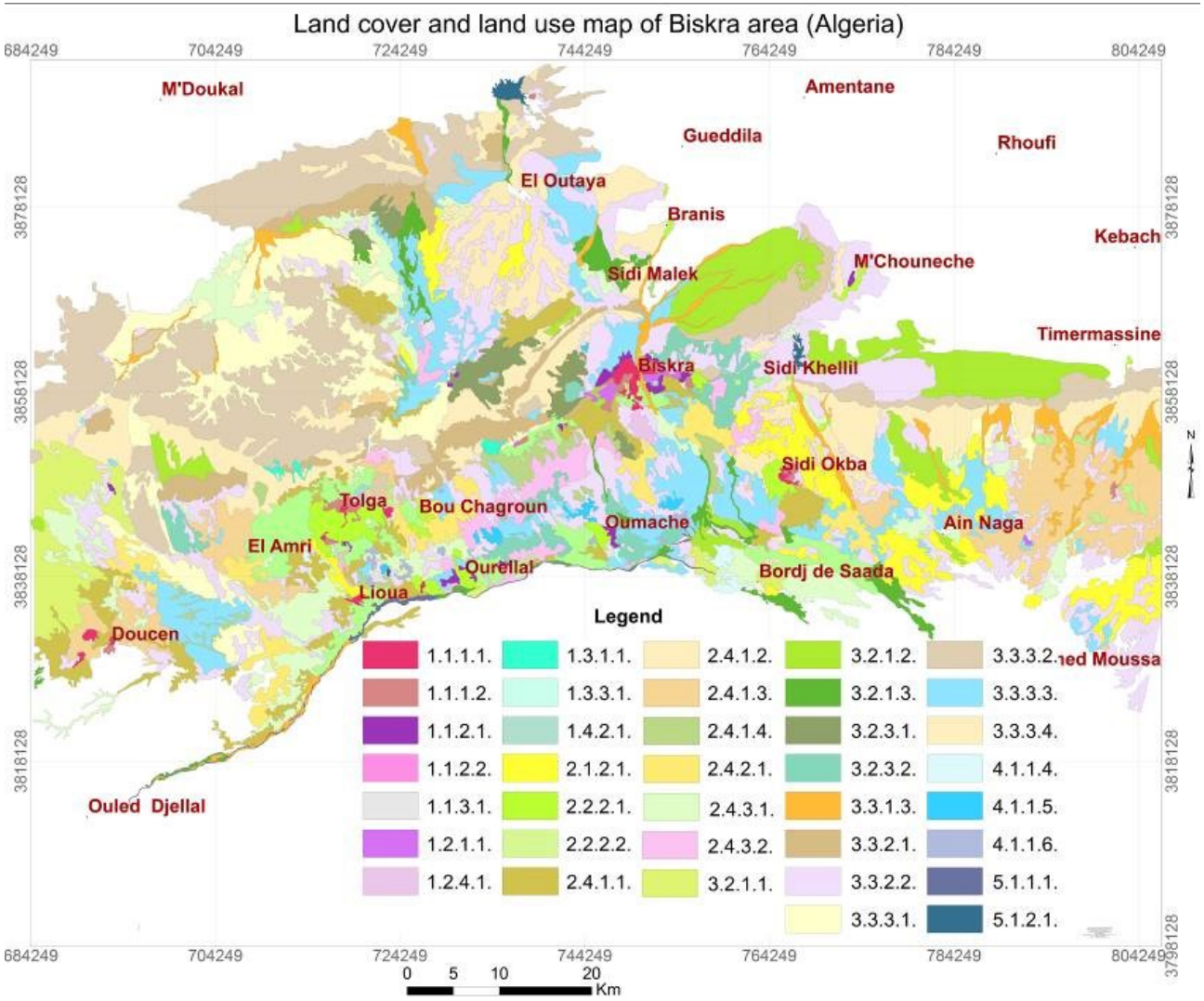

Figure 60. Land cover and land use map of Biskra area – visual interpretation.

5.1.2. Oum Zessar area

For the Oum Zessar area, 36 LCLU classes were defined based on visual interpretation of Landsat 8 images of 17 May 2013, path 190, row 37 and 24 May 2013, path 191, row 37 and ground truth data of a total of 400 observation points. The classes of the LCLU codes in the legend of figure 5 are:

1. Artificial surfaces

1.1. Urban fabric

1.1.1. Continuous urban fabric

Areas of urban centres with public, administrative and commercial buildings, roads, parking lots and artificial surfaces (e.g. cemeteries without vegetation) cover more than 80% of the total surface. Urban greenery is exceptional.

1.1.2. Discontinuous urban fabric

1.1.2.1. Discontinuous built-up areas with bare land

Most of the land is covered by structures. Buildings, roads and artificially surfaced areas are associated with bare soil, which occupy discontinuous but significant surfaces.

1.1.2.2. Discontinuous built-up areas with areas arable irrigated perimeters

The land is covered by impervious elements, such as houses, roads and artificially surfaced areas that are associated with small farming areas: cultivated irrigated private parcels (vegetables, aromatic plants, fruit trees) of subsistence agricultural practices, which occupy discontinuous but significant surfaces. The ratio is approximately 50-50%.

1.2. Industrial, commercial and transport units

1.2.4. Airports

1.2.4.1. Airports with grass surfaces of runways

Areas of airports with grass surface of runways with associated airport buildings.

1.3. Mine, dump and construction sites

1.3.1. Mineral extraction sites

1.3.1.1. Quarries and open-cast mines

Areas with open-pit extraction of construction material (sandpits, quarries) or other minerals (open-cast mines that include oil-shale mines, gravel, sand, and clay pits). Includes flooded gravel pits, except for river-bed extraction.

2. Agricultural areas

2.1. Arable land

2.1.2. Permanently irrigated land

2.1.2.1. Small-farming irrigated perimeters

Small-farming irrigated perimeters, in which crops are irrigated permanently or periodically, using a permanent infrastructure (irrigation channels, drainage network). It differs from the irrigated parcels in 1122, by increased size and homogeneous in composition. They usually consist of Olive nurseries or in combination with other fruit trees (orange, peach, almond) but also pine or Eucalyptus nurseries (used widely for “mis – en – defence”), but also legumes cultivation, rarely cereals, with a boundary of Eucalyptus or Pine species as a protection from sand encroachment. They

are usually found outside inhabited centres, build around surface wells, near Oued beds, where the phreatic is near to the surface. May include sporadically irrigated land.

2.2. Permanent crops

2.2.3. Olive groves

Extended areas planted with rain fed Olive trees which can have a low spectral response. The space between trees is usually of 2 m and that may be the main reason for feeble signal. They can be found in the plain sand encroached or even on saline, unfertile lands, with natural or cultivated vegetation. They are the only ones able to resist harsh conditions and low nutrient land with major water scarcity, due to the dual type of radicular system: longitudinal and transversal in order to maximise the capacity of water absorption. Locally or sporadically, arable land rectangular parcels pattern can be noticed, as they are ploughed. The NDVI gives null vegetation values for these areas. Generally, thay are identified through field ground truth or by the use of high-resolution imagery (Quickbird from Google Earth) as they are perennial vegetation and in order to be visible on the imagery, they must be tens of years old.

2.3. Pastures

2.3.1. Pastures

Dense grass cover, of floral composition, dominated by graminaceae, not under a rotation system. Mainly for grazing, but the fodder may be harvested mechanically. Includes areas with hedges (bocage).

2.4.1. Annual crops associated with permanent crops

2.4.1.1. Annual crops associated with Olive groves

Non-permanent crops (arable land or pasture) associated with Olive groves on the same parcel. This category covers associations within a single parcel, identifiable by specific spectral responses and not in tabias and jessour systems. It differs from areas of polyculture with parcels given over either to annual crops or to permanent crops. Land units in a typical mosaic of small parcels of annual crops, pasture and permanent crops should be classified under category 2.4.2 (complex cultivation patterns).

2.4.1.2. Tabias plantations

Permanent crops, usually Olive plantations cultivated in tabias water harvesting systems, usually in the plain areas, on slopes less than 3%, which are typical for the Tunisia arid and semiarid areas. They may be associated with annual crops within the tabias bodies, depending on the annual and seasonal rainfall regime and on their proximity to houses for small-scale farming or even for personal production. For this reason, this type of land use also includes sparse and discontinuous built-up features (houses, deposits, animal shelters). Locally, there may also be associated with other permanent crops such as figues, almond, pistachio and peach trees, where the soil is prone to this type of arboriculture. It may also contain portions of bare land or natural vegetation, but not of significant proportions (less than 30%). They are easily recognisable from their linear, leaf-veins pattern as they follow ephemeral oued courses, afluents and small torrential bodies in plain areas.

2.4.1.3. Jessour plantations

Permanent crops consisting mainly out of Olive plantations but can also be associated with figues and other fruit trees, cultivated in jessour systems (water harvesting techniques), typical for the mountain arid and semiarid areas in Tunisia, on slopes greater than 3%. It may also contain portions of bare land or natural vegetation on slopes, but not of significant proportion (less than 30%). They are easily recognisable from their linear, leaf-veins pattern as they follow

ephemeral oued courses, affluent and small torrential bodies in mountainous areas. Unlike 2.4.1.2, the spectral response is more intense and with a dot-pattern as in the mountain areas Olives are older and with richer canopies (the age of the trees gets smaller from mountain to plane, from west to east and due to different microclimate conditions).

2.4.2. Complex cultivation patterns

Juxtaposition of small parcels of diverse annual crops, pasture and/or permanent crops. On satellite images this category always presents a rectangular very fragmented pattern of easily recognizable parcel pattern. This heading covers land units identifiable by characteristic spectral responses and composed of small parcels of diverse annual crops, not necessarily sprouted but usually ploughed, pasture and/or permanent crops, provided that none of these three categories covers an identifiable surface unit of more than 25 ha within a single land unit. Arable land, pasture and orchards each occupy less than 75% of the total surface area of the unit. City gardens are included under this heading.

2.4.3. Land principally occupied by agriculture, with significant areas of natural vegetation

Areas principally occupied by agriculture, interspersed with significant natural areas. In these units, no homogeneous subset of 25 ha or more should be isolated in agricultural land or in natural areas (natural vegetation, forests, moors, grassland, water bodies or bare rock). Agricultural land occupies between 25 and 75% of the total surface of the unit. Hedged (bocage) areas are excluded from this heading (see heading 2.3.1).

2.4.3.1. Agricultural areas with significant share of natural vegetation, with Tabias cultivations.

Tabias water harvesting and agricultural type of management are typical for the plain areas, along Oued and small torrential valleys, usually consisting of small parcels of annual crops with olive trees and locally also fruit trees such as figs, almonds, peach trees and pistachio. It differs from Tabias heading through the fact that parcels of annual crops, not necessarily sprouted and usually ploughed are outside the tabias bodies, with sporadic distribution and a significant share on natural vegetation.

2.4.3.2. Agricultural areas with significant share of natural vegetation, with Jessour cultivations.

Jessour water harvesting and agricultural type of management are typical for mountainous areas, along Oued and small torrential valleys and usually consist of mature Olive trees and figs associated with parcels of annual crops, not necessarily sprouted, but usually ploughed and with an easily recognisable pattern. It may also contain significant areas of natural vegetation with a discontinuous distribution among the other land facets.

2.4.3.3. Agricultural areas with visible cultivation pattern, with significant share of natural vegetation

Agricultural areas with visible cultivation pattern, with significant share of natural vegetation, with the prevalence of annual crops in early phenological stage or not yet sprouted (ploughed land prevailingly)

2.4.3.4. Agricultural areas with significant share of annual and permanent crops, and with presence of scattered vegetation

Olive groves associated with fragmented parcels of annual crops, usually not yet sprouted, recognisable by pattern, with natural vegetation, with a discontinuous distribution (not in tabias or jessour).

2.4.4. Agro-forestry areas

This category appears frequently in Southern Europe. It is usually linked to very extensive areas with a very variable spectral signature (different species, tree density, soil types). Delineation is not always easy as there is often a transitional zone between the natural vegetation and the Ploughed land. A good knowledge of the area and the use of

aerial photographs are recommended. Small areas of planted trees, for sand blocking purposes, typical mis-en-defence plantations, prevailingly made out of Eucalyptus, but also pine species or acacia (wattle).

3. Forests and semi-natural areas

3.2. Shrub and/or herbaceous vegetation associations

3.2.1. Natural grassland

3.2.1.1. Open grassland

Low productivity grassland. Often situated in areas of rough, uneven ground. Frequently includes rocky areas, briars and heathland. Graminaceae, herbaceous cover between 20 - 40% and less than 15% shrub canopy.

3.2.1.2. Closed grassland with shrubs

Areas of grassland with small trees (acacia, tamarix) and shrubs (more than 40%).

3.2.1.3. Riparian vegetation

Natural riparian vegetation consisting of rich herbaceous, shrub vegetation and reed (can reach 3m height, attested from ground truth).

3.2.2. Mountain rangeland

This class is the equivalent of "moors and heathland" class in CORINE land cover nomenclature. Vegetation with low and closed cover, dominated by bushes, shrubs and herbaceous plants. Usually composed of mixed xerophillous vegetation, sparse on Southern and Western slopes and a rather uniform dense distribution on Northern and Eastern slopes. Contains palatable species.

3.2.3. Shrubland

3.2.3.1. Shrubland

This class is the equivalent of "sclerophyllous vegetation" class in CORINE land cover nomenclature. It is usually composed of mixed sclerophyllous but also xerophillous dense vegetation, but may also contain palatable species. Steppes of *Artemisia herba alba*, *stipa tenacissima* and *rosmarinus officinalis* in association with *hammada scoparia*, *fartesia aegyptica*, *chrysanthemum fustacum*, *centaurea furfuracaea* etc.

3.2.3.2. Oued vegetation

Shrubland associated with trees (Eucalyptus, pine, acacia – silver wattle, tamarix) and shrubland, with very sporadic annual cultivations or greenhouses. Mostly characterised by thin skeletal soil and coarse alluvial deposits

3.2.4. Xerophillous vegetation

3.2.4.1. Halophile vegetation

Steppes of lygenum spartum, astragalus armatus in association with erodium glaucophyllum, aristidia ciliate.

3.2.4.2. Psamophile vegetation

Speppes of *Retama raetam*, *rhanterium suaveolens*, *Artemisia campestris* in association with *astragalus gomba*, *astragalus gombiformis*, *Hammada schimittiana* (*arthrophytum schittianum*), *cleone Arabica*

3.2.4.3. Steppes of *Rhanterium suaveolens* and *Artemisia campestris*, *Retama raetam*

These may also be used as pastures, as they are palatable species. Vegetation found in areas of active aeolian deflation or accumulation, with calcareous crust at a depth inferior to 50 cm from surface. Mostly characterised by thin skeletal soil, with calcareous clasts (if re-worked), calcareous crust or concretions.

3.3. Open spaces with little or no vegetation

3.3.1. Beaches, dunes, sands

3.3.1.3. River banks/beds – sandy, Oued paleo valleys

Belts of river banks formed mainly by deposits of sands and gravel prevailingly without vegetation.

3.3.2. Bare rocks

3.3.2.1. Reg

Vast rocky desert plateau, usually represented by eroded calcareous plaque or with calcareous concretions.

Sparse shrubs, attested by ground truth as being sporadic and spontaneous, with no distribution pattern, represented by typical species: anthyllis sericea subsp. Henoniana, associated with gymnocarpos decander.

3.3.2.2. Bare rock/soil

In plain areas, it usually overlays sandy or saline areas. In the mountain areas, it refers to bare rock. Scree, cliffs, including active erosion flats situated above the high-water mark. Processing at an interactive station (mineralization index, principal component analysis) may be used in order to better distinguish class 3321 from 3322, given that in semiarid areas the location and spatial distribution of salt-affected soils is primary for agricultural activities and not only.

3.3.3. Sparsely vegetated areas

3.3.3.1. Nebkas

Coppice dunes, areas of sand plains (dunes) covered by sparse vegetation.

Typical semiarid aeolian dune landscapes consisting of areas covered by a rather thin layer of blowout sand and sometimes pebbles, forming coppice dunes, stabilised by vegetation, but too small to be considered a sand dune. They can be visually identified as they present a blurred homogenous colour indicating the blown - out sand. Isolated mounds are formed around individual plants, usually sparse within the defined area.

3.3.3.2. Sparse vegetation on rocks/reg

Areas of xerothermic grasses and shrubs of calcareous terrain, or areas of discontinuous grasslands.

3.3.3.3. Sparse vegetation on saline/alkali soils

3.3.3.4. Sparse psamophyte vegetation

3.3.3.5. Sparse Oued vegetation

3.3.3.6. Other sparse vegetation areas

4. Wetlands

4.1. Inland wetlands

4.1.1. Inland marshes

Low-lying inner land usually flooded and more or less saturated by water all year round. These areas are usually saline (alkali) inland marshes without reed beds (<20%) and with other water plants.

4.2. Coastal wetlands

4.2.1. Salt marshes

4.2.1.1. Sebkha

Sebkha: Salt – flats characterized by evaporitic – carbonate, saline deposits with some siliciclastic, usually without vegetation

4.2.1.2. Temporary humid areas – floodable areas with no or little vegetation

It differentiates from other wetlands through high humidity on the satellite imagery, but it cannot be considered a marsh nor a Sebkha.

5. Water bodies

5.1. Inland waters

5.1.1. Water courses

5.1.1.1. Oueds

Natural or artificial water courses serving as water drainage channels. Includes canals. Minimum width for inclusion: 50 m. By definition, they are temporary.

The minimum mapping unit (MMU) is 25 ha and the used mapping scale was 1: 40 000, the mximum allowed by the spatial resolution of Landsat imagery. To meet visual interpretation needs, image pre-processing methods, such as radiometric and atmospheric correction, were not necessary and attention was focused on band composition and radiometric enhancement (Zhang, Wang et al. 2014). Figure 15

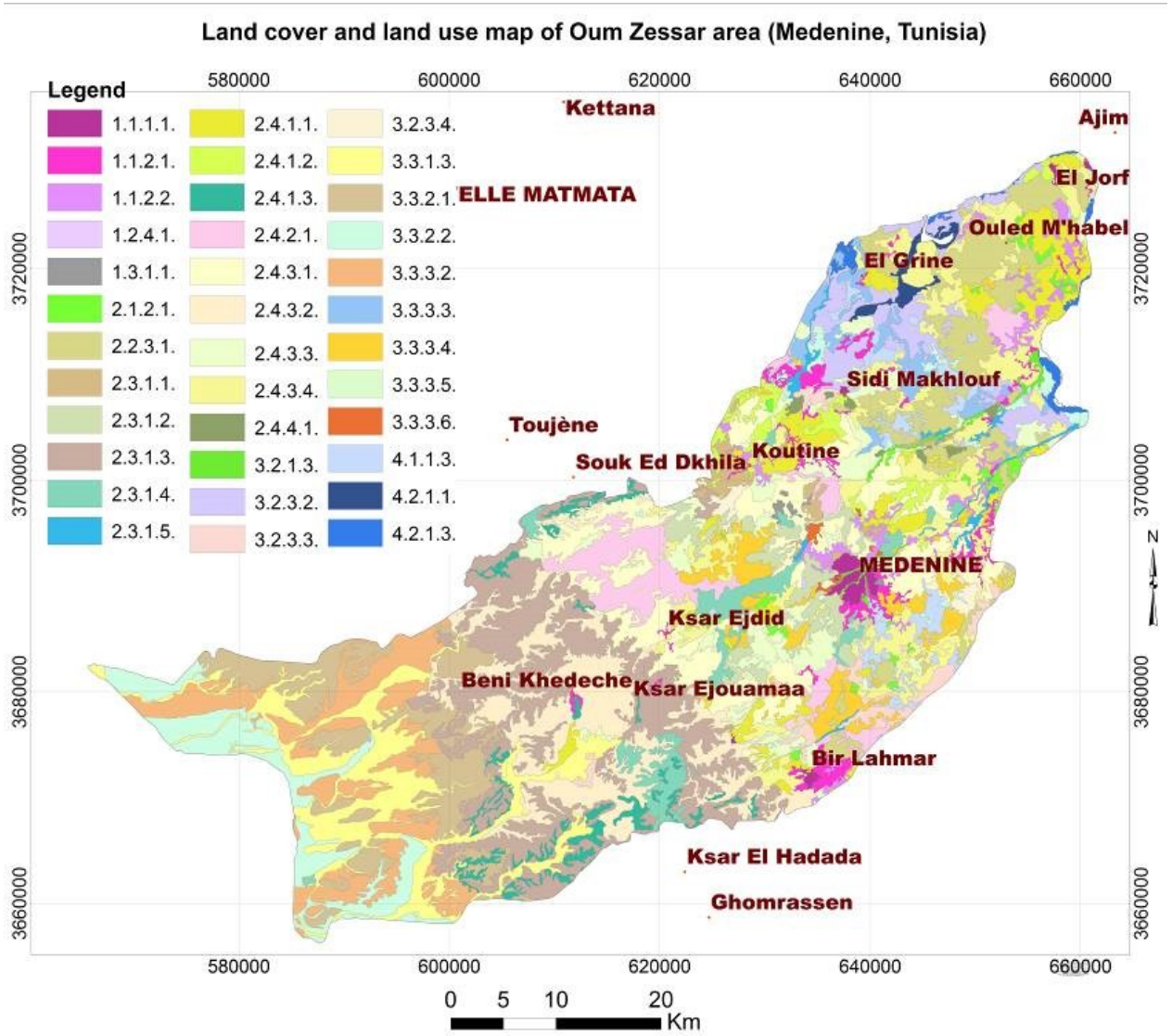

Figure 61. Land cover and land use map of Oum Zessar area – visual interpretation.

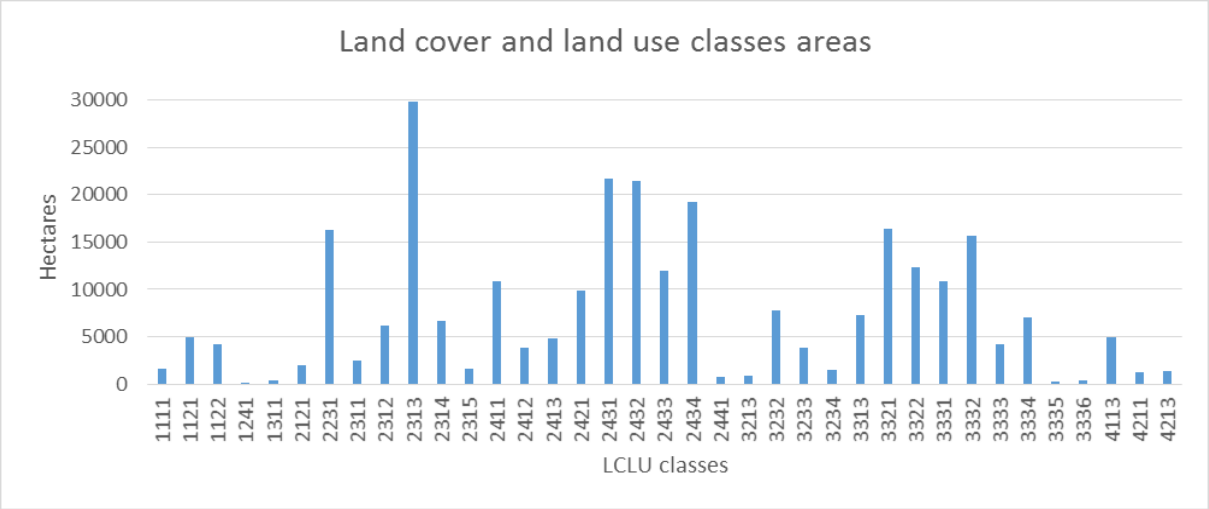

Figure 62. Oum Zessar distribution of land cover and land use classes areas

5.2. Spectral Libraries Analysis

Regarding the spectral analysis of the areas affected by sand encroachment, preliminary spectral analysis through visual inspection have shown a clear distinction between the areas west of the domain of Dahar and the inner-plain ones, within Jeffara, indicating different physical and/or chemical, namely mineralogical, characteristics. Spectral signatures were compared with existing USGS mineral libraries (ENVI 5.2) for matching analysis, as shown in the figures 63-65 (Afrasinei, Melis et al. 2015).

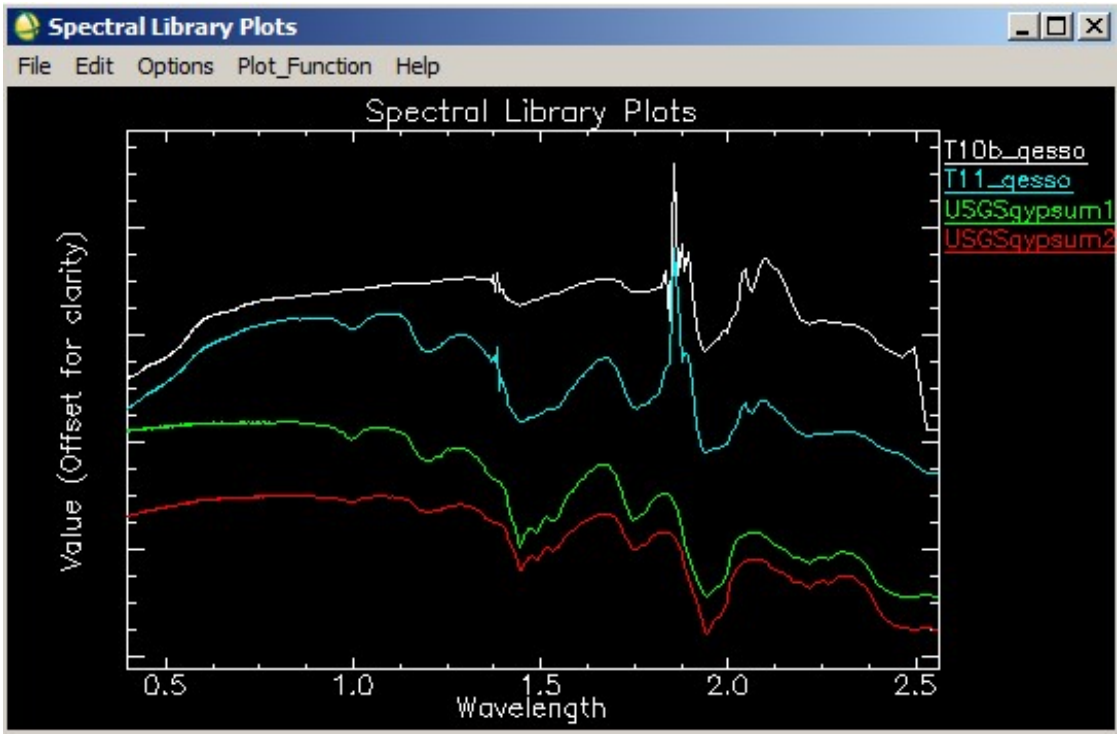

Figure 63. Display of spectral signatures of T10 and T11 and two USGS library gypsum signatures

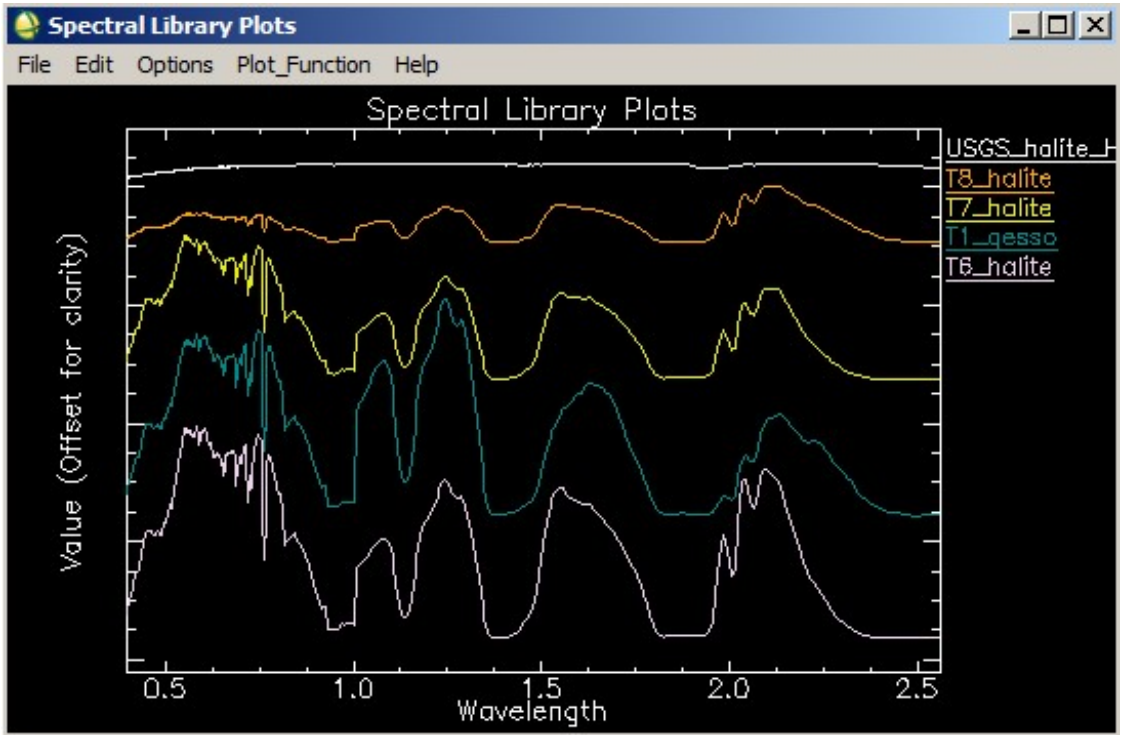

Figure 64. Display of spectral signatures of T10 (gypsum supposed), T6, T7 and T8 (the latter 3 - halite) and the USGS library halite signature

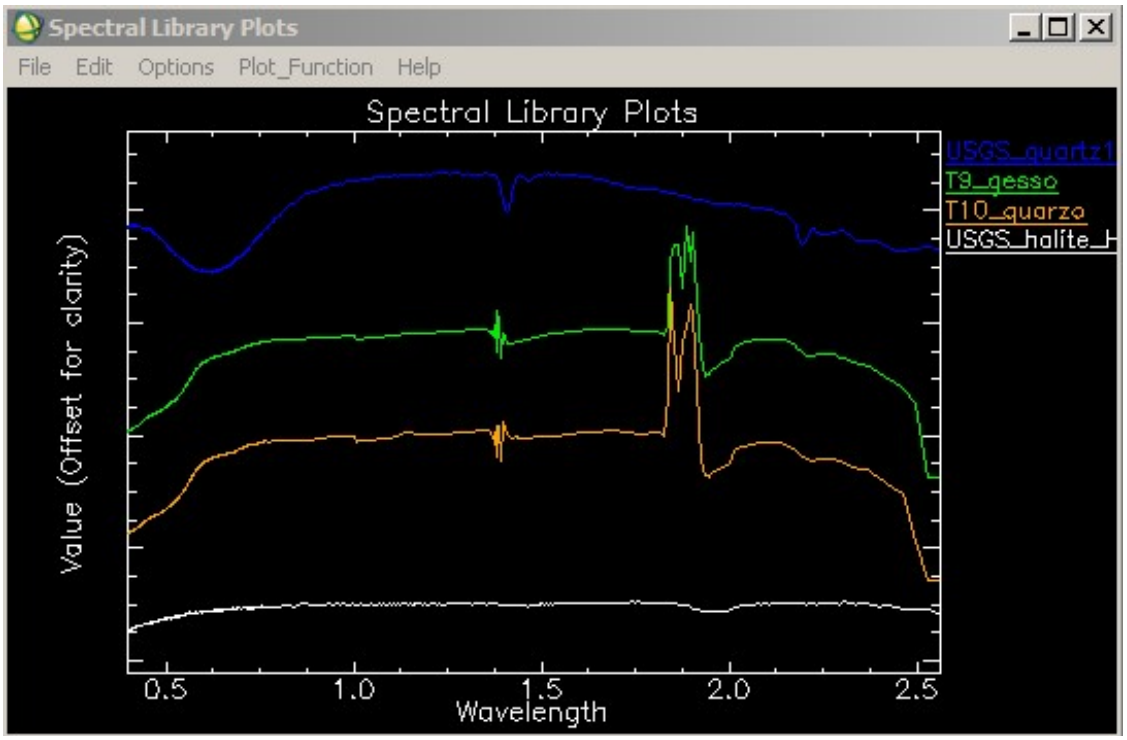

Figure 65. Display of spectral signatures of T9 and T10 and two USGS library quartz and halite signatures

5.3. XRD analysis

In order to obtain information on the mineralogy of salt crusts the 18 samples of salts and sand collected in the Oum Zessar area have been analysed through the X-ray diffraction method.

The main minerals of the salt samples are gypsum and halite, according to the pedogenetic, geochemical and sedimentological processes as driving factors of the geomorphological contexts from which they were taken. There were identified nine different mineral phases in total. The main minerals are found to be gypsum, halite, calcite and quartz; in most cases, it was also possible to estimate weight percentage. The bar graph shows the distribution of the main mineral phases within the samples. The T1, T3, T9, T10b, T11 samples are characterized by a high amount of gypsum, while the T6, T7, T8 samples present a high proportion of halite.

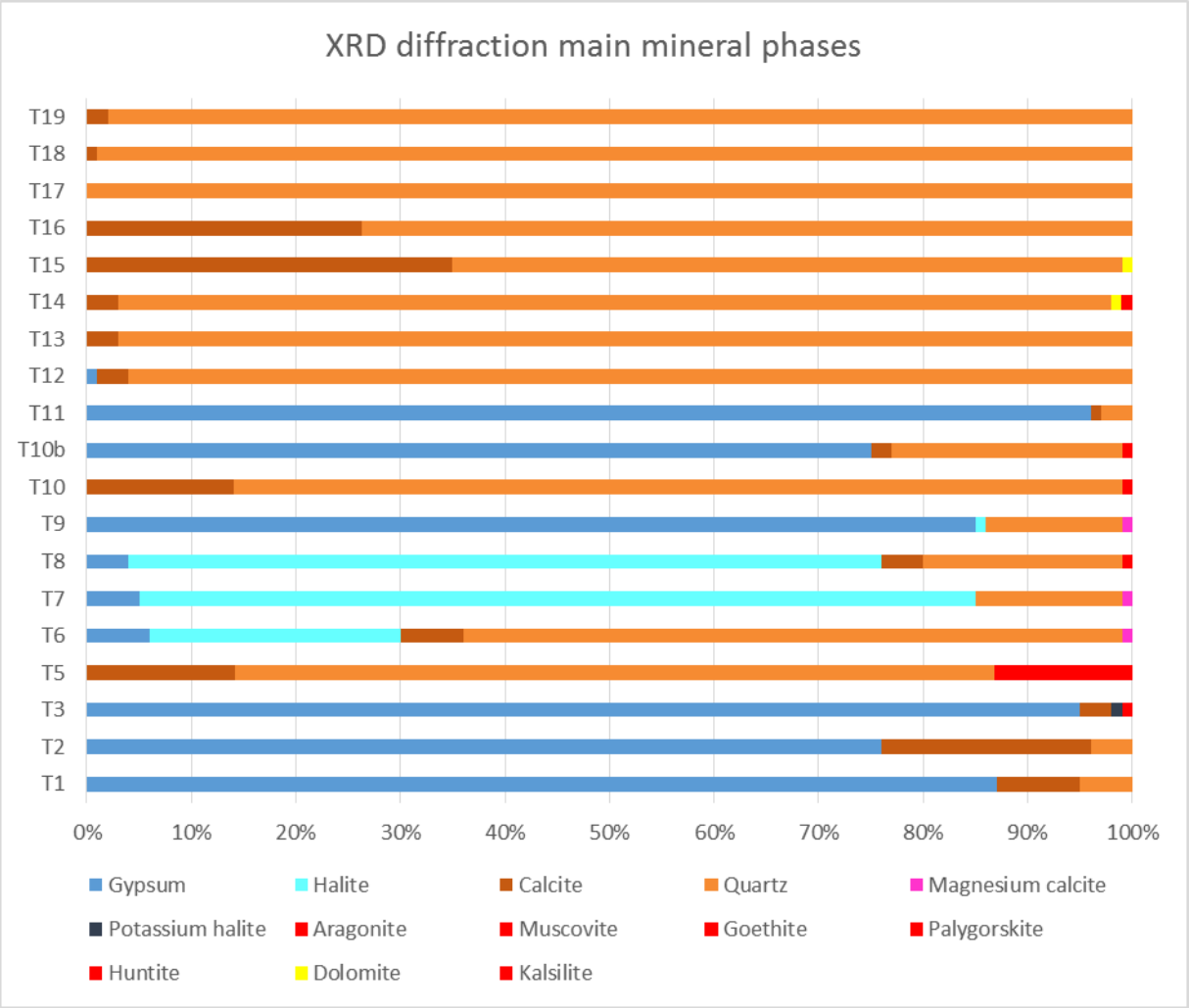

Figure 66. Main mineralogical phases of the salt and sand samples identified through XRD

The main minerals of the sand samples are quartz, calcite and dolomite, adding to these small proportions of clay or feldspar minerals. In figure 62, the distribution of sample points can be observed, in particular the fact that sand samples 13-19 that are located west of Dahar can be easily distinguished in figure 61 as being different in mineral composition (proportion and types) from the other ones.

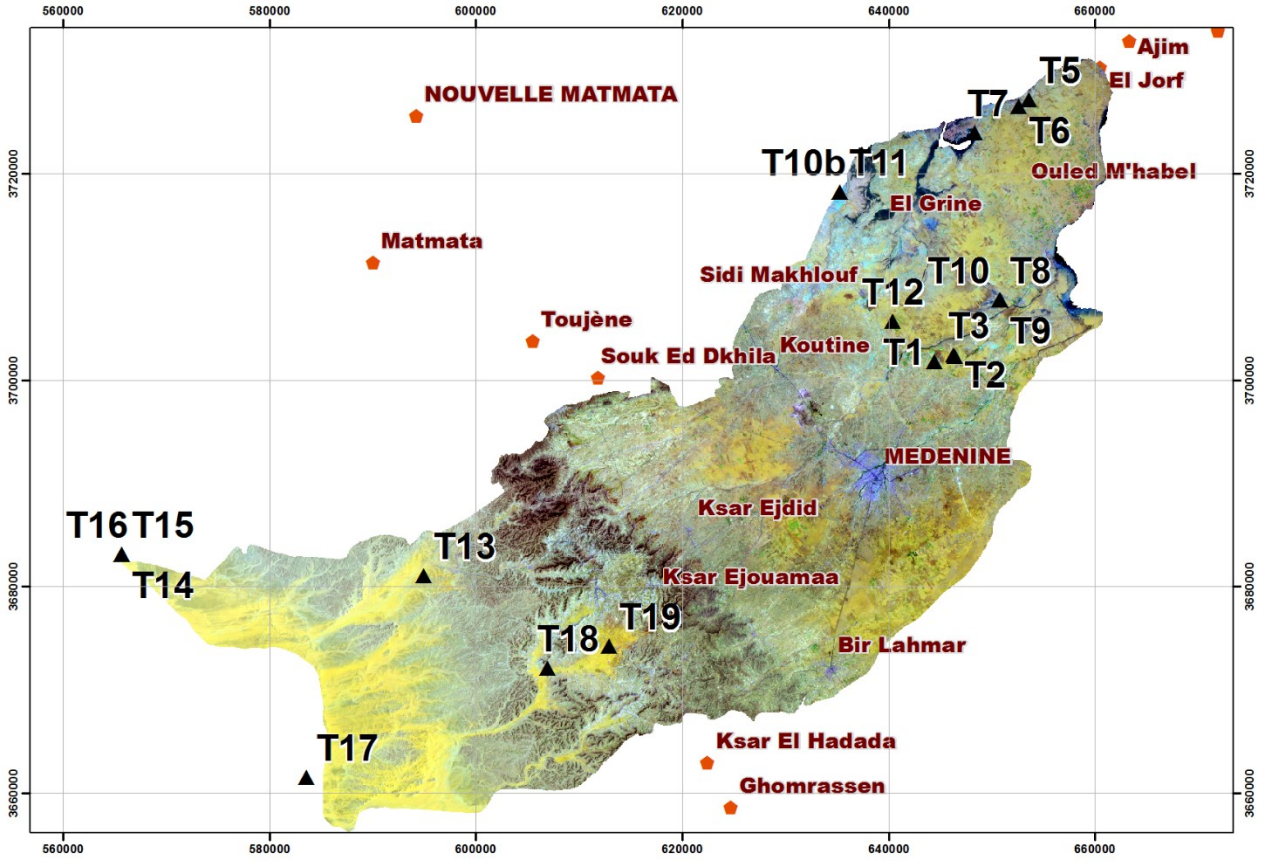
560000
580000
600000
620000
640000
660000
3720000
3700000
3680000
3660000
Ajim
El Jorf
NOUVELLE MATMATA
T5
T7
T6
T10b
T11
Ouled M'habel
El Grine
Matmata
Sidi Makhlouf
T10
T8
T12
T3
T9
Toujène
Souk Ed Dkhila
Koutine
T1
T2
MEDENINE
Ksar Ejdid
T16
T15
T13
T14
Ksar Ejouamaa
T19
T18
Bir Lahmar
T17
Ksar El Hadada
Ghomrassen

Figure 67

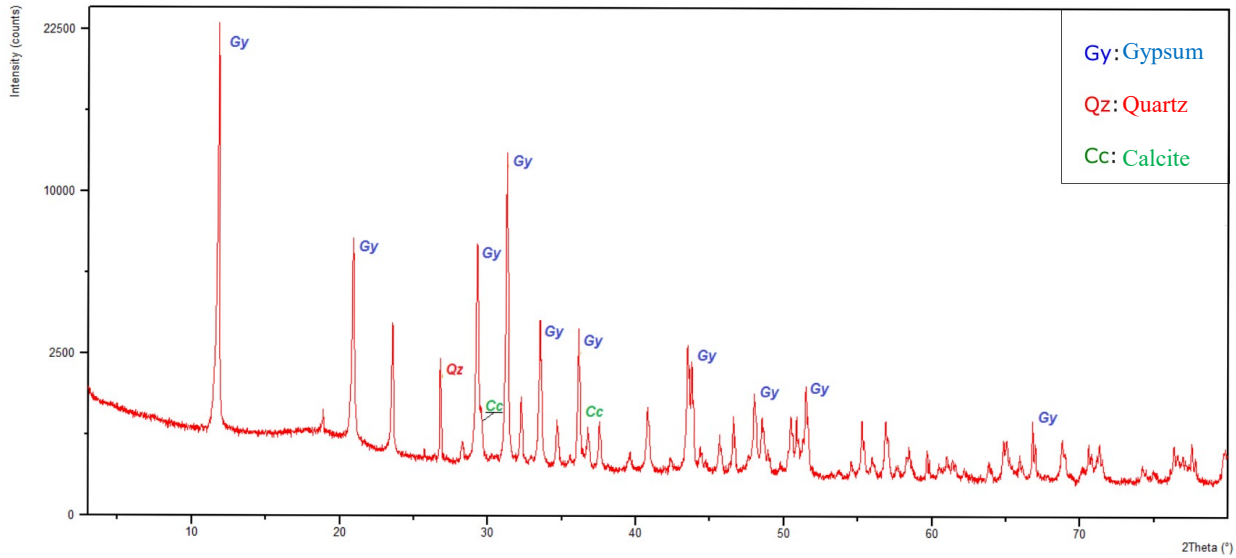

Gypsum	$CaSO_4 \cdot 2H_2O$	87%
Calcite	$Ca(CO_3)$	8%
Quartz	SiO_2	5%

Figure 68.Example of T1 graphic showing the main identified mineral phases correspondent to diffraction peaks

Sample	Photos	Y	X	Z	Target	LC	OBS	clouds	Date	Time	XRD
T1	Nikon 1051, 1054, 1055	33.4458	10.55333	45	fine loam, conglomerates, gypsum crust	sparse natural bushy veg, degradation indicating species		100%	16-06-14	8:55:00 AM	gypsum87, calcite8, quartz5
T2	Nikon 1056	33.4496	10.57483	43	gypsum crust, oxydised, reddish loam of fine texture	sparse desert vegetation		50%	16-06-14	9:41:00 AM	gypsum76, calcite21, quartz4
T3	Nikon 1060, 1061	33.4512	10.57383	45	gypsum crust	graminaceae, annual veg, sparse, small; fFuji 6142	software crash, files saved in new folder; all 3 sets of measurm taken in the same point	30%	16-06-14	10:06:00 AM	gypsum97, quartz3, potassium halite
T4	Nikon 1066	33.4517	10.57419	45	sand dune	nude dune, sourrounded by palms, sparse psammophyte		30%	16-06-14	10:17:00 AM	
T5	Nikon 1088, 1089	33.6726	10.6563	10	50m loam	arable land of olive groves with sparse natural graminaceae	50m loam in a depressionary area, instrument attached to car battery supply	100%	16-06-14	3:02:00 PM	quatrtz72, calcite14, aragonite13, muscovite
T6	Nikon 1108, 1109	33.6674	10.64563	10	salt efflorescence			20%	16-06-14	4:00:00 PM	quartz64, halite24, calcite6,gypsum6
T7	Nikon 1114, 1115	33.6447	10.59942	9	sebkha	bare land, sebkha, sparse and sporadic halophyte vegetation	shells presence	40%	16-06-14	4:36:00 PM	halite80, quartz15, gypsum5, magnesium calcite
T8	Fuji 116-6281/82	33.4987	10.62308	14	sandy soil with efflorescence	halophyte dry vegetation		0%	18-06-14	8:37:00 AM	halite73, quartz19, calcite4, gypsum4, goethite
T9	Fuji 6313/14	33.4983	10.6227	14	clay minerals with salt efflorescence	halophyte veg, panoramic Fuji6319-22	sub-surficial gypsum salt; same measurem point, 2 samples: T9-gypsum salt and T10 clay sample	0%	18-06-14	9:18:00 AM	gypsum86, quartz13, halite1, magnesium calcite
T10	Fuji 6317/18	33.4982	10.62267	14	clay minerals with salt efflorescence	halophyte veg, panoramic Fuji6319-23	sub-surficial gypsum salt; same measurem point, 2 samples: T9-gypsum salt and T10 clay sample	0%	18-06-14	9:18:00 AM	quartz86, calcite14, palygorskyte
T10b	Fuji 6351/52/57	33.5948	10.45755	20	gypsum crust	halophyte, haloclinum	near T11	0%	18-06-14	11:29:00 AM	gypsum76, quartz22, calcite2, huntite
T11	Fuji 6358/59	33.5948	10.45757	20	gypsum crystalls, sebkha	halophyte, haloclinum	near T10b, panoramic N172 Fuji6364-68	0%	18-06-14	11:40:00 AM	gypsum96, quartz3, calcite1
T12	Fuji 6377/78	33.48114	10.51069	49	sand encroachment	psammophyte, retama reatm	sand accumulation due to palissade (anthropical)	0%	18-06-14	12:50:00 PM	quatrz97, calcite3, gypsum
T13	Nikon 1203/04	33.26401	10.01943	338	sand dune, aeolian deposit	Beghil Guzah Dahar rangeland, gurdab, a	dand dunes due to the presence of tabias	0%	19-06-14	10:07:00 AM	quartz97, calcite3

						xerophyte species					
T14	Nikon 1238-44?	33.28489	9.705543	186	sand, oued valley, fine granulometry	psammophyte veg	within Oued bed, valley	0%	19-06-14	12:05:00 PM	quartz96, calcite3, dolomite, kalsilite
T15	Nikon 1245-50	33.2849	9.705497	186	sand, coarse granulometry	psammophyte veg	within Oued bed, valley	0%	19-06-14	12:05:00 PM	quartz65, calcite35, dolomite
T16	Nikon 1251-56	33.28515	9.705403	190	clay deposit in riverbed	bare land	within riverbed	0%	19-06-14	12:50:00 PM	quartz74, calcite26, dolomite, sylvite
T17	Nikon 1317/18	33.0889	9.895655	310	sand dune, aeolian deposit on carbonate surface	sparse psammophyte veg, retama	sand accumulation on carbonate surface, after artesian well visit	0%	19-06-14	3:20:00 PM	quartz99
T18	Nikon 1347/63	33	9	353	sand, cleaner	psammophyte, aristidia pungens, retama		0%	19-06-14	4:20:00 PM	quartz99, clacite1
T19	Nikon 1370-72	33.20127	10.21137	427	sand	psammophyte, aristidia pungens, retama	T18bis?	0%	19-06-14	5:04:00 PM	quartz98, calcite2

5.4. Classification Outputs

5.4.1. Decision Tree Classifier

5.4.1.1. Biskra Area

The decision tree map was obtained by applying vegetation, wetness, mineral and salinity indices as well as simple band ratios, mostly derived from the analysis of bands statistics, scatter plots and vertical and horizontal profiles of interest features but also from literature (Khan, Rastoskuev et al. 2001, Metternicht and Zinck 2008, Elnaggar and Noller 2010, Hamid Reza and Majid Shadman 2012, Allbed and Kumar 2013, Melis, Afrasinei et al. 2013, Mulder, de Bruin et al. 2013). The indices proposed for this study are constructed based on bands which present high spectral information covariance of the feature to be extracted. For example, in the case of highly saline areas class extraction, TM bands 1, 2 and 3 information are usually put together, in order to enhance the "brightness" features, divided by band 7, which presented the lowest reflectance values of salt features. Exponential or square root functions were used to force the emphasis of extreme values, helping in delineating high or moderate saline areas. The statistics of each index/math image were used in order to establish the thresholds for each decision node. The decision nodes and the resulting map are thus obtained, for each of the 8 dates. According to the lithological and vegetation cover of the area, the DT analysis and legend was adapted in order to classify the main land cover classes as well as classes of lithology distinguishable according to their spectral lithological response, which are described in table 6.

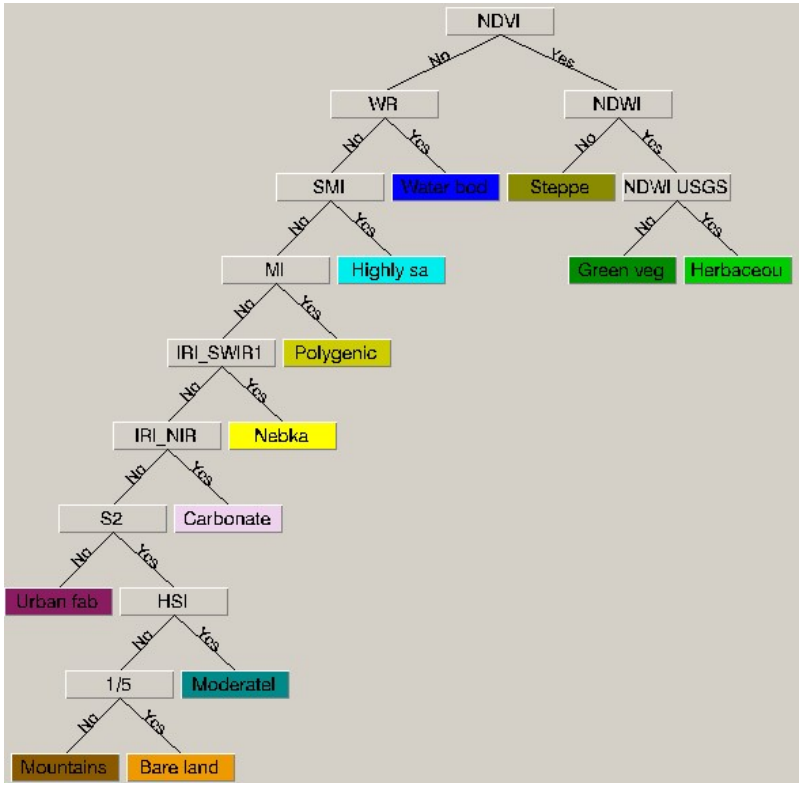

Figure 69. Decision tree binary decision nodes and resulting classes

Table 6. Description of the resulting classes of the Decision Tree Analysis

Green vegetation	Oasis vegetation, mainly palm groves, fruit trees plantation, types of small trees and tall shrubs rich in biomass or chlorophyll
Herbaceous vegetation	Annual crops, small natural herbaceous vegetation, small shrubs
Steppe	Typical dry shrub vegetation, woody correspondent to mountainous and piedmont areas
Urban fabric	Artificial, build-up surfaces, usually impervious
Nebka	Typical semiarid aeolian coppice dunes, areas of sand plains (dunes) covered by sparse or no vegetation
Mountains/outcropping bedrock	Mountain ranges and slopes, scree, cliffs, including active erosion flats, outcropping bedrock
Carbonate-rich areas	Areas with a high carbonate component, limestone crust, outcropping limestone
Polygenic deposits	Deposits correspondent to alluvial fans, recent alluvial deposits, piedmont and glacis accumulations, with a strong clay, sand and coarse materials
Bare land	Land with no vegetation cover and of no land use
Highly saline areas	Areas rich in salt minerals components
Moderately saline areas	Areas that present moderate salinity
Water bodies	Water areas of natural or artificial origin

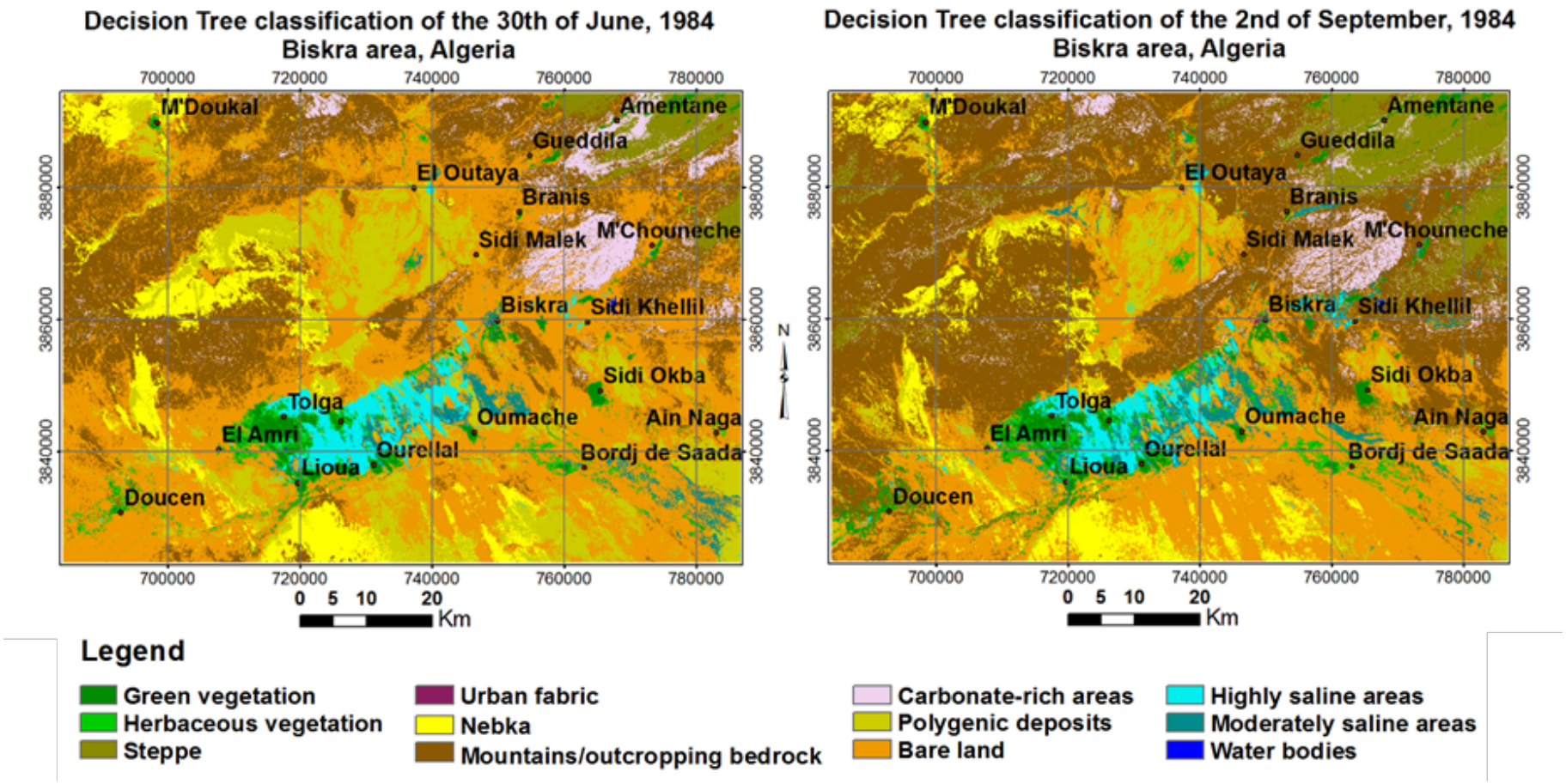

Figure 70. Decision Tree classification applied to 1984 images

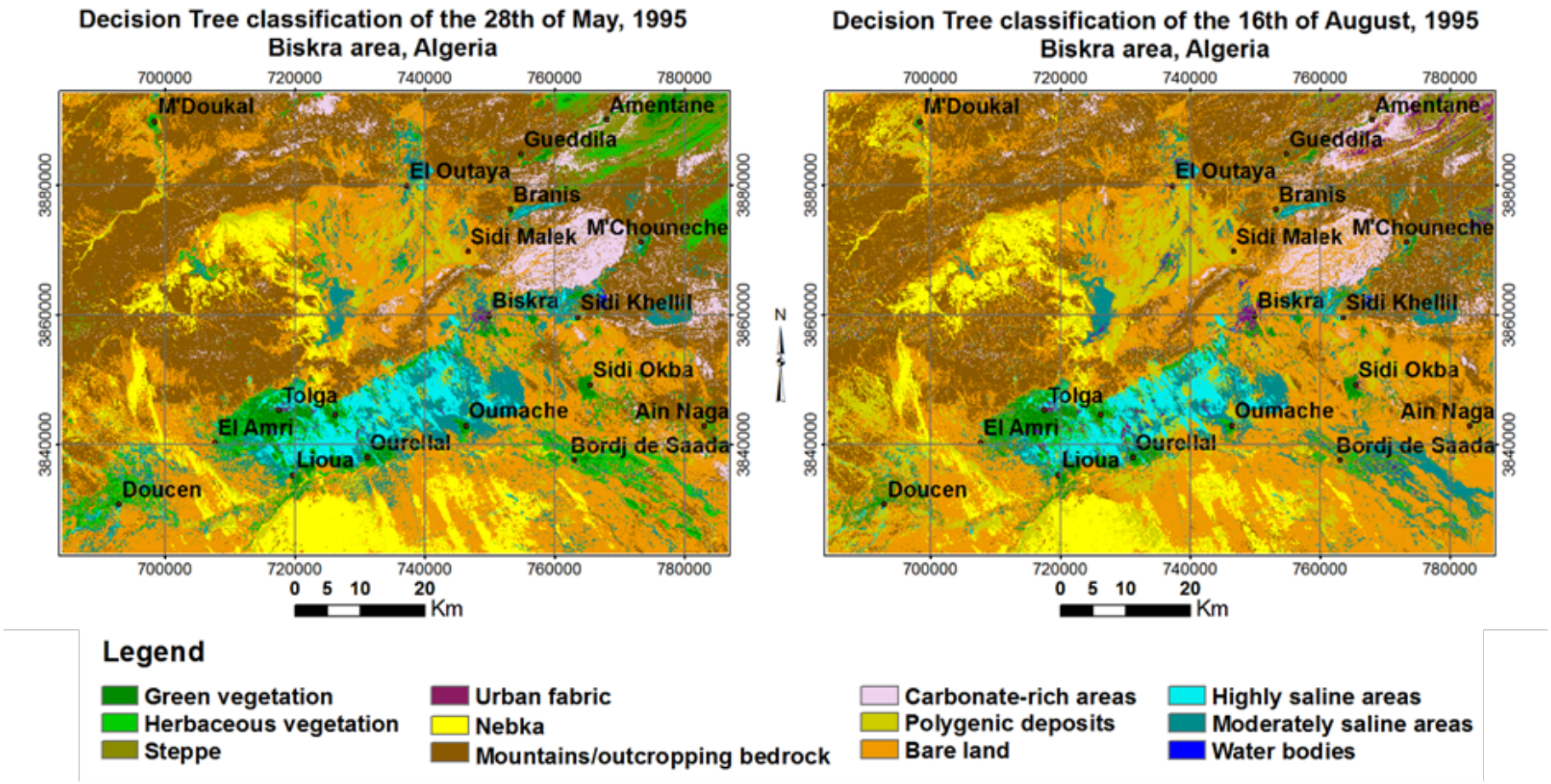

Figure 71. Decision Tree classification applied to 1995 images

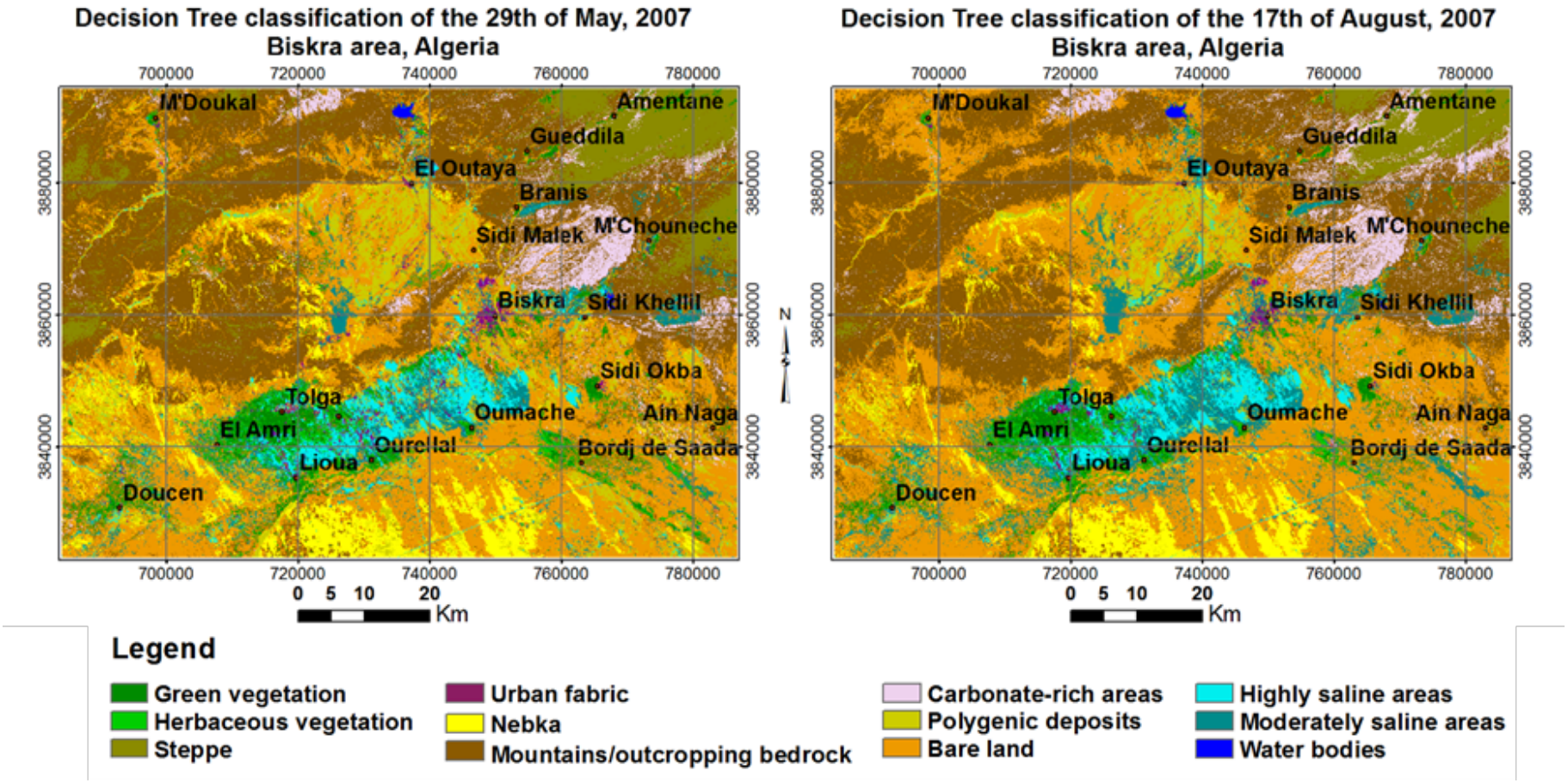

Figure 72. Decision Tree classification applied to 2007 images

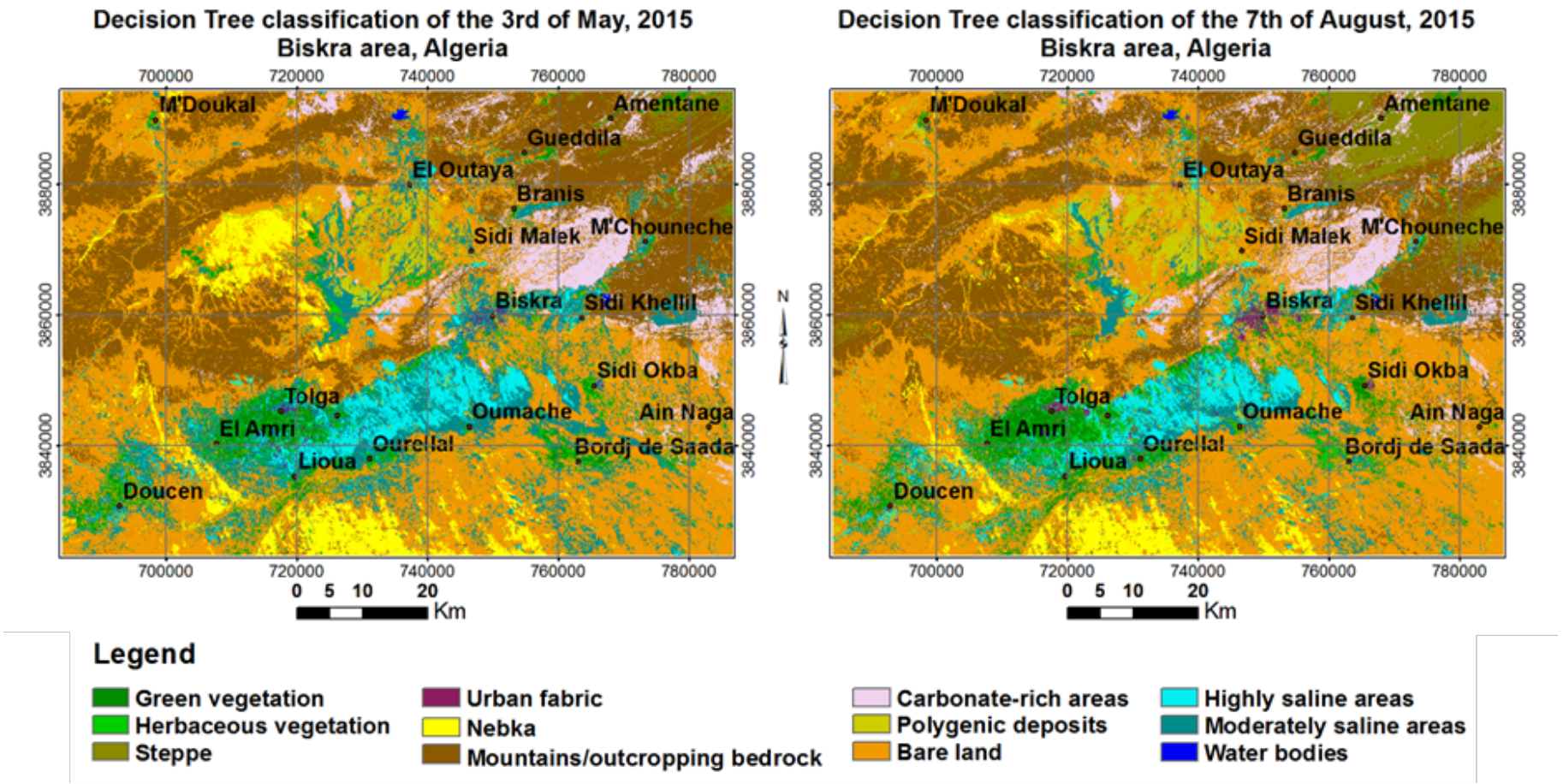

Figure 73. Decision Tree classification applied to 2015 images

5.4.1.2. Oum Zessar Area

The decision tree applied in the Oum Zessar study area followed the same construction flow and nodes as the one employed in the Biskra area. The only difference is that the order of some nodes was changed for reasons of correct extraction of classes in terms of priority. This issue appeared because some of the indices identify several features but with different degrees of intensity. This is where threshold correct calculation is of crucial importance. However,

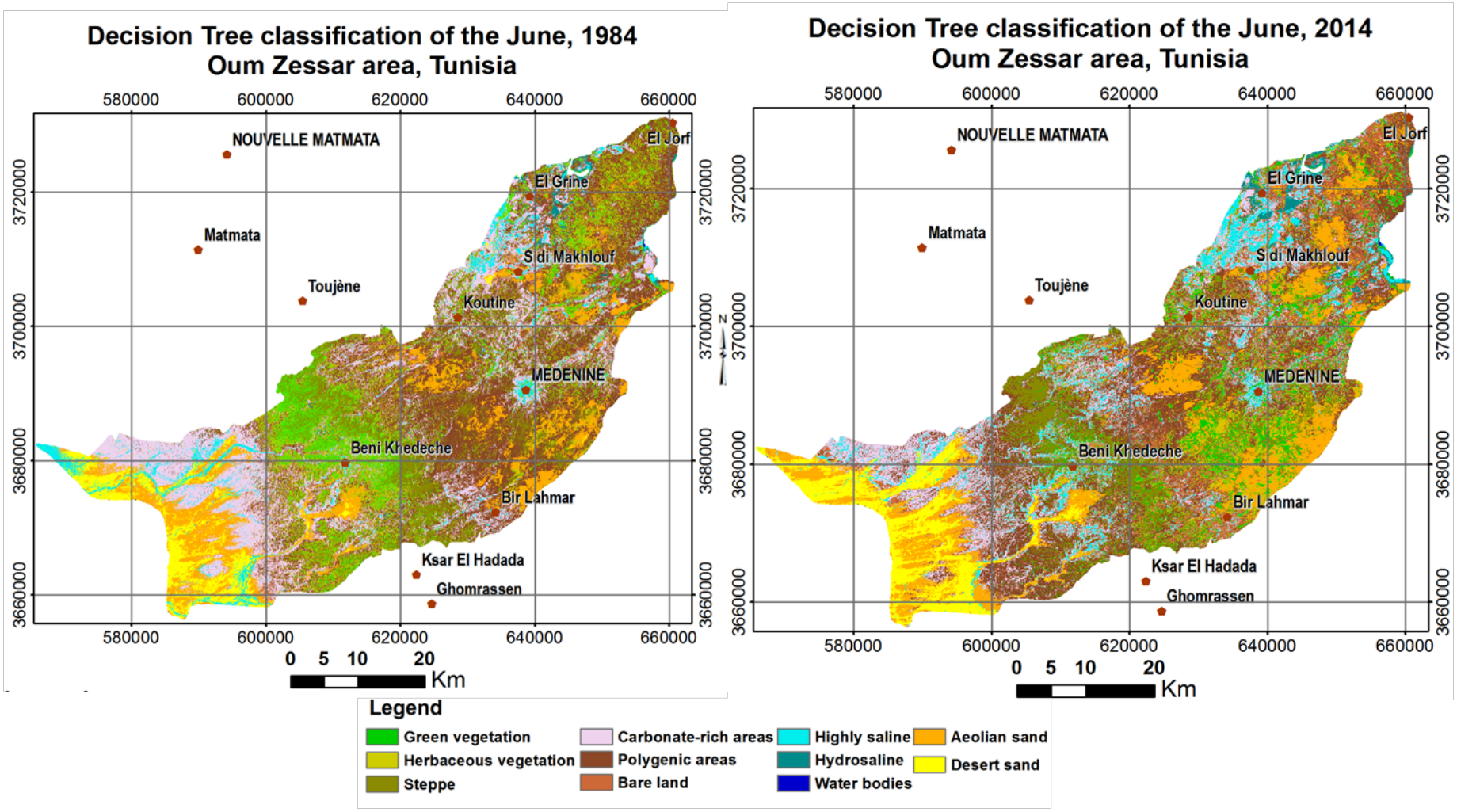

Figure 74. Decision tree classification applied to June 1984 and 2014 images, Oum Zessar area

5.4.2. IsoDATA of Knepper ratios Principal Components

5.4.2.1. Biskra area

In the Biskra area, the results showed that the third principal component mostly contained salt minerals – related information. The first component, representing the highest covariance between the 3 ratio images, mostly contained important information on the sand component, and the second one, clay minerals, that mostly overlaid areas of alluvial fans, with sand, loam and clay components.

The obtained PC bands were further classified using unsupervised classification, IsoData in ENVI 5.0 software (Exelis VIS, Boulder, CO), applied with 100 iterations and a 2% threshold in order to obtain a clear delineation of sa-line areas and sandy areas. The IsoData classification has presented difficulty in delineating the requested 12 main classes, some of which presenting similar characteristics to other existing ones, being unable to separate the moderately saline areas class. In order to allow comparison between the two sets of classification, the resulting DTA classification images to IsoDATA Knepper PCA classification images, the classes were evaluated for correspondence and the "improper" classes were not considered for analysis. In the figures 3 and 4, the classes which do not correspond to the expected resulting classes, are presented in white-grey-black levels and the class name denotes the fact that it is more likely to belong to that one. Thus, only highly saline areas class was considered for confusion matrix and the other ones were merged into one class of land in order to obtain the statistics for the image difference (Afrasinei, Melis et al. 2015)

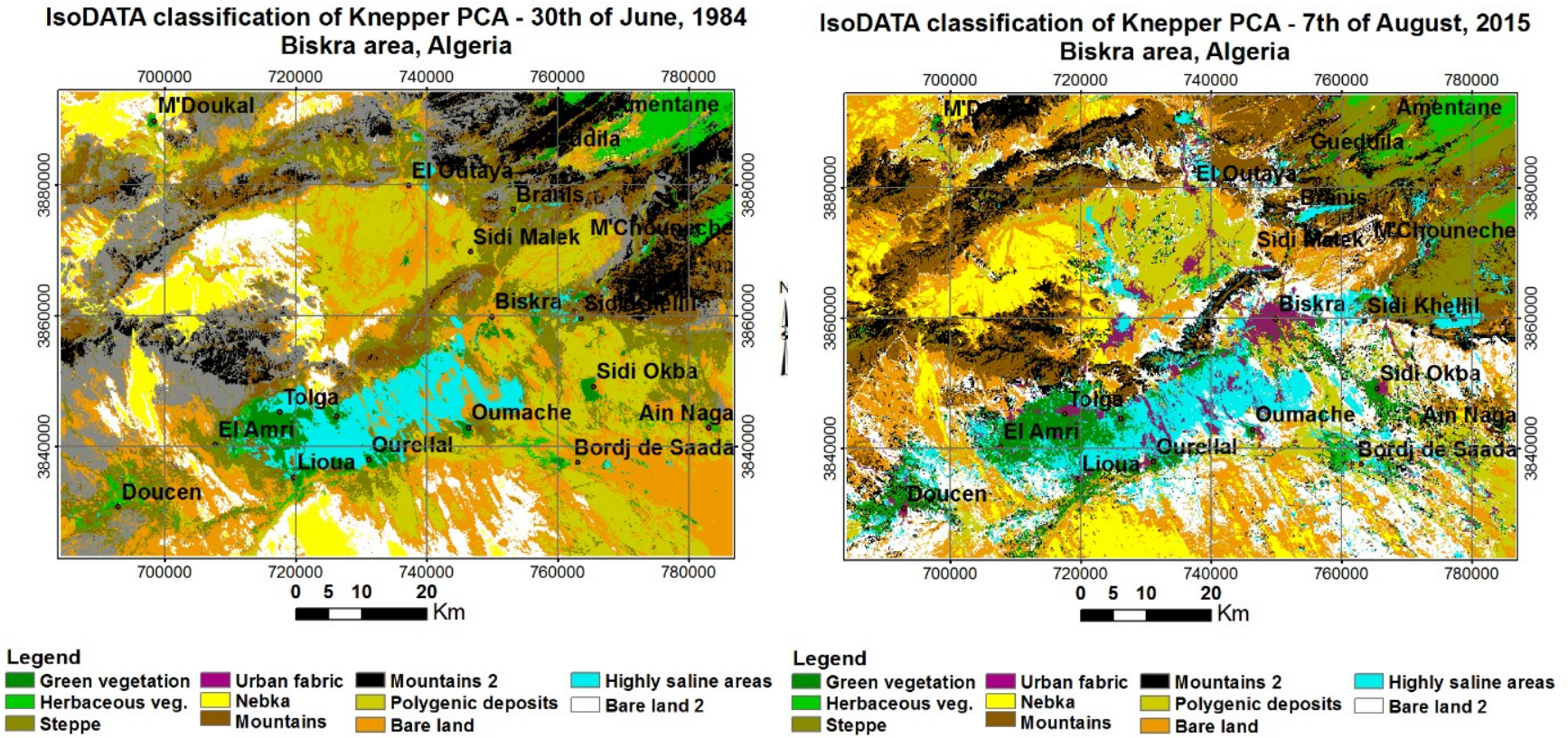
IsoDATA classification of Knepper PCA - 30th of June, 1984
Biskra area, Algeria
700000
720000
740000
760000
780000
3880000
3860000
3840000
M'Doukal
El Outaya
Sidi Malek
Biskra
Sidi Okba
Tolga
Oumache
Ain Naga
El Amri
Ourellal
Bordj de Saada
Lioua
Doucen
0 5 10 20
Km
IsoDATA classification of Knepper PCA - 7th of August, 2015
Biskra area, Algeria
Amentane
Guedtila
El Outaya
Sidi Malek
M'Chouneche
Biskra
Sidi Khelil
Sidi Okba
Tolga
Oumache
Ain Naga
El Amri
Ourellal
Bordj de Saada
Lioua
Doucen
Legend
Green vegetation
Herbaceous veg.
Steppe
Urban fabric
Nebka
Mountains
Mountains 2
Polygenic deposits
Bare land
Highly saline areas
Bare land 2

5.4.2.2. Oum Zessar area

In the Oum Zessar area, the IsoDATA was applied in the same manner as for Biskra area. In this case, however, the third principal component contained the sandy areas information and good results have also been obtained on the spectral distinction between the desert sand West of Dahar and the inner-plain aeolian one, as shown in figure . IsoData has been applied the three principal components but it has not succeeded in delineating correctly the eleven classes. For example, the *sparse vegetation on saline areas* class is an heterogeneous class, comprising carbonate-rich and saline areas with little, sporadic or no vegetation and it has been named consequently.

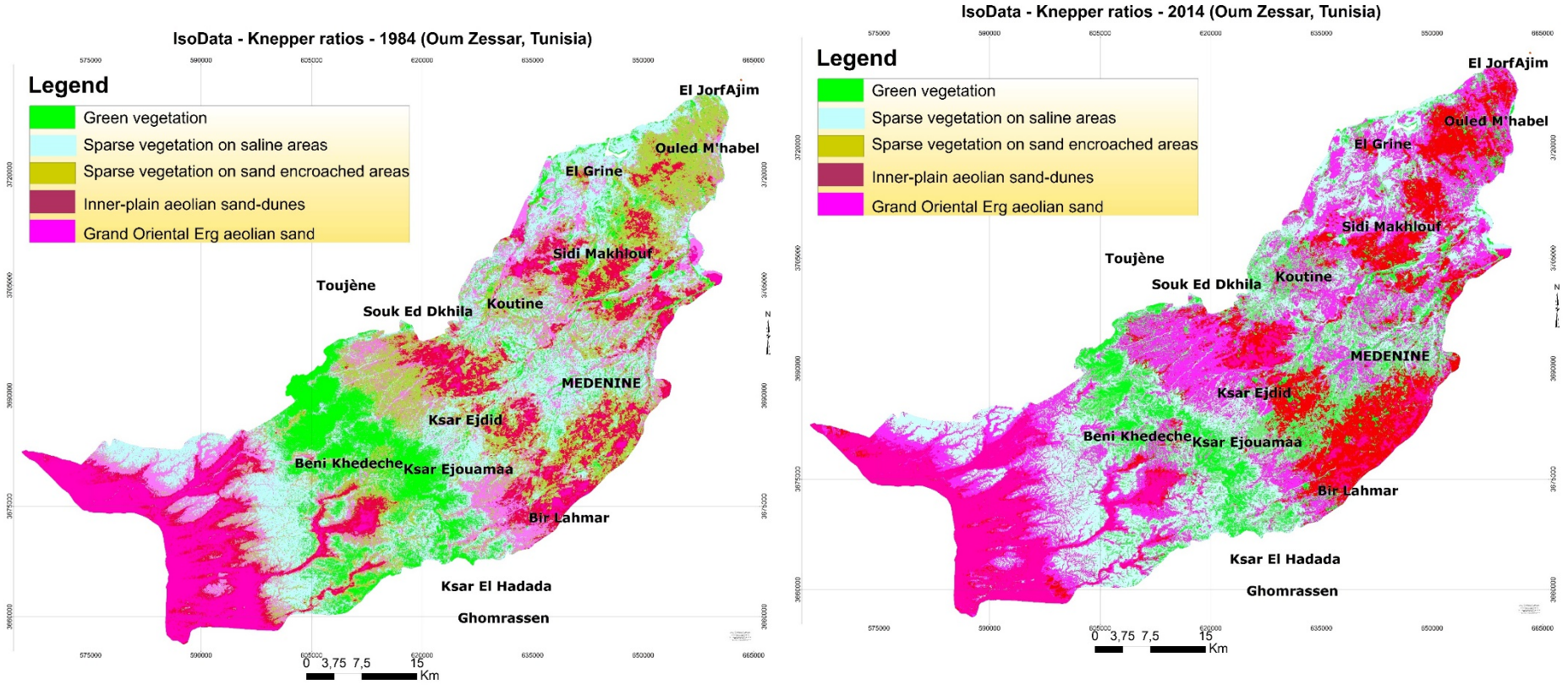

Figure 75. IsoData applied to principal components of Knepper ratios images of 1984 and 2014 in Oum Zessar area

5.5. Error Assessment

5.5.1. Biskra area

Confusion matrix was applied for the error assessment between the three methods in turn: visually interpreted land cover/use map, DTA map and IsoData of Knepper PCA. Firstly, the DTA images were set as "input files" and Knepper PCA images as "ground truth images". This analysis was applied for the 30 June 1984 pair of DT map and IsoData Knepper PCA map, the 9 June 2011 pair and 7 August 2015 pair, for both seasons. The first pair has given an overall accuracy of 70% (the lowest of all pairs) but a kappa coefficient of 0.71 (the highest of all pairs); the third pair, on the other hand, has given an overall accuracy of 79.97% and a kappa coefficient of 0.58, as presented in table 4. This discrepancy may be related to the disadvantages of the IsoData classification method, its threshold set for class separation and number of iterations, as well as the different quality of satellite data, either in terms of noise or radiometric resolution. In fact, it must be mentioned that the 30 June 1984 image was more laborious for the construction of the DT and its node thresholds very different from the rest of the images, whilst the other 7 images have maintained very close threshold values of correspondent indices.

Table 7. Comparison and error assessment of DTA according to LC map and IsoDATA of Knepper PCA map (date expressed in year_JDN)

	1984_182	2011_160	2011_160	2015_219
Classification methods pairing	DT_IsoData & Knepper_PCA	DT_IsoData & Knepper_PCA	DT & LC visual interpretation	DT_IsoData & Knepper_PCA
Kappa coefficient	0.71	0.57	0.41	0.58
Overall accuracy	70.30%	77.91%	72.71%	79.97%

An important aspect to be emphasized is the fact that the decision tree offered more flexibility, as a multistage classifier, thus managing to delineate classes with higher control. The amount, complexity and types of spectral information put together in this single classifier makes it highly controllable, as opposed to other classification flows. The comparison to the visually interpreted land cover map was undergone through visual inspection for all classes, but for a quantitative

assessment, the DTA map of 2011 was reduced to only two classes: “land” and “highly saline areas” and compared with the “saline areas” class of the LCLU map. Error matrix showed a matching of 72% and the lowest kappa coefficient of all pairs, that can be due to the subjectivity of the user, not necessarily a constraint, since visual interpretation implies a series of variables taken into consideration by the user when delineating features (contours, hue, size, texture, location etc), a multi-tasking and distributive interpretation that so far no mathematical algorithm has competed with. However, a drawback is that visual interpretation did not allow the delineation of moderately saline areas. This class has a particular spectral response, not discriminative enough through visual interpretation, but only through spectral information extraction, i.e. an adequate index, like the one proposed in this study, the HIS (Hue Salinity Index).

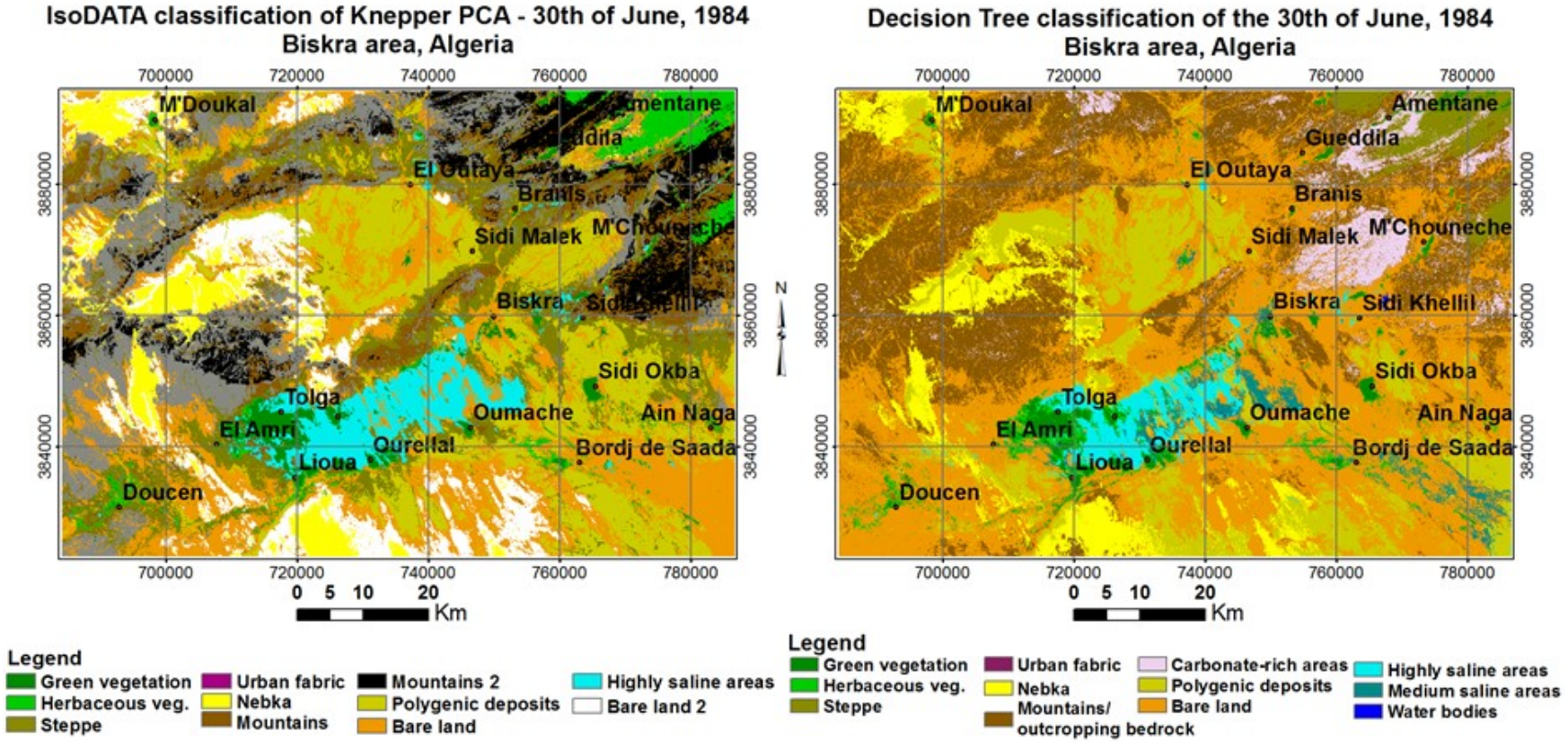

Figure 76. IsoDATA classification applied to Knepper ratios PCA and DTA classification of 30 June 1984 image

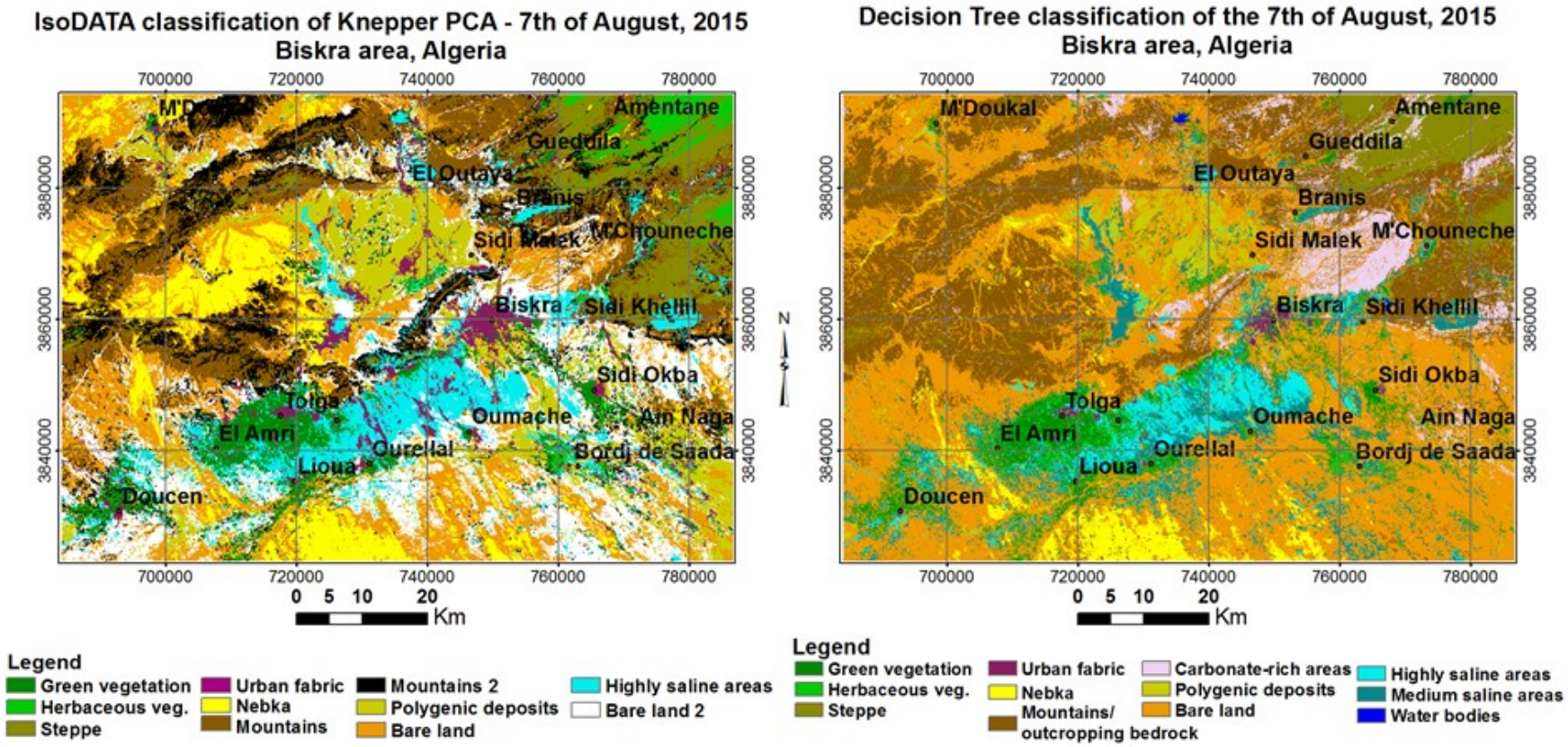

Figure 77. IsoDATA classification applied to Knepper ratios PCA and DTA classification of 7 August 2015 image

5.5.2. Oum Zessar area

Confusion matrix resulted in a match inferior to 60% between the DT and the IsoData images.

5.6. Change Detection

We approached change detection analysis in two ways: we have compared the images of each of the two analysed seasons from 1984 to 2015, but we have also looked at changes between one season and another, within a year. The changes of each class surface, expressed in percentages, for each date can be observed in figure 63. For the easiness of the interpretation discussion, we will refer to the May-June images as belonging to the "wet season" and to the August-September images as "dry season".

5.6.1. Biskra Area

As a result of the DTA classification, we obtained the salinity/land cover maps for the chosen dates, as presented in figure 5. We approached change detection analysis in two ways: we have compared the images of each of the two analysed seasons from 1984 to 2015, but we have also looked at changes between one season and another, within a year. The changes of each class surface, expressed in percentages, for each date can be observed in figure 9, and the maps are presented in figures 5 to 8. For the easiness of the interpretation discussion, we will refer to the May-June images as belonging to the "wet season" and to the August-September images as "dry season".

From the intra-annual point of view, in all years, changes that occur between the end of the wet season and the end of the dry season, maintain similar pattern of change. More specifically, classes that are interchangeable remain as follows: *highly saline areas* have the most frequent interchange with *moderately saline areas*, *polygenic deposits* and *herbaceous vegetation* classes (decreasing in 1995, by 1.53% and in 2015 by 1.69% and increasing in 2007 by 17.63%); moderately saline areas mostly interchange with *highly saline areas*, *urban fabric*, *bare land* and *herbaceous vegetation* (with an increase of 60% in 1984, 100% in 1995, 93% in 2007 and 106% in 2015.

As an example of intra-annual change, the results of the detection analysis of 30 June and 2 September images of the year 1984, show that the *highly saline areas* class has decreased by 26%, mainly in the favour of *urban fabric* class, by 18.7%, *polygenic deposits* by 4.2% and *herbaceous vegetation*, by 2.1%, gaining only 1.4% and 1.9% of *water bodies* and *herbaceous vegetation* classes, respectively. The total changes, with gains and losses, represent -19.8%.

It must be mentioned that throughout the classification process, both in DTA and Knepper PCA, there has been a strong spectral confusion of "highly saline areas" class and the "water bodies" one (consisting of one lake in the hole image in 1984 and 1995, after which another one is visible after 2007, in the northern part of the areas, which is reported to be due to the construction of a dam). This confusion problem has been solved only throughout the DTA, using the ratio Red/Infrared (presented as WR in table 2). The urban fabric are expected to be classified under saline areas as it has been noticed to have similar spectral behaviour to these latter ones in all the analysed images. Thus, the changes regarding saline areas-urban fabric may not be a true change, but a misclassification due to this spectral confusion. In the year 1984, the *moderately saline areas* have an overall increase of 60%, mainly in the disfavour of urban fabric, water bodies and herbaceous vegetation.

The fact that there is a constant interchange between either highly saline areas and *herbaceous vegetation* classes or between *moderately saline area* and *herbaceous vegetation*, gives way to the scenario that agricultural practices have the tendency to intensify the salinization processes, as the *herbaceous vegetation* class delineated in all images correspond more than 80% to agricultural areas, parcels of cultivated land, mostly recognizable by their rectangular shape, that may or not present chlorophyll response, but in some images denote the presence of humidity or re-worked land hues. These are found mainly in the Occidental Zab, in south-western part of the study area, in the Doucen area, around the Tolga Oasis, especially in the western part of it, known as El Amri and in Oriental Zab, the extended agricultural area between Sidi Okba and Ain Naga, as in can be observed in figure 5.

Concerning the inter annual changes analysis, the main trends observed from the change detection statistics are that *herbaceous vegetation* class presents a major increase (of 34%) in the disfavour of *green vegetation* class when comparing the 1984 and 2015 images dated at the beginning of the dry season, as opposed to a major increase of the *green vegetation* class in the disfavour of *herbaceous vegetation* class at the end of the dry season, of the same pair of years. This comes as a natural

change as the *herbaceous vegetation* class tends to be more sensitive to lack of rainfall and high temperature, as opposed to *green vegetation* class which is mainly composed of aridity-resistive palm groves, fruit trees and shrub vegetation.

Change detection results applied to the 1984 and 2015 pair (table 5 shows the dry season results) show that, in both seasons, the main classes with which *highly saline areas* class has interchanged are the *urban fabric*, *moderately saline areas*, *herbaceous vegetation* and *green vegetation* classes. It must be mentioned that both the *highly saline areas* and *moderately saline areas* classes have a major increase in the dry season (of 52 and 239%, respectively) compared to the wet season (of 24 and 164%, respectively).

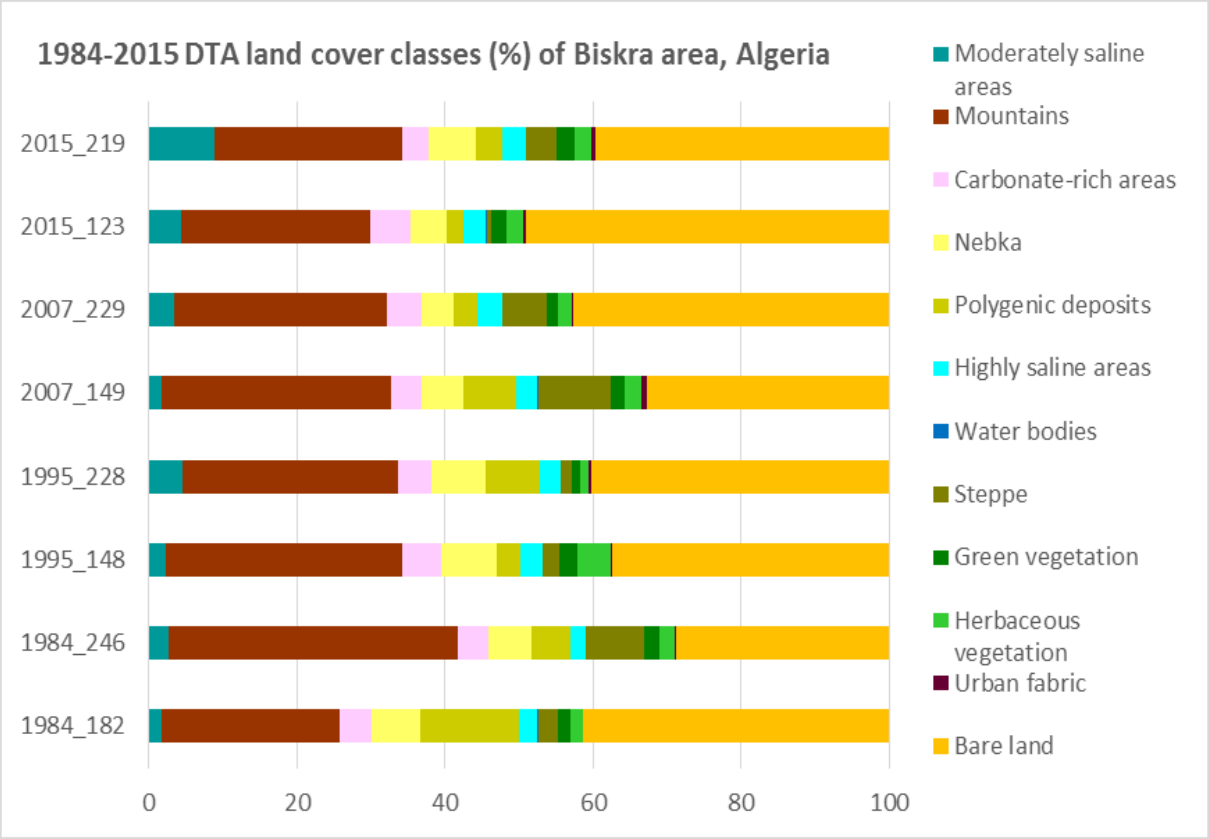

Figure 78. Class coverage statistics for each analysed date (percentage)

Table 8. Change detection statistics between the 1984 and 2014 images of the decision tree classification of Biskra area

%	Moderately saline	Mountains	Carbonate -rich	Nebka	Polygenic deposits	Highly saline	Water	Steppe	Green veg.	Herb. Veg.	Urban	Bare land
Moderately saline	***45.92***	***2.83***	***0.31***	***1.69***	***9.867***	***25.6***	***5.91***	***0.48***	***4.96***	***19.4***	***25.74***	***16.98***
Mountains	***0.124***	45.8	41.3	16.9	1.399	***0.002***	1.19	53.7	0.36	0.71	1.31	1.21
Carbonate-rich	***0.054***	2.55	47.7	0.06	0.573	***0.024***	0.59	6.09	0.06	0.14	1.57	0.54
Nebka	***0.147***	2.43	0.01	52.09	11.436	***0.06***	0.13	0.02	0.12	0.69	0.013	5.92
Polygenic deposits	***3.78***	0.89	0.21	0.92	26.554	***4.1***	0	0.073	0.31	2.23	2.79	5.35
Highly saline	***28.17***	***0.41***	***0.05***	***0.39***	***3.52***	***46.7***	***5.51***	***0.031***	***1.07***	***6.98***	***5.75***	***2.97***
Water	***0.09***	0.03	0.008	0	0.031	***0.001***	76.02	0.005	0.009	0.028	0.45	0.043
Steppe	***0.95***	0.85	1.33	0.39	1.37	***0.52***	4.51	35.3	15.03	7.404	4.03	1.47
Green veg.	***3.33***	0.58	0.09	0.37	0.75	***8.58***	0.93	0.72	46.93	17.56	1.65	1.71
Herb. Veg.	***4.77***	0.6	0.13	0.61	1.39	***9.33***	2.52	0.5	18.55	16.83	3.011	2.39
Urban	***1.45***	0.09	0.08	0.012	0.17	***3.11***	0.53	0.09	2.14	2.88	38.61	0.69
Bare land	***11.16***	42.8	8.62	26.468	42.9	***1.77***	2.12	2.876	10.41	25	15.02	60.68
Class Total	***100***	100	100	100	100	***100***	100	100	100	100	100	100
Class Changes	***54.07***	54.1	52.2	47.904	73.4	***53.3***	23.97	64.64	53.06	83.16	61.38	39.31
Image Difference	***239***	-35.4	-10.7	7.961	-31.9	***52.9***	154.3	-46.29	16.81	0.36	442.6	37.91

5.6.2. Oum Zessar area

In the Oum Zessar area, the Decision Tree Analysis showed that the aeolian sand class presented an increase of 27, 69% and the desert one, of 0, 58%, between 1984 and 2014. However, the PCA of the Knepper composites, between the same years, have shown in an increase of 21% of aeolian sand class and 19% of desert sand class, as resulted from the change detection statistics. In the DT image of 1984, the desert sand class may have presented problems of spectral confusion with another feature (possibly saline areas in the western extremity of the image). Comparing it to both IsoDATA of Knepper PCA of 1984 or to ground truth data (but from 2014), we observed that in that sector, none of these have presented the saline patch present in the DT 1984 image. Two hypothesis can be formulated: (1) either the employed saline index within the DT analysis have managed to detect that sector as saline and Knepper PCA did not detect it because of insufficient efficiency; or (2) the index presented a prectal confusion, thus it needs revision or we need to deepen the analysis in order to understand the cause of that classification. However, we must mention that this issue cannot be verified through ground truth, since it corresponds to 2014. Nevertheless, that sector is characterised mainly by carbonate surfaces, with calcareous concretions and ground truth has also acknowledged the presence of densely distributed small stripes of gypsum, which have managed to reflect enough as to change an entire pixel's value. It is quite possible that in 1984 that area was not covered with sand, thus presenting a different spectral signature, whereas in 2014, a sheet of sand that covered it may have been thick enough to hide it.

Nonetheless, we do not exclude the scenario in which carbonate surfaces reflect similarly to saline surfaces, being themselves saline surfaces also in terms of internal vibration modes of the anion group that determines the presence or absence of absorption features in the electromagnetic spectrum.

Thus the index employed to extract it needs further revision. The class has been identified but it has been overestimated. Thus, we have reached our goal of separating desert sand class from the inner plain aeolian sand, but we cannot appreciate the change between the two dates, as it needs further revision. It is also important to mention that the sparse vegetation on sand encroached areas, mainly psamophyte species have decreased by 40% which can be argued by the fact that in the past decades

the rainfed agriculture and especially olive plantations overlay mostly to the sandy areas of the plain.

The most important aspect obtained from this analysis was the net separation between inner-plain aeolian sandy areas and the desert ones along paleo-valleys that converge towards the Great Oriental Erg. Both classification methods have shown good separability between the two classes, for both years in discussion.

Table 9. Change detection statistics between the 1984 and 2014 images of the decision tree classification of Oum Zessar area

	Hydrosaline	Bare land	Carbonate	Water	Aeolian sand	Desert sand	Highly saline	Steppe	Green vegetation	Herbaceous	Polygenic
Unclassified	0	0	0	0	***0***	***0***	0	0	0	0	0
Hydrosaline	28.33	1.723	2.007	27.53	***0.24***	***0.123***	3.052	0.28	1.49	1.82	0.57
Bare land	12.78	20.497	13.619	0	***6.312***	***3.99***	4.186	3.467	8.81	16.04	10.20
Carbonate	13.78	16.046	48.304	0	***0.813***	***3.636***	24.883	1.841	5.09	10.15	4.19
Water	0.03	0	0	64.06	***0***	***0***	0.109	0	0.01	0.004	0
Aeolian sand	***0.05***	***1.719***	***0.376***	***0***	***35.773***	***13.478***	***1.205***	***4.237***	***1.24***	***4.07***	***9.33***
Desert sand	***0.024***	***1.351***	***2.778***	***0***	***8.872***	***62.185***	***38.734***	***0.239***	***0.63***	***1.728***	***0.75***
Highly saline	12.385	3.389	11.409	1.449	***0.334***	***0.995***	21.474	0.187	1.22	2.09	0.45
Steppe	1.183	1.939	0.207	0.29	***6.519***	***0.725***	0.03	38.903	19.023	4.472	9.44
Green vegetation	4.513	4.459	1.37	4.928	***8.033***	***1.538***	1.14	9.686	23.424	8.915	9.52
Herbaceous vegetation	6.718	8.57	2.487	1.449	***14.501***	***3.1***	1.149	10.002	12.867	12.425	13.84
Polygenic	20.189	40.304	17.441	0	***18.595***	***10.228***	4.037	31.158	26.169	38.265	41.67
Class Total	100	100	100	100	***100***	***100***	100	100	100	100	100
Class Changes	71.663	79.503	51.696	35.94	***64.227***	***37.815***	78.526	61.1	76.57	87.575	58.32
Image Difference	-0.003	-61.181	56.259	58.55	***27.699***	***0.583***	-43.092	-3.815	-21.448	-9.623	218.92

6. CHAPTER SIX: CONCLUSIONS

6.1. Limitations

In both areas, the encountered difficulties were related to salty features spectral extraction when existing indices were applied. We managed to solve or minimise this issue through the new indices proposed in this study.

The spectral analysis undertaken in both areas showed that the main factors affecting the reflectance of salt-affected soils are quantity and mineralogic composition salts, together with soil moisture, colour, impurities content and surface roughness. The mineralogy of carbonate, sulphate and chloride salts determines the presence or absence of absorption features in the electromagnetic spectrum, associated with internal vibration modes due to excitation of overtones and combination tones of the fundamental anion groups (e.g. HOH, OH^-, CO_3^{2-}, SO_4^{2-}) (Szabolcs 1989, Metternicht and Zinck 2008). The issues encountered in the current study were mainly those related to spectral confusion between saline areas, alluvial clayey material, carbonate – rich soils, and outcropping limestone. Applying solely salinization indices reported as having high accuracy when mapping salinity in similar areas (Khan, Rastoskuev et al. 2005, Allbed and Kumar 2013, Masoud 2014), results were not completely satisfactory, since clay and silt-rich soils, urban fabric features, bare land and carbonate-rich surfaces were identified altogether with saline areas. The application of both decision tree and IsoDATA of Knepper ratios PCA showed satisfactory results but an overall accuracy of around 87 % which may be due to the user-dependency of the two datasets (DTA, LCLU map) of the total of three employed (the aforementioned ones and Knepper PCA). However, the results confirm that surface features common in drylands, such as braided stream beds, eroded terrain surfaces with truncated soils, and non-saline silt-rich structural crusts, can generate high levels of reflectance, similar to those of areas with high salt concentration, as stated by (Metternicht and Zinck 2008). For example, in the Oum Zessar area, the braided paleo valleys located west of Dahar, that are visible until the limit with the Grand Oriental Erg, have presented difficulties in the spectral separation from saline areas. Even if the ground truth did reveal the presence of gypsum formations, this was in very small patches, difficultly detectable at a resolution of 30 m. Moreover, in this area, the prevalent formations are the Cretaceous carbonate series, which may have caused this confusion.

Other issues encountered specifically during the processing phase concerned the lack of performance of the NDVI in such environments. The results were anomalous, either underestimating the vegetation cover (in Biskra area's case) or overestimating it (in Oum Zessar's case). We tried to overcome this drawback by employing also two different NDWIs (the one proposed by USGS (McFeeters 1996) and in the decision tree classifier which have corrected these anomalies, but further research is needed in order to deepen the understanding of this spectral behaviour, identify the problem and propose solutions.

6.2. Methodology

The methodology used in this study tackled with two types of problems: 1) the two main environmental issues present in the areas of study, hence soil salinity and sand encroachment, delineating them, defining their current state, driving forces and trends 2) from the methodical point of view, hence the spectral confusion among very reflective desert features; in some cases, limited or no access to field data or to undergo field survey oneself. In order to cope with several constraints, the visually interpreted classification of land cover and land use was performed for both areas and two different automated classification schemes were assessed and set up: 1) a decision tree analysis (DTA) employing also indices proposed for this particular study, and 2) IsoDATA classification applied to the Principal Components Analysis (PCA) of Knepper ratios, for in the fast, user-independent, spectral-based delineation of mineral components.

In the case of Biskra area, the employment of the Decision Tree classifier has proven to be more flexible and adequate for the extraction of highly and moderately saline areas and major land cover types, as it allows multi-source information and higher user control. The results were compared with IsoDATA classification maps applied to Knepper ratios Principal Component Analysis and were proven to have a substantial advantage over this latter method. Five of the indices employed in the Decision Tree construction proposed for the current study have given satisfactory results. The error assessment of the salinity index (SMI) proposed in this research for the extraction of highly saline areas was verified through comparison with 2 other mapping methods, being of around 76,06%. The decision tree applied in this area has been applied and tested in the Oum Zessar area of Tunisia. In the latter one, it has also been validated, given the amount of ground truth points, thus giving it an additional degree of reliability to be applied and functional in the Biskra area too.

In the case of Oum Zessar area, the employed methodology combined with the use of the latest satellite data of the Landsat series, with many improved features, as well as the latest accurate worldwide 30 m resolution SRTM DEM, have provided valid results as to sustain the existence of a correlation between the mineralogy of the analysed surfaces, obtained from XRD, and the correspondent spectral signatures extracted from both remote and proximal sensing data; samples of the same mineral composition are characterized by a similar spectral response; halite-dominated surfaces show a specific spectral response compared to those of high gypsum content and the sand accumulations West of Dahar showed distinct characteristics from the inner-plain ones, related to quartz proportion but also the presence or absence of other minerals. Positive results were obtained for sand encroached areas delineation, this being confirmed also by the spectral signatures analysis and comparison to the existing USGS spectral libraries and by the mineralogical X-ray diffraction analysis, which confirmed the spectral variances between the inner-plain sand and the West of Dahar range sand.

In summary, this analysis' validity was provided by means of remote and proximal sensing, integrated with ground truth and X-ray diffraction data, which allowed the discrimination of different sand types and the salt-affected surfaces from other types of land cover (carbonate-rich ones, bare land, urban or impervious surfaces) and distinguish the gypsum surfaces those containing halite. The first results presented in this study confirm the validity and need to use the multispectral data for the construction of a knowledge framework of the territory. The phenomena of soil salinization and sand encroachment can be approached throughout a combined spectral analysis so that they can be monitored with an extremely controllable methodology such as the one proposed herein. A future step of this research would be the analysis of different decision tree algorithms, particularly the machine learning ones and their efficiency compared to the manual DT used in this study.

6.3. Land degradation dynamics: driving factors and trends

In the Biskra area of Algeria, one of the important aspects that emerged from the diachronic series analyses is that the expansion of open field and industrial agriculture practices in the last three decades have led and continue to contribute to a secondary salinization of soils. In the Occidental Zab, the increase in salinized soils correspond to the expansion of phoeniciculture and market gardening (often greenhouse) but in the Oriental Zab, the large scale industrial agriculture, that required also a large number of deep wells (given the 200-300 m depth of the exploitable groundwater), has caused sporadic local appearance of small patches of salinized surfaces all along the lower slope of the alluvial fan area, patches that were not present in the '80s and started to appear only after 2007. Applying post classification change detection (ENVI), the statistics for the 1984 to 2015 diachronic analysis, comprising images acquired at the end of the wet season and at the end of the dry season, have shown an overall increase of 53 % of the highly saline areas surface, but no substantial change between the seasons. This is an important aspect, given that currently the specific literature emphasizes the importance of image acquisition date being at the end of dry season for optimal results. The *moderately saline areas* class *Moderately saline areas* class presented an overall increase of over 100% from 1984 to 2015 and was noticed to have some variations from one year to another, in terms of fluctuant increase-decrease and also within the same year, but still of insignificant extent. Nonetheless, it was observed to be slightly more sensitive to seasonal conditions than the *highly saline areas* class. This may be also due to the fact that saline soils tend to retain high moisture content and it is possible that hydro-saline areas where detected and included in the *moderately saline areas* class by the HIS index and not in the *highly saline areas* class. In this way, we can confirm the findings of (Elnaggar and Noller 2010) on the fact that we significant correlation with electro-conductivity values (thus, soil salinity) as saline soils tend to retain high moisture content.

In the Oum Zessar study area, in Tunisia, the analyses show a substantial change in several components of the environment since the 80s, related to increased anthropic pressure, settlement and agricultural policies and national development strategies. One of the concerning aspects that emerged from this study is that the Jeffara plain, is more affected by sand encroachment over the last decade, namely by around 27%, adding also changes in several other classes of land cover. Results show that sand accumulation and encroachment has reached a worrying magnitude in this

area, but it is not limited to it. Other studies show that the whole south of Tunisia is interested by this alarming situation (Khatelli and Gabriels 2000, Ouerchefani, Dhaou et al. 2013, Afrasinei, Melis et al. 2015).

Sand accumulation and encroachment are very dynamic phenomena and their evolution depends not only on the bio-physical conditions of such arid and semi-arid environment but also on the management and overexploitation of natural resources through overgrazing, expansion of cultivation, use of tillage or mouldboard ploughing instead of deep mole plough etc. Mouldboard or turn plough is applied in less fertile areas. In order to grow crops regularly the soil must be turned to bring nutrients to the surface. Even if the trigger is found at a very big scale, a micro local one, agricultural practices have a deep and direct impact on this process. In the Oum Zessar area, mouldboard ploughing is practiced locally, on small patches for crops and trees (private family cultivated perimeters, subsistence agriculture) but also on extended surfaces for Olive trees plantations (in the whole Jeffara coastal plain and inner, east of Dahar plain, mainly in areas already affected by sand encroachment).

Furthermore, it is important to address the matter of Olive tree groves that cover an extended area in the Jeffara coastal and inner plain, near the limit of the glacis of Dahar, mainly in areas already affected by sand encroachment. In the coastal areas, an important aspect is that Olive plantation require holes deep enough (even a few meters) to exceed the carbonate crust layer that would limit the tree's growth, access to water etc. Thus, the land presents itself with many such holes, whereas carbonate material is reworked and brought to surface that eventually is dissolved by the torrential rainfalls, re-entering into the soil matrix where it can re-precipitate and form another layer. This may also have an impact from the agronomic, vegetation health point of view related to limiting plant absorption of certain nutrients etc.

Alternatives to ploughing, such as the no-till method, have the potential to actually build soil levels and humus. These are suitable to soils encountered in this study area, since they are mainly private perimeters of small, intensively cultivated plots on poor, shallow or degraded soils that ploughing would further degrade.

No-till improves soil quality (soil function), carbon, organic matter, aggregates, protecting the soil from erosion, evaporation of water and structural breakdown, let alone the deflation of sand particles. A reduction in tillage passes helps prevent the compaction of soil. Tilling a field reduces

the amount of water, via evaporation, around 0.85 to 1.9 cm per pass. By no-tilling, this water stays in the soil, available to the plants. Tillage lowers the albedo of croplands. The potential for global cooling as a result of increased Albedo in no till croplands is similar in magnitude to the biogeochemical (carbon sequestration) potential (Ouessar 2011).

6.4. Overall Conclusion

The conducted research has its originality in the critical analysis, multi-lateral approach and valid application. The development and description of a customised methodological approach for the analysis of the spatial and temporal dynamics of land degradation phenomena represents the first achievement of this work. Based on a vast bibliography, this work combines and proposes a specific workflow for thematic mapping, indices construction and classification built-up and change detection analysis. The employment of two different classification approaches, of either visual interpretation or automated provided invaluable support for identification and correct delineation of features of interest and an additional validity to the results.

Five of the eleven indices employed in the Decision Tree construction were constructed throughout the current study, among which we propose also a salinity index (SMI) for the extraction of highly saline areas.

Tree classifier has proven to be more flexible and adequate for the extraction of highly and moderately saline areas and major land cover types, as it allows multi-source information and higher user control, with an accuracy of more than 80%.

Another added value is the tailored methodology for arid and semi-arid areas' assessment of land degradation state, a contemporary issue with which many parts of the world are currently confronting with. This is a small step toward a possible standardisation of methodology and guidelines to follow in similar studies, since in this work we provided:

- A methodology for constructing valid land cover and land use maps at 1:70 000 scale, of two areas of 500 000 and 300 000 hectares.
- Steps for defining 4th level land cover and land use nomenclature according to the local bio-geographical context

- Input on integrating proximal sensing (spectroradiometric field measurements) into spectral analysis for higher precision and validity in identifying features
- Input on integrating mineralogical analysis, namely X-ray diffraction, for the understanding of the spectral behaviour and discrimination of land features
- Means of constructing new indices for the extraction of specific land cover or mineral features, not present in the up-to-date scientific literature
- Five new validated mineral indices
- Results that contend with common knowledge of remote sensing of saline areas related to restrictions on the acquisition date of satellite images to the end of the dry season only: two-seasonal approach of change detection
- Methodological flow employing remote and proximal sensing techniques with user-interpreted land cover mapping, multifunctional field data, and XRD data enhancing validity and reliability

Applying both classical research methods as well as the ones developed in this work, we have obtained results which: improve the knowledge on this territory; offer a new perspective on the functional and spatio-temporal dynamics of its components; partly confirm and partly disputes previous knowledge; allows a more precise delineation of land features. At the same time, the development of the concepts and methods (including the results) presented in this work create new possibilities for further research in similar arid and semi-arid areas and they can be used successfully for the study of other similar geographical spaces.

7. List of Figures

8. References

(2013). ENVI Classic Tutorials.

Abbas, A., S. Khan, N. Hussain, M. A. Hanjra and S. Akbar (2013). "Characterizing soil salinity in irrigated agriculture using a remote sensing approach." Physics and Chemistry of the Earth **55-57**(0): 43-52.

Abubaker Haroun Mohamed Adam, E. A. M. H., Salih, Abdelrahim . M (2013). "Accuracy Assessment of Land Use & Land Cover Classification (LU/LC) "Case study of Shomadi area- Renk County-Upper Nile State, South Sudan"." International Journal of Scientific and Research Publications **3**(5).

Afrasinei, G.-M., M. T. Melis, F. Frau, V. Demurtas, C. Buttau, C. Arras and G. Ghiglieri (2015). "Spectral characterization methodology of saline and sand encroachment areas using proximal sensing e remote sensing in Tunisia." ASITA.

Afrasinei, G. M., M. T. Melis, C. Buttau, J. M. Bradd, C. Arras and G. Ghiglieri (2015). Diachronic analysis of salt-affected areas using remote sensing techniques: the case study of Biskra area, Algeria.

Afrasinei, G. M., M. T. Melis, C. Buttau, J. M. Bradd, C. Arras and G. Ghiglieri (2015). Diachronic analysis of salt-affected areas using remote sensing techniques: the case study of Biskra area, Algeria. Proc. SPIE 9644, Earth Resources and Environmental Remote Sensing/GIS Applications VI.

Aldabaa, A. A. A., D. C. Weindorf, S. Chakraborty, A. Sharma and B. Li (2015). "Combination of proximal and remote sensing methods for rapid soil salinity quantification." Geoderma **239-240**: 34-46.

Aleksandrowicz, S., K. Turlej, S. Lewiński and Z. Bochenek (2014). "Change Detection Algorithm for the Production of Land Cover Change Maps over the European Union Countries." Remote Sensing **6**(7): 5976-5994.

Algerienne, M. d. l. H. (1980). Notice explicative de la Carte Hydrogeologique de Biskra au 1/200.000. Alger, Algeria, Ministere de l'Hydraulique Algerienne MdH.

Allbed, A. and L. Kumar (2013). "Soil Salinity Mapping and Monitoring in Arid and Semi-Arid Regions Using Remote Sensing Technology: A Review." Advances in Remote Sensing **02**(04): 373-385.

Allbed, A., L. Kumar and Y. Y. Aldakheel (2014). "Assessing soil salinity using soil salinity and vegetation indices derived from IKONOS high-spatial resolution imageries: Applications in a date palm dominated region." Geoderma **230-231**: 1-8.

Anna, D., L. Megan and O. Bertram (2008). The Suitability of Airborne Hyperspectral Imagery for Mapping Surface Indicators of Salinity in Dryland Farming Areas. Remote Sensing of Soil Salinization, CRC Press.

Antonio Di, G. and O. B. Douglas (2012). Overview of Land-Cover Classifications and Their Interoperability. Remote Sensing of Land Use and Land Cover, CRC Press**:** 37-48.

Avelar, S. and P. Tokarczyk (2014). "Analysis of land use and land cover change in a coastal area of Rio de Janeiro using high-resolution remotely sensed data." Journal of Applied Remote Sensing **8**(1): 083631.

Becerril-Piña, R., C. A. Mastachi-Loza, E. González-Sosa, C. Díaz-Delgado and K. M. Bâ (2015). "Assessing desertification risk in the semi-arid highlands of central Mexico." Journal of Arid Environments **120**: 4-13.

Bouaziz, M., R. Gloaguen and B. Samir (2011). Remote mapping of susceptible areas to soil salinity, based on hyperspectral data and geochemical, in the southern part of Tunisia.

Bougherara, A. and B. Lacaze (2009). Etude preliminaire des images Landsat et Alsat pour le suivi des mutations agraires des Ziban (extrême nord-est du Sahara algérien) de 1973 à 2007. Journées d'Animation

Scientifique (JAS09) de l'AUF Alger J. d. A. S. J. d. l. A. Alger. Journées d'Animation Scientifique (JAS09) de l'AUF Alger Journées d'Animation Scientifique (JAS09) de l'AUF Alger

Bracene, R. and D. F. d. Lamotte (2002). "The origin of intraplate deformation in the Atlas system of western and central Algeria: from Jurassic rifting to Cenozoic–Quaternary inversion." Tectonophysics **357**: 207–226.

Bullock, P. and H. L. Houerou (1995). Land Degradation and Desertification. IPCC SECOND ASSESSMENT REPORT. Climate Change. W. G. I. S. f. P. IPCC.

Buttau, C., A. Funedda, A. Carletti, S. Virdis and G. Ghiglieri (2013). "Studio geologico strutturale per indagini idrogeologiche dell'area compresa tra le regioni di Batna e Biskra (NE Algeria)." Rend Online Soc Geol It **29**: 13-16.

Büttner, G., G. Maucha, M. Bíró, B. Kosztra and O.Petrik (2000). National CORINE Land Cover mapping at scale 1:50.000 in Hungary. Hungary, FÖMI Remote Sensing Centre, Budapest.

CLC2006TechnicalGuidelines (2007). CLC2006 Technical Guidelines. Copenhagen.

D'Odorico, P., A. Bhattachan, K. F. Davis, S. Ravi and C. W. Runyan (2013). "Global desertification: Drivers and feedbacks." Advances in Water Resources **51**(0): 326-344.

Dalel Ouerchefani, H. T. e. A. B. (2008). "Apport de la classification spectrale des compositions colorées des indices pour la cartographie des sols salins dans un milieu aride du Sud tunisien." Journal Canadien de Télédétection **vol. 34**(no 5): p. 438–446.

Dregne, H. E. (2002). "Land Degradation in the Drylands." Arid Land Research and Management **16**(2): 99-132.

Duan, H. C., T. Wang, X. Xue, S. L. Liu and J. Guo (2014). "Dynamics of aeolian desertification and its driving forces in the Horqin Sandy Land, Northern China." Environ Monit Assess **186**(10): 6083-6096.

Elnaggar, A. A. and J. S. Noller (2010). "Application of Remote-sensing Data and Decision-Tree Analysis to Mapping Salt-Affected Soils over Large Areas." Remote Sensing **2**(1): 151-165.

Escadafal, R., C. Barbero-Sierra, W. Exbrayat, M. J. Marques, M. Akhtar-Schuster, A. El Haddadi and M. Ruiz (2015). "First Appraisal of the Current Structure of Research on Land and Soil Degradation as Evidenced by Bibliometric Analysis of Publications on Desertification." Land Degradation & Development **26**(5): 413-422.

Escadafal, R. and M. Pouget (1985). Luminance spectrale et caracteres de la surface des sols en region aride mediterraneenne (Sud Tunisien). 4th Symposium of ISS Working Group Remote Sensing for Soil Survey.

Essifi, B., M. Ouessar and M. C. Rabia (2009). "Mapping long-term variability of vegetation greenness and sand dunes around watering points in the rangelands of Dahar and El Ouara (Tataouine-Tunisia) during the period 1975-2000 using remote sensing." Journal of Arid Land Studies **19**(1): 319-322.

ETC/LC and E. E. Agency (1999). CORINE Land cover. Technical guide, ETC/LC, European Environment Agency.

Eyal, B.-D., M. Graciela, G. Naftaly, M. Eshel, M. Vladmir and B. Uri (2008). Review of Remote Sensing-Based Methods to Assess Soil Salinity. Remote Sensing of Soil Salinization, CRC Press.

FAO (1999). Soil salinity assessment, FAO.

Fares, M. H. and C. G. Philip (2008). Characterization of Salt-Crust Build-Up and Soil Salinization in the United Arab Emirates by Means of Field and Remote Sensing Techniques. Remote Sensing of Soil Salinization, CRC Press.

Farifteh, J. (2007). Imaging Spectroscopy of salt-affected soils: Model-based integrated method. Netherlands, International Institute for Geo-information Science and Earth Observation, Enschede.

Farifteh, J., A. Farshad and R. J. George (2006). "Assessing salt-affected soils using remote sensing, solute modelling, and geophysics." Geoderma **130**(3–4): 191-206.

Farifteh, J., F. Van der Meer, C. Atzberger and E. J. M. Carranza (2007). "Quantitative analysis of salt-affected soil reflectance spectra: A comparison of two adaptive methods (PLSR and ANN)." Remote Sensing of Environment **110**(1): 59-78.

Farifteh, J., F. van der Meer, M. van der Meijde and C. Atzberger (2008). "Spectral characteristics of salt-affected soils: A laboratory experiment." Geoderma **145**(3–4): 196-206.

Feranec, J. and J. Otahel (2000). THE 4TH LEVEL CORINE LAND COVER NOMENCLATURE FOR THE PHARE COUNTRIES. EEA Phare Topic Link on Land Cover Slovak Republic, Institute of Geography, Slovak Academy of Sciences, Bratislava.

Frizon de Lamotte, D., B. Saint Bezar, R. Bracène and E. Mercier (2000). "The two main steps of the Atlas building and geodynamics of the western Mediterranean." Tectonics **19**(4): 740-761.

Fu, H., L. Gu, R. Ren and J. Sun (2014). Land salinization classification method using Landsat TM in western Jilin Province of China.

Gao, B.-c. (1996). "NDWI—A normalized difference water index for remote sensing of vegetation liquid water from space." Remote Sensing of Environment **58**(3): 257-266.

Ge, X., K. Dong, A. E. Luloff, L. Wang, J. Xiao, S. Wang and Q. Wang (2016). "Correlation between landscape fragmentation and sandy desertification: a case study in Horqin Sandy Land, China." Environ Monit Assess **188**(1): 62.

Ghiglieri, G., M. O. B. Sy, H. Yahyaoui, M. Ouessar, A. Ouldamara, A. S. Gil, C. Arras, M. Barbieri, O. Belkheiri, M. B. Zaied, C. Buttau, A. Carletti, S. D. Pelo, A. Dodo, Antonio, Funedda, I. Iocola, E. Meftah, F. Mokh, K. Nagaz, M. T. Melis, D. Pittalis, M. Said, M. Sghaier, C. Torrentó, S. Virdis, Abderezak, Zahrouna and G. Enne (2014). Design of artificial aquifer recharge systems in dry regions of Maghreb (North Africa). FlowPath2014 - National meeting on nydrogeology, Viterbo, Dipartimento di Scienze Ecologiche e Biologiche,

Università degli Studi della Tuscia.

Gitelson, A. A., Y. J. Kaufman and M. N. Merzlyak (1996). "Use of a green channel in remote sensing of global vegetation from EOS-MODIS." Remote Sensing of Environment **58**(3): 289-298.

Gitelson, A. A., Y. Peng, T. J. Arkebauer and J. Schepers (2014). "Relationships between gross primary production, green LAI, and canopy chlorophyll content in maize: Implications for remote sensing of primary production." Remote Sensing of Environment **144**(0): 65-72.

Gorji, T., A. Tanik and E. Sertel (2015). "Soil Salinity Prediction, Monitoring and Mapping Using Modern Technologies." Procedia Earth and Planetary Science **15**: 507-512.

Guiraud, R., W. Bosworth, J. Thierry and A. Delplanque (2005). "Phanerozoic geological evolution of Northern and Central Africa: An overview." Journal of African Earth Sciences **43**(1-3): 83-143.

Guo, Y., Z. Shi, L.-q. Zhou, X. Jin, Y.-f. Tian and H.-f. Teng (2013). "Integrating Remote Sensing and Proximal Sensors for the Detection of Soil Moisture and Salinity Variability in Coastal Areas." Journal of Integrative Agriculture **12**(4): 723-731.

Haijiang, L., Z. Chenghu, C. Weiming, L. En and L. Rui (2008). "Monitoring sandy desertification of Otindag Sandy Land based on multi-date remote sensing images." Acta Ecologica Sinica **28**(2): 627-635.

Hamid Reza, M. and R. Majid Shadman (2012). "Decision Tree Land Use/ Land Cover Change Detection of Khoram Abad City Using Landsat Imagery and Ancillary SRTM Data." Scholars Research Library(Annals of Biological Research): 4045-4053.

Hirche, A., M. Salamani, A. Abdellaoui, S. Benhouhou and J. M. Valderrama (2011). "Landscape changes of desertification in arid areas: the case of south-west Algeria." Environ Monit Assess **179**(1-4): 403-420.

Jaffrain, G. and EEA (2011). CORINE land cover outside of Europe. Nomenclature adaptation to other bio-geographical regions. Spain, Universidad de Malaga, ETCSIA.

Kang, Q., R. Yu, Z. Zhang and X. Zhao (2005). Remote sensing application of soil salinization based on multi-source images.

Khan, N. M., V. V. Rastoskuev, Y. Sato and S. Shiozawa (2005). "Assessment of hydrosaline land degradation by using a simple approach of remote sensing indicators." Agricultural Water Management **77**(1-3): 96-109.

Khan, N. M., V. V. Rastoskuev, E. V.Shalina and Y. Sato (2001). Mapping Salt-affected Soils Using Remote Sensing Indicators - A Simple Approach With the Use of GIS IDRISI -. 22nd Asian Conference on Remote Sensing. Singapore, Centre for Remote Imaging, Sensing and Processing; National University of Singapore; Singapore Institute of Surveyors and Valuers; Asian Association on Remote Sensing.

Khatelli, H. and D. Gabriels (1998). "A study on the dynamics of sand dunes in Tunisia: Mobile barkhans move in the direction of the Sahara." Arid Soil Research and Rehabilitation **12**(1): 47-54.

Khatelli, H. and D. Gabriels (2000). "EFFECT OF WIND DIRECTION ON AEOLIAN SAND TRANSPORT IN SOUTHERN TUNISIA." Int. Agrophysics **14**: 291-296.

Kross, A., H. McNairn, D. Lapen, M. Sunohara and C. Champagne (2015). "Assessment of RapidEye vegetation indices for estimation of leaf area index and biomass in corn and soybean crops." International Journal of Applied Earth Observation and Geoinformation **34**(0): 235-248.

Langford, R. L. (2015). "Temporal merging of remote sensing data to enhance spectral regolith, lithological and alteration patterns for regional mineral exploration." Ore Geology Reviews **68**(0): 14-29.

Li, J., Y. Zhao, H. Liu and Z. Su (2016). "Sandy desertification cycles in the southwestern Mu Us Desert in China over the past 80years recorded based on nebkha sediments." Aeolian Research **20**: 100-107.

Li, L., S. L. Ustin, A. Palacios-Orueta, S. Jacquemoud and M. L. Whiting (2009). Remote sensing based assessment of biophysical indicators for land degradation and desertification. Recent Advances in Remote Sensing and Geoinformation Processing for Land Degradation Assessment, CRC Press**:** 15-44.

Lorenz, R. D., N. Gasmi, J. Radebaugh, J. W. Barnes and G. G. Ori (2013). "Dunes on planet Tatooine: Observation of barchan migration at the Star Wars film set in Tunisia." Geomorphology **201**: 264-271.

Masoud, A. A. (2014). "Predicting salt abundance in slightly saline soils from Landsat ETM+ imagery using Spectral Mixture Analysis and soil spectrometry." Geoderma **217-218**: 45-56.

Masoud, A. A. and K. Koike (2006). "Arid land salinization detected by remotely-sensed landcover changes: A case study in the Siwa region, NW Egypt." Journal of Arid Environments **66**(1): 151-167.

Matthew, C. H. (2012). Classification Trees and Mixed Pixel Training Data. Remote Sensing of Land Use and Land Cover, CRC Press**:** 127-136.

McFeeters, S. K. (1996). "The use of Normalized Difference Water Index (NDWI) in the delineation of open water features." International Journal of Remote Sensing **17**(7): 1425–1432.

Melis, M. T., G. Afrasinei, O. Belkheir, A. Carletti, I. Iocola, D. Pittalis, S. Virdis and G. Ghiglieri (2013). Caratterizzazione spettrale delle aree interessate da salinizzazione nel bacino del Oued Biskra in Algeria a supporto delle politiche di gestione dell'acqua nell'ambito del progetto WADIS-MAR. Atti 17a Conferenza Nazionale ASITA, 5 – 7 novembre 2013, Riva del Garda. Riva del Garda, ASITA. **Atti 17a Conferenza Nazionale ASITA, 5 – 7 novembre 2013, Riva del Garda**.

Metternicht, G. and J. A. Zinck (2008). Soil Salinity and Salinization Hazard. Remote Sensing of Soil Salinization, CRC Press.

Metternicht, G. and J. A. Zinck (2008). Spectral Behavior of Salt Types. Remote Sensing of Soil Salinization, CRC Press.

Metternicht, G. I. and J. A. Zinck (2003). "Remote sensing of soil salinity: potentials and constraints." Remote Sensing of Environment **85**(1): 1-20.

Mia, B. and Y. Fujimitsu (2012). "Mapping hydrothermal altered mineral deposits using Landsat 7 ETM+ image in and around Kuju volcano, Kyushu, Japan." Journal of Earth System Science **121**(4): 1049-1057.

Mulder, V. L., S. de Bruin, M. E. Schaepman and T. R. Mayr (2011). "The use of remote sensing in soil and terrain mapping — A review." Geoderma **162**(1–2): 1-19.

Mulder, V. L., S. de Bruin, J. Weyermann, R. F. Kokaly and M. E. Schaepman (2013). "Characterizing regional soil mineral composition using spectroscopy and geostatistics." Remote Sensing of Environment **139**: 415-429.

NRD (2011). WADIS-MAR Water harvesting and Agricultural techniques in Dry lands: an Integrated and Sustainable model in MAghreb Regions. Project Document.

Nutini, F., M. Boschetti, P. A. Brivio, S. Bocchi and M. Antoninetti (2013). "Land-use and land-cover change detection in a semi-arid area of Niger using multi-temporal analysis of Landsat images." International Journal of Remote Sensing **34**(13): 4769-4790.

Olofsson, P., G. M. Foody, M. Herold, S. V. Stehman, C. E. Woodcock and M. A. Wulder (2014). "Good practices for estimating area and assessing accuracy of land change." Remote Sensing of Environment **148**(0): 42-57.

Otukei, J. R. and T. Blaschke (2010). "Land cover change assessment using decision trees, support vector machines and maximum likelihood classification algorithms." International Journal of Applied Earth Observation and Geoinformation **12, Supplement 1**(0): S27-S31.

Ouerchefani, D. (2012). CARACTERISATION ET SUIVI DES ETATS DE SURFACES ÉOLISÉS EN TUNISIE PRÉ-SAHARIENNE : APPROCHES STATIONNELLE ET SPATIALE, Laboratoire de Ressources Minérales et Environnement, Université de Tunis El Manar, Faculté des Sciences de Tunis.

Ouerchefani, D., H. Dhaou, E. Delaitre, Y. Callot and S. Abdeljaoued (2013). "Geographic information system (GIS) and remote sensing for multi-temporal analysis of sand encroachment at Oglet Merteba (South Tunisia)." African Journal of Environmental Science and Technology **Vol. 7**(10): pp. 938-943.

Ouessar, M. (2007). Hydrological impacts of rainwater harvesting in wadi Oum Zessar watershed (Southern Tunisia). Ph.D, Ghent University

Ouessar, M. (2010). WATER HARVESTING AND CC ADAPTATION IN THE DRY AREAS OF TUNISIA. Damascus , Syria Regional Consultation Meeting Climate Change Impacts in the Arab Region: Water Scarcity, Drought, and Population Mobility.

Ouessar, M. (2011). Physical and socio-economic characteristics of the watershed of Wadi Oum Zessar, Tunisia.

Pal, M. (2012). Advanced algorithms for land use and cover classification. Advances in Mapping from Remote Sensor Imagery, CRC Press**:** 69-90.

Pal, M. and P. M. Mather (2003). "An assessment of the effectiveness of decision tree methods for land cover classification." Remote Sensing of Environment **86**(4): 554-565.

Pons, X., L. Pesquer, J. Cristóbal and O. González-Guerrero (2014). "Automatic and improved radiometric correction of Landsat imagery using reference values from MODIS surface reflectance images." International Journal of Applied Earth Observation and Geoinformation **33**(0): 243-254.

R.L. Dehaan, G. R. T. (2002). "Field-derived spectra of salinized soils and vegetation as indicators of irrigation-induced soil salinization." Remote Sensing of Environment **80**: 406–417.

Rao, P., S. Chen and K. Sun (2006). Improved classification of soil salinity by decision tree on remotely sensed images.

Richa Sharma, A. G. a. P. (2013). "Decision tree approach for classification of remotely sensed satellite data using open source support." J. Earth Syst. Sci. **122**(5): 1237–1247.

Rogan, J., J. Franklin and D. A. Roberts (2002). "A comparison of methods for monitoring multitemporal vegetation change using Thematic Mapper imagery." Remote Sensing of Environment **80**(1): 143-156.

Rogan, J., J. Franklin, D. Stow, J. Miller, C. Woodcock and D. Roberts (2008). "Mapping land-cover modifications over large areas: A comparison of machine learning algorithms." Remote Sensing of Environment **112**(5): 2272-2283.

Roy, D. P., M. A. Wulder, T. R. Loveland, W. C.E, R. G. Allen, M. C. Anderson, D. Helder, J. R. Irons, D. M. Johnson, R. Kennedy, T. A. Scambos, C. B. Schaaf, J. R. Schott, Y. Sheng, E. F. Vermote, A. S. Belward, R. Bindschadler, W. B. Cohen, F. Gao, J. D. Hipple, P. Hostert, J. Huntington, C. O. Justice, A. Kilic, V. Kovalskyy, Z. P. Lee, L. Lymburner, J. G. Masek, J. McCorkel, Y. Shuai, R. Trezza, J. Vogelmann, R. H. Wynne and Z. Zhu (2014). "Landsat-8: Science and product vision for terrestrial global change research." Remote Sensing of Environment **145**(0): 154-172.

Schiettecatte, W., M. Ouessar, D. Gabriels, S. Tanghe, S. Heirman and F. Abdelli (2005). "Impact of water harvesting techniques on soil and water conservation: a case study on a micro catchment in southeastern Tunisia." Journal of Arid Environments **61**(2): 297-313.

Scudiero, E., T. H. Skaggs and D. L. Corwin (2015). "Regional-scale soil salinity assessment using Landsat ETM+ canopy reflectance." Remote Sensing of Environment **169**: 335-343.

Sghaier, M., M. Ouessar, A. O. Belgacem, H. Taamallah and H. Khatteli (2010). Vulnerability of olive production sector to climate change in the governorate of Médenine (Tunisia). Final report. CI:GRASP project.

Srimani, P. K. and N. Prasad (2012). "Decision tree classification model for land use and land cover mapping - a case study." International Journal of Current Research **4**(05): 177-181.

Srimani, P. K. and S. N. Prasad (2012). "DECISION TREE CLASSIFICATION MODEL FOR LAND USE AND LAND COVER MAPPING- A CASE STUDY." International Journal of Current Research.

Szabolcs, I. (1989). Salt Affected Soils, CRC Press.

van der Meer, F. D., H. M. A. van der Werff, F. J. A. van Ruitenbeek, C. A. Hecker, W. H. Bakker, M. F. Noomen, M. van der Meijde, E. J. M. Carranza, J. B. d. Smeth and T. Woldai (2012). "Multi- and hyperspectral geologic remote sensing: A review." International Journal of Applied Earth Observation and Geoinformation **14**(1): 112-128.

Vanonckelen, S., S. Lhermitte, V. Balthazar and A. Van Rompaey (2014). "Performance of atmospheric and topographic correction methods on Landsat imagery in mountain areas." International Journal of Remote Sensing **35**(13): 4952-4972.

Vanonckelen, S., S. Lhermitte and A. Van Rompaey (2013). "The effect of atmospheric and topographic correction methods on land cover classification accuracy." International Journal of Applied Earth Observation and Geoinformation **24**(0): 9-21.

Wang, T., C. Z. Yan, X. Song and S. Li (2011). "Landsat Images Reveal Trends in the Aeolian Desertification in a Source Area for Sand and Dust Storms in China's Alashan Plateau (1975-2007)." Land Degradation & Development: n/a-n/a.

Wang, X., G. Wang, L. Lang, T. Hua and H. Wang (2013). "Aeolian Transport and Sandy Desertification in Semiarid China: A Wind Tunnel Approach." Land Degradation & Development **24**(6): 605-612.

Zhang, Z., X. Wang, X. Zhao, B. Liu, L. Yi, L. Zuo, Q. Wen, F. Liu, J. Xu and S. Hu (2014). "A 2010 update of National Land Use/Cover Database of China at 1:100000 scale using medium spatial resolution satellite images." Remote Sensing of Environment **149**(0): 142-154.

Zhu, Z. and C. E. Woodcock (2014). "Continuous change detection and classification of land cover using all available Landsat data." Remote Sensing of Environment **144**(0): 152-171.